National Library of Canada
Canadian Theses Service
Ottawa, Canada
K1A 0N4

Bibliothèque nationale du Canada
Services des thèses canadiennes

CANADIAN THESES

THÈSES CANADIENNES

NOTICE

The quality of this microfiche is heavily dependent upon the quality of the original thesis submitted for microfilming. Every effort has been made to ensure the highest quality of reproduction possible.

If pages are missing, contact the university which granted the degree.

Some pages may have indistinct print especially if the original pages were typed with a poor typewriter ribbon or if the university sent us an inferior photocopy.

Previously copyrighted materials (journal articles, published tests, etc.) are not filmed.

Reproduction in full or in part of this film is governed by the Canadian Copyright Act, R.S.C. 1970, c. C-30. Please read the authorization forms which accompany this thesis.

AVIS

La qualité de cette microfiche dépend grandement de la qualité de la thèse soumise au microfilmage. Nous avons tout fait pour assurer une qualité supérieure de reproduction.

S'il manque des pages, veuillez communiquer avec l'université qui a conféré le grade.

La qualité d'impression de certaines pages peut laisser à désirer, surtout si les pages originales ont été dactylographiées à l'aide d'un ruban usé ou si l'université nous a fait parvenir une photocopie de qualité inférieure.

Les documents qui font déjà l'objet d'un droit d'auteur (articles de revue, examens publiés, etc.) ne sont pas microfilmés.

La reproduction, même partielle, de ce microfilm est soumise à la Loi canadienne sur le droit d'auteur, SRC 1970, c. C-30. Veuillez prendre connaissance des formules d'autorisation qui accompagnent cette thèse.

THIS DISSERTATION
HAS BEEN MICROFILMED
EXACTLY AS RECEIVED

LA THÈSE A ÉTÉ
MICROFILMÉE TELLE QUE
NOUS L'AVONS REÇUE

NL 339 (r. 86/01)

Canada

National Library of Canada
Bibliothèque nationale du Canada

136

Ottawa, Canada
K1A 0N4

TC –

0-315-23333-8

CANADIAN THESES ON MICROFICHE SERVICE – SERVICE DES THÈSES CANADIENNES SUR MICROFICHE

PERMISION TO MICROFILM – AUTORISATION DE MICROFILMER

• Please print or type – Écrire en lettres moulées ou dactylographier

AUTHOR – AUTEUR

Full Name of Author – Nom complet de l'auteur

STACY KENT GRANT

Date of Birth – Date de naissance
27 JANUARY 1985

Canadian Citizen – Citoyen canadien
☑ Yes / Oui ☐ No / Non

Country of Birth – Lieu de naissance
CANADA

Permanent Address – Résidence fixe
1202 KNOTTWOOD ROAD EAST
EDMONTON, ALTA
T6K 2J8

THESIS – THÈSE

Title of Thesis – Titre de la thèse

GEOLOGIC STUDY OF THE VIKING FORMATION, HARMATTAN EAST FIELD

Degree for which thesis was presented
Grade pour lequel cette thèse fut présentée
MSc

Year this degree conferred
Année d'obtention de ce grade
1985

University – Université
UNIVERSITY OF ALBERTA

Name of Supervisor – Nom du directeur de thèse
Dr. F.J. LONGSTAFFE
Dr. F.J. HEIN

AUTHORIZATION – AUTORISATION

Permission is hereby granted to the NATIONAL LIBRARY OF CANADA to **microfilm** this thesis and to **lend** or **sell copies of the film.**

The author reserves other publication rights, and neither the thesis nor extensive extracts from it may be printed or, otherwise reproduced without the author's written permission.

L'autorisation est, par la présente, accordée à la BIBLIOTHÈQUE NATIONALE DU CANADA de **microfilmer** cette thèse et de **prêter** ou de **vendre des exemplaires du film.**

L'auteur se réserve les autres droits de publication; ni la thèse ni de longs extraits de celle-ci ne doivent être imprimés ou autrement reproduits sans l'autorisation écrite de l'auteur.

ATTACH FORM TO THESIS – VEUILLEZ JOINDRE CE FORMULAIRE À LA THÈSE

Signature
Kent Grant

Date
11 October 1985

NL-91 (r. 84/03)

Canada

THE UNIVERSITY OF ALBERTA

GEOLOGIC STUDY OF THE VIKING FORMATION, HARMATTAN EAST FIELD

by

S. KENT GRANT

A THESIS

SUBMITTED TO THE FACULTY OF GRADUATE STUDIES AND RESEARCH

IN PARTIAL FULFILMENT OF THE REQUIREMENTS FOR THE DEGREE

OF MASTER OF SCIENCE

DEPARTMENT OF GEOLOGY

EDMONTON, ALBERTA

FALL, 1985

THE UNIVERSITY OF ALBERTA

RELEASE FORM

NAME OF AUTHOR S. KENT GRANT

TITLE OF THESIS GEOLOGIC STUDY OF THE VIKING FORMATION, HARMATTAN EAST FIELD

DEGREE FOR WHICH THESIS WAS PRESENTED MASTER OF SCIENCE

YEAR THIS DEGREE GRANTED FALL, 1985

Permission is hereby granted to THE UNIVERSITY OF ALBERTA LIBRARY to reproduce single copies of this thesis and to lend or sell such copies for private, scholarly or scientific research purposes only.

The author reserves other publication rights, and neither the thesis nor extensive extracts from it may be printed or otherwise reproduced without the author's written permission.

(SIGNED) Kent Grant

PERMANENT ADDRESS:

1202 KNOTTWOOD ROAD EAST

EDMONTON ALBERTA

T6K 2J8

DATED 11 October 1985

THE UNIVERSITY OF ALBERTA

FACULTY OF GRADUATE STUDIES AND RESEARCH

The undersigned certify that they have read, and recommend to the Faculty of Graduate Studies and Research, for acceptance, a thesis entitled GEOLOGIC STUDY OF THE VIKING FORMATION, HARMATTAN EAST FIELD submitted by S. KENT GRANT in partial fulfilment of the requirements for the degree of MASTER OF SCIENCE.

F. J. Longstaffe

Supervisor

Frances J. Hein

Supervisor

Frank W. Schwartz

Jennifer Whiting

Date 11 October 1985

DEDICATION

I dedicate this thesis to my wife Lynn, my parents Norma and Alex and my parents-in-law Dee and Jack who all provided support throughout the duration of this project.

ABSTRACT

The coarsening-upward clastic sequence of the Viking Formation within the Harmattan East field was deposited approximately 5 km seaward of a storm-dominated shoreline. This clastic sequence consists of fine-grained sandstone, medium or coarse-grained sandstone and chert-pebble conglomerate. Unidirectional currents (wave and/or storm-induced) transported the two sandstones into the lower shoreface environment, forming a northeast/southwest oriented trough. This trough focused the sediment-gravity flows (storm-induced) which transported the conglomerate into the lower shoreface or inner-shelf environment. Subsequent reworking of the conglomerate was minimized by this trough.

The Viking Formation consists of sublitharenites containing 10-40% cement. The upper two lithologic units are cemented (10-20%) primarily by quartz and clay minerals. These clay minerals include kaolinite and illite, with minor illite/smectite, chlorite and smectite. The fine-grained sandstone is cemented (30-40%) by quartz, carbonate minerals (siderite, minor dolomite and ankerite) and minor clay minerals.

This formation has undergone burial and subsequent uplift. During burial these clastic rocks have passed through both early and late stages of diagenesis, reaching a maximum temperature and burial depth of 140-150°C and 3600 metres, respectively. Early diagenesis is marked by pyrite, siderite, quartz, chlorite and possibly dolomite. Late diagenesis is characterized by illitization of smectite, the formation of illite and later kaolinite, ankeritization of dolomite and possible albitization of feldspar. This diagenetic sequence has been followed throughout the study area except in the lower portion of the fine-grained sandstone which was totally cemented prior to late diagenesis.

The producing horizon consists of three laterally continuous zones of conglomerate overlying a medium or coarse-grained sandstone. For primary production the reservoir quality is determined by the depositional pattern of the conglomerate if a low rate of production is maintained. However, if stimulation or secondary recovery (with high flushing rates) is attempted the mineralogy will have a significant influence on reservoir quality. Possible formation damage may result from the migration of fines, sensitivity to fresh water and precipiation of ferric hydroxide gels, in decreasing order of importance.

ACKNOWLEDGEMENT

Greatly appreciated is the guidance provided by my supervisors Dr. F.J. Longstaffe and Dr. F.J. Hein. I would also like to thank Diane Caird for her assistance in the labratory. In addition I would like to thank Canadian Superior Oil Ltd. for providing financial support and access to well data. Finally I would like to thank the other members of my committee, Dr. F.W. Schwartz and Dr. J Whiting, whose comments improved the thesis.

Table of Contents

Chapter — Page

I. INTRODUCTION 1
A. PURPOSE OF THE STUDY 3
B. STRATIGRAPHY 5
C. GEOLOGIC HISTORY 8
D. PREVIOUS WORK 15
E. METHODS 17
Core Description 17
Facies Definition 17
Correlation of Logs 17
Sampling 17
Hydrometer Analysis 20
X-ray Diffraction Analysis 21
Scanning Electron Microscopy 22
Thin Section Analysis 23
II. SEDIMENTOLOGY 24
A. LITHOFACIES 24
B. FACIES ASSOCIATIONS 31
C. SHELF PROCESSES 31
D. FACIES INTERPRETATION 37
E. PALEOGEOGRAPHY 48
F. DEPOSITIONAL PROCESSES 55
Fine-grained sandstone 55
Medium or coarse-grained sandstone 55
Conglomerate 58
G. DEPOSITIONAL PATTERN 63
Fine-grained sandstone 63
Medium or coarse-grained sandstone 63
Conglomerate 69
III. MINERALOGY 75

A. PETROGRAPHY 75
B. GRAIN-SIZE ANALYSIS (by hydrometer) 89
C. X-RAY DIFFRACTION ANALYSIS 93
Bulk Mineralogy 93
Clay Mineralogy 93
D. SCANNING ELECTRON MICROSCOPY 104
Conglomerate 104
Medium or Coarse-grained Sandstone 104
Fine-grained Sandstone 111
E. DIAGENESIS 114
IV. RESERVOIR STUDY 119
A. HARMATTAN EAST RESERVOIR 119
B. FORMATION DAMAGE 125
C. RESERVOIR EVALUATION 126
V. CONCLUSION 129
BIBLIOGRAPHY 131
VI. APPENDIX I 145
VII. APPENDIX II 155

LIST OF TABLES

Table 3.1 Samples investigated 76
Table 3.2a Rock components 79
Table 3.2b Bulk mineralogy 80
Table 3.3a Hydrometer analysis 90
Table 3.3b Hydrometer analysis 92
Table 3.4a Mineralogy 5-20 μm size-fraction 94
Table 3.4b Mineralogy $>$ 5μm size-fraction 96
Table 3.5a Mineralogy 2-5 μm size-fraction 98
Table 3.5b Mineralogy $<$ 5 μm size-fraction 100
Table 3.6 Mineralogy $<$ 2 μm size-fraction 102

LIST OF FIGURES

Figure 1.1 Location Map 2
Figure 1.2 Map of the Gas and Oil fields in Alberta 6
Figure 1.3 Stratigraphic Table 7
Figure 1.4 Tectonic Elements 9
Figure 1.5 Early Late Albian Seas 11
Figure 1.6 Late late Albian Seas 12
Figure 1.7 Late Early Turonian Seas 13
Figure 1.8 Basins and arches of western Canada 14
Figure 1.9 Grain-size scale 18
Figure 1.10 Symbols for lithologs 19
Figure 2.1 Fence diagram of Harmattan East 32
Figure 2.2 Facies 8, Facies 1, Facies 2 (core photographs) 38
Figure 2.3 Position of transitional zone 40
Figure 2.4 Storm deposit (photograph) 41
Figure 2.5 Facies 3, Facies 4, Facies 5, Facies 9 (core photographs) 45
Figure 2.6 Lithofacies, top of clastic wedge 49
Figure 2.7 Correlation, lower conglomerate to rooted zone 50
Figure 2.8 Cross-section, Harmattan East to shoreline 51
Figure 2.9 Correlation, Harmattan East to western complex 53
Figure 2.10 Bentonite correlation 54
Figure 2.11 Generalized lithology, Viking Formation 56
Figure 2.12 Shoaling sequence 57
Figure 2.13 Stages in movement of sediment gravity flow 59
Figure 2.14 Flow pattern in rip-currents 62
Figure 2.15 Paleotopgraphy of fine-grained sandstone 64
Figure 2.16 Isopach of medium or coarse-grained sandstone 65
Figure 2.17 Paleotopography of the medium or coarse-grained sandstone 66
Figure 2.18 Block diagram, paleotopography medium or coarse-grained sandstone 67
Figure 2.19 Block diagram, paleotopography conglomerate 70
Figure 2.20 Isopach of the conglomerate 72

Figure 2.21 Depositional pattern on the banks of trough 73
Figure 2.22 Boundaries of the Harmattan East conglomerate 74
Figure 3.1 Rock classification 81
Figure 3.2 Petrography (conglomerate) 82
Figure 3.3 Petrography (medium or coarse-grained sandstone) 84
Figure 3.4 Petrography (fine-grained sandstone) 87
Figure 3.5 Conglomerate (SEM) 105
Figure 3.6 Medium or coarse-grained sandstone (SEM) 107
Figure 3.7 Carbonate cements (SEM) 109
Figure 3.8 Fine-grained sandstone (SEM) 112
Figure 3.9 Diagenetic model 115
Figure 4.1 Boundaries of Harmattan East conglomerate 120
Figure 4.2 Harmattan East lithology 121
Figure 4.3 Fence diagram of reservoir 122
Figure 4.4 Porosity permeability correlation 124
Figure 4.5 Reservoir configuration (primary & secondary recovery) 127

LIST OF ABBREVIATIONS

Tables and Figures presented throughout the report employ the following abbreviations:

ROCK TYPES

Congl. = Conglomerate

C.Sst. = Coarse-Grained Sandstone

M.Sst. = Medium-Grained Sandstone

F.Sst. = Fine-Grained Sandstone

BULK MINERALOGY FROM THIN SECTION

Ch= Chert

Q = Quartz

F = Feldspar

RF= Rock Fragments

Ca= Carbonate

S = Siderite

C = Clay Minerals

MINERALOGY FROM X-RAY DIFFRACTION, THIN SECTION, AND SCANNING ELECTRON MICROSCOPY

μm= Micrometer (1×10^{-6} meters)

Q = Quartz

F = Feldspar

C = Clay Minerals

IS= Illite/Smectite

SM= Smectite

Chl= Chlorite

I = Illite

K = Kaolinite

AF= Authigenic Feldspar

LIST OF ABBREVIATIONS (CONTINUED)

AQ= Authigenic Quartz

2°P = Secondary Porosity

Sh= Shale Rock Fragment

An = Ankerite

D = Dolomite

S = Siderite

Py= Pyrite

MINERAL ABUNDANCES

nd= Not Detected

t = Trace (<2%)

mt= Minor or Trace (2-5%)

m = Minor (5-10%)

mM= Moderate (10-35%)

M = Major (>35%)

I. INTRODUCTION

The Harmattan East oil field occurs in clastic sedimentary rocks of the Cretaceous Viking Formation. This clastic sequence is a shallow marine, coarsening-upward wedge which is bound above and below by marine shales. The field is located approximately one hundred kilometers north of Calgary (Fig. 1.1).

The Viking Formation in the Harmattan East field lies at an average depth of 2200 metres and is considered to be an underpressured zone. The oil-in-place is 8.2 X 10^6 M^3 (51.81 mmSTB)[1] with a gas cap consisting of 172.7 X 10^6 M^3 (6.13 BCF)[1].

The Harmattan East Viking 'A' pool was discovered in November, 1979 with the drilling of well 13-26-32 3W5. Later drilling penetrated the western edge of the pool at 11-20-32 3W5, which at the time was designated as the discovery well for the Harmattan East Viking 'B' pool by the Energy and Resources Conservation Board (ERCB). As of January 1984, 62 wells had been drilled by 9 different operators within the Harmattan East field, which encompasses the ERCB designated Viking pools A, B, E, F and L. The Harmattan East Viking oil field comprises an area of approximately 11,400 ha (44 sections/28,160 acres). The oil bearing units within the field include 35 sections, with the gas cap to the east side of the pool occurring in nearly 9 sections. This study is confined to Township 32 and the lower half of Township 33, Range 2,3 and 4 west of the Fifth Meridian (Fig. 1.1).

Within the Harmattan East field, the stratigraphic section is divided into the Upper and Lower Viking horizons. The Lower Viking (20 metres thick) unit conformably overlies the silty shales of the Joli Fou Formation. The basal part of the Lower Viking consists of approximately 10 metres of interbedded and bioturbated fine-grained sandstones and silty shales. This is overlain by approximately 10 metres of fine to very fine-grained cross-bedded sandstones. The Upper Viking (4 - 7 metres thick) consists of medium or coarse-grained sandstone overlain by chert-pebble conglomerate. This unit has good permeability (average 25 md) and porosity which averages 9%. This Upper Viking unit has a sharp erosional contact with the Lower Viking stratigraphic unit.

---

[1]estimated volumetrically

Figure 1.1 Location map for the Harmattan East Field

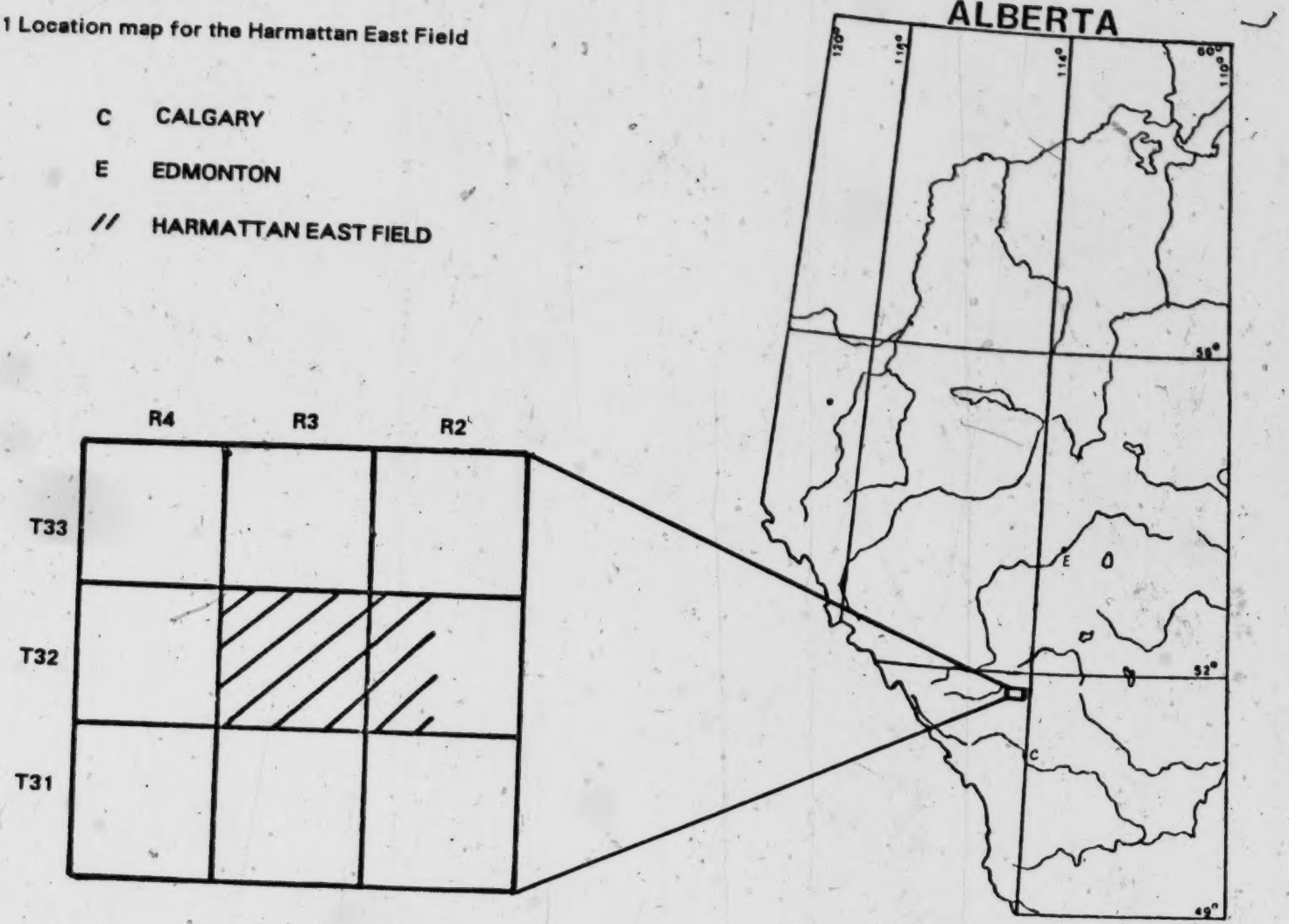

A. PURPOSE OF THE STUDY

This study will examine both sedimentology and mineralogy of the Viking Formation within the Harmattan East oil field. The purpose of this study is to development of a diagenetic sequence and to confront the lack of a well developed shallow-marine facies model for coarse-grained sediment. The specific objectives of this study are to define:

1. the sedimentary facies present within the Harmattan East study area,
2. the facies associations and their lateral continuity within the study area,
3. the depositional processes and environment within the study area,
4. the nature and distributions of authigenic minerals within the Viking Formation,
5. mineralogical controls on potential formation damage resulting from fluid injection, and
6. sedimentary and mineralogic factors controlling the distribution of hydrocarbons.

As this Viking reservoir has undergone burial and subsequent uplift, mineral transformations can not be directly correlated to present formation conditions. This requires that the Viking Formation be compared to established models for sandstone diagenesis (e.g. Gulf Coast). However, direct comparison with these diagenetic models is difficult due to variation in the original detrital component and subsequent uplift of the Viking Formation.

At present there is no well developed shallow-marine facies model (or models) because of the complex correlation between processes and results. Within this environment two distinct processes (tidal and storms) may produce the same bedform (linear sand ridge), or conversely one process (tidal currents) may produce different types of deposits (linear sand ridge or smaller bedforms). In trying to establish the correlation between processes and results two major problems exist. Firstly, how is the sediment transported into water depths ranging form 10 to 200 metres? Secondly, to what extent is the sediment remolded by tidal, storm and oceanographic currents (Walker, 1979)?

Removal of the coastal sands is a problem because fairweather shore-parallel currents and shoaling waves maintain the sands in the nearshore environment (Komar, 1976). Swift (1976) referred to this retaining force as the 'littoral energy fence'. Sediment which penetrates this 'fence' generally falls within two types: river-mouth bypass or shoreface bypass. The 'river-mouth bypass' consists of seaward moving currents generated by either ebb-tidal jets or flood-stage jets of a river mouth, generally occurring during a regression (Swift, 1976). The 'shoreface-bypass' results from the erosional retreat of the shoreface during a marine

transgression (Swift, 1976). These two types of bypass represent end members and may have a combined influence during a still-stand of the sea.

Movement of sediment from the nearshore into the shallow-marine environment and possible reworking will be controlled by processes such as intruding oceanic currents, tidal currents, meteorological currents (wind, wave and storm-induced) and density current. Of these processes storm and tidal currents are the most important (Walker, 1979) giving rise to the concept of storm-dominated and tide-dominated shelves. Within these two environments a variety of mechanisms have been proposed for the transport and reworking of sand size material. However, many of these mechanisms will not be capable of transporting coarse sediment (gravel).

This study will discuss both a possible diagenetic sequence for this Viking reservoir and one mechanism by which coarse sediment may be transported into the shallow marine environment.

B. STRATIGRAPHY

The name 'Viking' was first used by Slipper (1917) to denote the gas reservoir sandstone of the Viking-Kinsella field in east-central Alberta (Fig. 1.2). These Viking sandstones were considered to be marine because they overlie the marine Joli Fou Shales and, in turn, are overlain by the marine Lloydminster Shales. The Viking was initially classified as a member of the Colorado Group (Hunt, 1954; Reasoner and Hunt, 1954; Gammell, 1958) but was later upgraded to formation status (Magdich, 1955; Stelck, 1958).

During mid-Cretaceous time the Colorado Sea transgressed the continental deposits of the Upper Mannville Group, with initial deposition of the Joli Fou Shales. The Joli Fou Shales pinch out to the west in the foothills, where the Viking Formation unconformably overlies the non-marine Mannville Group (Fig. 1.3). To the south, the Joli Fou shales become indistinct from the Viking Formation because of an increased silt content within the Joli Fou. Further southward both formations grade into the Bow Island Formation. To the northeast and east, in the vicinity of St. Paul (Township 58, Range 9 W5M),(Fig. 1.2), the Viking Formation thins and finally pinches out (Gammell, 1955). Here the sandstones of the Pelican Formation and a portion of the Paddy member of the Peace River Formation lie at the same biostratigraphic position as the Viking Formation. Other biostratigraphic equivalents of the Viking Formation include the Silt Member of the Ashville Formation of southwest Manitoba, the Muddy Sandstone of Wyoming and the Newcastle Sandstone of Montana and North Dakota (Stelck, 1958, 1975; Glaister, 1959; Rubkin, 1964; Berg and David, 1968) (Fig. 1.3).

Using macro-faunal and micro-faunal evidence from the overlying Lloydminster Shales and the lower Joli Fou Shales, the age of the Viking Formation was established as the mid-upper Albian stage of the Lower Cretaceous (Stelck, 1958, 1975). The underlying Joli Fou shales contain the foraminifera *Haplophragmoides gigas* and the pelecypod *Inoceramus comancheanus* which establishes an age ranging from the uppermost Mid-Albian to the lowest part of the Upper Albian. The overlying Lloydminster Shales contain the foraminifera *Miliamina manitobensis* and stratigraphically higher, *Neogastroplites*. Thus the Viking Formation is estimated to be mid-upper Albian in age, which is in agreement with K-Ar absolute dates calculated by Tizzard (1974). K-Ar dates for biotite and sanidine from bentonites within the Viking Formation range from 94 to 118 ma with an average of 100 $\pm$2 ma.

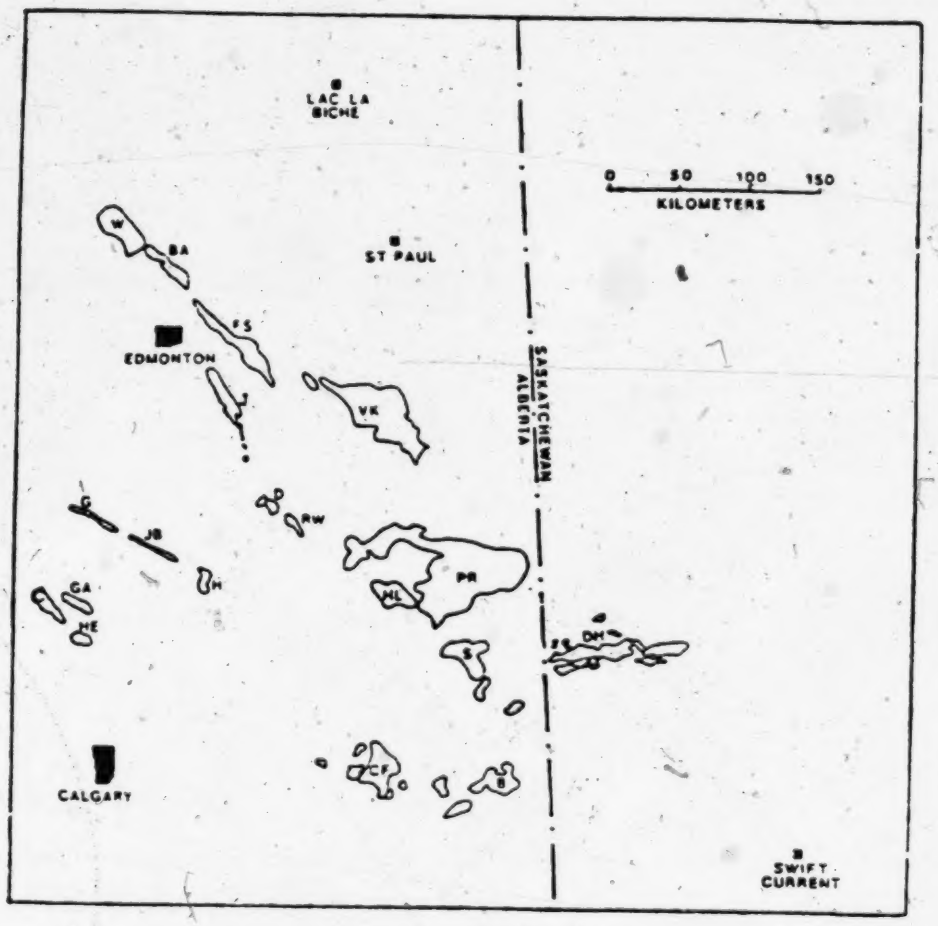

Figure 2.2

Location of some Viking Formation Oil and Gas Fields in Alberta and Saskatchewan. W = Westlock, FS = Fort Saskatchewan, VK = Viking-Kinsella, J = Joarcam, D = Donalda, RW = Red Willow, G = Gilby, JB = Joffre-Bentley, H = Huxley, C = Caroline, GA = Garrington, HE = Harmattan East, PR = Provost, HL = Harrison Lake, S = Sedalia, CF = Cessford, B = Blindloss, DH = Dodslands-Hoosier (after Amajor, 1980).

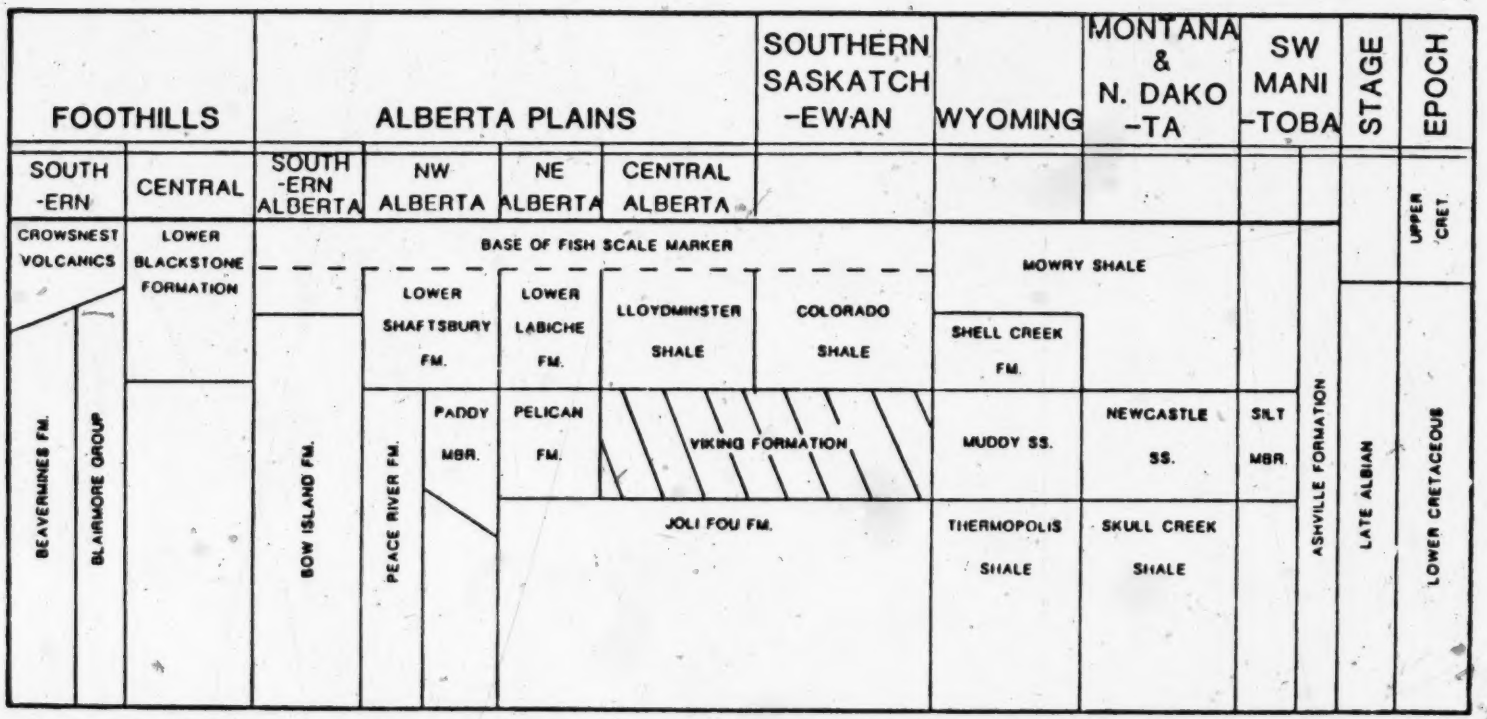

Figure 1.3 STRATIGRAPHIC CORRELATION OF THE VIKING FORMATION IN CENTRAL ALBERTA AND NEIGHBOURING AREAS.

(MODIFIED FROM AMAJOR, 1980)

C. GEOLOGIC HISTORY

Sediments comprising the Cretaceous rocks of the Rocky Mountain foothills and Alberta plains were deposited in an elongate, asymmetrical trough, referred to as the Western Interior Basin. This basin is bounded to the west by the Cordillera and to the east by the PreCambrian Shield (craton). This elongate trough is structurally a foreland basin (Dickinson, 1974) which can be divided into four zones on the basis of water depths, sedimentation accumulation rates, subsidence rates and tectonic stability (Kauffman, 1977). The Harmattan East field occurs within the western foredeep zone, characterized by maximum subsidence and sedimentation. The sediment is generally coarse-grained clastic material derived from tectonically active highlands to the west. The inferred depositional environment within the Viking varies from shallow marine to marginal marine, with an estimated maximum water depth of 30 metres, on the basis of biostratigraphic data (McNeil and Caldwell, 1981).

The foreland basin formed in the late Jurassic by subduction of the oceanic crust beneath the North American craton (Dickinson and Snyder, 1978). Subduction in the deepest western portion of the basin was greatly enhanced by the development of an elongate thrust belt on the western margin of the basin in the Cordillera (Weimer, 1983). Maximum subsidence is best explained by loading of the lithosphere in the adjacent thrust belt (Price, 1973; Beaumont, 1980; Jordon, 1981). Subduction was also enhanced by redistribution of the sediment load after the thrusting events as a result of erosion (Rice, 1980). To the east where marine deposition was taking place, the subsidence has not been clearly demonstrated to be related to the crustal loading by thrust plates; instead it was probably due to compaction associated with sediment loading.

The Columbian orogeny commenced in the late Jurassic and continued to the early late Cretaceous and was characterized by pulses of thrusting (Amajor, 1980). This thrusting affected both the subsidence of the foreland basin and the dispersal of sediment into the basin. With time, the thrust belt and the foreland basin migrated eastward. The early phase of the Nevadan orogeny (late Jurassic) was restricted to the Omineca Geanticline and was a period of intense activity. The Coastal Range orogeny (Aptian-Albian) was widespread, resulting in intense deformation, metamorphism and uplift of the Cordilleran geosyncline. During this period there was also extensive intrusion of granitic masses, accompanied by volcanism (Fig. 1.4). The volcanic centres were concentrated in the northern Rockies (Utah, Montana, British

LEGEND:

- Granitic Batholiths
  - A- Southern Cassiar-Omenica
  - B- South Coast Range
  - C- Nelson
- Volcanic Islands
- Volcanic Deposits
  - ① Crowsnest Volcanics
  - ② Vaughn Bentonite
- Probable location of subduction zone
- Edge of the foothills disturbed belt
- Probable outcrop edge of the PreCambrian Shield
- Spreading direction of the Pacific Plate
- E Edmonton
- C Calgary
- CF Caroline flexure

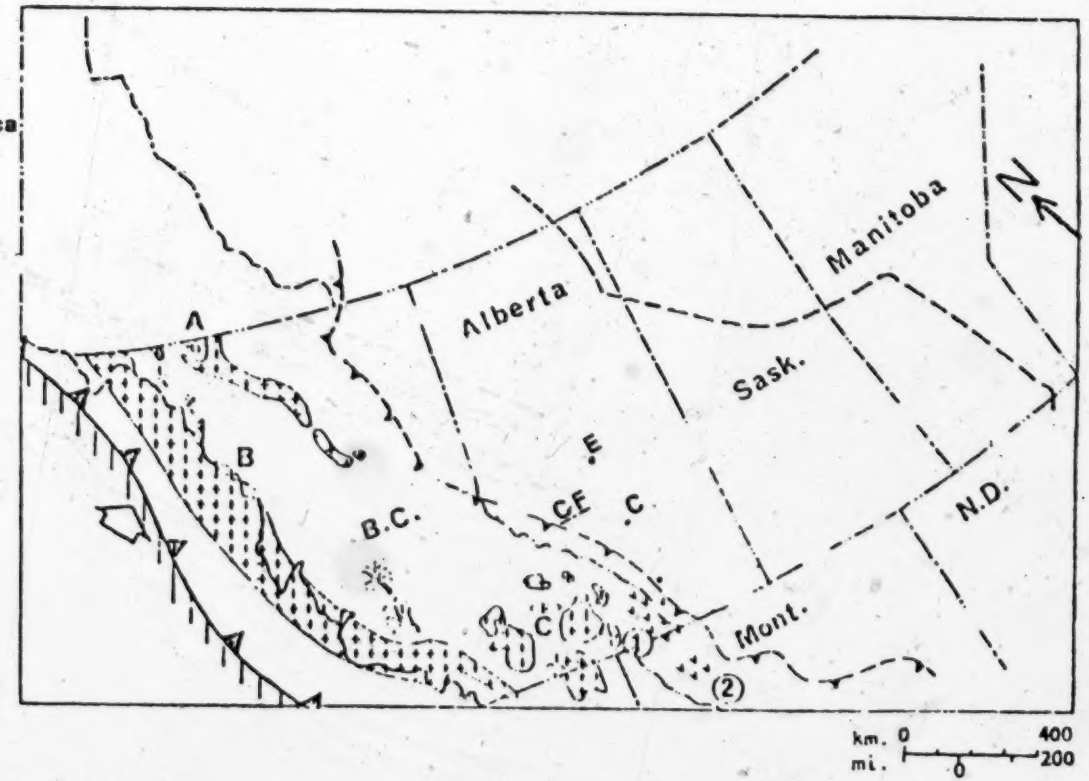

Figure 1.4

Major tectonic elements of the Lower Cretaceous of Western Canada. The location of the Caroline Flexure and Harmattan East Field are shown. Modified from (Wheeler et al.,1972; Douglas et al.,1970; Dickinson, 1971, 1976; Rudkin, 1964; Williams and Stelck, 1975; Eisbacher, 1977; Simpson, 1975; Amoco ,1976).

Columbia and Idaho); peak periods of explosive activity are recorded by the occurrence of widespread bentonite beds. Kauffman (1977) noted a strong correlation between this accelerated volcanic activity and transgressions which he related to plate tectonic activity.

During the late Albian, two major transgressions occurred as the basin was invaded by the southward-advancing Boreal Sea and, to a lesser extent, by the northward-advancing Gulfian Sea. Evidence based on macro-faunal and micro-faunal biostratigraphy suggests that the seas merged at least once during the early late Albian (William and Stelck, 1975) (Fig. 1.5). The Joli Fou Formation of the Albian Skull Creek sequence was deposited during this period when the two seas had merged (Fig. 1.4). By late Albian, a regressive phase resulted in the Mowry Sea becoming landlocked with access only from the north (Fig. 1.6). Within this regressive cycle, during which Viking deposition occurred, a series of small transgressive/regressive phases can be identified. Viking deposition was eventually terminated by the next transgressive cycle which began at approximately the Albian-Cenomanian boundary of the late Cretaceous (Fig. 1.3, 1.7).

The pattern of Cretaceous sedimentation was locally controlled by the structural features within the Mowry Sea. These include the Williston Basin of southern Saskatchewan, the Key River-Hay River Basin of northern British Columbia and the West Alberta Basin in western Alberta (Fig. 1.8). The Western Alberta Basin is bounded to the southeast by the Sweet Grass Arch, to the north by the Peace River Arch and to the west by the West Alberta Arch. The West Alberta Basin was subdivided by the Caroline upwarp and the Meadowlake escarpment (Williams and Stelck, 1975).

Figure 1.5 Map showing early late Albian seas at the time of *Inoceramus comancheanus*.
(after Williams and Stelck, 1975)

Figure 1.6 Map showing extent of the late late Albian sea at the time of *Neogastroplites cornutus*.
(after Williams and Stelck, 1975)

Figure 1.7 Map showing extent of late early Turonian seas at the time of *Watinoceras*. (after Williams and Stelck, 1975)

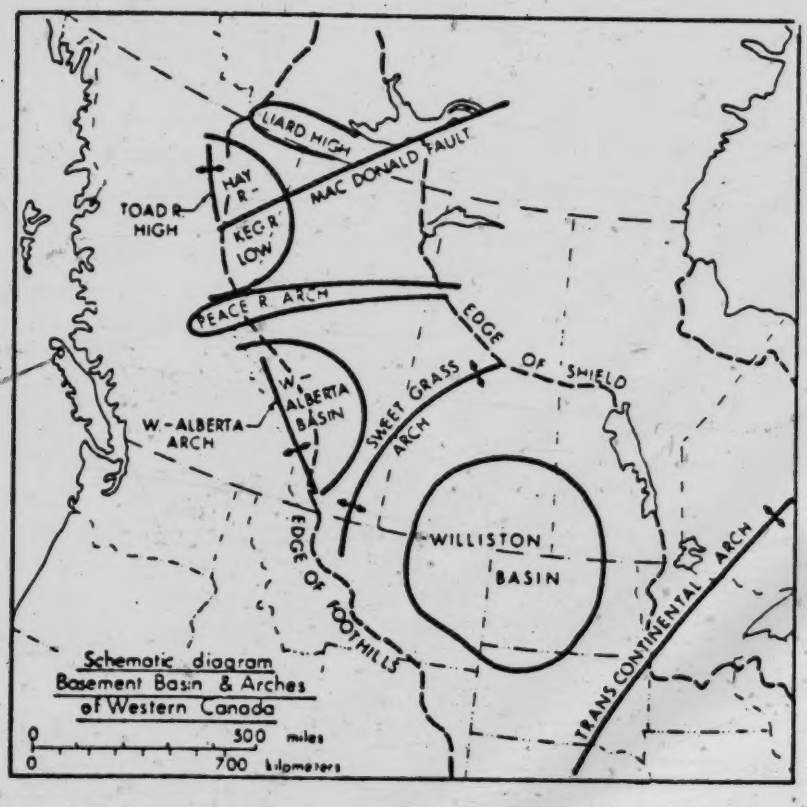

Figure 1.8

Schematic diagram of Precambrian basement features of western Canada. (after Williams and Stelck, 1975).

D. PREVIOUS WORK

Since 1917 when Slipper first used the name 'Viking' to denote a sandstone gas reservoir in south-central Alberta, numerous studies of this formation have been carried out. The generalized subsurface lithostratigraphy was examined by Hume (1933), Nauss (1945), Gammell (1955), Love (1955), Glaister (1958, 1959), Stelck (1958), Tizzard (1974) and Amajor (1977, 1980). The foraminiferal biostratigraphy and paleoecology of this formation were studied by Nauss (1947), Bullock (1950), Bahn (1951), Stansberry (1957), Stelck (1958, 1975) and North and Caldwell (1975). Recently, the research emphasis on the Viking Formation has been concerned with the sedimentary processes which influenced the facies patterns. To date, at least six interpretations have been proposed:

1. regressive and transgressive shoreline deposits,
2. turbidites,
3. beach-barrier islands and offshore bars,
4. deltaic deposits,
5. tidal current ridges, and
6. storm surge deposits.

The regressive-transgressive shoreline concept, proposed by Bullock (1950), interpreted the Viking as the sandstone facies of the early Lloydminster transgression. This concept was further modified by Gammell (1955) who stated that the Viking sandstone of central Alberta was a regressive sand wedge which had been reworked by currents. The idea of current activity was advanced by DeWeil (1956) who inferred that the Viking sediment was transported by longshore currents which operated seaward of the strandline. Glaister (1959), working on the Bow Island Formation of southern Alberta, interpreted the sandstone as a series of minor regressions within a major transgression. More recently the Viking sandstone in the Provost area (Fig. 1.2) was described as a transgressive deposit (Thomas, 1977; Beaumont, 1984).

The idea of turbidity currents as a depositional mechanism for the emplacement of the Viking chert-pebble conglomerate was advanced by Beach (1955, 1956, 1962) and Roessingh (1959). This concept is also supported by paleogeographic reconstructions using bentonites within the Viking Formation. The bentonites were associated with active tectonism and volcanism which generated earthquakes. These earthquakes may have triggered submarine slides resulting in offshore moving slumps and turbidity currents, which transported the coarse

detritus into the shallow offshore-shelf environment.

The Viking sandstone has been interpreted both as offshore bars and shoreline deposits. These sandstones were deposited in the Joli Fou sea (Stelck, 1958). Shelton (1973) interpreted the Viking sandstone at Joffre and Joarcam (Fig. 1.2) to be barrier islands. It was proposed that Joarcam was deposited after Joffre, as the sea regressed to the northeast. Similar interpretations for Viking sandstones have been made by Tizzard (1974), Tizzard and Lerbekmo (1975) and Thomas (1977). These local studies are supported by the regional work of Amajor (1980). Amajor's study of the West Alberta Basin suggests that two distinct sand complexes were present, a northeasterly prograding, regressive meso-tidal barrier island complex, and a southwesterly migrating, offshore tide-dominated sand body. In western Saskatchewan, the Viking sandstone at Township 23, Ranges 20-30 W3M was interpreted as a beach deposit (Jones, 1969). Shoreline deposits were also described in the Viking sandstone by Rice and Gautier (1983). They have interpreted much of the Viking sandstones to have been deposited in an interdeltaic strandplain environment and that the coastal Viking sandstone was derived from reworked deltas.

A lower Viking delta was mapped in the area east of Jasper National Park by the Amoco Canada Petroleum Company Limited (1976). Further to the south, the deltaic systems have been interpreted as wave-dominated (Rice and Gautier, 1983). A well-documented example of a wave-dominated delta has been described in the Upper Cretaceous Eagle Sandstone in north-central Montana (Rice, 1980).

Further offshore in the Western Interior Seaway, various currents emplaced and modified the sediment in the epeiric sea. Thin sandstone units (in southwest Saskatchewan) trend at a high angle relative to the shoreline. These units may have been deposited by eastward flowing tidal currents, forming offshore tidal shoals (Evans, 1970). Tidal currents were also evoked by Amajor (1980) to explain a southward migrating sand ridge.

The idea of storm-induced currents as a mechanism for sand dispersal during Viking time was introduced by Hunt (1954) for the Joseph Lake-Armena-Camrose trend of central Alberta. A similar storm current origin for the Gilby Viking 'B' sandstone (south-central Alberta) was described by Koldijk (1976) and Thomas (1977).

E. METHODS

Core Description

In core, units were identified on a minimum scale of one centimetre. Grain size was recorded using the phi (ø) scale and equivalent metric scale, as defined by the Canstrat charts (Fig. 1.9). The core was examined with careful notation of grain size, sedimentary structures such as ripples, cross-bedding and trough cross-bedding, biogenic structures and the nature of all lithologic contacts. These data were used to produce lithosections (Fig. 1.10). Problems with logging of core occurred where portions of the core were missing, broken or scored by the core barrel.

Facies Definition

The clastic sedimentary rocks have been divided into ten distinct facies (Table 2.1), extending from the Joli Fou Shale at the base of the section to the Lower Colorado Shale at the top. Facies were defined on the basis of lithology, grain size, sedimentary structures, biogenic structures, type of grading and the matrix versus clast-supported nature of the conglomerates.

Correlation of Logs

Correlation between lithologs and geophysical logs (gamma ray, spontaneous potential, shallow resistivity) for the major facies (Table 2.1) shows a high degree of reliability and can be used to predict the location and thickness of the major facies. Lithology, except for conglomerate, was defined by the gamma ray and/or spontaneous potential logs. The geophysical identification of conglomerate units has been accomplished using a combination of gamma-ray and shallow resistivity logs, provided the thickness of the unit is > 0.5 metres. For lesser thicknesses, the characteristic response of the conglomerate is masked by the lithologies bounding it. Care must be exercised as the shallow resistivity log also reacts to variations in the quantity and type of pore fluids.

Sampling

Samples were collected from all lithologies, with special emphasis on the conglomerates and the medium or coarse-grained sandstones located stratigraphically below the conglomerate.

Grain Size Scales

Millimeters	Phi (ϕ)	Wentworth Size Class	
4096	-12		
1024	-10	Boulder (-8 to -12ϕ)	GRAVEL
256	- 8		
		Cobble (-6 to -8ϕ)	
64	- 6		
16	- 4	Pebble (-2 to -6ϕ)	
4	- 2		
3.36	- 1.75		
2.83	- 1.5	Granule	
2.38	- 1.25		
2.00	- 1.0		
1.68	- 0.75		
1.41	- 0.5	Very coarse sand	
1.19	- 0.25		
1.00	0.0		
0.84	0.25		
0.71	0.5	Coarse sand	
0.59	0.75		
1/2 — 0.50	1.0		SAND
0.42	1.25		
0.35	1.5	Medium sand	
0.30	1.75		
1/4 — 0.25	2.0		
0.210	2.25		
0.177	2.5	Fine sand	
0.149	2.75		
1/8 — 0.125	3.0		
0.105	3.25		
0.088	3.5	Very fine sand	
0.074	3.75		
1/16 — 0.0625	4.0		
0.053	4.25		
0.044	4.5	Coarse silt	
0.037	4.75		
1/32 — 0.031	5.0		
1/64 0.0156	6.0	Medium silt	MUD
1/128 0.0078	7.0	Fine silt	
1/256 — 0.0039	8.0	Very fine silt	
0.0020	9.0		
0.00098	10.0	Clay	
0.00049	11.0		
0.00024	12.0		
0.00012	13.0		
0.00006	14.0		

Figure 1.9 **(after FOLK, 1968)**

Figure 1.10 Lithologic Symbols and Sedimentary Structures

These samples were used for grain size analysis, X-ray diffraction (XRD) and scanning electron microscopy (SEM). Porosity and permeability data for core were provided by Canadian Superior Oil Company.

Hydrometer Analysis

The percentage of fine-grained material in each sample was determined using hydrometer analysis. Each sample was disaggregated, care being taken to preserve the original grain size distribution. Grains larger than 2 mm were removed by sieving. A minimum of 20 grams of material from each sample was soaked in 125 ml of a 4% sodium hexametaphosphate solution for 8 hours to further disperse the particles. Ultrasonic disaggregation was used as a final step to ensure thorough dispersion of clay-sized particles. The solution was placed in a graduated cylinder and diluted with distilled water to a total of 1000 ml.

To initiate the analysis, each cylinder was agitated and the dispersed particles then allowed to settle. Hydrometer measurements were taken at 0.25, 0.5, 1.0, 2.0, 5.0, 10.0, 15.0, 30.0, 60.0, 120.0, 240.0, 480.0, and 1440.0 minutes elapsed time for the sample and a control column containing only the Na-hexametaphosphate solution. From these data, the following calculation were performed:

1. The hydrometer readings were corrected for variations in temperature and then subtracted from the control hydrometer readings (which takes into account the density of the Na-hexametaphosphate in solution);
2. The corrected hydrometer readings were converted to values of effective depth using calibrated tables;
3. The maximum particle diameter still in suspension at any time was calculated by multiplying its specific gravity (2.65) by the square root of effective depth divided by time. Particle diameter (d) is expressed in units of phi (phi = $-\log_2 d$);
4. The percentage of material still in suspension at any time was calculated by dividing the corrected hydrometer reading by the mass of the sample before sieving (e.g., the mass of any material greater than 2 mm in diameter is included here).

To calculate the percentage of the various size-fractions in each sample a log-probability graph was constructed using particle size (log scale) and percent sediment (probability scale). A smooth curve was drawn through the points. From this graph the

percentages of material <2 μm, <5 μm and <20 μm were determined.

X-ray Diffraction Analysis

Following hydrometer analysis, the solutions were redispersed and the requisite size-fractions separated at the appropriate time, according to Stoke's Law. To ensure complete separation, the dispersion and settling process was repeated three times for each size-fraction. The size fractions collected were then heated for two days at 60°C to destroy any residual organic matter. The solutions were then thoroughly washed with distilled water using a high speed centrifuge. The <2 μm size fraction was then divided into two portions; one was saturated with Ca^{2+} and the other with K^{+}. All size fractions were freeze-dried and deposited by suction onto a ceramic disc.

X-ray diffractograms for the discs were obtained using the following conditions (Ignasiak et al., 1983):

1. Co K-alpha radiation, with graphite monochromator;
2. 1 degree divergent slit; time constant = 2;
3. 1 degree two theta/minute at 600 mm/h;
4. 50 kV, 20mA.

The following X-ray charts were obtained for the <2 μm material:

1. Ca-disc at 54% relative humidity, 2-40 degrees two-theta;
2. Ca-glycolated, 2-62 degrees two-theta;
3. K-disc at 0% relative humidity, 2-40 degrees two-theta;
4. K-disc at 54% relative humidity, 2-22 degrees two-theta;
5. K-disc at 300°C, 2-28 degrees two-theta;
6. K-disc at 550°C, 2-28 degrees two-theta.

For the 2-5 μm and the 5-20 μm material, X-ray data was obtained for the unsaturated discs at 54% relative humidity. For all samples the appropriate conditions were maintained prior to, and throughout, the X-ray analysis. This combination of procedures permits unambiguous identification of the various clay mineral families present in the samples.

The relative percentage of clay minerals in each size-fraction was determined using Scafe's method (personal communication). For the <2 μm material, the heights of (001)

X-ray diffractions were measured for smectite, illite and kaolinite using XRD charts for the Ca-saturated, ethlyene-glycol treated samples. The (002) or (003) X-ray diffractions (d = 13 Å[2]) were used for mixed-layer clays present in the samples. For chlorite, the height of the (001) X-ray diffraction was determined from the K-saturated, heat-treated (550°C) XRD pattern. For the 2-5 μm and the 5-20 μm size-fractions, all measurements were made using the XRD patterns obtained at 54% relative humidity. To account for the variation in crystallinity of each clay mineral family, form factors were assigned in the following manner:

1. Illite (10 Å) = 1.000;
2. Mixed-layer clay (13 Å) = height of 13 Å peak/2 x height of 10 Å peak;
3. Smectite (17 Å) = height of 17 Å peak/4 x height of 10 Å peak;
4. Chlorite (14 Å) = height of 14 Å peak/3 x height of 10 Å peak;
5. Kaolinite (7 Å) = height of 7 Å peak/2.5 x height of 10 Å peak.

These form factors were summed and the relative percentages calculated for all the phases. For samples containing both chlorite and kaolinite, the kaolinite (001) and the chlorite (002) basal diffractions overlap. Hence, the amount of kaolinite may be overestimated. To correct for this discrepancy, percentage of chlorite (14 Å) is subtracted from the percentage of kaolinite (7 Å); all results are renormalized to 100% and rounded to the nearest 5%.

Scanning Electron Microscopy

A small chip from the center of each sample was mounted on SEM stubs using conductive silver paint. The stubs were sputter-coated with 20 nm[3] of gold to ensure proper grounding during the analysis. The instrument used for the microscopy was the Cambridge Stereoscan S100. Its accelerating voltage was fixed at 25 KV.

The ratio of crystal widths to pore-throat diameters was determined using SEM. *It is important to note that the pore-throat sizes determined in this manner are only an approximation*; other techniques, such as acetate peels and mercury injection, can be used to quantify these estimates.

---

[2]1 Å = 1 X 10^{-10} meters
[3]1 nm = 1 X 10^{-9} meters

Thin Section Analysis

Thin section analysis was performed to determine nature and relative abundance of framework grains in the samples. The thin sections were impregnated with blue epoxy to emphasize porosity. Relative abundances were obtained by point counts (500 counts per thin section). Classification of rocks was based on the types of framework grains present or originally present, prior to diagenesis.

II. SEDIMENTOLOGY

The sedimentology of the Viking Formation within the Harmattan East field is examined in this chapter. This study was designed to determine the sedimentary facies, to define the sediment dispersal mechanisms, to identify the depositional pattern, and to define the major controls on deposition.

The sedimentology is presented in five parts: (1) detailed description of the lithofacies; (2) description of the facies associations; (3) interpretation of the sedimentary structures and depositional origins of the facies; (4) paleogeography and depositional processes, and (5) the depositional pattern within the Harmattan East field.

A. LITHOFACIES

The Viking Formation has been subdivided into 9 facies. An additional facies (Facies 10) represents the marine shales which bound the Viking Formation. These ten facies, along with the subfacies, are described below, and summarized in Table 2.1.

Facies 1. The *Interbedded Shale/ Fine-Grained Sandstone Facies* has two end-members, (A) fine-grained sandstones (2 to 3ø) with argillaceous laminations, in which bedding is horizontal to wavy and bioturbation is minor, and (B) shale beds (1 to 2 cm thick) with fine-grained sandstone lenses, showing lenticular bedding. The shales are black and have varying amounts of coaly or pyritized plant material. Facies 1 units average 1 metre in thickness (range: 0.8 to 1.0 m). Shale rip-up clasts occur are scarce.

Facies 2. *Fine to Very Fine-Grained Sandstone* (2 to 4ø) constitutes the majority of the Viking Formation. This facies is divided into seven subfacies;

Subfacies 2A. The *Structureless, Fine to Very Fine-Grained Sandstone* is massive having no visible sedimentary structures. This subfacies is rarely hydrocarbon stained. Subfacies 2A averages 50 cm in thickness (range: 0.2 to 8 m) and comprises 5-10% of Facies 2.

Subfacies 2B. The *Parallel-Stratified, Fine-Grained Sandstone* is parallel laminated with bedding varying from flat to low-angle wavy and a dip angle ranging from 0°-5°. Localized

sideritized zones and nodules are present. Hydrocarbon staining is rare. Subfacies 2B averages 1.0 m in thickness (range: 0.3 to 1.5 m) and comprises 40-50% of Facies 2.

Subfacies 2C. The *Low-angle (<10°), Cross-Bedded, Fine-Grained Sandstone* occurs in association with Subfacies 2B. Rare occurrences of glauconite have been identified. Subfacies 2C averages 60 cm in thickness (range: 0.4 to 1.2 m) and comprises 20-30% of Facies 2.

Subfacies 2D and 2E. *Trough Cross-stratified* and *Ripple Cross-stratified, Fine to Very Fine-Grained Sandstone* generally overlies subfacies 2B (parallel-laminated fine-grained sandstone). Subfacies 2D and 2E are generally 3 to 5 cm thick (range: 1 to 25 cm) and represent 5-10% of Facies 2.

Subfacies 2F. *Bioturbated, Fine-Grained Sandstone* occurs in beds which are generally 5 to 10 cm in thickness. Subfacies 2F contains well preserved burrows (1 cm diameter) in the western part of the regional study area (DeIure et al., 1984) To the north and east, in the regional study area, subfacies 2F is more abundant and contains a large variety of trace fossils. Subfacies 2F represents 2 to 5% of Facies 2.

Subfacies 2G. *High-angle (>10°), Cross-bedded, Fine to Very-Fine-Grained Sandstone* occurs primarily where high-angle scour surfaces truncate underlying beds. Generally, the dip decreases rapidly to low-angle (<10°) over a thickness interval of 5 or 10 cm. Minor occurrences of glauconite were also observed. Subfacies 2G represents 2 to 5% of Facies 2.

Subfacies 2H. *Convolute Cross-bedded, Fine to Very-Fine-Grained Sandstone* is rare within the study area. Small scale structures include 2-3 cm thick beds with convolute (distorted) laminae. Larger scale structures (50 to 60 cm thick) show overturned lamination and may be associated with underlying ball-and-pillow structures.

Conglomerate facies have been defined based on the following criteria. A conglomerate has greater than 25% of its components >2 mm in diameter. A unit with less than 25% of its components >2 mm in diameter is a pebbly sandstone. Matrix-supported conglomerates have <30% clast contact; clast-supported conglomerates have >30% clast contact.

Facies 3. *Ungraded Matrix-supported, Chert-Pebble Conglomerate.* This facies averages 25 cm in thickness (range: 0.25 to 1.0 m). Where facies 3 approaches its maximum thickness the matrix-supported conglomerate may be interbedded with zones of clast-supported conglomerate. Facies 3 may show hydrocarbon staining.

Subfacies 3A. Structureless, ungraded, matrix-supported conglomerate which is poorly sorted. The matrix is medium or coarse-grained sandstone (0 to 2ø). Subfacies 3A is a predominate component of facies 3, representing approximately 50% of the conglomerate observed.

Subfacies 3B. Horizontally stratified, ungraded matrix-supported conglomerate. Parallel stratified beds will vary between flat and low angle dips. The matrix (medium or coarse-grained sandstone) may show normal grading where the conglomerate has a graded contact with the overlying Lloydminster Shales. This facies rarely occurs within the Harmattan East field.

Subfacies 3C. High angle or trough cross-bedded, matrix-supported conglomerate. High angle cross-bedding is very rare and was not identified within the Harmattan East field, but is observed elsewhere within the regional study area.

Facies 4. *Ungraded, Clast-supported Conglomerate* is generally a structureless, poorly sorted, chert-pebble conglomerate. This facies is generally 20 cm in thickness (range: 5 to 35 cm) and may be hydrocarbon stained.

Subfacies 4A. Structureless, ungraded, clast-supported conglomerate is generally found at the base of a graded conglomerate sequence. This subfacies represents approximately 10% of the conglomerate observed.

Subfacies 4B. Horizontal to low-angle, parallel laminated or stratified clast-supported conglomerate. Dip angle varies between flat and low angle (<10°). Low angle cross-bedding is rare.

Facies 5. *Graded, Matrix-supported Conglomerate* is a common facies. Normally graded beds are dominant. Sorting is poor, with clast size varying from 0.3 to 6 cm. The grading mainly reflects variations in the percentage of matrix, relative to clasts in the conglomerate. The average thickness of Facies 5 is 30 cm (range: 15 to 80 cm). This facies represents approximately 35% of the conglomerate observed.

Facies 6. *Graded, Clast-supported Conglomerate* is rarely seen. Individual normally graded beds average 50 cm in thickness (range: 0.1 to 1.5 m). Inversely graded beds were not identified within the Harmattan East field.

Facies 7. *Mixed Conglomerate/Shale* is common at the top of the section (in contact with the Lower Colorado Shale, Subfacies 10A) and at the base of the section (in contact with bioturbated silty shales, Subfacies 10C in Table 5.1). This mixed lithology is usually structureless with pebbles floating in shale matrix. Facies 7 averages 10 cm in thickness.

Facies 8. *Mixed Sandstone/Shale* facies is characterized by a mixing of sandstone and shale by loading or bioturbation. Internal load or biogenic structures are characteristic. Load structures are commonly well defined ball-and-pillow or flame structures. Bioturbation is indicated by the presence of well preserved burrows. Thick sections of intensively mixed fine-grained sandstone and shale occur in the lower portion of the Viking Formation. The amount of bioturbation and shale increase downsection within the Viking Formation. Mixed fine-grained sandstone/shale units up to 1 metre thick are present within predominantly fine-grained sandstone (Facies 2)

units. Mixed coarse-grained sandstone/shale units are generally restricted to the overlying Lloydminster Shale where the Viking 'A' is often present and can be locally correlated between wells.

Facies 9. *Medium or Coarse and Pebbly Coarse-Grained Sandstone* (1ø to -1ø) commonly occurs within the Upper Viking unit. This sandstone unit may contain low (<10°) to high-angle (>10°) cross-bedding and pebble stringers. This facies generally has good porosity and may be hydrocarbon strained. Beds average 0.1 m in thickness (range: 0.1 to 0.2 m). This facies represents 5% of the Viking Formation.

Facies 10. *Shales* seen in the core are black or dark grey in color. The Lloydminster Shales (Subfacies 10A, Table 2.1) exhibit conchoidal fracture and contain abundant fish scales and minor plant debris. These shales range between 10 and 60 metres thick from the Base of Fish Scales to the top of the Viking Formation. Small lenses of rippled very fine-grained sandstone are commonly interbedded within the shales. Coarse-grained sandstones (Viking 'A' of Facies 8 and 9) are locally abundant.

Shales within the Viking Formation (Subfacies 10B, Table 2.1) average about 20 cm in thickness (range: 0.1 to 4 m). No fish scales are present. These shales often contain coaly and pyritized plant debris. Where this subfacies is thicker than one metre, leaf imprints and twig fragments may be present.

Bioturbated silty shales (Subfacies 10C, Table 2.1) occur at the very base of most sections. This unit is completely homogeneous due to extensive bioturbation. Silty shales are commonly dark grey in colour and have a blocky or massive texture due to the prescence of silt-sized quartz grains. Extensive sideritization of this unit occurs where it is overlain by coarser detritus.

Table 2.1. Summary of Facies

1. Interbedded Shale/Fine Sandstone (average grain size: 2 to 3 ϕ):

   Fine-grained sandstone with argillaceous laminations to shale beds 1 to 2 cm thick with sandstone lenses. Many beds show flaser and lenticular bedding.

   A. Sandstones with argillaceous interlaminae.

   B. Shale beds with fine-grained sandstone lenses.

2. Fine-Grained Sandstone:

   A. Structureless: massive sandstones which exhibit no visible sedimentary structures.

   B. Parallel stratified: stratification varies from flat to slightly wavy.

   C. Low-angle cross-bedded (< 10° dips on cross-laminae).

   D. Trough cross-beds: variable size festoon crossbeds (range 2 to 10cm), usually occurring above horizontally stratified sandstones.

   E. Ripple cross-stratified: formsets of variable size (range 2 to 8cm), commonly occurring above horizontally stratified sandstones.

   F. Bioturbated: primary sedimentary structures destroyed by burrowing activity.

   G. High angle cross-bedded (> 10° dips on cross-laminae).

   H. Convolute cross-stratified.

3. Conglomerate (Ungraded matrix-supported; more than 25% of clasts are > 2mm):

   A. Structureless.

   B. Horizontal stratification: parallel beds, flat to low-angle dip (<10° dips on cross-laminae).

   C. High-angle cross-stratified (> 10° dips on cross-laminae).

4. Conglomerate (Ungraded clast-supported; more than 25% of clasts are > 2mm):

   A. Structureless to disorganized.

   B. Horizontal to low-angle stratified: parallel beds, flat to low-angle dip (< 10° dips on cross-laminae).

   C. Trough cross-bedded.

5. Conglomerate (graded, matrix-supported; more than 25% of clasts are > 2mm):

   A. Structureless with normal grading,

   B. Structureless with inverse grading.

6. Conglomerate (graded, clast-supported; more than 25% of clasts are > 2mm):

   A. Structureless with normal grading,

   B. Structureless with inverse grading.

7. Mixed Conglomerate/Shale:

   A. Structureless,

   B. Burrowed,

   C. Loaded,

8. Mixed Sandstone/Shale:

   A. Structureless,

   B. Burrowed,

   C. Loaded,

9. Medium or Coarse and Pebbly Coarse Sandstone:

   A. Structureless,

   B. High-angle, cross-stratified (> 10° dips on laminae),

   C. Low-angle, cross-stratified (< 10° dips on laminae).

10. Shale:

   A. Black, with conchoidal fracture, fish scales, small lenses of rippled very fine-grained sandstone (Lloydminster Shale),

   B. Black, often with coaly and pyritized plant debris (shales within the Viking Formation).

   C. Dark-grey, bioturbated, mixed with silt, blocky or massive texture (shales at the base of the Viking Formation).

B. FACIES ASSOCIATIONS

The facies described above can be grouped into five facies association:

1. Shale (Lower Colorado Shales): subfacies 10A,
2. Conglomerate: facies 3, 4, 5, 6, 7,
3. Medium or coarse-grained and pebbly coarse-grained sandstone: facies 9,
4. Fine to very fine-grained sandstone: facies 2,
5. Interbedded, fine-grained sandstone and shale: facies 1, 8 and subfacies 10B, 10C.

The lateral continuity of these facies associations within the Harmattan East field are indicated on Figure 2.1.

C. SHELF PROCESSES

The processes which are active in the shallow-marine environment are intruding oceanic currents, tidal currents, meteorological currents (wind, wave, and storm currents) and density currents. The intruding oceanic currents occur well offshore and will not be discussed in detail. Tidal and meterological (storm) currents are the most important processes (Walker, 1979) and have give rise to the concept of tide-dominated and strom-dominated shelves.

Tidal Currents

Tidal currents are always at work, on the continental shelf, and must be considered with other sediment-moving forces (Brenner, 1980). Where tidal currents are great, high-velocity currents constantly rework shelf-bottom sediments. While in areas of low tidal range, low-velocity currents combine with storm-generated currents to move sediment both along the sea bottom and in suspension (Mofjeld,1976).

In the Cretaceous Western Interior Seaway tidal ranges were reconstructed to be approximately 0.86 metres (Slater, 1984). It is questionable whether this tidal range would generate flow velocities adequate to be the primary physical process during Viking deposition. The interpretation of tidal-dominated sandwave complexes (Amajor, 1980) within the Cretaceous seaway, analogous to the North Sea sand ridges, would indicate that tidal currents were active. However, because of the small tidal range, it is suggested that the tidal currents were supplemented by storm currents. These processes may also be responsible for the formation of the Garrington oil field.

Well Locations

	3W5
1.	14-12-32
2.	16-14-32
3.	6-23-32
4.	6-25-32
5.	6-27-32
6.	16-15-32
7.	16-10-32
8.	6-16-32

	4W5
9.	7-24V-32
10.	15-14V-32

Datum: 12 m below Base of Fish Scales

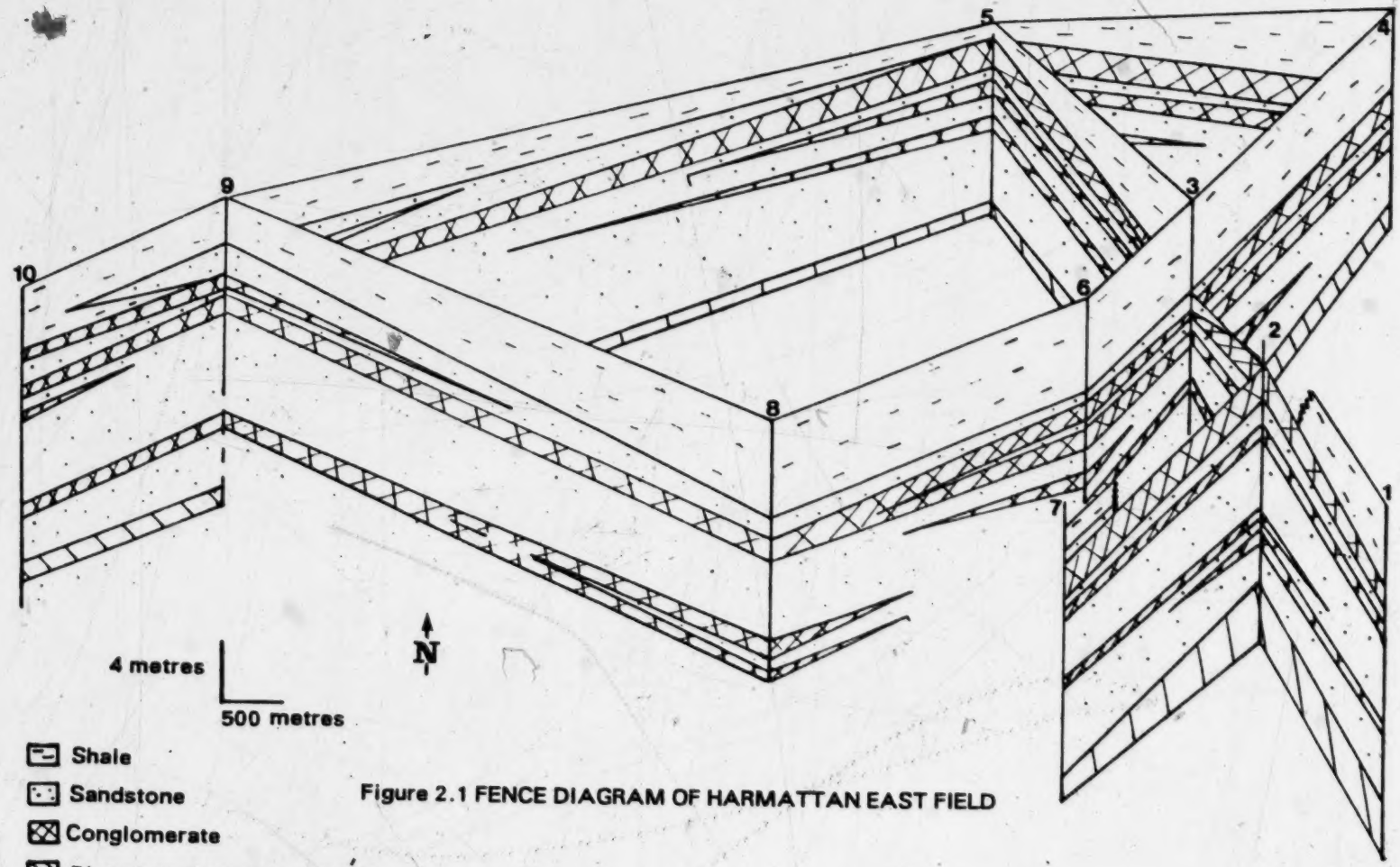

Figure 2.1 FENCE DIAGRAM OF HARMATTAN EAST FIELD

Closer toward shore the low tidal range produces currents which are overshadowed by wave action and storm-induced currents, perhaps characteristic of the Harmattan East field.

Meteorological Currents

A variety of unidirectional currents are generated by meteorological disturbances. These include wave and storm-generated currents, often with an oscillatory wave component. These currents are capable of entraining and and transporting sediment, when in contact with the sea floor (Komar, 1976; Madsen, 1976). The orbital motions tend to be of high-velocity, short duration beneath wave crests and lower-velocity, longer duration beneath troughs (Komar, 1976). These orbital currents produce a pulsating disruptive effect which lifts the sediment into suspension, making it vulnerable to transport by relatively weak unidirectional currents (Kumar, 1976; Madsen, 1976).

In the shoaling water of the nearshore environment waves develop a disharmonic oscillation at the bed surface. This results in the formation of asymmetrical ripples, which are the most common bedform in wave-dominated nearshore environments (de Raaf et al., 1977). The most important diagnostic features of wave ripples are (Boersma, 1970):

1. the degree and directions of ripple asymmetry varies considerably along a train of ripples.
2. form-discordant cross-lamination,
3. internal structure of wave ripples
   a. composed of bundles of laminae,
   b. cross-laminae strongly tangential toward lower set boundary,
   c. angle of repose variable between very flat ($\pm 10^{\circ}$ to steep (45°),
   d. cross-lamination varies within a single ripple,
   e. lower boundary of a wave ripple set is often scooping or undulatory;
4. even lamination of straight, slightly undulatory or low angle types.

Also associated with wave action are rip-currents, which are a unidirectional flow returning water carried landward by waves. The main effect of rip-currents is the removal of resuspended sediment from the breaker zone to the upper shoreface, where it is temporarily stored until transported seaward by bottom currents (Field and Roy, 1984): These rip-currents are not capable of carrying significant amounts of sediment to depths of >45 m unless the flow gives rise to a near-bottom sediment-laden component that is in part driven by gravity (Field

and Roy, 1984).

During Viking deposition storm-generated currents were also believed to be active. These currents represent a large undirectional back-flow of water caused by the set-up during a storm. These currents combined with wave cyclic loading and liquefaction to transport sediment offshore (Clukey et al., 1980; Nelson, 1982). The amount of sediment which is put into suspension will be controlled by the intensity of the wave action. A low intensity storm may produce an 80% increase in suspended sediment load while a hurricane can produce a 400% increase (Drake, 1976). This suspended sediment is transported downslope by storm-generated currents which are also capable of scouring sand size material (Cacchione et al.,1984; Field and Roy, 1984).

These unidirectional currents may produce a graded deposit which mimics the classic Bouma Ta-e sequence (Bouma, 1962) of a turbidity current (Kreisa, 1981; Nelson, 1982). Therefore, Nelson (1982) suggested that generation of a density current is not necessary to produce a turbidite-like deposits over a shallow shelf (Nelson, 1982). These shallow-water graded layers may be distinguished from similar deep water turbidites by the predominance of trough cross-stratification, in the proximal part of the system, the dominance of plant debris, the gradation to common shallow marine fossils, bioturbation and the storm lag layers in distal areas (Nelson, 1982). Diagnostic features of such storm surge ebb-current deposits include (Kreisa, 1980):

1. sharp bases and burrowed or diffuse upper contacts,
2. couplets of shell or gravel lag and laminated sand or silt,
3. weakly graded and often laminated sands and silts,
4. escape burrows,
5. decrease in thickness and abundance of sand and silt layers away from shore,
6. lamination is generally horizontal but 'gentle discordances' are common.

As the storms which initiate these currents may result in an 80-400% increase in suspended sediment load it is questionable whether the flow will give rise to a near-bottom sediment-laden component that is in part driven by gravity. For this reason it is difficult to distinguish between sediment deposited from storm-induced unidirectional currents and storm-induced gravity flows.

In the shallow-marine environment sediment may also be transported by density currents, which are the result of rapid sediment accumulation, catastrophic events or storm activity. These processes may generate slumps, slides or sediment-gravity flows. Of these mechanisms sediment-gravity flows will be most important as they do not require steep slopes, rapid sediment accumulation or catastrophic events to occur. Storm-induced sediment-gravity flows have been described by Hayes (1967) and Hamblin and Walker (1979). The erosional basal contact and the fining-upward sequence suggests transport as either a debris flow or by a turbidity current. Debris flows are typically sluggish, consisting of granular solids 'floating' in a clay-water matrix (Curray, 1966). In contrast, turbidity currents move rapidly and may have either high or low sediment concentrations, depositing conglomerate and sandstone or classical turbidites, respectively. These turbidity currents will have a sharp base and a fining-upward sequence, characteristic of initial high energy flow, decreasing vertically.

These storm-generated currents may have combined with tidal currents to form the dominant process in the deposition of the offshore Cretaceous Viking sand bodies (Brenner, 1978; Amajor, 1980). The Cretaceous sand bodies are composed of sand ridges tens of kilometers long, less than 3 kilometers wide and having crests approximately 10 metres above the adjacent swale. These sand ridges are spaced 2 to 5 kilometres apart and may be linear, or comma shaped. They are generally subparallel and trend either diagonally across the shelf or perpendicular to the coast (Brenner, 1978; Amajor, 1980).

D. FACIES INTERPRETATION

Using the sedimentary structures observed in core, the facies can be interpreted with respect to depositional processes. These facies are discussed in order, beginning at the base of the section.

Facies 8 is a bioturbated very fine to fine-grained sandstone and shale (Fig. 2.2a) which shows an increase in primary sedimentary structures over biogenic structures upsection. Burrows are the dominant sedimentary structures, representing 50-70% of the facies. This amount of sediment reworking by burrowing organisms implies a relatively low energy environment. Deposition is interpreted to have occurred near the base of the transitional zone, which lies between the offshore and nearshore environments (Fig. 2.3). The transitional zone is a low energy environment in which both shelf and basinal depositional processes occur (Reinson, 1979). In general this zone is characterized by fine-grained or silty fine-grained sandstone and a change from biogenic structures to primary physical sedimentary structures upsection. The physical sedimentary structures are preserved as laminated to burrowed beds, wave-rippled bedding and parallel lamination (Howard and Reineck, 1981).

Near the base of Facies 8 thin low-angle parallel laminated to ripple cross-bedded fine-grained sandstone units occur (Bouma Tb-c divisions, Bouma, 1962). This sequence is generally capped by low-angle parallel laminated sandstone and shale (Bouma Td-e divisions, Bouma, 1962). These sandstones are interpreted as pulses of higher energy which periodically intrude into the transitional and offshore environments (Fig. 2.4). A possible modern analogue for these sandstones has been described by Nelson (1982) on the Bering Shelf.

Nelson (1982) examined modern shallow-water graded sand layers which were produced by storm surges on the Bering Shelf. He observed that the proximal graded sand beds mimic a Bouma Ta-e turbidite sequence. Nelson's (1982) idealized vertical sequence of sedimentary structures include a basal parallel laminated medium to fine-grained sand (Sb), cross and convoluted lamination (Sc), upper parallel-laminated very fine-grained sand to coarse silt (Sd), and mud cap (Se). The upper parallel-laminated sand (Sd) commonly contained laminated beds of epiclastic plant fragments. Nelson (1982) also observed that the nearshore graded sand layers have the lower parallel-lamination (Sb) but lack the distal sand layers.

Figure 2.2 Fine-grained Sandstone Facies

A. Photograph of core showing Facies 8; bioturbated very fine-grained sandstone and shale. Well 14-14-32 3W5, 2222.9 m.

B. Photograph of core showing Facies 1; interbedded fine-grained sandstone and shale. Well 8-12-32 3W5, 2207.6 m.

C. Photograph of core showing subfacies 2C and 2D; low-angle ($< 10°$) cross-bedded fine-grained sandstone and trough cross-stratified fine-grained sandstone. Note trough cross-stratification (TR) and cross-bedding (X-B). Well 6-25-32 3W5, 2190.9 m.

D. Photograph of core showing subfacies 2C; low-angle ($< 10°$) cross-bedded fine-grained sandstone. Note scour contacts and the truncation of lower beds as indicated by arrows. Well 14-18-32 2W5, 2176.6 m.

All core is 10.2 cm (4.0 in) in diameter.

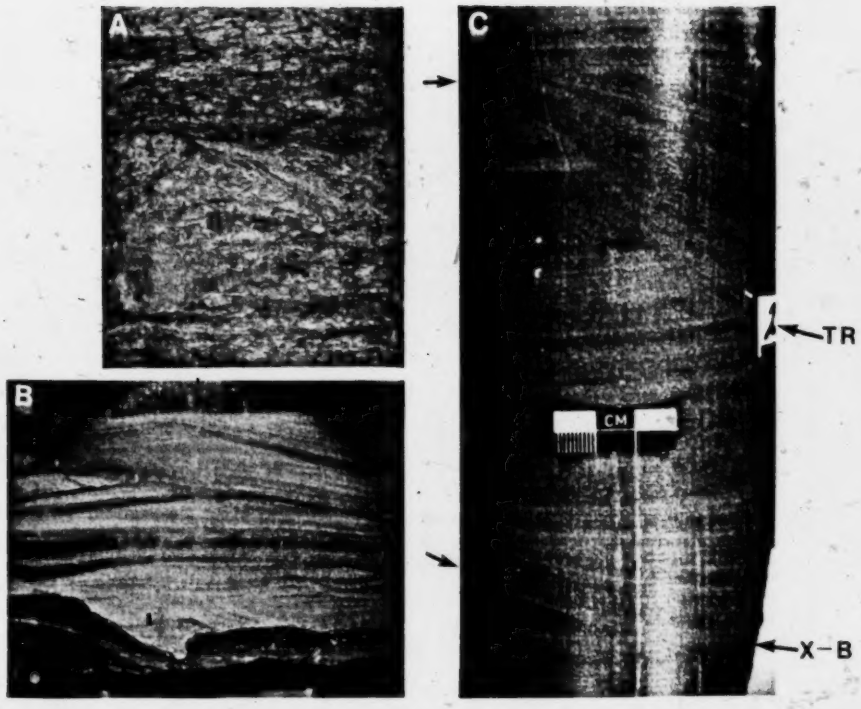
A
B
C
TR
CM
X-B

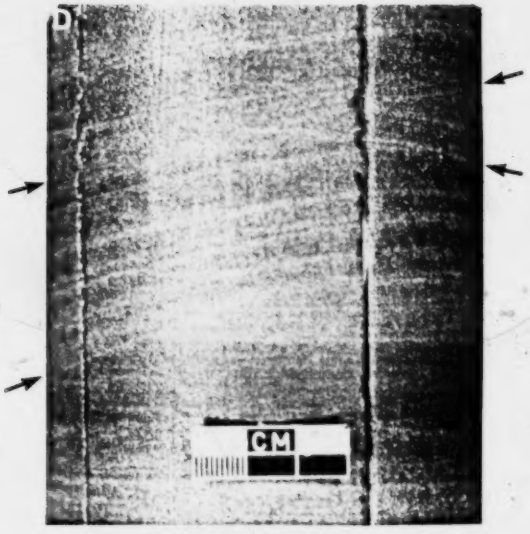
D
CM

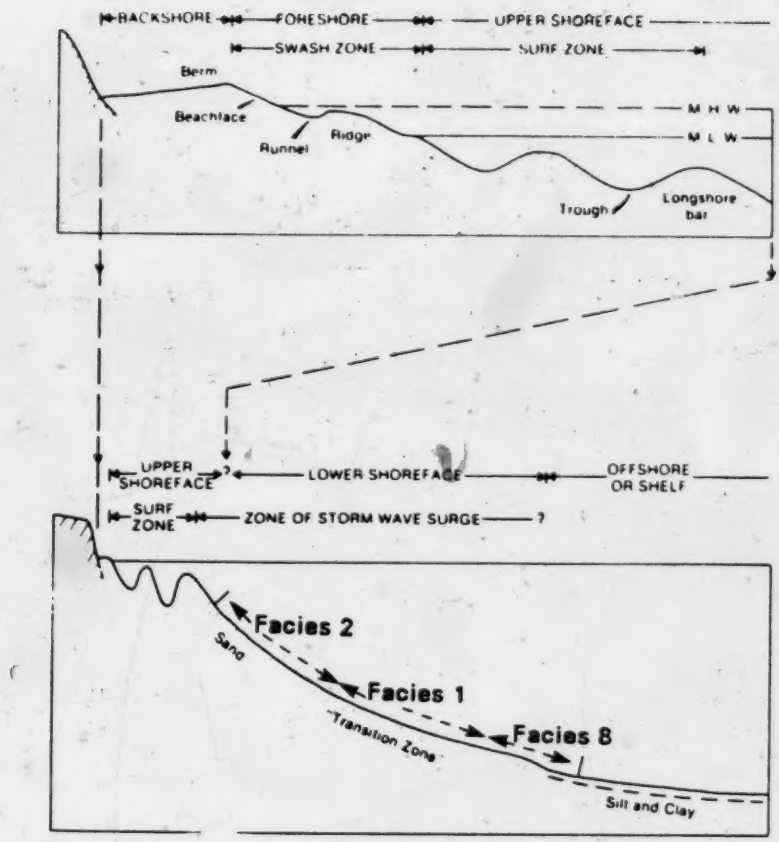

Figure 2.3—Generalized beach-to-offshore profiles showing terminology applied to principal morphological features and zones.

(after D.G. McCubbin, 1982)

Figure 2.4 Storm Deposit

A. Photograph showing storm deposit which has intruded into the base of the lower shoreface environment. Note lower parallel-lamination (Sb), cross-lamination (Sc), upper parallel-lamination (Sd) and mud cap (Se).
Well 8-17-32 2W5, 2116.9 m.

B. Photograph showing storm deposit which has intruded into lower shoreface environment. Note lack of lower parallel-lamination. Cross-lamination (Sc), poorly defined upper parallel-lamination (Sd) and mud cap (Se). Lack of lower parallel-lamination suggest deposition occurred further from the source than photograph 2.4A. This is the result of shoaling water depths.
Well 16-22-32 3W5, 2222.5 m.

All core is 10.2 cm (4.0 in) in diameter.

A
Se
Sd
Sc
CM
Sb

B
Se
Sd
Sc

Nelson's (1982) model for the formation of graded sand layers in a shallow water environment is in agreement with Kreisa (1981). These models suggest that the storm-induced deposit will have a sharp base, horizontal laminations, poor grading and a decreased thickness away from shore. These seaward-flowing currents are driven by storm surge ebb-currents (Nelson, 1982).

The lack of evidence of reworking within these sandstones suggests that deposition began below fairweather wave base, in the offshore shelf or base of the transition zone. Moving upsection, it is difficult to identify storm layers because of extensive reworking by marine currents above fairweather wave base.

Facies 1 is an interbedded fine-grained sandstone and shale (Fig. 2.2b). The sandstone is generally laminated with less common wave ripples (Fig. 2.2b). Bioturbation occurs both within the shale and at the upper contacts between the sandstone and shale. Facies 1 is interpreted to have been deposited in the middle portion of the transitional zone (Fig. 2.3). The laminated sandstones within the bioturbated unit indicate fluctuations between biogenic activity and sediment deposition. Deposition occurs above fairweather wave base and is interpreted to have resulted from unidirectional flows, probably wave-induced.

Facies 2 is a very fine to fine-grained sandstone which has an abundance of cross-bedding. This sandstone is interpreted as having been deposited near the top of the lower shoreface environment (Fig. 2.3) The predominance of sandstone versus shale, the abundance of cross-bedding and the absence of bioturbation suggest a shallow-water high energy environment. The low-angle cross-stratification and trough cross-stratification indicate that the current strength was sufficient for tractional transport of the fine-grained sandstone (Fig. 2.2c,d). The planar lamination which is associated with the cross-stratification is interpreted as having formed under high flow conditions. These conditions are the result of unidirectional flow, possibly wave-surge. As the flow strength decreased, climbing ripples were formed, eventually maturing into small scale trough cross-stratification. This sequence of sedimentary structures indicates a decreasing flow strength and sedimentation rate. Thin shale partings, which are less commonly found within the parallel-laminated sandstone, suggest that this sequence was not deposited as one unit.

Facies 3, 4 and 5 are chert-pebble conglomerates which are interpreted as having been transported as storm-induced sediment gravity flows, a process described by Hayes (1967) and

Hamblin and Walker (1979). The sharp contact at the base and the large clast size suggests that the conglomerate was not deposited as a continuous sequence with the underlying fine-grained sandstone (Facies 2).

Facies 3 is an ungraded, matrix-supported, chert-pebble conglomerate (Fig. 2.5a). The lack of grading is the result of the amalgamation of a series of sediment gravity flows. The basal surface of each of the gravity flows erodes into the underlying storm deposit. This results in the amalgamation of the beds into one thick, ungraded, matrix-supported conglomerate.

Facies 4 (Fig. 2.5b) is an ungraded, clast-supported, chert-pebble conglomerate which occurs along the sides of a trough within this field. Facies 4 represents deposition from a flow with a lower concentration of fines than those which formed Facies 3.

Facies 5 (Fig. 2.5c) is a graded, matrix-supported, chert-pebble conglomerate. The beds are matrix-supported at the base and grade upward into a medium or coarse-grained pebbly sandstone, with better sorting. The sandstone may be massive or show vague parallel-stratification. This sequence is similar to the graded and graded stratified conglomerate/pebbly sandstone seen in most deep water marine sequences (Walker, 1975; Hein, 1984). These sequences are generally associated with large scale turbidity currents and/or basal dispersions. This would support the interpretation of a sediment-gravity-flow origin for these conglomerates.

Facies 9 is a medium or coarse-grained and pebbly coarse-grained sandstone which is interpreted has having been deposited by a high energy flow, possibly storm-induced. This sandstone lies below the conglomerate and may be massive (subfacies 9A) or low-angle cross-stratified (Subfacies 9C). The low-angle cross-stratification would indicate that fairweather conditions were not capable of reworking this sandstone. The massive sandstone, which is generally clean and well sorted, is also interpreted as having been deposited by a high energy flow. This is indicated by the concentration of pebbles and mudstone clasts above the sharp contact with the fine-grained sandstone (Fig. 2.5e). This sandstone was deposited by pulses of high energy as indicated by thin shale partings and minor amounts of bioturbation which have been identified within this unit. The high-angle cross-stratified sandstone (Subfacies 9B) is restricted to the trough within this field and generally occurs within the conglomerate unit (Fig. 2.5b,d). The high-angle cross-stratification is interpreted to have been deposited by storm currents and later reworked by wave-induced rip-currents and storm -

Figure 2.5 Conglomerate and Coarse-grained Sandstone Facies

A. Photograph of core showing subfacies 3A; structureless, matrix-supported conglomerate.
Well 6-25-32 3W5, 2187.8 m.

B. Photograph of core showing subfacies 4A; structureless, clast-supported conglomerate. Note scour contact with subfacies 9B (high-angle cross-bedding ($>$ 10° dip) indicated by arrows.
Well 8-12-32 3W5, 2192.0 m.

C. Photograph of core showing subfacies 5A; normally graded, matrix-supported conglomerate. Normal grading is indicated by arrows. This photograph also shows subfacies 3C, high-angle, cross-bedded, matrix-supported conglomerate indicated by arrows.
Well 15-14V-32 4W5, 2353.8 m.

D. Photograph of core showing subfacies 9B; high-angle, cross-bedded ($>$ 10° dip on laminae) medium or coarse-grained pebbly sandstone. Note high-angle cross-bedding indicated by arrows.
Well 14-18-32 2W5, 2171.0 m.

E. Photograph of core showing erosional contact between subfacies 9A and subfacies 2B. Note scour contact, pebble concentration at contact and shale clasts indicated by arrows.
Well 14-24-32 3W5, 2197.2 m.

All core is 10.2 cm (4.0 in) in diameter.

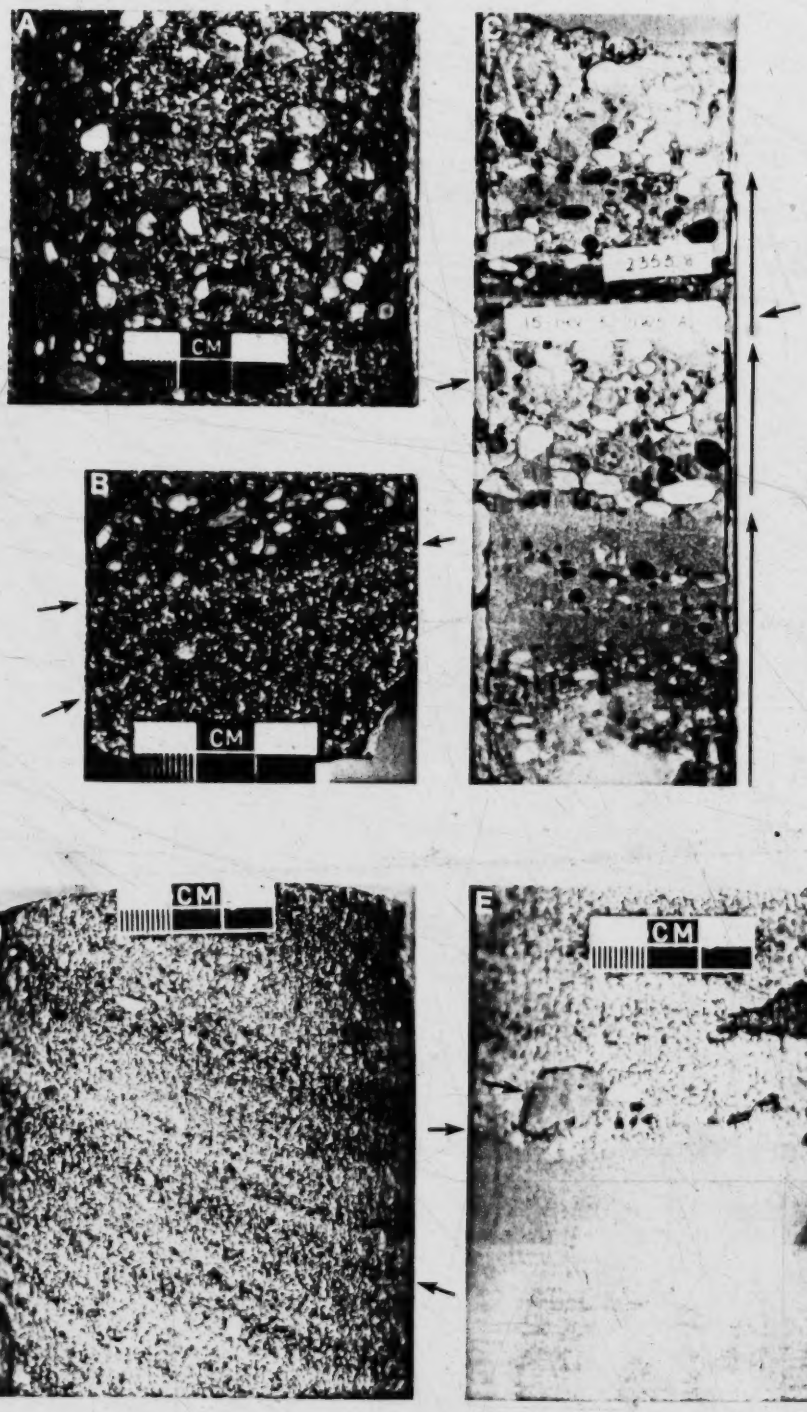
A
CM
B
CM
C
D
CM
E
CM

surge-ebb currents, a processes described by Cacchione et al., 1984. These higher velocity currents are directed along a trough, allowing for tractional transport of the sand, and the formation of large-scale two-dimensional ripples.

Facies 10 is a marine shale which bounds the Viking Formation. These shales represent deposition of mud and silt from suspension in a low energy environment. The sediment is confined to mud and silt.

E. PALEOGEOGRAPHY

The Viking Formation within the Harmattan East field is a coarsening-upward clastic sequence, deposited in a storm-dominated, shallow-marine environment. The storm influence is indicated by:

1. a sharp base with a burrowed or diffuse upper contact,
2. couplets of conglomerate lag and laminated sandstone,
3. laminated and poorly graded sandstone,
4. laminated sandstone containing escape-traces,
5. a decrease in the thickness of the sandstone layers away from shore,
6. horizontal or gentle discordant lamination, and
7. graded sand layers containing:
    a. trough cross-lamination,
    b. abundant laminated plant debris,
    c. high quantity of starved ripples,
    d. shallow marine fossils and
    e. increased bioturbation distally.

As the shoreline (Fig. 2.6) prograded to the northeast the fine-grained sandstone was deposited as two units which were separated by a thin chert-pebble conglomerate (Fig. 2.7). The sharp contact at the base of this conglomerate indicates deposition under high energy conditions and that the sandstone and conglomerate are not a continuous sequence. The depositional environment grades from the transitional to the nearshore, as the water depth shoals.

The rooted zone to the southwest has been identified as both a shoreline (Delure et al., 1984) and a barrier island complex (Amajor, 1980) (Fig. 2.6). This rooted zone does not occur within the Harmattan East field. However, it is proposed that the thin conglomerate, which separates the two fine-grained sandstones, is stratigraphically equivalent to the rooted zone (Fig. 2.8). This implies that the upper fine-grained sandstone (Fig. 2,7) represents a second sand body which prograded seaward of the rooted zone (shoreline). This depositional pattern would account for the shoaling water depths within the Harmattan East field. The depositional environment of the lower fine-grained sandstone is interpreted to have extended from the offshore to the transitional environment (Fig. 2.3). The upper fine-grained sandstone is

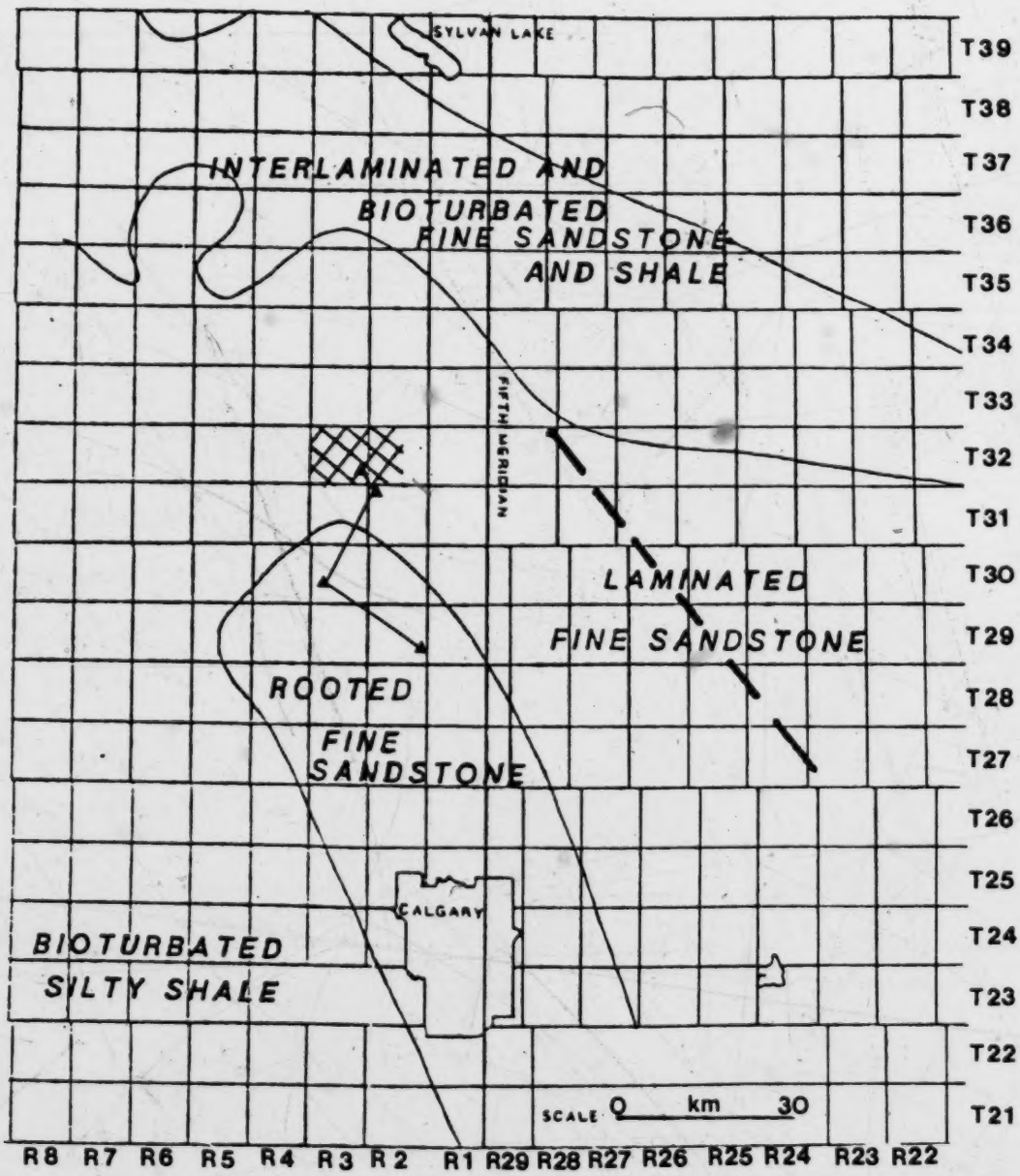

Figure 2.6 Lithofacies at the top of the clastic wedge.

----shelf break inferred from bentonite beds (after Amajor, 1980)

Harmattan East

location of cross-section (Fig. 2.8)

(from Delure et al., 1984)

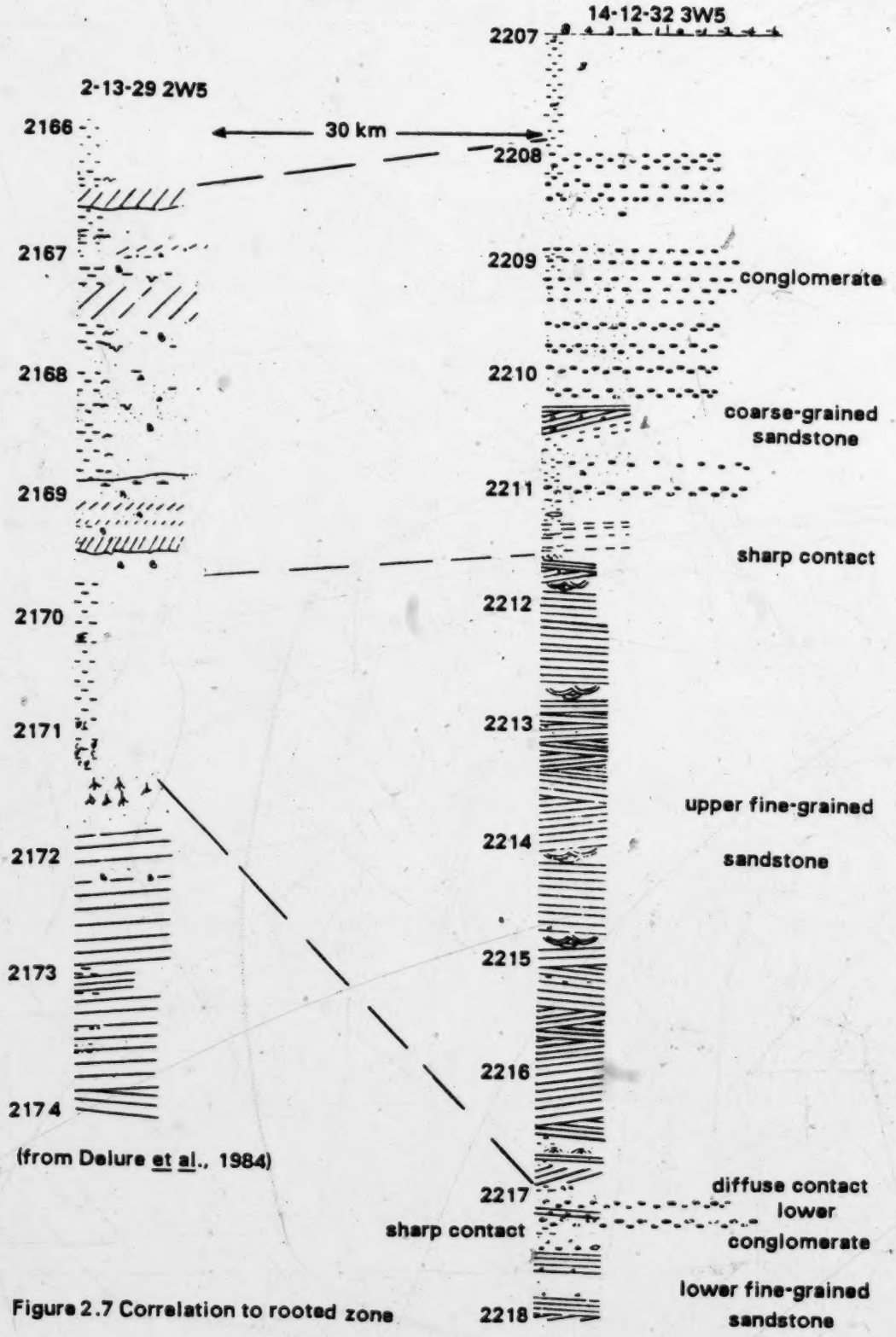

(from Delure et al., 1984)

Figure 2.7 Correlation to rooted zone

14-12-32 3W5

11-31-31 2W5

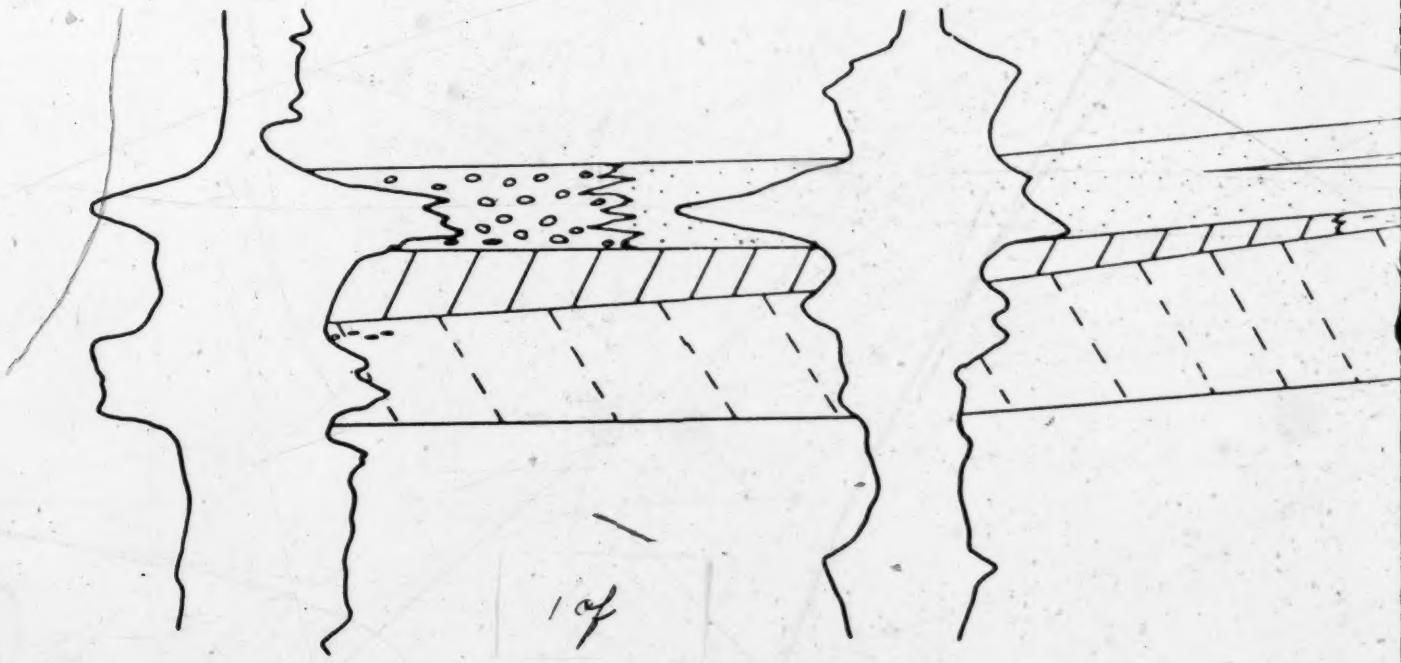

LEGEND

C coal

shale

rooted zone

conglomerate

coarse-grained sandstone

//// upper fine-grained sandstone

lower fine-grained sandstone

Datum: Base of Fish Scales

5 metres

location of cross-section on Figure 2.6

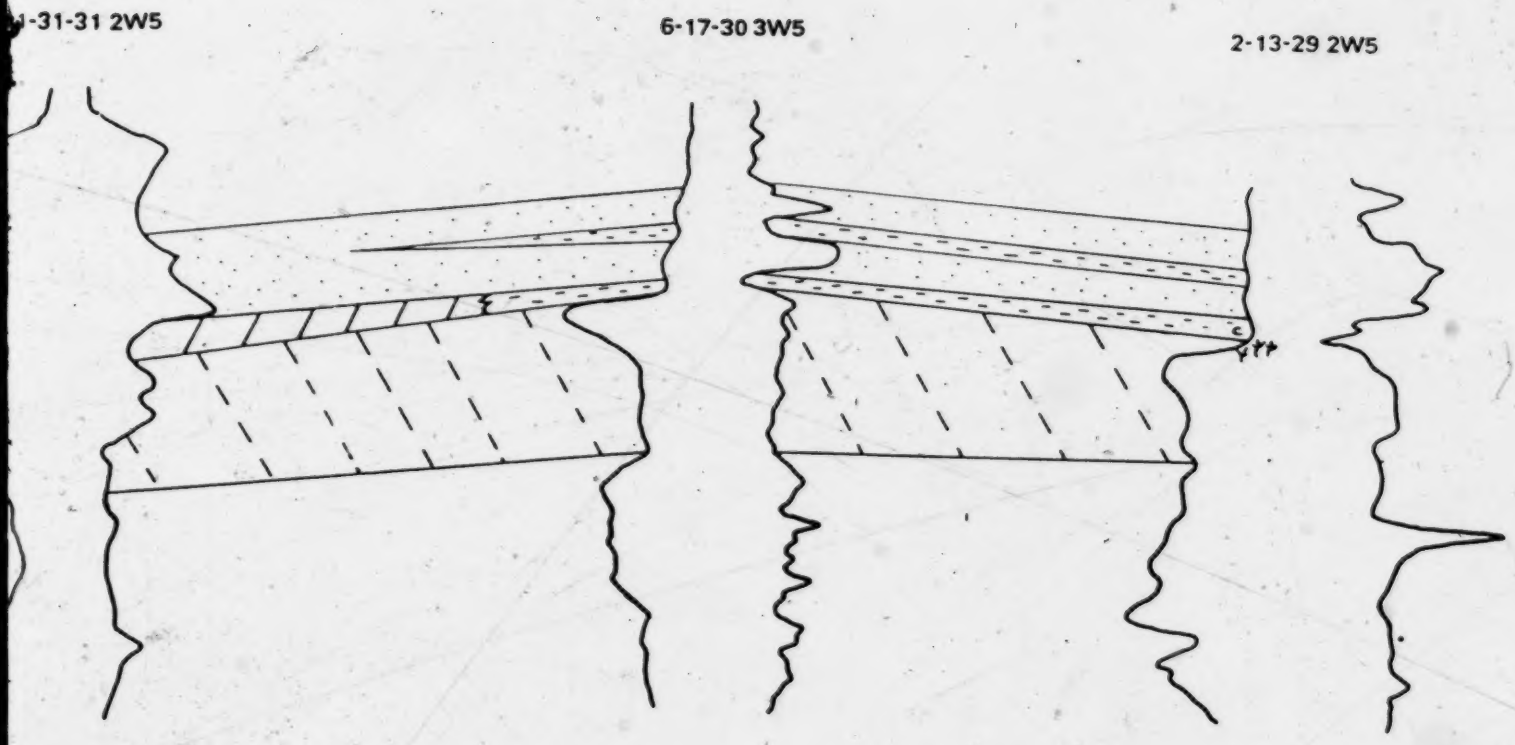

cales

2 of 2

Figure 2.8 Cross-section (north-south) from Harmattan East to rooted fine-grained sandstone

on on Figure 2.6

interpreted to have extended from the transitional zone into the nearshore environment (as discussed previously).

The medium or coarse-grained sandstone has a sharp contact with the underlying fine-grained sandstone (Fig. 2.5e). This would suggest that the medium or coarse-grained sandstone was deposited from a high energy flow and was not deposited as one continuous sequence with the underlying fine-grained sandstone. Overlying the medium or coarse-grained sandstone is a chert-pebble conglomerate. This conglomerate is interpreted as having been deposited by a series of sediment gravity flows (as discussed previously). The medium or coarse-grained sandstone and the conglomerate do not constitute one gradational sequence or continum of deposition. Because of a significant break between these units it is difficult to infer a depositional setting. It is suggested that the conglomerate was deposited near the base of the lower shoreface or in the offshore (inner shelf) environment.

Regionally, the lithologic units described above, correlate to the upper western sand complex of Amajor (1980) (Fig. 2.9). The two fine-grained sandstones within the Harmattan East field correlate to Amajor's upper west 1 and 2 units, respectively. The medium or coarse-grained sandstone and conglomerate correlate to the upper west 3 unit. This unit was bound by two bentonites which are believed to occur within the Harmattan East field (Fig. 2.10). Thus the conglomerate and medium or coarse-grained sandstone, of Harmattan East, can be correlated to four (4) thin coarsening-upward sequences located at Township 27, Range 21W4M. These four coarsening upward sequences may represent the distal portion of major storm events.

CORRELATION OF LITHOLOG TO GEOPHYSICAL LOG

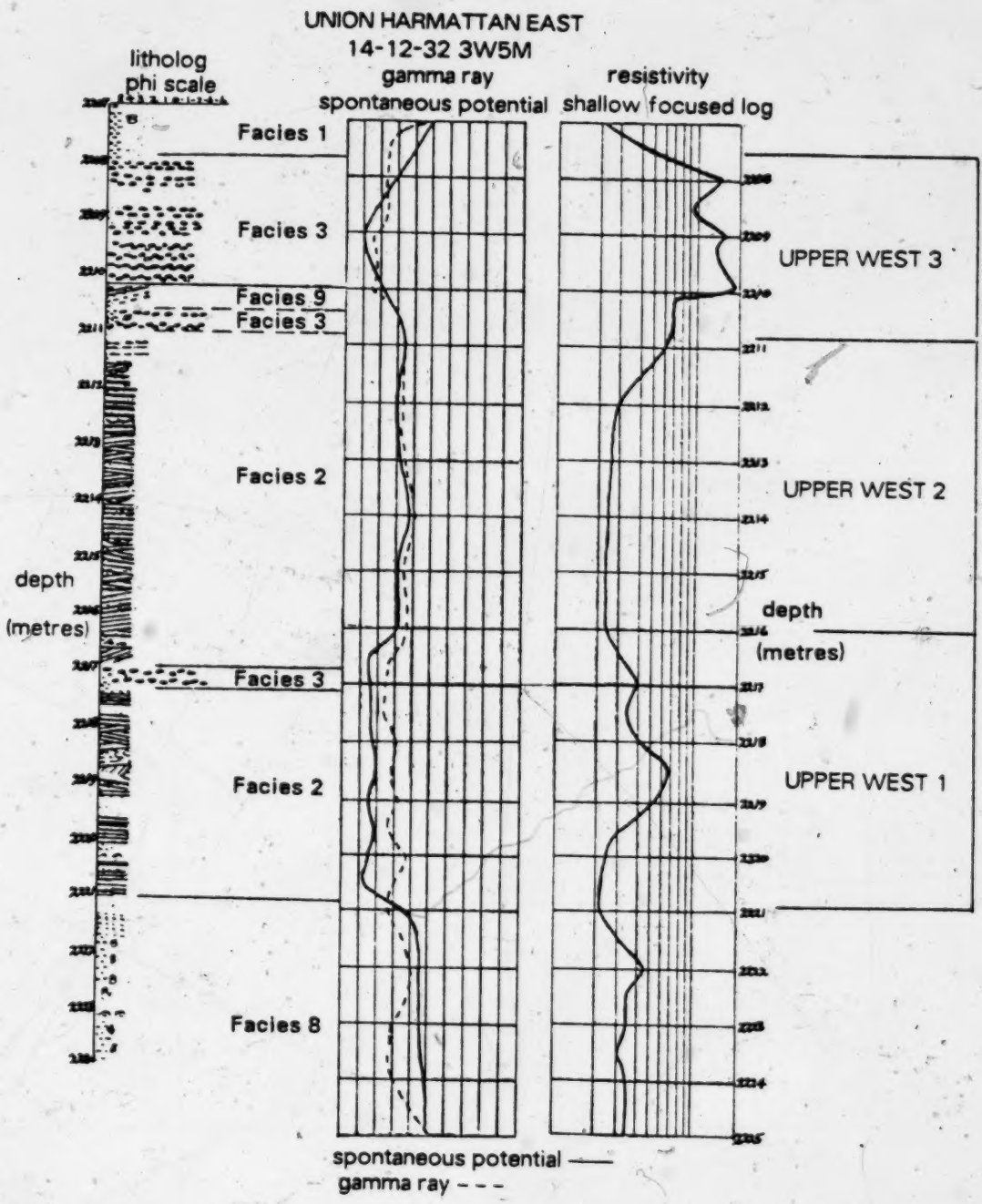

Figure 2.9

Correlation of Harmattan East Viking Section with Upper Western Complex

(after Amajor, 1980)

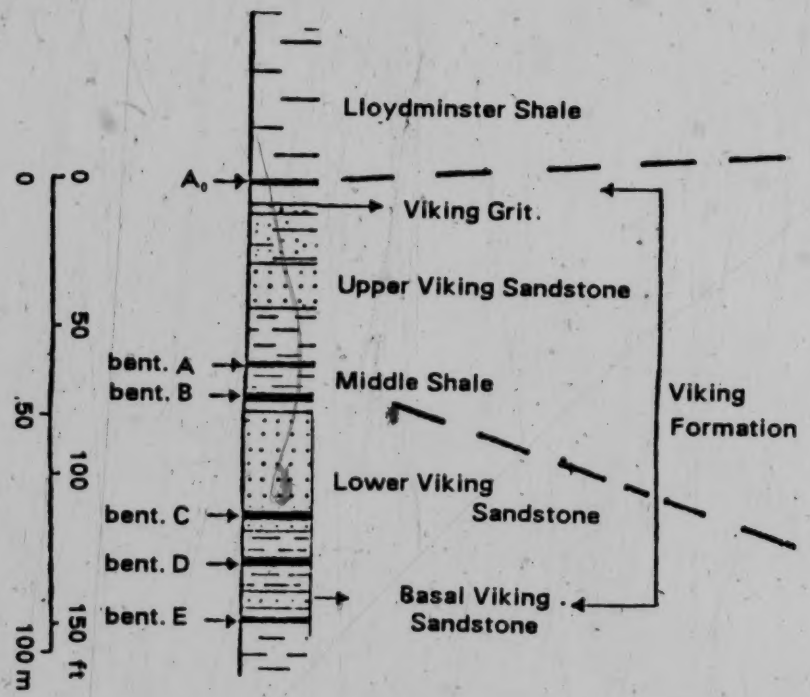

Generalized Viking section east-central Alberta

(after Amajor, 1980)

Thin Viking section Haramattan

East south-central Alberta

Figure 2.10 Bentonite Correlation

F. DEPOSITIONAL PROCESSES

The Harmattan East field can be divided into three major lithologic units: fine-grained sandstone, medium or coarse-grained sandstone and chert-pebble conglomerate (Fig. 2.11). The fine-grained sandstone unit represents the thickest portion of the Viking Formation (up to 20 metres). The actual thickness of this unit is difficult to establish as the lower contact grades into the underlying Joli Fou Shales.

Fine-grained sandstone

Deposition occurred in a still-stand of the Haplophragmoides gigas- Inoceramus comacheanus tidal sea (Stelck, 1975), as part of the northeasterly prograding shoreline. Initial deposition began in the offshore environment and graded upward into the transitional zone. This fine-grained sandstone, which is predominately low-angle cross-stratified (subfacies 2C), was deposited by unidirectional currents, probably wave-induced. Deposition began below fairweather wave base where the slow rate of sand accumulation allowed mixing of the sand and muddy substrate through bioturbation. Less commonly, storm activity provides pulses of clean sand which mimic a Bouma Ta-e sequence (Fig. 2.12). These sands are moved seaward by storm surge-ebb currents. With continued shoaling sand deposition moves into the transitional zone, where currents produced by the wave action have sufficient strength for tractional transport of the sand. Deposition occurred above fairweather wave-base.

Medium or coarse-grained sandstone

The medium or coarse-grained sandstone was transported downslope by unidirectional wave and storm currents. The sharp erosional contact at the base of this sandstone indicates that initial deposition was from a high energy flow (Fig. 2.5e). These periods of higher energy are indicated by scour surfaces which are associated with pebble stringers. Deposition occurred in a moderate to low energy environment as indicated by the presence of shale partings and minor bioturbation.

The abrupt change in grain size between the medium or coarse-grained sandstone and the underlying fine-grained sandstone suggests either a change in sediment input or flow velocities. The high-angle cross-stratified sandstones (subfacies 9B) represent storm deposits

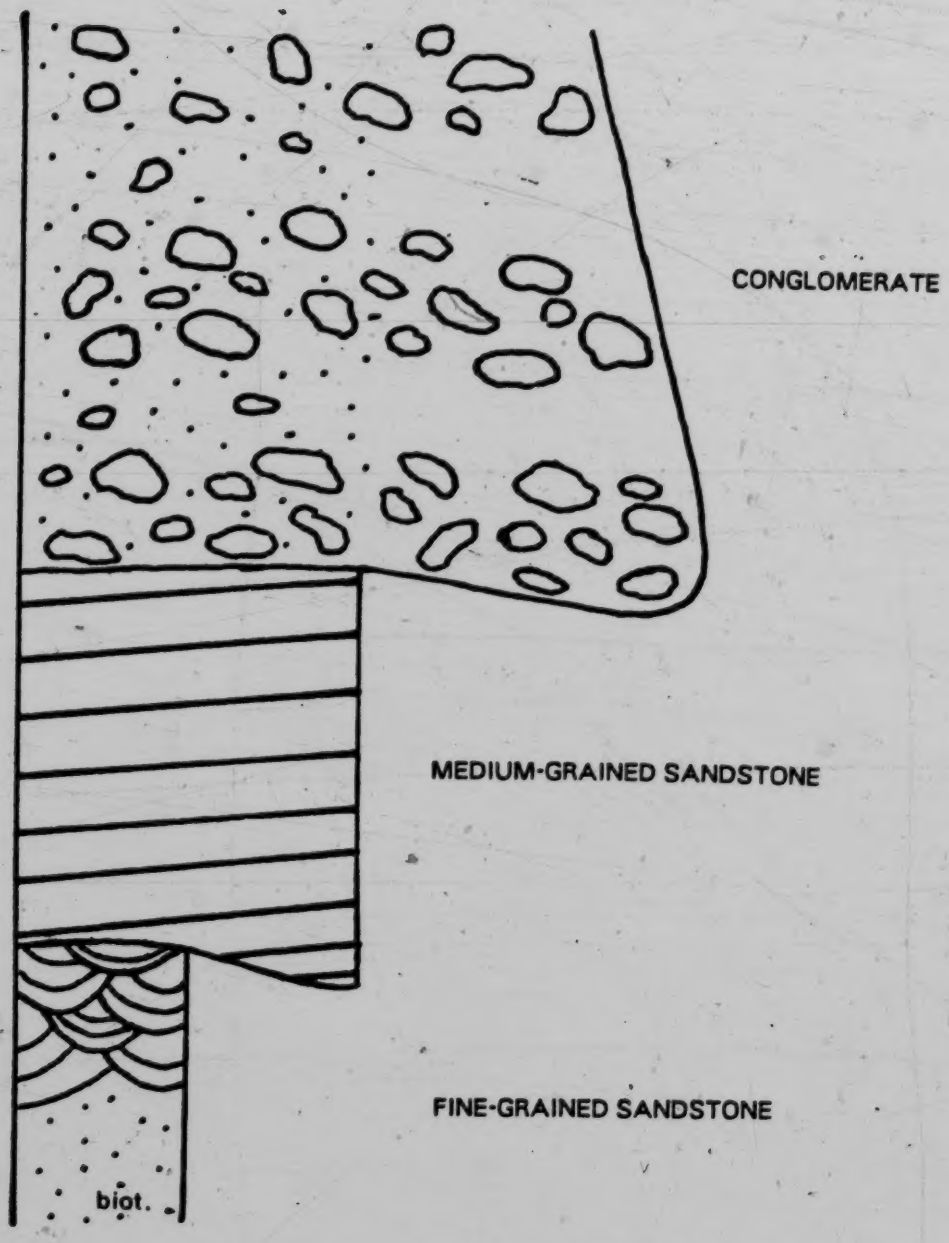

General lithology of the Viking Formation within the Harmattan East field.
Figure 2.11

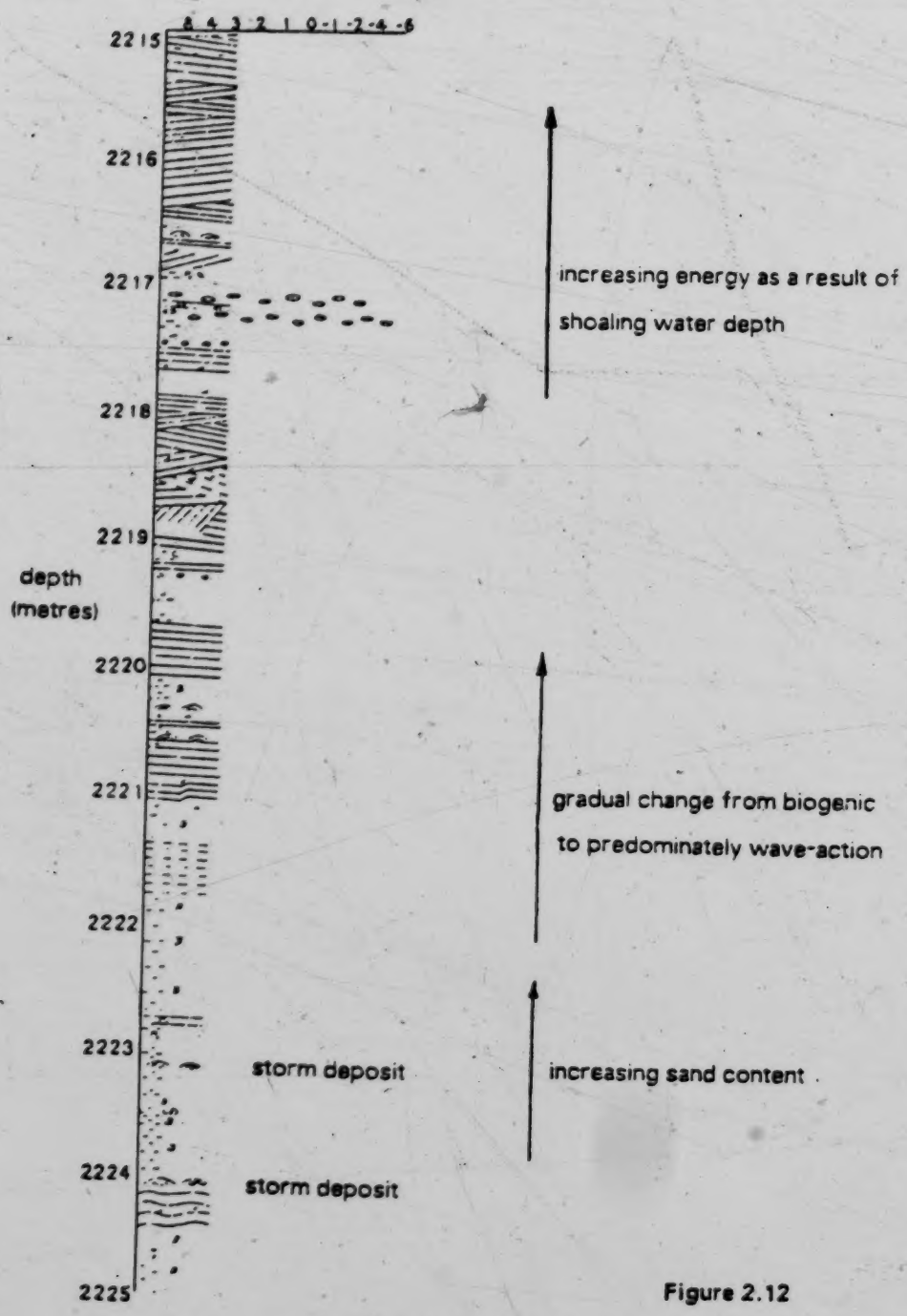
LITHOLOG
PHI SCALE
8 4 3 2 1 0 -1 -2 -4 -6
2215
2216
2217
2218
2219
depth
(metres)
2220
2221
2222
2223
2224
2225
storm deposit
storm deposit
increasing energy as a result of
shoaling water depth
gradual change from biogenic
to predominately wave-action
increasing sand content

Figure 2.12

which have been reworked by either wave-induced rip-currents or small storm surge-ebb currents. This sandstone may also have been reworked by southeasterly flowing currents.

Conglomerate

Within the Harmattan East field the conglomerate is interpreted as a storm-induced sediment-gravity flow. The beds vary in thickness, ranging from 20 to 40 cm. Variation in the maximum clast size within conglomerate beds results from sorting or variations in the properites of individual flows. Each of these beds have a concentration of clasts near a sharp erosional base, and an increased matrix content upsection. This is characteristic of modern day storm deposits (Hayes, 1976; Rodolfo et al., 1971 and Kumar and Sanders, 1976).

It has been proposed that these sediment-gravity flows are initiated by wave-shock which induces liquefaction and subsequent movement of the bottom sediment (Fig. 2.13) (Clukey et al., 1980; Nelson, 1982). The initial slumps, which are transported by unidirectional currents, become more turbulent and change into offshore moving gravity flows, which are focused along the trough. During maximum storm surge-ebb flow this sediment can not be contained within the trough. This allows the gravity flow to spread laterally onto the levee of the trough. As the flow begins to wane a fining-upward sequence is deposited both on the levee and within the trough. During normal flow, rip-currents and smaller storm events result in tractional transport of the medium or coarse-grained sandstone (Cacchione et al., 1984). As this sequence is repeated the next gravity flow will scour into the underlying pebbly sandstone. This results in the amalgamation of a series of 'fining-upward' beds into one ungraded matrix-supported conglomerate.

Large storms are capable of generating both high velocity, seaward moving currents and bottom shear stress which could induce liquefaction of the sediment. This is supported by the work of Kumar and Sanders (1976) who measured the currents produced by hurricane Camille off the coast of the Florida Panhandle. These currents flowed directly offshore with a velocity 3 to 5 time faster than the normal shore parallel currents (Murray, 1970). At water depths of 63 m maximum current velocities of 1.6 m/sec were measured. This current velocity would be capable of transporting the large clasts within the Viking Formation. Also, as the bottom shear stress associated with the oscillatory component of these storm-induced currents is generally

Figure 2.13 Sediment Gravity Flow

I. Storm activity results in the dispersion of the sand directly beneath the conglomerate. This dispersion is the result of storm induce waves. The difference in pressure between the crest and the trough of the waves results in dispersive pressure between sands grains.

II. The return flow, which results from the storm setup, is capable of moving the sand which has an increased dispersive pressure. The storm ebb-current initiates the sediment gravity flow. During maximum flow the sediment gravity flow extends out of the trough. This creates the thin overbank deposits.

III. As the storm ebb-current begins to wane the sediment gravity flow can be contained within the trough. The reducing flow creates the thin fining-upward sequence formed on the banks of the trough.

IV. During normal flow conditions rip-currents are focused along the trough. These rip-currents are capable of moving the coarse-grained sand as tractionally transported bedload. This tractional transport forms ripples within the trough.

V. This sequence of steps is repeated with the next major storm activity. On the banks of this trough another thin fining-upward sequence is formed. Within the trough, bedforms created during normal flow conditions are reworked by the next storm event, resulting in amalgamation of the conglomerate beds.

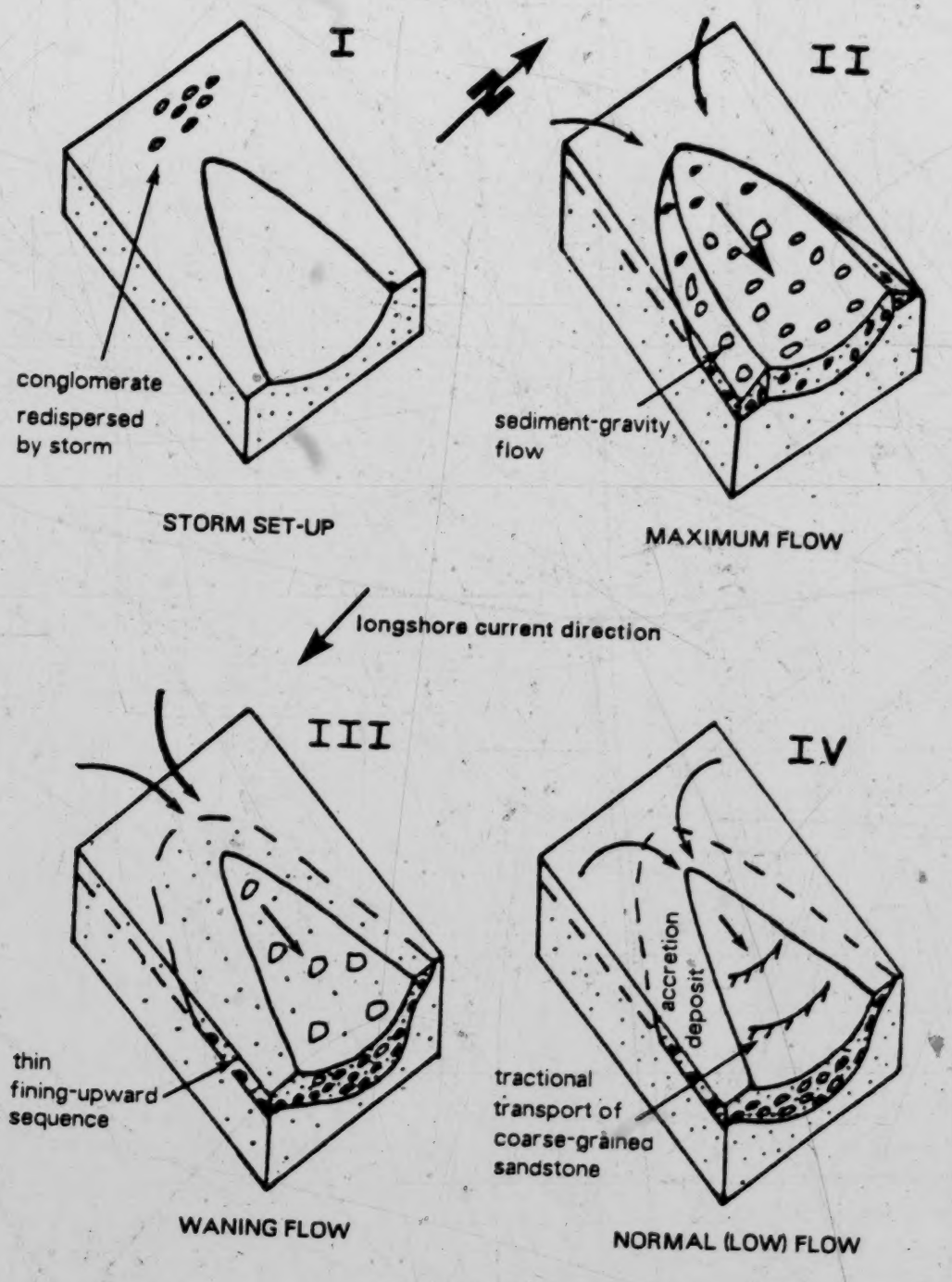
I
II
conglomerate
redispersed
by storm
sediment-gravity
flow
STORM SET-UP
MAXIMUM FLOW
longshore current direction
III
IV
thin
fining-upward
sequence
accretion
deposit
tractional
transport of
coarse-grained
sandstone
WANING FLOW
NORMAL (LOW) FLOW
flow direction
bedforms produced by tractional transport

Figure 2.13

several times larger than the unidirectional flow, this could induce liquefaction of the sediment (Madsen, 1976).

In addition to the high energy of the storm environment a feature such as a trough will serve to focus the flow of rip-currents (Felix and Gorsline, 1972) and bottom currents (Cacchione et al., 1984) (Fig. 2.14). Surface waves are refracted as they approach the head of the trough forming a zone of divergence along the shoreline. Local circulation drives the nearshore currents back toward the lower energy divergent zone, over the head of the trough. This results in turbid waters moving seaward and down the trough (Karl, 1983). The increased flow velocity will result in tractional transport of the medium or coarse-grained sandstone which separates the zones of conglomerate. These sandstones (Subfacies 9B) are reworked into two-dimensional ripples which are identified by the high-angle cross-stratification within the core (Fig. 2.5c,d).

In summary, both the fine-grained sandstone and the medium or coarse-grained sandstones were transported offshore by unidirectional wave and/or storm currents. The chert-pebble conglomerate was transported offshore as storm-induced, sediment-gravity flows. The initial slumping is the result of liquefaction of the bottom sediment by wave-shock. These slumps rapidly change into offshore moving sediment-gravity flows, which are focused by a trough and modified by strong storm surge-ebb currents.

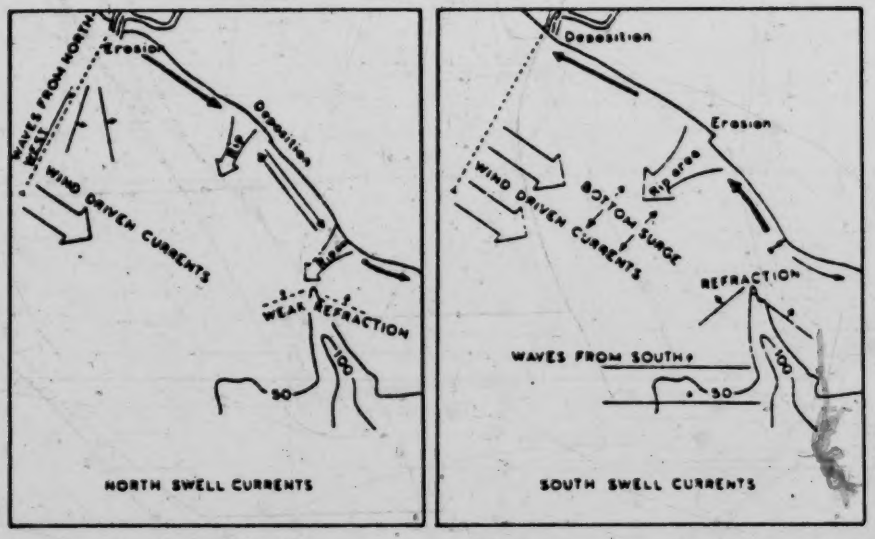

Figure 2.14

Longshore drift and current systems for the two major local wave directions. Magnitudes of flow and direction are schematically shown.

(after Felix and Gorsline, 1972)

G. DEPOSITIONAL PATTERN

The depositional pattern of the Harmattan East field is primarily controlled by the paleotopography of the two sandstone units. These sandstones combine to form a broad shallow east-west oriented trough which serves to focus the sediment-gravity flows. The thickest portion of conglomerate is located along the axis of this trough with thinner beds extending laterally (north-south) away from the trough.

Fine-grained sandstone

The major depositional feature of this sandstone is an east/west oriented shallow-embayment (Fig. 2.15). Slump structures identified within the core suggests that this paleotopographic feature may have resulted from slumping, which was initiated by either tectonic or volcanic activity. The fine-grained sandstone has a sharp erosional contact with the overlying medium or coarse-grained sandstone.

Medium or coarse-grained sandstone

As the medium or coarse sand moved to the northeast it smoothed the underlying paleotopography, resulting in two areas of increased thickness, in the west and southern portion of the field (Fig. 2.16). Medium or coarse sand filled the southern portion of the shallow embayment created by the fine-grained sandstone. This forms a well defined trough (Fig. 2.17, 2.18) which is 5 km long, 4 km wide at the mouth (distally), has a gradient of approximately 0.6m/km and a maximum relief of 4 to 5 m.

Uneven topography along the banks of the trough (Fig. 2.18) has been interpreted as resulting from either overbank levee deposition or reworking of the margins by marine currents. In the study area a current system flowed to the southeast (see chapter 4); however this type of current system, as seen on the Hudson Shelf Valley, reworks only the upcurrent bank (Freeland et al., 1981). Therefore, overbank flows are favoured because both banks of the trough appear to have been reworked.

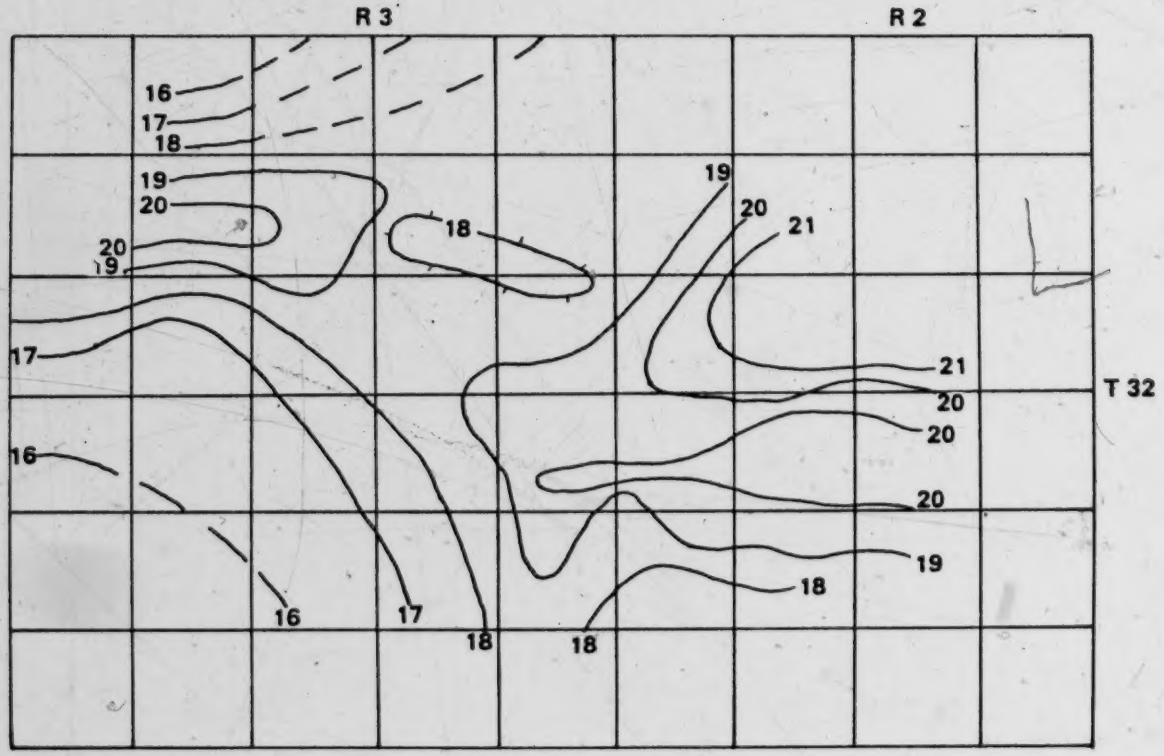

-20-
depth below
base of
Fish Scales

Figure 2.15 Paleotopography of the Fine-grained Sandstone

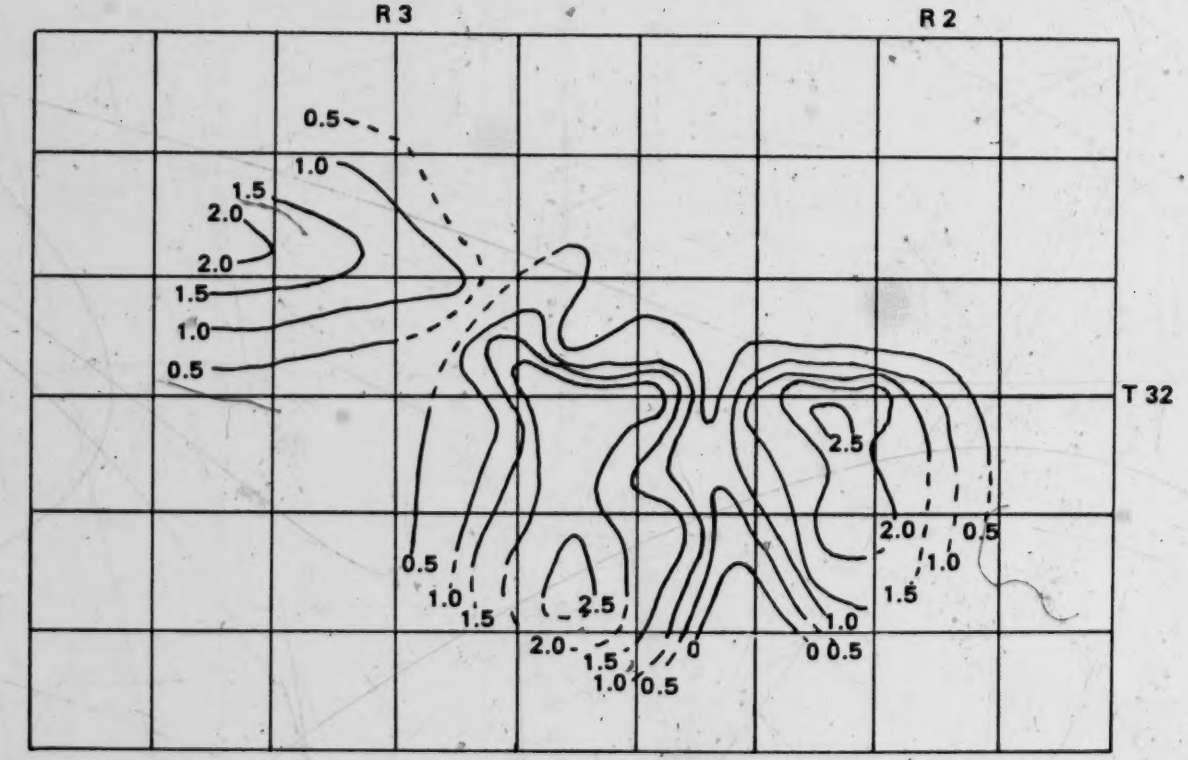

Figure 2.16 Isopach of the Medium or Coarse-grained Sandstone

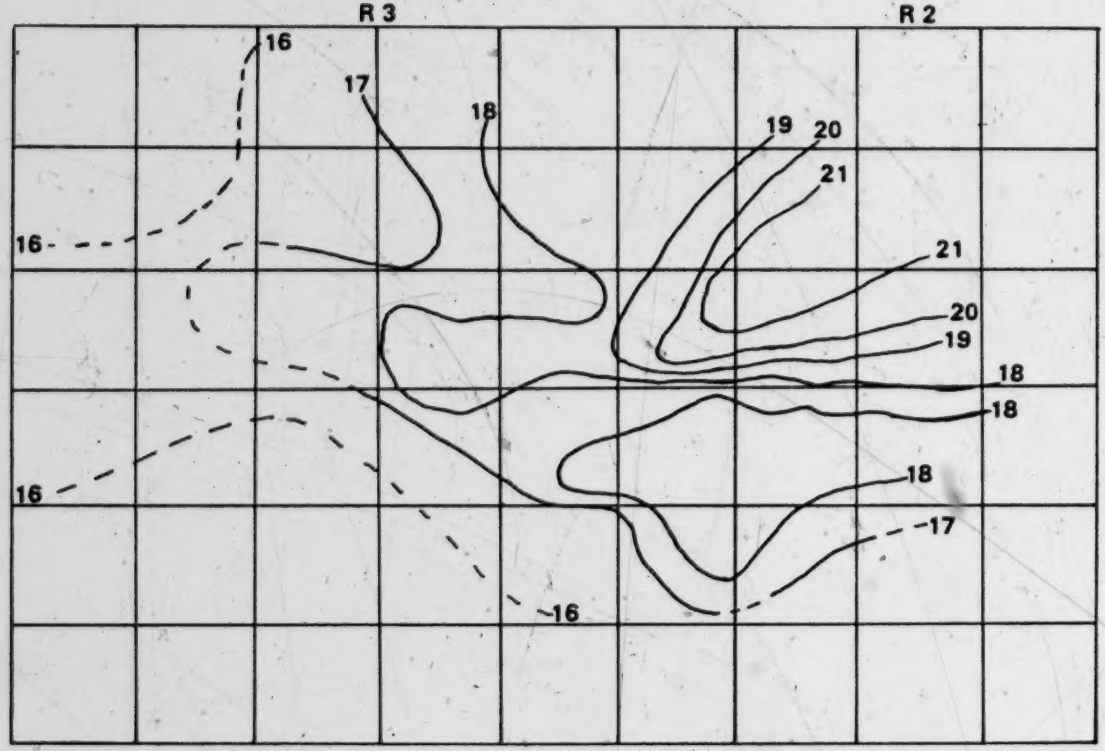

Figure 2.17 Paleotopography of the Medium or Coarse-grained Sandstone

-20-
depth below
base of
Fish Scales

Figure 2.18 is a 3D diagram produced by the computer package "surface II" (Sampson, 1978). The grid was produced using x,y co-ordinates from the base map and the Base of the Fish Scales as a datum. Contacts were picked brom geophysical logs. This figure represents the paleotopographic surface of the medium to coarse-grained sandstone wedge. The two major features are an east/west oriented trough and a plateau located to the west and south of the trough.

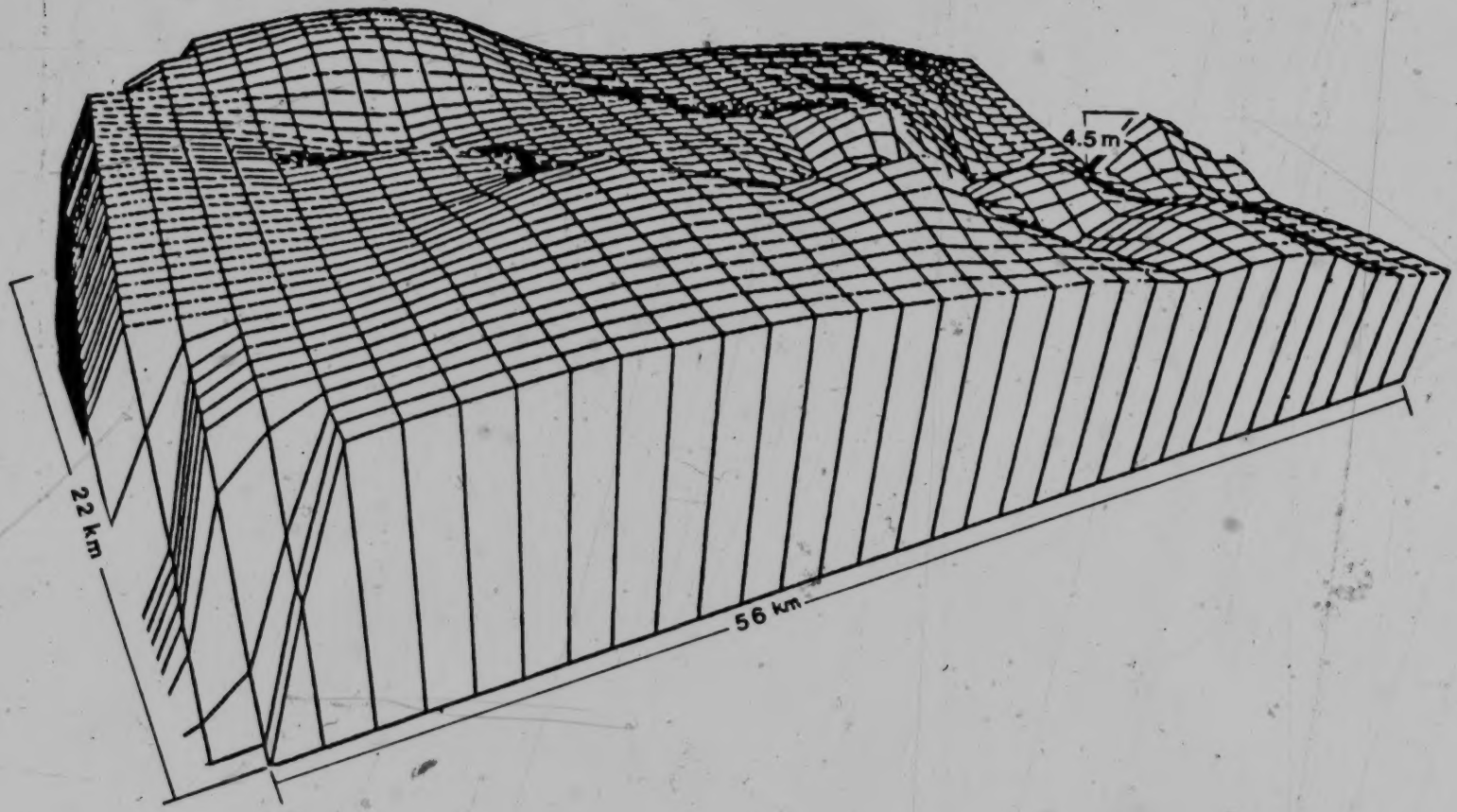

Figure 2.18 Paleotopography of the Medium-grained sandstone

Conglomerate

The depositional pattern of the chert-pebble conglomerate results in the trough being filled prior to the next major transgressive event (Fig. 2.19). This conglomerate horizon attains its maximum thickness (4.5 m) along the axis of the trough, decreasing laterally (north/south) (Fig. 2.20). The conglomerate horizon consists of three zones (0.6 m thick), separated by medium or coarse-grained pebbly sandstone. Within the trough each of the three zones of conglomerate comprise one thick, ungraded, matrix-supported conglomerate. This has resulted from the amalgamation of a series of sediment gravity flows. Moving laterally (north/south) from the trough, each of these zones of conglomerate grade into a series (maximum 6) of fining-upward beds, each deposited from a sediment-gravity flow (Fig. 2.21). This results in a concentration of clasts at a sharp erosional base and an increased matrix content upsection, grading into a pebbly sandstone.

The southern limit of the conglomerate horizon is skewed to the southeast, suggesting possible reworking and winnowing of the conglomerate by southeasterly flowing currents systems (Fig. 2.22). The northern limit occurs at approximately the boundary between Township 32 and 33, Range 3W5. This margin is patchy and is not a zero isopach, which may indicate that a thin (<0.2 m) reworked conglomerate lag overlaps the Harmattan East conglomerate. To the northeast a thin conglomerate lies along the trend of the Garrington system (Robb et al., 1984). The southern limit for the conglomerate, which is a zero isopach, is difficult to delineate because of poor well control and the problems of identifying a thin conglomerate on geophysical logs. The east/west boundaries are also tentative due to the lack of core.

Figure 2.19 is a 3D diagram produced by the computer package "surface II" (Sampson, 1978). The grid was produced using x,y co-ordinates from the base map and the Base of the Fish Scales as a datum. Contacts were picked from geophysical logs. This figure represents the paleotopographic surface of the conglomerate unit. The major feature is the loss of the trough which is represented in Figure 2.18.

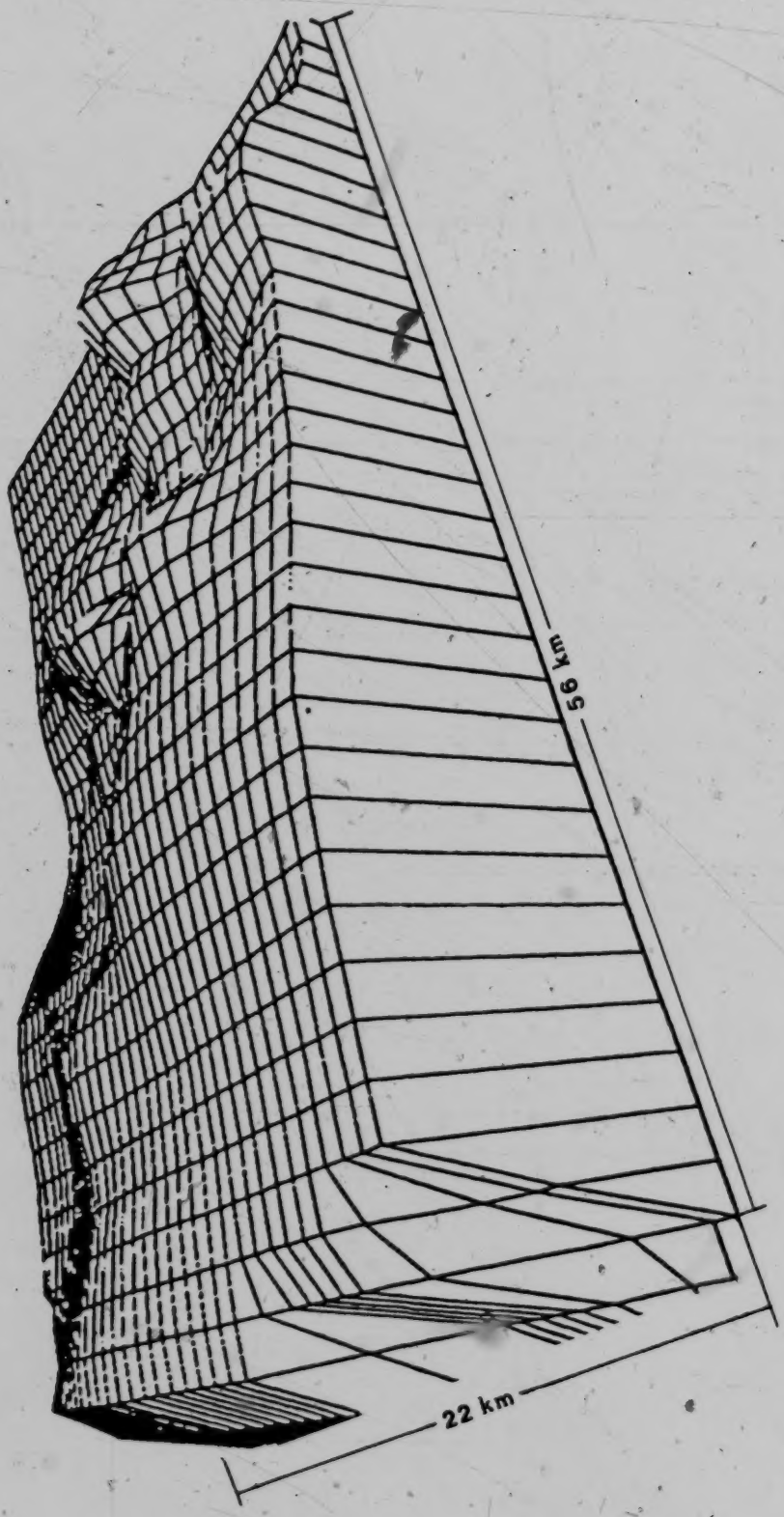

Figure 2.19 Paleotopography of the Conglomerate

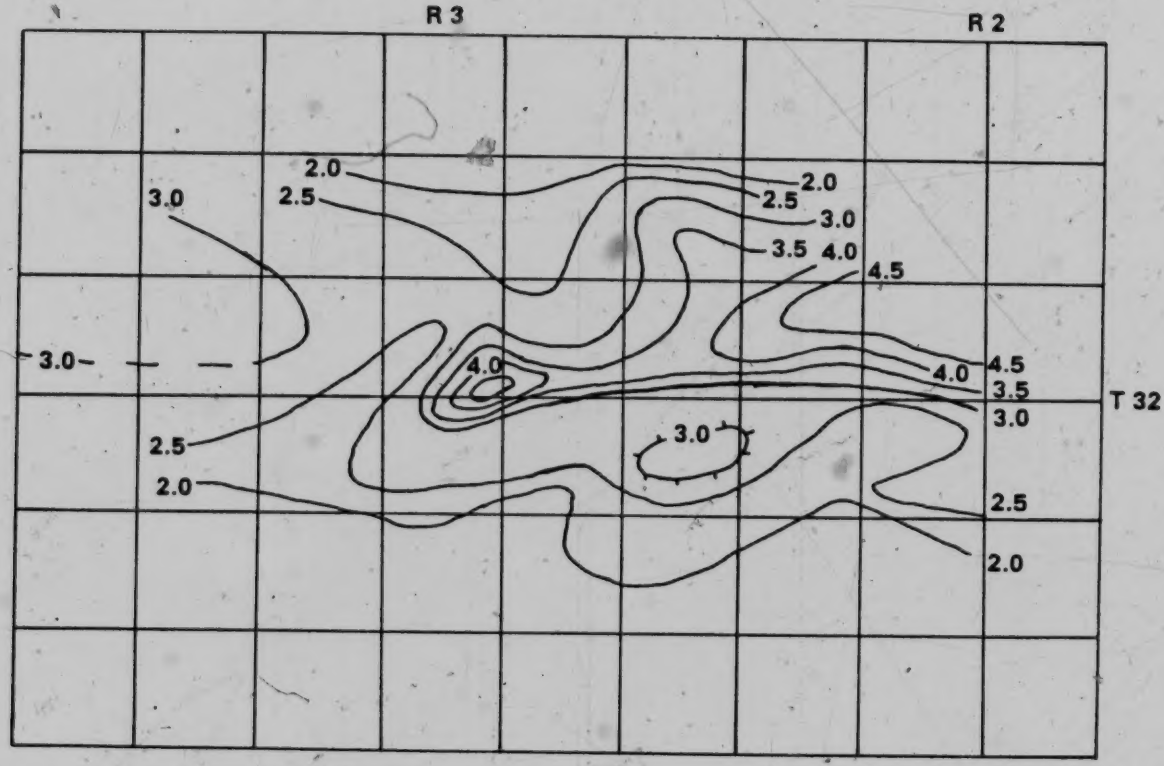

Figure 2.20 ISOPACH OF THE CONGLOMERATE

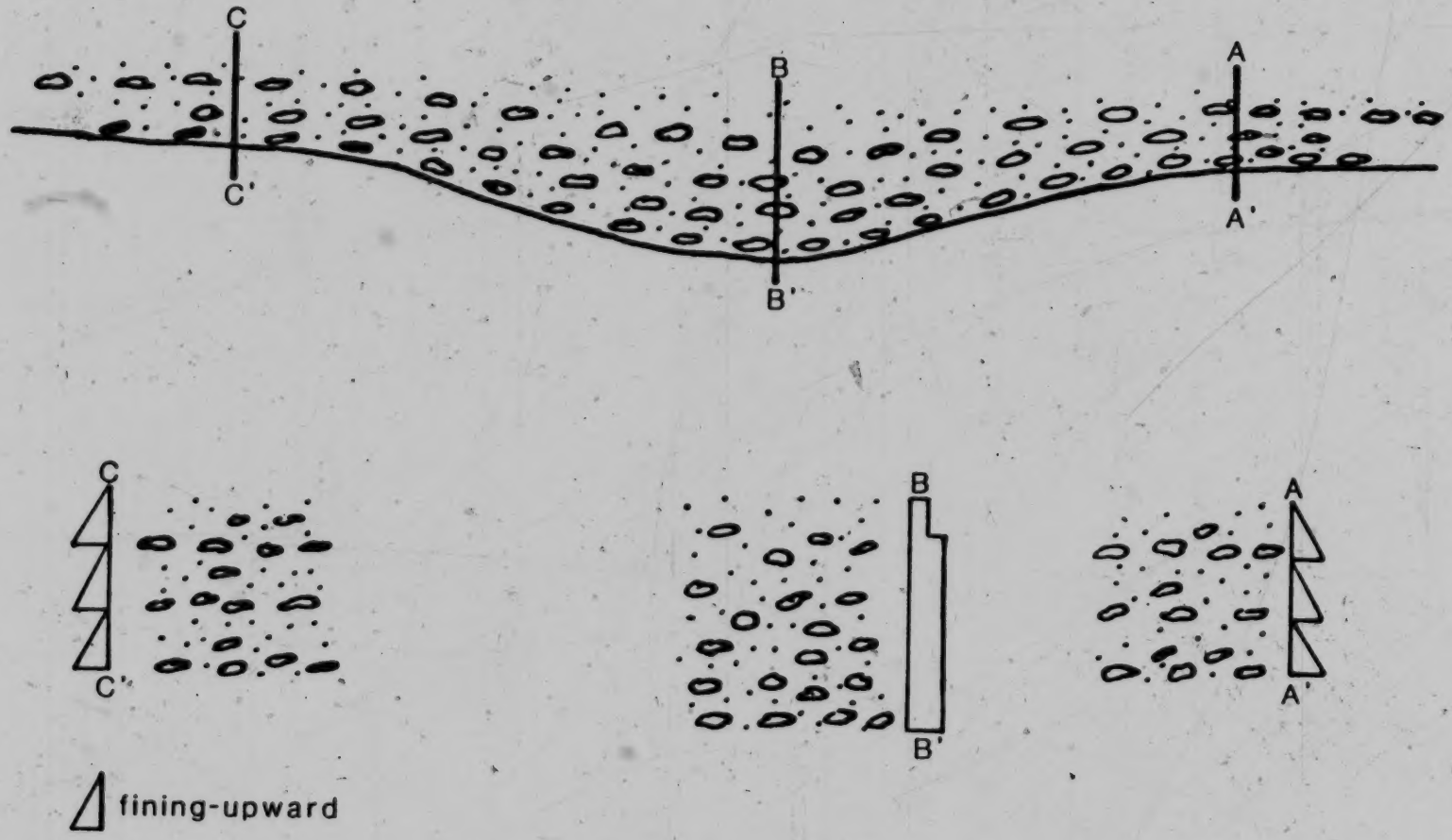

Figure 2.21

Depositional pattern of one of the three zones of conglomerate.

Looking down the axis of the trough.

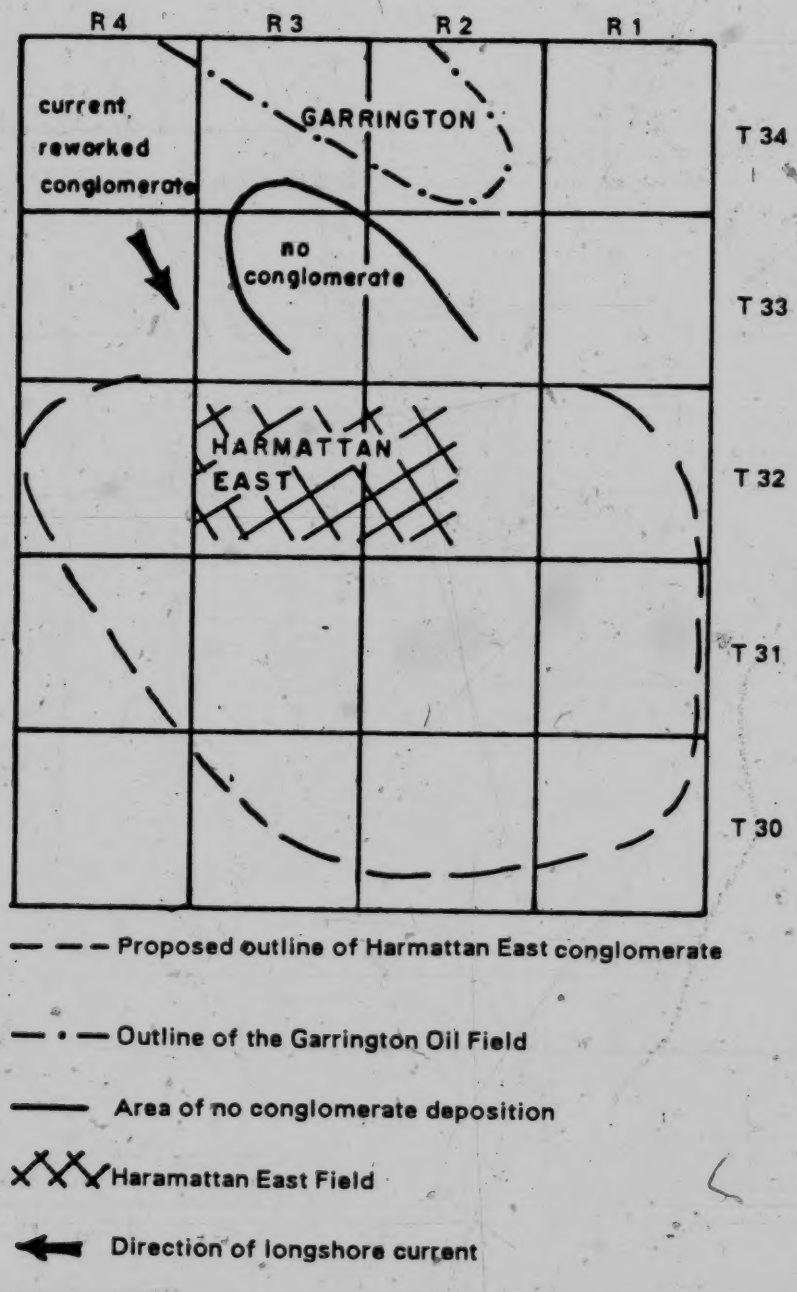

Figure 2.22 shows the skewed nature of the conglomerate which has originated from the Harmattan East field. Also, the northern margin of the Harmattan East field is located on the boundary between Township 32 and 33. At this location conglomerate, which is reworked by longshore currents, overlaps the Harmattan East conglomerate.

III. MINERALOGY

The mineralogy of the Viking Formation in the Harmattan East oil field is examined in this chapter. Sixty-seven samples from 15 wells were studied (Table 3.1). The mineralogic data are used to predict reservoir damage that could arise from secondary recovery techniques, and to develop a model of sandstone diagenesis for the unit.

Methods include thin-section examination, grain-size analysis, X-ray diffraction (XRD), energy dispersive analysis (EDA), and scanning electron microscopy (SEM). Thin-section examination was used to obtain the bulk composition, location of clay minerals, amount and types of cement, and the textures of the rocks. The amount of clay-sized material in the sample was determined by grain-size analysis. X-ray diffraction of bulk samples was used to determine the relative abundance and types of carbonates and feldspars present in the sample. The < 2 μm, 2-5 μm and 5-20 μm size fractions were also examined by X-ray diffraction to determine their clay mineralogy. The scanning electron microscope, with the attached energy dispersive analyzer (EDA), was used to examine the habit and distribution of clay minerals and carbonates, especially authigenic phases.

A. PETROGRAPHY

The conglomerates are composed of framework grains (80-85%), cement (4-10%) and porosity (5-13%) (Table 3.2a). Framework grains are quartz (15-20%), chert (50-65%), feldspar (predominately plagioclase) (3-5%) and rock fragments (5-10%) (Table 3.2b). The conglomerates are classified as sublitharenites (Fig. 3.1). Quartz overgrowths (t-7%) and kaolinite (3-8%) (Fig. 3.2a) comprise most of the cement. The conglomerate has an average porosity of 10%; sorting and grain-size distribution is consistent throughout the unit. Permeability varies drastically, ranging from 2-70 md, because of localized variation in the quantity of the cements.

The medium or coarse-grained sandstone is composed of framework grains (74-80%), cement (9-16%) and porosity (4-13%) (Table 3.2a). Framework grains are quartz (35-40%), chert (20-30%), feldspar (5-10%) (predominately plagioclase) and rock fragments (5-10%)(Table 3.2b); these rocks are sublitharenites (Fig. 3.1). Quartz overgrowths (5-10%), clays (3-10%) and carbonates (t) comprise most of the cement (Fig. 3.3a). The porosity and permeability range from 4-13% and 10-25 md, respectively.

TABLE 3.1 SAMPLES INVESTIGATED

SAMPLE NUMBER	ROCK TYPE	DEPTH (m)	HYDROMETER ANALYSIS	THIN SECTION	XRD SIZE-FRACTION <2μm	XRD SIZE-FRACTION 2-5μm	XRD SIZE-FRACTION 5-20μm	SEM
HARMATTAN EAST								
6-17-32-3W5								
K87	Congl.	2133.4	X	X		X	X	
K88	M.Sst.	2134.2	X	X	X	X	X	X
K90	F.Sst.	2136.3	X	X	X	X	X	X
K92	F.Sst.	2142.5	X	X	X	X	X	
K93	Congl.	2146.7	X	X	X	X	X	
6-18-32-2W5								
K74	Congl.	2175.9	X	X	X	X	X	
K75	M.Sst.	2176.5	X	X	X	X	X	
K77	C.Sst.	2178.8	X	X	X	X	X	
K80	F.Sst.	2185.2	X	X	X	X	X	
K82	F.Sst.	2187.1	X	X	X	X	X	
K85	Congl.	2194.6	X	X	X	X	X	
6-20-32-2W5								
K52	Congl.	2125.1	X	X	X	X	X	X
K53	F.Sst.	2121.5	X	X	X	X	X	X
K54	Congl.	2126.4	X		X	X	X	
K56	F.Sst.	2127.5	X		X	X	X	X
K58	F.Sst.	2128.9	X		X	X	X	
K61	F.Sst.	2131.2	X		X	X	X	
K62	Congl.	2134.1	X	X	X	X	X	
K63	F.Sst.	2134.6	X	X	X	X	X	
14-12-32-3W5								
K11	C.Sst.	2208.3	X		X	X	X	
K13	F.Sst.	2212.5	X		X	X	X	
K17	F.Sst.	2220.0	X	X	X	X	X	
16-14-32-3W5								
K162	Congl.	2207.4	X	X	X	X	X	
K163	C.Sst.	2208.0	X		X	X	X	
K165	M.Sst.	2210.5	X	X	X	X	X	
K168	F.Sst.	2217.0	X	X	X	X	X	
6-16-32-3W5								
K22	M.Sst.	2210.6	X		X	X	X	
K26	F.Sst.	2215.3	X	X	X	X	X	
K29	Congl.	2218.3	X		X	X	X	
K31	F.Sst.	2219.9	X	X	X	X	X	

TABLE 3.1 SAMPLES INVESTIGATED (CONTINUED)

SAMPLE NUMBER	ROCK TYPE	DEPTH (m)	HYDROMETER ANALYSIS	THIN SECTION	XRD SIZE-FRACTION <2μm	XRD SIZE-FRACTION 2-5μm	XRD SIZE-FRACTION 5-20μm	SEM
16-22-32-3W5								
K133	C.Sst.	2211.3	X		X	X	X	
K134	Congl.	2211.8	X		X	X	X	
K136	M.Sst.	2213.7		X	X	X	X	
K137	F.Sst.	2214.4		X	X	X	X	
6-25-32-3W5								
K149	Congl.	2187.1	X		X	X	X	
K151	Congl.	2189.1	X		X	X	X	
K152	C.Sst.	2189.4	X		X	X	X	
K153	F.Sst.	2190.4	X	X	X	X	X	
K154	F.Sst.	2192.6	X	X	X	X	X	
7-24V-32-4W5								
K155	C.Sst.	2296.5	X	X	X	X	X	
K159	F.Sst.	2299.8	X	X	X	X	X	
11-31-33-4W5								
K43	C.Sst.	2391.5	X	X	X	X	X	
K44	Congl.	2393.0	X	X	X	X	X	
K46	F.Sst.	2395.7		X	X	X	X	
K48	F.Sst.	2402.2		X	X	X	X	
16-10-32-3W5								
M1	Congl.	2215.3	X	X	X	X	X	X
M2	C.Sst.	2215.6	X	X	X	X	X	X
M3	Congl.	2217.6	X	X	X	X	X	X
M4	C.Sst.	2218.4	X	X	X	X	X	X
M5	F.Sst.	2219.4	X	X	X	X	X	X
M6	C.Sst.	2217.2	X	X	X	X	X	X
M7	Congl.	2223.3	X	X	X	X	X	X
M8	F.Sst.	2226.3	X	X	X	X	X	X
M9	C.Sst.	2217.9	X	X	X	X	X	X
16-23-32-3W5								
M1	Congl.	2204.8	X	X	X	X	X	X
M2	Congl.	2205.7	X	X	X	X	X	X
M3	C.Sst.	2206.4	X	X	X	X	X	X
M4	C.Sst.	2206.6	X	X	X	X	X	X
6-24-32-3W5								
M1	C.Sst.		X	X	X	X	X	
M2	F.Sst.		X	X	X	X	X	
M3	Congl.		X	X	X	X	X	
M4	F.Sst.		X	X	X	X	X	

TABLE 3.1 SAMPLES INVESTIGATED (CONTINUED)

SAMPLE NUMBER	ROCK TYPE	DEPTH (m)	HYDROMETER ANALYSIS	THIN SECTION	XRD SIZE-FRACTION <5μm	XRD SIZE-FRACTION >5μm	SEM
6-19-32-2W5							
SP3	Congl.	2170.6	X		X	X	X
SP6	Congl.	2171.1	X		X	X	X
SP21	M.Sst.	2173.1	X		X	X	X
SP29	C.Sst.	2174.3	X		X	X	X
SP45	F.Sst.	2177.5	X		X	X	X

TABLE 3.2a ROCK COMPONENTS, THIN SECTION ANALYSIS

SAMPLE NUMBER	ROCK TYPE	DEPTH (m)	FRAMEWORK GRAINS (%)	CEMENTS (%)	POROSITY (%)
16-14-32-3W5					
K162	Congl.	2208.3	85	10	5
K165	M.Sst.	2210.5	80	16	4
K168	F.Sst.	2217.0	63	36	t
6-18-32-3W5					
K74	Congl.	2175.9	85	9	6
K77	C.Sst.	2178.8	74	18	8
K80	F.Sst.	2185.2	60	39	t
6-16-32-3W5					
K21	C.Sst.	2210.4	77	13	10
K23	M.Sst.	2211.5	82	13	5
K31	F.Sst.	2219.9	70	29	t
6-20-32-2W5					
K53	M.Sst.	2125.5	78	9	13
K55	Congl.	2126.7	83	4	13
K57	F.Sst.	2128.5	55	44	t
K63	F.Sst.	2134.6	57	39	4

TABLE 3.2b BULK MINERALOGY, THIN SECTION ANALYSIS

SAMPLE NUMBER	FRAMEWORK GRAINS (%)					CEMENTS (%)			ROCK CLASS (FOLK, 1968)
	Ch	Q	F	RF	Q	Ca	S	C	
16-14-32-3W5									
K162	60	13	3	9	2	nd	nd	8	Sublitharenite
K165	29	36	4	11	9	nd	nd	7	Sublitharenite
K168	12	38	3	10	20	2	5	9	Sublitharenite
6-18-32-2W5									
K74	56	16	5	8	7	nd	nd	2	Sublitharenite
K77	22	38	7	7	9	nd	nd	9	Sublitharenite
K80	5	41	6	8	19	nd	nd	20	Sublitharenite
6-16-32-3W5									
K21	25	39	5	8	8	nd	nd	5	Sublitharenite
K23	30	39	4	9	7	nd	nd	6	Sublitharenite
K31	11	49	2	8	14	1	8	6	Sublitharenite
6-20-32-2W5									
K53	21	39	10	8	5	1	nd	3	Sublitharenite
K55	63	13	3	4	1	nd	nd	3	Sublitharenite
K57	10	35	4	6	12	13	2	17	Sublitharenite
K63	8	37	4	8	13	2	23	1	Sublitharenite

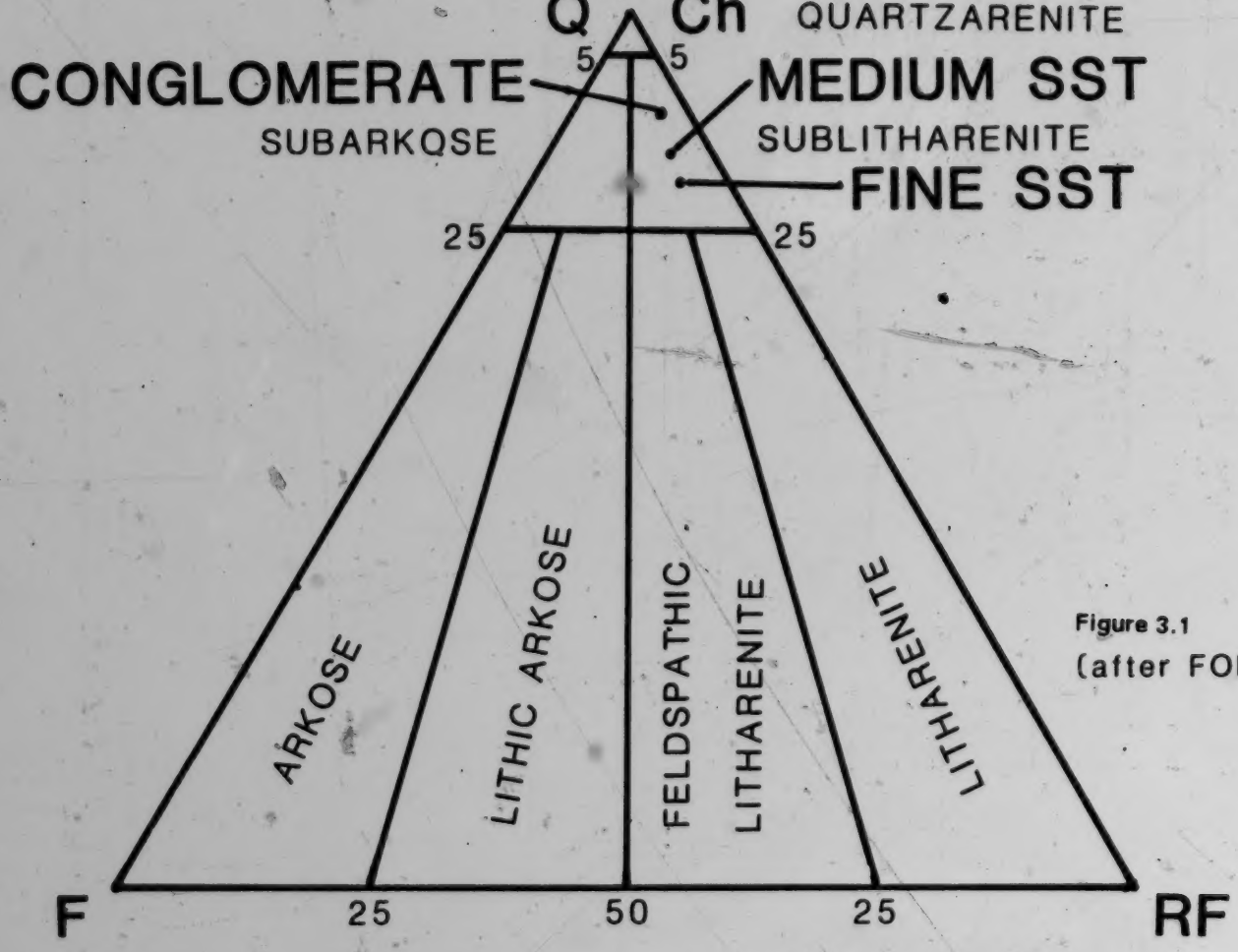

Figure 3.1
(after FOLK, 1968)

Figure 3.2 Conglomerate

(thin section photographs)

A. Sample K162, showing the bulk composition of the chert-pebble conglomerate. Predominately chert (Ch), with lesser amounts of quartz (Q), rock fragments (RF) and feldspar (F).
Well 6-20-32 3W5, depth 2207.4 m.

B. Sample K162, showing the two main cements, quartz overgrowths (AQ) and clays (kaolinite) (K).
Well 16-14-32 3W5, depth 2207.4 m.

C. Sample K162, showing both primary and secondary porosity of the chert-pebble conglomerate. Secondary porosity (2°P) includes, solutioning of feldspars, fracture porosity and intercrystalline within the kaolinite.
Well 16-14-32 3W5, depth 2207.4 m.

D. Sample K12, showing composite quartz grains containing muscovite flakes. This suggests a metamorphic source terrain for the detrital matrix within the conglomerate.
Well 14-12-32 3W5, depth 2209.4 m.

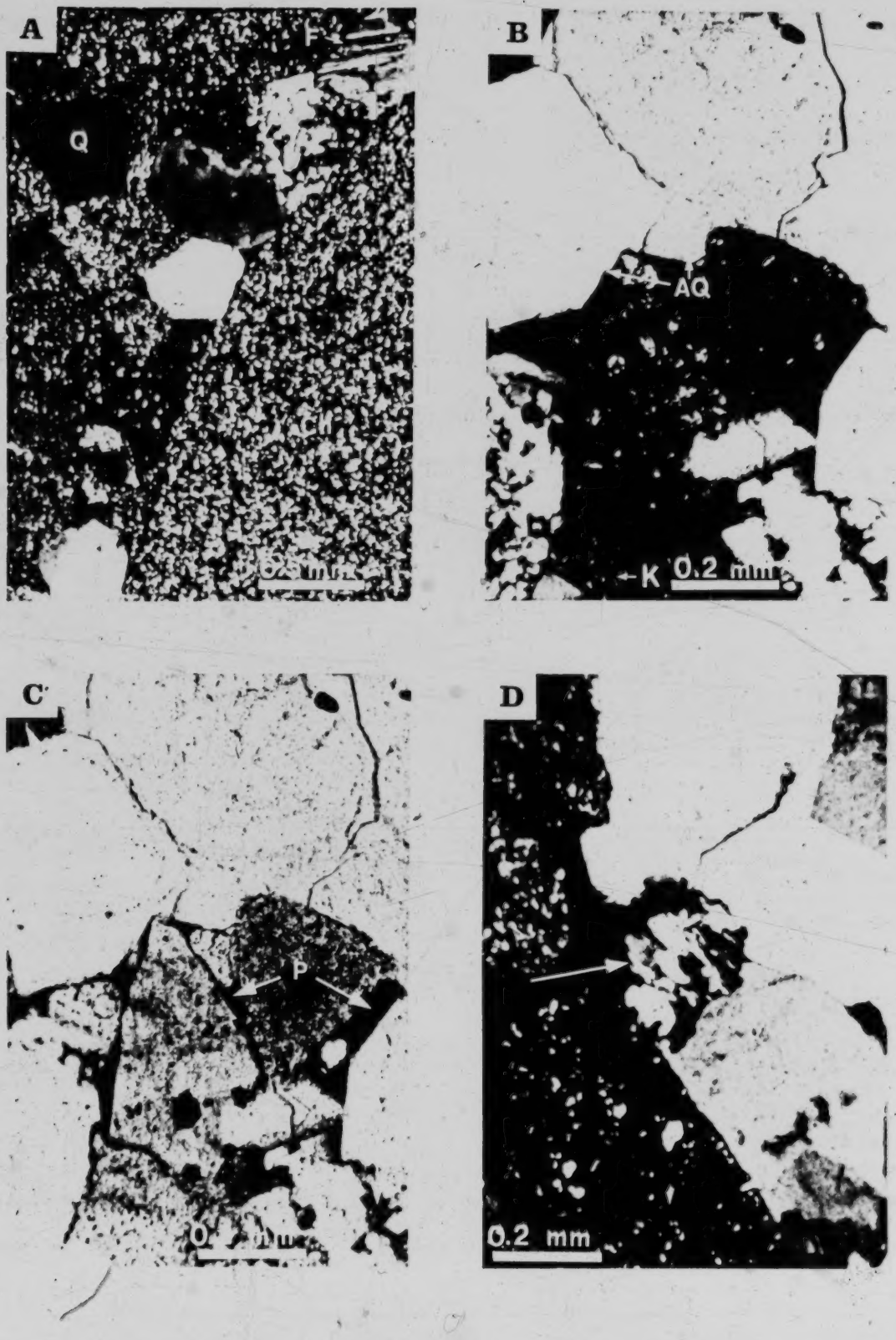
A
F
Q
Ch
0.2 mm
B
AQ
K
0.2 mm
C
P
0.2 mm
D
0.2 mm

Figure 3.3 Medium or Coarse-grained Sandstone

(thin section photographs)

A. Sample K175, showing the bulk composition which is predominately quartz (Q), with lesser amounts of chert (Ch), rock fragments (RF) and feldspar (F).
Well 14-18-32 3W5, depth 2171.4 m.

B. Sample K100, showing the two main cements quartz overgrowths (AQ) and clays (kaolinite K).
Well 16-23-32 3W5, depth 2206.9 m.

C. Sample K100, showing both primary and secondary porosity. Secondary porosity includes intercrystalline, within the kaolinite, dissolution of feldspar (Fig. 3.3B) and minor fracture porosity.
Well 16-23-32 3W5, depth 2206.9 m.

D. Sample K100, showing the dissolution of feldspar forming secondary porosity.
Well 16-23-32 3W5 depth 2206.9 m.

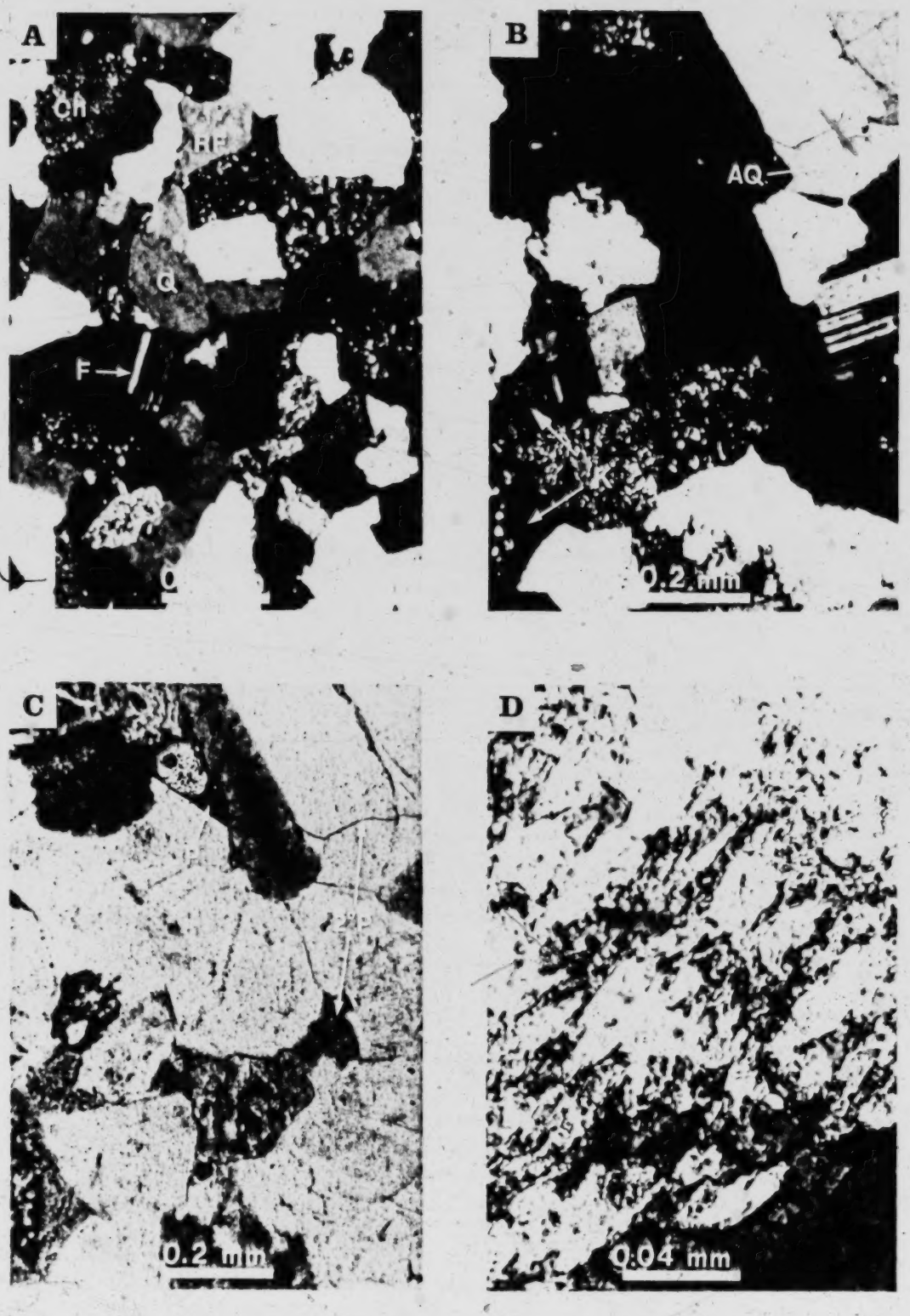
A
CH
ARF
Q
F
Q
B
AQ
0.2 mm
C
0.2 mm
D
0.04 mm

The fine-grained sandstone is composed of framework grains (55-70%), cements (29-44%) and porosity (t-4%) (Table 3.2a). Framework grains are quartz (35-50%), chert (5-15%), feldspar (1-6%) (predominately plagioclase) and rock fragments (5-10%); these rocks are sublitharenites (Fig. 3.1). Cement types vary both laterally and with depth. In the upper portion of the fine-grained sandstone, cements consist of clay minerals + quartz overgrowths ± ankerite (Fig. 3.4a). Ankerite cement is characteristic of areas where the overlying medium or coarse-grained sandstones are absent. Lower in the fine-grained sandstone, siderite is the predominate cement, with lesser amounts of Fe-dolomite/ankerite and clay minerals (Fig. 3.4b).

A change in source area between the fine-grained sandstone and the overlying coarser-grained units is suggested by the petrographic study. The conglomerate and medium or coarse-grained sandstone have a common source area that contains both sedimentary (chert pebbles) and metamorphic (composite quartz containing muscovite) rock types (Fig. 3.2b). Within the coarser units, the quartz and feldspar grains are of comparable size, suggesting a short distance of transport. Regional uplift of the source area may have caused the change from sandstone to conglomerate. In contrast, the fine-grained sandstone has a source area which is predominately plutonic with a minor metamorphic contribution (Fig. 3.4c). This is supported by the presence of vacuoles within most of the quartz grains. Feldspars are generally smaller than the quartz grains, indicating a longer distance of transport than the overlying coarser-grained units.

Within the Viking 'B', which contains the three lithologic units discussed above, feldspars comprise only 5-10% of the framework grains (Table 3.2b). The low percentage of feldspar in the Viking 'B' is in contrast to the greater than 20% feldspar in an overlying coarse-grained sandstone (Viking 'A') (Robb et al., 1984). This difference may be a function of source area and preferential loss due to diagenetic processes (e.g., solution of feldspars, formation of kaolinite, etc.)

Figure 3.4 Fine-grained Sandstone

(thin-section photograph)

A. Sample K92, showing the bulk composition which is predominately quartz (Q), with lesser amounts of chert (Ch), rock fragments (RF) and feldspar (F).
Well 6-17-32 2W5, depth 2142.5 m.

B. Sample K92, showing the cements found in the fine-grained sandstone located directly beneath the medium or coarse-grained sandstone. The cement ranges from 20-40% of the whole rock and consists of equal amounts of clays (C) and quartz overgrowths (AQ).
Well 6-17-32 2W5, depth 2141.5 m.

C. Sample K14 showing the cements found in the fine-grained sandstone in the absence of overlying medium or coarse-grained sandstone. The cement ranges from 15-35% of the whole rock. The cement consists of clays, with lesser amounts of quartz overgrowths (AQ) and carbonate (Ca).
Well 14-12-32 3W5, depth 2216.2 m.

D. Sample K82 showing the cements found in the fine-grained sandstone, 10 metres below the upper contact of this sandstone. The cement ranges from 20-45% of the whole rock, consisting of predominately siderite (S), with minor amounts of clay (C) and carbonate (Ca). The carbonates are stained blue.
Well 6-18-32 2W5, depth 2187.1 m.

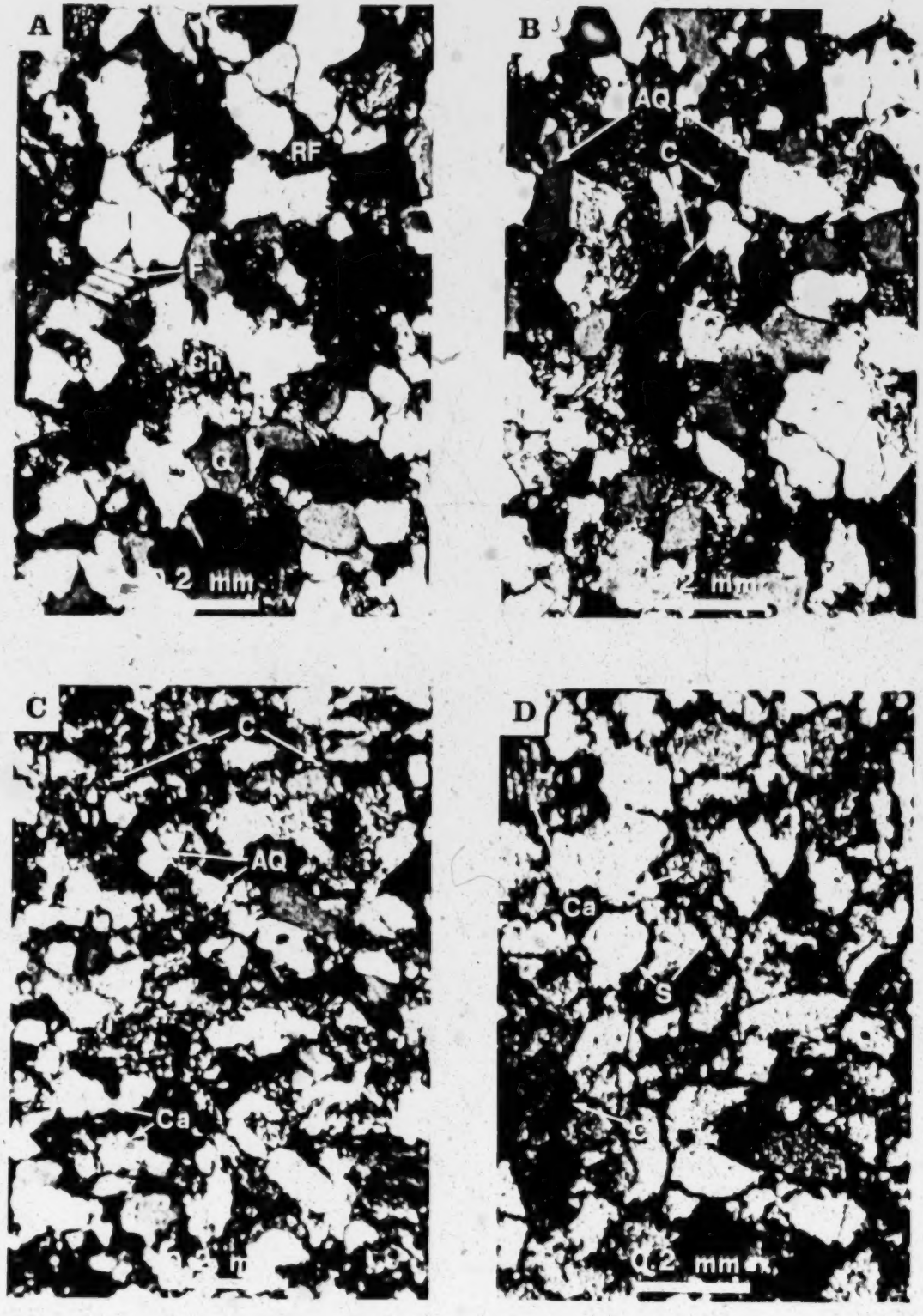
A
RF
F
Ch
Q
2 mm
B
AQ
C
2 mm
C
C
AQ
Ca
D
Ca
S
C
2 mm

B. GRAIN-SIZE ANALYSIS (by hydrometer)

The percentage of the whole rock within the three size fractions examined was calculated base on the grain-size analysis (Table 3.3). There is an apparent increase in the abundance of fine-grained material from the conglomerate to the fine-grained sandstone.

The average abundance of fine-grained material in each lithology is:

Conglomerate

5-20μm	1.3%
2-5μm	0.8%
<2μm	1.7%

Medium or coarse-grained sandstone

5-20μm	3.9%
2-5μm	0.9%
<2μm	3.7%

Fine-grained sandstone

5-20μm	6.5%
2-5μm	2.2%
<2μm	5.0%

TABLE 3.3a HYDROMETER ANALYSIS

SAMPLE NUMBER	ROCK TYPE	DEPTH (m)	% MATERIAL IN SAMPLE <2μm	2-5μm	5-20μm
6-17-32-2W5					
K87	Congl.	2133.4	0.4	0.7	0.6
K88	M.Sst.	2134.2	0.6	1.8	3.6
K90	F.Sst.	2136.3	4.7	3.1	6.0
K92	F.Sst.	2142.5	4.3	2.3	4.6
K93	Congl.	2146.7	1.7	0.9	0.2
6-18-32-2W5					
K74	Congl.	2175.9	0.8	0.1	0.9
K75	M.Sst.	2176.5	1.2	0.8	1.1
K77	C.Sst.	2178.8	0.5	1.2	1.2
K80	F.Sst.	2185.2	4.8	1.9	5.1
K82	F.Sst.	2187.1	5.1	1.8	10.5
K85	Congl.	2194.6	0.7	1.1	0.8
6-20-32-2W5					
K52	Congl.	2125.1	0.5	2.3	1.3
K53	F.Sst.	2125.5	0.7	1.3	6.0
K54	Congl.	2126.4	0.9	0.3	1.4
K56	F.Sst.	2127.5	5.2	5.1	7.2
K58	F.Sst.	2128.9	5.2	4.8	9.3
K61	F.Sst.	2131.2	5.0	4.0	4.0
K62	Congl.	2134.1	0.5	0.5	1.4
K63	F.Sst.	2134.6	1.0	4.0	7.5
14-12-32-3W5					
K11	C.Sst.	2208.3	1.3	1.3	2.3
K13	F.Sst.	2212.5	5.6	2.2	8.6
K17	F.Sst.	2220.0	4.4	1.6	4.8
16-14-32-3W5					
K162	Congl.	2207.4	1.1	0.6	2.5
K163	C.Sst.	2208.0	1.2	1.3	2.7
K165	M.Sst.	2210.5	9.4	2.4	14.2
K168	F.Sst.	2217.0	5.2	1.6	6.7
6-16-32-3W5					
K22	C.Sst.	2210.6	0.5	0.5	3.0
K26	F.Sst.	2215.3	4.0	3.0	8.0
K29	Congl.	2218.3	0.9	1.0	1.0
K31	F.Sst.	2219.9			
16-22-32-3W5					
K133	C.Sst.	2211.3	3.5	1.3	1.3
K134	Congl.	2211.8	1.7	1.7	1.1
K136	M.Sst.	2213.7	-	-	
K137	F.Sst.	2214.4	7.3	3.6	5.3

TABLE 3.3a HYDROMETER ANALYSIS (CONTINUED)

SAMPLE NUMBER	ROCK TYPE	DEPTH (m)	% MATERIAL IN SAMPLE <2μm	2-5μm	5-20μm
6-25-32-3W5					
K149	Congl.	2187.1	2.5	0.3	0.9
K151	Congl.	2189.1	2.5	0.4	1.2
K152	C.Sst.	2189.4	5.1	0.4	1.5
K153	F.Sst.	2190.4	8.2	2.8	7.2
K154	F.Sst.	2192.6	4.6	1.7	7.2
7-24V-32-4W5					
K155	C.Sst.	2296.5	2.8	2.0	9.4
K159	F.Sst.	2299.8	3.9	2.9	8.8
11-31-33-4W5					
K43	C.Sst.	2391.5	2.3	0.7	3.6
K44	Congl.	2393.0	1.1	0.3	1.7
K46	F.Sst.	2395.7	4.2	3.1	5.9
K48	F.Sst.	2402.1	1.9	0.1	0.1
16-10-32-3W5					
M1	Congl.	2215.3	4.2	1.3	
M2	C.Sst.	2215.6	3.3	0.3	
M3	Congl.	2217.6	3.3	0.2	
M4	C.Sst.	2218.4	4.7	0.3	
M5	F.Sst.	2223.3	9.6	0.5	
16-23-32-3W5					
M1	Congl.	2204.8	3.1	0.2	
M2	Congl.	2205.7	1.7	0.1	
M3	C.Sst.	2206.4	10.1	0.4	
M4	C.Sst.	2206.6	3.4	0.2	
6-24-32-3W5					
M1	C.Sst.	-	7.5	0.3	
M2	F.Sst.	-	7.4	0.3	
M3	Congl.	-	2.6	0.9	
M4	F.Sst.	-	7.2	0.9	

TABLE 3.3b HYDROMETER ANALYSIS

SAMPLE NUMBER	ROCK TYPE	DEPTH (m)	% MATERIAL IN SAMPLE <5μm	>5μm
6-19-32-2W5				
SP3	Congl.	2170.7	5.8	94.2
SP6	Congl.	2171.1	10.7	89.3
SP21	M.Sst.	2173.2	25.9	74.1
SP29	C.Sst.	2174.3	6.4	93.6
SP45	F.Sst.	2177.6	13.1	86.9

C. X-RAY DIFFRACTION ANALYSIS

Bulk Mineralogy

Eleven whole rock samples representing the three main lithologies were studied using X-ray diffraction. These samples contained mostly quartz with lesser amounts of plagioclase, carbonates and clay minerals. Carbonate minerals include siderite and dolomite/ankerite. Siderite was detected in all samples, ranging from trace to moderate amounts. Generally, if siderite occurred in greater than trace amounts, other carbonate minerals were not detected. The Fe-rich dolomite/ankerite is restricted to the upper portion of the fine-grained sandstone and the two coarser-grained units.

Clay Mineralogy

A. 5-20 μm size-fraction

Minerals identified in the 5-20 μm size fraction are quartz, feldspar and clays (Table 3.4a,b). Quartz is of major abundance in each lithology. Clays range in abundance from minor to moderate. Feldspars were detected in trace to minor amounts. Carbonates were not considered.

In the conglomerate and medium or coarse-grained sandstone, kaolinite is the most abundant clay mineral (85-95%), followed by illite (t-15%). Both illite/smectite and chlorite occur in minor or trace amounts. Within the fine-grained sandstone, illite (45-60%) is most abundant, with lesser amounts of kaolinite (20-45%), illite/smectite (2-15%) and chlorite (5-10%). Smectite was not detected.

TABLE 3.4a MINERALOGY 5-20 μm SIZE-FRACTION

SAMPLE NUMBER	ROCK TYPE	DEPTH (m)	Q	F	C	RELATIVE % CLAYS IS	SM	CL	I	K
6-17-32-2W5										
K87	Congl.	2133.4	M	t	M	nd	nd	t	mt	95
K88	M.Sst.	2134.2	M	m	mM	mt	nd	t	5	90
K90	F.Sst.	2136.3	M	m	mM	mt	nd	m	40	50
K92	F.Sst.	2142.5	M	m	mM	mt	nd	m	65	25
K93	Congl.	2146.7	M	m	mM	20	t	m	40	35
6-18-32-2W5										
K74	Congl.	2175.9	M	t	mM	t	nd	t	mt	95
K75	M.Sst.	2176.5	M	t	mM	t	nd	t	mt	95
K77	C.Sst.	2178.8	M	m	mM	t	t	t	5	90
K80	F.Sst.	2185.2	M	m	mM	10	t	m	60	20
K82	F.Sst.	2187.1	M	m	mM	nd	nd	10	70	20
K85	Congl.	2194.6	M	m	mM	mt	nd	mt	10	85
6-20-32-2W5										
K52	Congl.	2125.1	M	mt	M	t	nd	t	t	95
K53	F.Sst.	2125.5	M	t	mM	nd	nd	t	mt	95
K54	Congl.	2126.4	M	t	mM	mt	nd	t	10	85
K56	F.Sst.	2127.5	M	t	mM	mt	nd	t	25	70
K58	F.Sst.	2128.9	M	t	mM	t	t	mt	30	65
K61	F.Sst.	2131.2	M	t	mM	nd	nd	5	40	55
K62	Congl.	2134.1	M	t	mM	t	nd	t	mt	95
K63	F.Sst.	2134.6	M	t	mM	nd	nd	5	30	65
14-12-32-3W5										
K11	C.Sst.	2208.3	M	mt	M	t	nd	t	mt	95
K13	F.Sst.	2212.5	M	mt	mM	5	nd	10	60	25
K17	F.Sst.	2220.0	M	mt	mM	10	nd	10	65	15
16-14-32-3W5										
K162	Congl.	2207.4	M	m	M	nd	nd	t	mt	95
K163	C.Sst.	2208.0	M	t	M	nd	nd	t	m	90
K165	M.Sst.	2210.5	M	t	mM	nd	nd	5	50	45
K168	F.Sst.	2217.0	M	t	mM	m	nd	m	50	40
6-26-32-3W5										
K22	C.Sst.	2210.6	M	m	M	t	nd	t	mt	95
K26	F.Sst.	2215.3	M	nd	mM	mt	nd	mt	40	50
K29	Congl.	2218.3	M	m	mM	m	nd	mt	25	65
K31	F.Sst.	2219.9	M	m	m	10	nd	10	55	25
16-22-32-3W5										
K133	C.Sst.	2211.3	M	mM	M	nd	nd	nd	mt	95
K134	Congl.	2211.8	M	t	M	nd	nd	nd	mt	95
K136	M.Sst.	2213.7	M	t	M	t	nd	t	mt	95
K137	F.Sst.	2214.4	M	t	mM	mt	nd	5	45	45

TABLE 3.4a MINERALOGY 5-20 μm SIZE-FRACTION (CONTINUED)

SAMPLE NUMBER	ROCK TYPE	DEPTH (m)	Q	F	C	RELATIVE % CLAYS IS	SM	CL	I	K
6-25-32-3W5										
K149	Congl.	2187.1	M	t	mM	nd	nd	nd	mt	95
K151	Congl.	2189.1	M	mt	M	t	nd	t	mt	95
K152	C.Sst.	2189.4	M	mt	M	nd	nd	nd	mt	95
K153	F.Sst.	2190.4	M	mt	mM	mt	nd	mt	35	60
K154	F.Sst.	2192.6	M	mt	mM	mt	nd	mt	35	60
7-24V-32-4W5										
K155	C.Sst.	2296.5	M	m	mM	nd	nd	t	mt	95
K159	F.Sst.	2299.8	M	nd	mM	nd	nd	5	45	50
11-31-33-4W5										
K43	C.Sst.	2391.5	M	mM	M	mt	nd	mt	5	90
K44	Congl.	2393.0	M	t	M	t	nd	t	mt	95
K46	F.Sst.	2395.7	M	t	mM	5	nd	5	45	45
K48	F.Sst.	2402.1	M	t	mM	15	nd	5	30	50
16-10-32-3W5										
M1	Congl.	2215.3	M	t	mM	5	nd	5	15	75
M2	C.Sst.	2215.6	M	m	mM	nd	nd	nd	nd	M
M3	Congl.	2217.6	M	m	mM	nd	nd	nd	t	M
M4	C.Sst.	2218.4	M	m	mM	t	nd	m	15	80
M5	F.Sst.	2219.4	M	m	mM	5	nd	5	45	45
M6	C.Sst.	2217.2	M	m	mM	15	nd	10	40	35
M7	Congl.	2223.3	M	m	mM	t	nd	t	t	M
M8	F.Sst.	2226.3	M	m	mM	15	nd	10	45	30
M9	C.Sst.	2217.9	M	m	mM	nd	nd	nd	10	90
16-23-32-3W5										
M1	Congl.	2204.8	M	t	mt	nd	nd	t	t	M
M2	Congl.	2205.7	M	t	mM	nd	nd	nd	t	M
M3	C.Sst.	2206.4	M	m	mM	m	nd	t	10	85
M4	C.Sst.	2206.6	M	m	mM	nd	nd	t	t	M
6-24-32-3W5										
M1	C.Sst.	-	M	mt	mM	5	nd	5	20	70
M2	F.Sst.	-	M	t	mM	10	nd	5	60	25
M3	Congl.	-	M	t	mM	mt	nd	mt	10	80
M4	F.Sst.	-	M	t	mM	15	nd	10	55	20

TABLE 3.4b MINERALOGY >5 μm SIZE-FRACTION

SAMPLE NUMBER	ROCK TYPE	DEPTH (m)	Q	F	C	RELATIVE % CLAYS IS	SM	CL	I	K
6-19-32-2W5										
SP3	Congl.	2170.7	15	10	M	t	nd	mt	15	60
SP6	Congl.	2171.1	5	5	M	t	nd	t	5	85
SP21	M.Sst.	2173.2	mt	mt	M	t	t	mt	5	90
SP29	C.Sst.	2174.4	15	10	M	t	nd	mt	10	65
SP45	F.Sst.	2174.6	20	10	M	t	nd	5	50	15

B. 2-5 μm size-fraction

Minerals identified in the 2-5 μm size fraction are quartz, clay minerals and feldspar (Table 3.5). Quartz is major in abundance for each of the lithologies. Clay minerals were detected in minor or moderate amounts. Feldspars occur in minor or trace amounts. Carbonates were not analyzed.

In the conglomerate and medium or coarse-grained sandstone, kaolinite is the most abundant clay mineral (45-95%). Present in lesser quantities are illite (5-35%), chlorite and illite/smectite ($<$ 5%). Smectite was not detected. Within the fine-grained sandstone the relative abundance of illite and kaolinite range from 25-65%. Illite increases in abundance downsection. Other clay minerals include illite/smectite (nd-20%), chlorite (nd-10%) and smectite (nd-9%).

TABLE 3.5a MINERALOGY 2-5 μm SIZE-FRACTION

SAMPLE NUMBER	ROCK TYPE	DEPTH (m)	Q	F	C	RELATIVE % CLAYS IS	SM	CL	I	K
6-17-32-2W5										
K87	Congl.	2133.4	M	t	mM	m	nd	t	10	80
K88	M.Sst.	2134.2	M	mt	M	mt	nd	t	10	85
K90	F.Sst.	2136.3	M	mt	mM	mt	nd	mt	30	65
K92	F.Sst.	2142.5	M	mt	mM	m	nd	m	60	20
K93	Congl.	2146.7	M	mt	mM	20	nd	5	50	25
6-18-32-2W5										
K74	Congl.	2175.9	M	mt	M	t	nd	t	5	90
K75	M.Sst.	2176.5	M	t	M	t	nd	t	mt	95
K77	C.Sst.	2178.8	mM	m	M	t	nd	t	5	90
K80	F.Sst.	2185.2	M	m	mM	m	t	m	55	25
K82	F.Sst.	2187.1	M	m	mM	nd	nd	20	56	15
K85	Congl.	2194.6	M	m	mM	15	nd	5	40	40
6-20-32-2W5										
K52	Congl.	2125.1	M	mt	mM	nd	nd	nd	5	95
K53	F.Sst.	2125.5	M	t	mM	t	nd	t	m	90
K54	Congl.	2126.4	M	t	mM	mt	nd	t	15	80
K56	F.Sst.	2127.5	mM	t	mM	nd	nd	t	mM	75
K58	F.Sst.	2128.9	mM	t	mM	nd	nd	mt	25	70
K61	F.Sst.	2131.2	M	t	mM	10	nd	5	40	45
K62	Congl.	2134.1	M	t	mM	5	nd	mt	15	75
K63	F.Sst.	2134.6	M	t	mM	nd	nd	5	40	55
14-12-32-3W5										
K11	C.Sst.	2208.3	mM	t	M	mt	nd	t	5	90
K13	F.Sst.	2212.5	M	t	mM	m	nd	mt	45	40
K17	F.Sst.	2220.0	M	t	mM	15	nd	10	60	15
16-14-32-3W5										
K162	Congl.	2207.4	M	m	M	nd	nd	t	m	90
K163	C.Sst.	2208.0	M	t	M	5	nd	t	10	80
K165	M.Sst.	2210.5	M	t	mM	mt	t	mt	40	55
K168	F.Sst.	2217.0	M	t	mM	15	nd	m	40	35
6-16-32-3W5										
K22	C.Sst.	2210.6	M	mt	M	mt	nd	mt	10	85
K26	F.Sst.	2215.3	M	t	mM	5	nd	5	50	40
K29	Congl.	2218.3	M	mt	mM	5	nd	t	20	70
K31	F.Sst.	2219.9	M	mt	mM	nd	nd	m	70	20
16-22-32-3W5										
K133	C.Sst.	2211.3	M	mM	M	mt	nd	t	mt	95
K134	Congl.	2211.8	mM	t	M	mt	nd	t	5	90
K136	M.Sst.	2213.7	M	t	M	t	nd	t	mt	95
K137	F.Sst.	2214.4	M	t	mM	5	nd	5	40	50

TABLE 3.5a MINERALOGY 2-5 μm SIZE-FRACTION (CONTINUED)

SAMPLE NUMBER	ROCK TYPE	DEPTH (m)	Q	F	C	RELATIVE % CLAYS IS	SM	CL	I	K
6-25-32-3W5										
K149	Congl.	2187.1	M	t	mM	nd	nd	nd	5	95
K151	Congl.	2189.1	M	t	M	mt	nd	t	5	90
K152	C.Sst.	2189.4	M	t	M	mt	nd	t	5	90
K153	F.Sst.	2190.4	M	t	mM	nd	nd	mt	35	60
K154	F.Sst.	2192.6	M	t	mM	5	nd	mt	30	60
7-24V-32-4W5										
K155	C.Sst.	2296.5	M	mM	M	nd	nd	5	10	85
K159	F.Sst.	2299.8	M	t	mM	nd	nd	5	40	55
11-31-33-4W5										
K43	C.Sst.	2391.5	mM	t	M	t	nd	mt	10	85
K44	Congl.	2393.0	M	t	mM	mt	nd	mt	5	90
K46	F.Sst.	2395.7	M	t	M	m	nd	m	40	45
K48	F.Sst.	2402.1								
16-10-32-3W5										
M1	Congl.	2215.3	M	mt	m	t	nd	nd	t	M
M2	C.Sst.	2215.6	M	t	mM	t	nd	nd	mM	80
M3	Congl.	2217.6	M	mt	m	t	nd	nd	t	M
M4	C.Sst.	2218.4	M	mt	m	mt	nd	mt	5	90
M5	F.Sst.	2219.4	M	mt	m	10	nd	5	35	50
M6	C.Sst.	2217.2	M	mt	m	15	nd	10	30	45
M7	Congl.	2223.3	M	mt	m	m	nd	m	25	65
M8	F.Sst.	2226.3	M	mt	m	20	nd	10	40	30
M9	C.Sst.	2217.9	M	mt	m	mt	nd	mt	15	80
16-23-32-3W5										
M1	Congl.	2204.8	M	mM	mM	mt	nd	t	10	85
M2	Congl.	2205.7	M	t	mM	5	nd	5	20	70
M3	C.Sst.	2206.4	M	t	mM	t	nd	nd	t	M
M4	C.Sst.	2206.6	M	t	mM	t	nd	t	mt	95
6-24-32-3W5										
M1	C.Sst.	-	M	t	mM	5	nd	5	20	70
M2	F.Sst.	-	M	t	mM	15	nd	5	30	50
M3	Congl.	-	M	t	mM	mt	nd	mt	15	80
M4	F.Sst.	-	M	t	mM	15	nd	10	50	25

TABLE 3.5b MINERALOGY < 5 μm FRACTION

SAMPLE NUMBER	ROCK TYPE	DEPTH (m)	Q	F	C	RELATIVE % CLAYS IS	SM	CL	I	K
6-19-32-2W5										
SP3	Congl.	2170.7	15	10	M	t	nd	mt	15	60
SP6	Congl.	2171.1	5	5	M	t	nd	t	5	85
SP21	M.Sst.	2171.2	mt	mt	M	t	t	t	5	90
SP29	C.Sst.	2174.3	15	10	M	t	nd	t	10	65
SP45	F.Sst.	2177.6	20	10	M	t	nd	5	50	15

C. <2 μm size-fraction

Minerals identified in the <2 μm size-fraction are clay minerals, quartz and feldspar (Table 3.6). Carbonates were not considered here. Clay minerals are major in abundance; quartz varies from moderate to major in abundance. Feldspar occurs in minor or trace amounts.

In the conglomerate and medium or coarse-grained sandstone kaolinite is the most abundant clay mineral (25-70%), with lesser amounts of illite (20-45%). Other clay minerals include illite/smectite (5-15%) (> 50% illite layers), chlorite (5-10%) and smectite (nd-10%). Within the fine-grained sandstone illite (30-65%) is the most abundant clay mineral, with lesser amounts of kaolinite (20-45%). Other clay minerals include illite/smectite (5-25%), chlorite (5-10%) and smectite (nd-5%).

The kaolin group mineral was examined in greater detail using X-ray powder camera techniques. In one sample, the polytype identified is dickite (Dean et al., 1983). Other samples were comprised mostly of kaolinite.

TABLE 3.6 MINERALOGY < 2 μm SIZE-FRACTION

SAMPLE NUMBER	ROCK TYPE	DEPTH (m)	Q	F	C	RELATIVE % CLAYS IS	SM	CL	I	K
6-17-32-2W5										
K87	Congl.	2134.2								
K88	M.Sst.	2134.2	M	t	M	m	t	mt	25	65
K90	F.Sst.	2136.3	M	t	M	m	nd	m	50	35
K92	F.Sst.	2142.5	M	t	M	15	nd	m	70	5
K93	Congl.	2146.7	M	t	M	20	nd	15	60	5
6-18-32-2W5										
K74	Congl.	2175.9	M	m	M	m	m	mt	35	45
K75	M.Sst.	2176.5	M	mt	M	m	mt	t	25	60
K77	C.Sst.	2178.8	M	t	M	mt	t	t	20	70
K80	F.Sst.	2185.2	M	t	M	15	nd	m	70	10
K82	F.Sst.	2187.1	M	t	M	15	t	m	75	5
K85	Congl.	2194.6								
6-20-32-2W5										
K52	Congl.	2125.1	M	t	M	m	t	m	30	60
K53	F.Sst.	2125.5	M	nd	M	mt	nd	m	20	75
K54	Congl.	2126.4	M	nd	M	m	t	m	50	45
K56	F.Sst.	2127.5	M	nd	M	m	nd	mt	50	40
K58	F.Sst.	2128.9	M	nd	M	m	t	m	50	40
K61	F.Sst.	2131.2	M	nd	M	m	nd	t	60	30
K62	Congl.	2134.1	M	nd	mM	mM	nd	mt	55	25
K63	F.Sst.	2134.6	M	nd	mM	m	nd	m	65	20
14-12-32-3W5										
K11	C.Sst.	2208.3	m	t	M	m	nd	m	40	40
K13	F.Sst.	2212.5	m	nd	M	m	nd	m	65	20
K17	F.Sst.	2220.0	m	nd	M	15	nd	m	70	5
16-14-32-3W5										
K162	Congl.	2207.4	M	m	M	10	nd	nd	20	70
K163	C.Sst.	2208.0	M	mt	M	m	t	m	30	55
K165	M.Sst.	2210.5	M	mt	M	m	t	m	50	30
K168	F.Sst.	2217.0	M	mt	M	20	t	m	65	10
6-16-32-3W5										
K22	C.Sst.	2210.6	M	t	mM	10	nd	5	35	50
K26	F.Sst.	2215.3	M	t	M	10	nd	m	60	20
K29	Congl.	2218.3	M	t	M	15	t	m	55	25
K31	F.Sst.	2219.9			mM	20	t	m	70	m
16-22-32-3W5										
K133	C.Sst.	2211.3	M	mM	M	m	t	mt	20	65
K134	Congl.	2211.8	M	m	M	m	t	mt	30	60
K136	M.Sst.	2213.7	M	m	M	m	t	mt	20	65
K137	F.Sst.	2214.4	M	m	M	10	nd	5	60	25

TABLE 3.6 MINERALOGY < 2 μm SIZE-FRACTION (CONTINUED)

SAMPLE NUMBER	ROCK TYPE	DEPTH (m)	Q	F	C	RELATIVE % CLAYS IS	SM	CL	I	K
6-25-32-3W5										
K149	Congl.	2187.1	M	t	M	5	nd	mt	30	60
K151	Congl.	2189.1	M	t	M	t	m	mt	20	65
K152	C.Sst.	2189.4	M	t	M	mt	mt	mt	20	70
K153	F.Sst.	2190.4	M	t	M	m	t	m	60	25
K154	F.Sst.	2192.6	M	t	M	m	nd	mt	50	40
7-24V-32-4W5										
K155	C.Sst.	2296.5	M	t	M	nd	t	mM	30	55
K159	F.Sst.	2299.8	M	t	M	m	t	m	55	25
11-31-33-4W5										
K43	C.Sst.	2391.5	M	t	M	5	nd	10	25	60
K44	Congl.	2393.0	M	t	M	m	m	10	25	50
K46	F.Sst.	2395.7	M	t	M	mt	m	m	65	20
K48	F.Sst.	2402.1	M	t	mM	20	nd	10	40	30
16-10-32-3W5										
M1	Congl.	2215.3	M	t	M	15	nd	5	45	35
M2	C.Sst.	2215.6	mM	mt	M	5	nd	5	20	70
M3	Congl.	2217.6	M	mM	M	10	nd	10	20	60
M4	C.Sst.	2218.4	M	mM	M	10	nd	5	30	55
M5	F.Sst.	2219.4	M	mM	M	10	nd	10	25	55
M6	C.Sst.	2217.2	M	mM	M	15	nd	10	30	45
M7	Congl.	2223.3	M	mM	M	15	nd	10	30	45
M8	F.Sst.	2226.3	M	mM	M	20	nd	10	50	20
M9	C.Sst.	2217.9	M	mM	M	10	nd	5	35	50
16-23-32-3W5										
M1	Congl.	2204.8	M	t	mM	10	nd	5	40	45
M2	Congl.	2205.7	mM	t	M	5	20	5	40	25
M3	C.Sst.	2206.4	mM	t	M	10	nd	5	30	55
M4	C.Sst.	2206.6	mM	t	M	10	nd	5	35	50
6-24-32-3W5										
M1	C.Sst.	-	M	mt	M	10	nd	10	35	45
M2	F.Sst.	-	M	mt	M	10	nd	10	65	15
M3	Congl.	-	M	mt	M	10	nd	5	30	55
M4	F.Sst.	-	M	mt	M	5	nd	10	60	25

D. SCANNING ELECTRON MICROSCOPY

Twenty-three samples have been examined using the scanning electron microscope (Table 3.1). The objectives of this portion of the study are to determine the nature and distribution of the pore-lining and pore-filling minerals and to estimate the size and shape of pore-throats.

Conglomerate

The main characteristics of the conglomerate are summarized in Figure 3.5. This conglomerate is poorly sorted, averages 12% porosity (moderate to poorly developed, Fig. 3.5a) and has an average pore-throat diameter of 55 μm. The two main authigenic minerals identified are quartz and kaolinite. Authigenic quartz is present as either small prismatic crystals on the crystal faces delineating pore spaces or as quartz overgrowths (Fig. 3.5b). The kaolinite, which is a pore-filling, formed as large pseudohexagonal crystals averaging 15 μm in diameter (Fig. 3.5d,e,f). Authigenic illite and illite/smectite, which were identified in minor or trace amounts, occurs as small fibrous networks of crystals on grain surfaces (Fig. 3.5h) or as pore-throat bridges (Fig. 3.5c). Carbonate minerals, pyrite (Fig. 3.5c,d,g) and feldspar were also observed.

Medium or Coarse-grained Sandstone

The major features of the medium or coarse-grained sandstone are summarized in Figure 3.6. This sandstone is moderate to well sorted, averages 10% porosity (Fig. 3.6a) and has an average pore-throats diameter of 25 μm. The two main authigenic minerals identified in this unit are kaolinite and quartz. The kaolinite, which occurs as a pore-filling, forms pseudohexagonal crystals ranging from 10-15 μm in diameter (Fig. 3.6 b,c,d). The authigenic quartz formed either small prismatic crystals, on the grain surfaces delineating the pore-spaces, (Fig. 3.6e,f) or as overgrowths. Illite and illite/smectite, which occurs in minor or trace amounts, forms a pore-lining consisting of a fibrous honeycomb-like structure (Fig. 3.6 g). Smectite, which ranges from trace to not detected in abundance, also occurs as a pore-lining (Fig. 3.6h). Minor amounts of pyrite and carbonate are also present. Carbonate occurs as siderite (Fig. 3.6 e,f), ankerite (Fig. 3.7 a,b) and possibly Fe-rich dolomite.

Figure 3.5 Conglomerate

A. Sample M3, well 16-10-32 3W5, showing poor sorting and moderately developed porosity. Authigenic quartz (AQ) and pore-filling kaolinite (K) are visible. Depth 2217.6 m.

B. Sample M3, well 6-25-32 3W5, showing authigenic quartz (AQ) which is present as either small prismatic crystals (druzy quartz), which forms on grain surfaces, or as overgrowths. Depth 2189.2 m.

C. Sample M7, well 16-10-32 3W5, showing pore bridging illite or illite/smectite and dolomite. Depth 2223.3 m.

D. Sample M7, well 16-10-32 3W5, showing pore filling kaolinite (K) and carbonate (Ca). Depth 2223.3 m.

E. Sample M3, well 16-10-32 3W5, showing well developed kaolinite (K) overlying authigenic quartz (AQ). Depth 2217.6m.

F. Sample M2, well 16-23-32 3W5 showing well developed kaolinite (K) booklets, with individual crystals which exceed 20 μm in diameter. Depth 2205.7 m.

G. Sample M3, well 16-13-32 3W5, showing framboidal pyrite (PI), authigenic quartz (AQ), pore-lining illite (I) and pore-filling kaolinite (K). Depth 2186.6 m.

H. Sample M3, well 16-13-32 3W5, showing illite (I) or illite/smectite (IS) which forms a fibrous network on grain surfaces. Depth 2186.8 m.

A
AQ
k

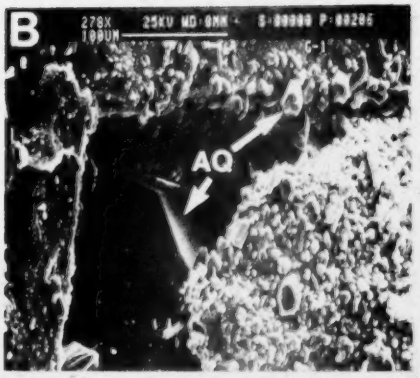
B
AQ

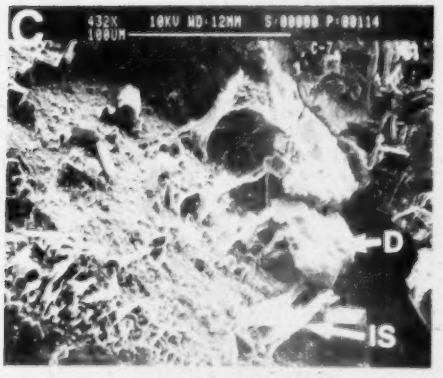
C
D
IS

D
k
C

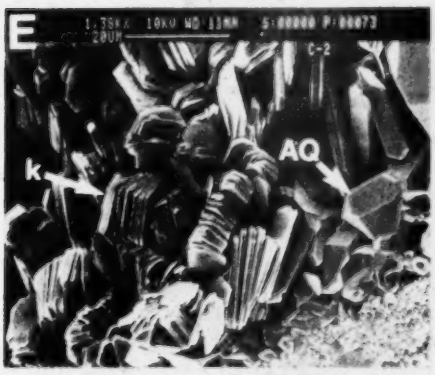
E
k
AQ

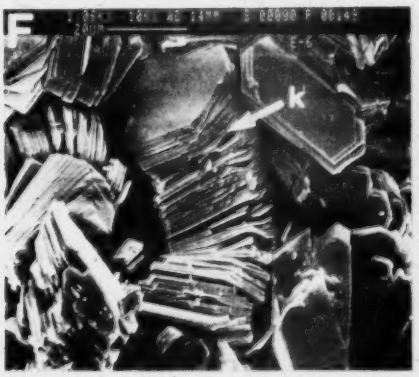
F
k

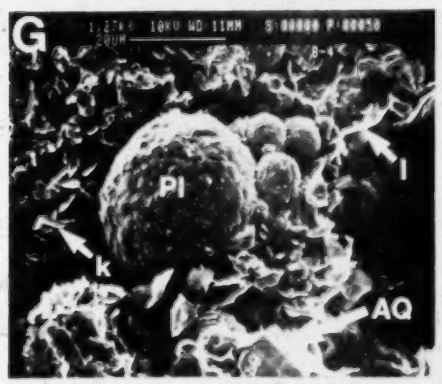
G
PI
I
k
AQ

H
I

Figure 3.6 Medium or Coasre-grained Sandstone

A. Sample M6, well 16-10-32 3W5, showing moderate to good sorting. The primary porosity is reduced as a result of the formation of abundant authigenic minerals within the pores and pore-throats. Depth 2217.2 m.

B. Sample M1, well 16-10-32 3W5, showing pore lining kaolinite (K). Depth 2164.7 m.

C. Sample M4, well 16-10-32 3W5, showing pore-lining and pore-filling kaolinite (K). Depth 2218.4 m.

D. Sample M3, well 6-25-32 3W5, showing large well formed pseudohexagonal kaolinite (K) crystals. Depth 2189.5 m.

E. Sample M1, well 16-13-32 3W5, showing pore-lining quartz (AQ) and siderite (S). Depth 2184.7 m.

F. Sample M1, well 16-13-32 3W5, showing what may be large euhedral siderite crystals (S) forming on grain surfaces, in association with authigenic quartz (AQ). Depth 2184.7 m.

G. Sample M4, well 16-13-32 3W5, showing fibrous honeycomb shaped net works of illite (I) and illite/smectite (IS). Late forming kaolinite booklet (K) on illite/smectite (IS). Depth 2187.9 m.

H. Sample M5, well 16-13-32 3W5, showing fibrous smectite (SM) which forms on grain surfaces. Depth 2188.6 m.

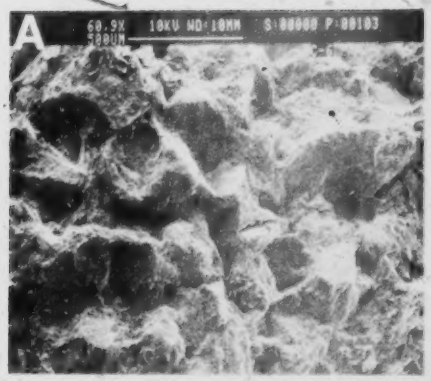
A

B
k

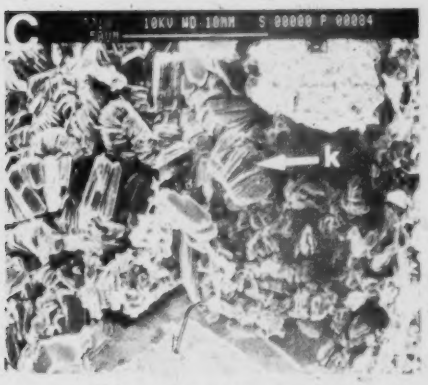
C
k

D
k

E
AQ
S

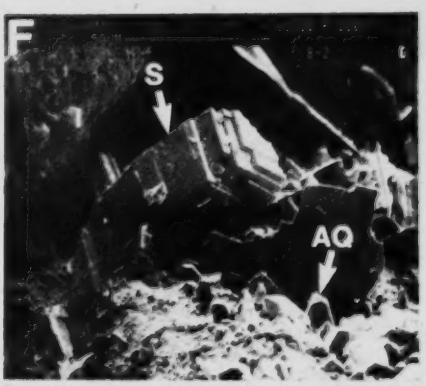
F
S
AQ

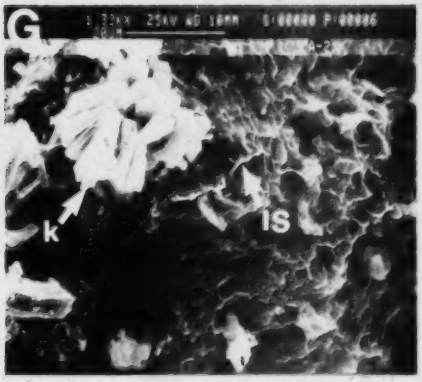
G
k
IS

H
SM

Figure 3.7 Carbonate Cements

A. Sample K88, medium or coarse-grained sandstone showing ankerite (An) cement. Well 6-17-32 2W5, depth 2134.2 m.

B. Sample K88, energy dispersive analyzer for the ankerite seen in Figure 3.7A. Run at 20 Kv.

C. Sample K90, fine-grained sandstone showing siderite (S) and Fe-rich dolomite (D). Illite/smectite (IS) is shown in close proximity to the siderite (S). Well 6-17-32 2W5, depth 2136.3 m.

D. Sample K90, energy dispersive analyzer for the siderite (S) shown in Figure 3.7C. Note, the high Al and Si are a result of scatter associated with the illite/smectite (IS). Run at 20 Kv.

E. Sample K90, energy dispersive analyzer for the Fe-rich dolomite (D) shown in Figure 3.7C. Note, the background was matched with Figure 3.7D to allow direct comparison. Run at 20 Kv.

A
An

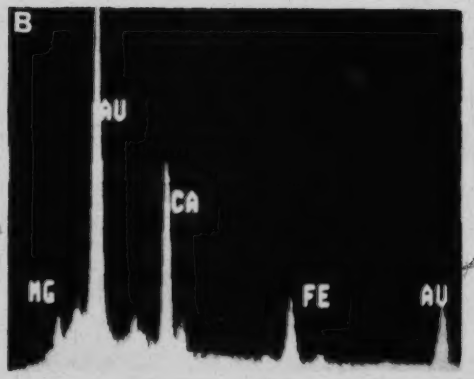
B
AU
CA
MG
FE
AU

C
D
S
IS

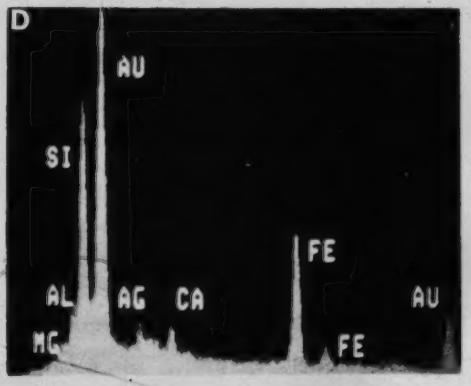
D
AU
SI
FE
AL
AG
CA
AU
MG
FE

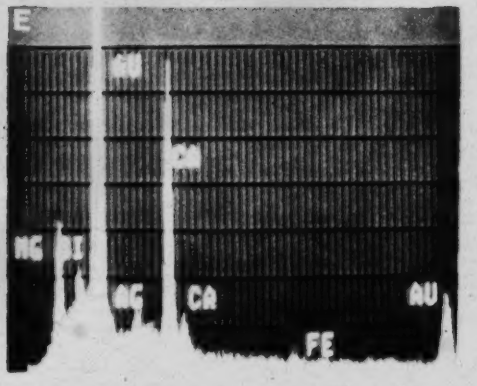
E
AU
CA
MG
SI
AG
CA
AU
FE

Fine-grained Sandstone

The main characteristics of the fine-grained sandstone are summarized in Figure 3.8. This sandstone is well sorted, averages <2% porosity and has an average pore-throat diameter of 15 μm. The low porosity within this unit results from the extensive development of authigenic pore-lining and pore-filling minerals (Fig. 3.8a). The most abundant of the authigenic clay minerals is pore-lining illite (Fig. 3.8 b,d,e,f,g,h), which is a late phase coating authigenic quartz (Fig. 3.8 f,g). Kaolinite, which occurs as pore-lining, is less abundant than illite and forms pseudohexagonal crystals ranging from 5-7μm in diameter (Fig. 3.8b). Also identified in minor quantities are feldspar, pyrite and carbonate. The carbonate minerals include siderite (S) (Fig. 3.7c,d), Fe-rich dolomite (D) (Fig. 3.7c,e) and possibly ankerite.

Figure 3.8 Fine-grained Sandstone

A. Sample M5, well 16-10-32 3W5 showing extensive pore-lining and pore-filling minerals, which results in low permeability. Depth 2219.4 m.

B Sample M8, well 16-13-32 3W5, showing pore-lining illite (I) and pore-filling kaolinite (K). Depth 2196.7 m.

C. Sample M8, well 16-13-32 3W5, showing authigenic pore-lining quartz (AQ). Depth 2196.7 m.

D. Sample M4, well 16-22-32 3W5, showing illite (I) forming on grain surface. Depth 2215.5 m.

E. Sample M5, well 16-10-32 3W5, showing the fibrous habit of pore-lining illite (I). Depth 2219.4 m.

F. Sample M8, well 16-13-32 3W5, showing pore-lining authigenic quartz (AQ) and illite (I). Depth 2196.7 m.

G. Sample M5, well 16-10-32 3W5, showing pore-lining illite (I) and late pore-filling kaolinite (K). Depth 2219.4 m.

H. Sample M8, well 16-10-32 3W5, showing pore-lining and pore-bridging illite (I). Depth 2226.3 m.

A
B
l
k
C
AQ
D
l
E
F
AQ
G
l
k
H
l

E. DIAGENESIS

Diagenesis can be divided into early and late stages. Early diagenesis occurs in the upper 30-40 metres of the sediment column, extending to the depth at which methane generating microrganisms (methanogens) cease activity. This early stage of diagenesis can be further subdivided into oxic and anoxic conditions (Berner, 1981). In the Cretaceous seaway, the oxic/anoxic boundary generally occurred at or below the sediment/water interface (Gautier, 1983) as little or no evidence of aerobic oxidation (oxic diagenesis) has been preserved. The anoxic conditions consist of a sulfate reduction zone and a zone of carbonate reduction/methane generation (Rice and Claypool, 1981). Within the sulfate reduction zone sulfidic conditions result from the bacterial reduction of the sulfate, which accompanies anaerobic oxidation of organic matter (Goldhaber and Kaplan, 1974). In the presence of excess aqueous sulfide, the monosulfides which formed initially commonly transform into framboidal pyrite (Gautier, 1983). Also derived from the anaerobic oxidation of organic matter is bicarbonate which may precipitate as a carbonate in the sulfate reduction zone. Within the carbonate reduction/methane generation zone carbondioxide from both the overlying sulfate reduction zone and sea water may be consumed in the precipitation of minerals such as siderite, vivianite and rhodocrosite (Berner, 1981). In marine sediments these minerals occur with dolomite and iron-bearing carbonates (Kelts and McKenzie, 1982).

Late diagenesis, which encompasses burial, uplift and/or recharge by meteoric water is marked by the change from microbial processes and mechanical dewatering to thermal transformations. The lower limit of this zone occurs at a depth where temperature and pressure are sufficient for metamorphism to occur.

During early diagenesis the Viking Formation in the Harmattan East field existed in anoxic conditions, characterized by an excess of organic matter (Claypool and Kaplan, 1974). The presence of framboidal pyrite and siderite indicates that the Viking Formation passed through both the sulfate reduction and carbonate reduction/methane generation zones of early diagenesis. Dolomite and ankerite were also identified; however, it is difficult to determine if these carbonates formed during early diagenesis or in conjunction with clay transformations during late diagenesis (Fig. 3.9). Quartz overgrowths may also have formed during both early and late stages of diagenesis, as a result of pressure solution and mineral transformations, respectively (Fig. 3.9).

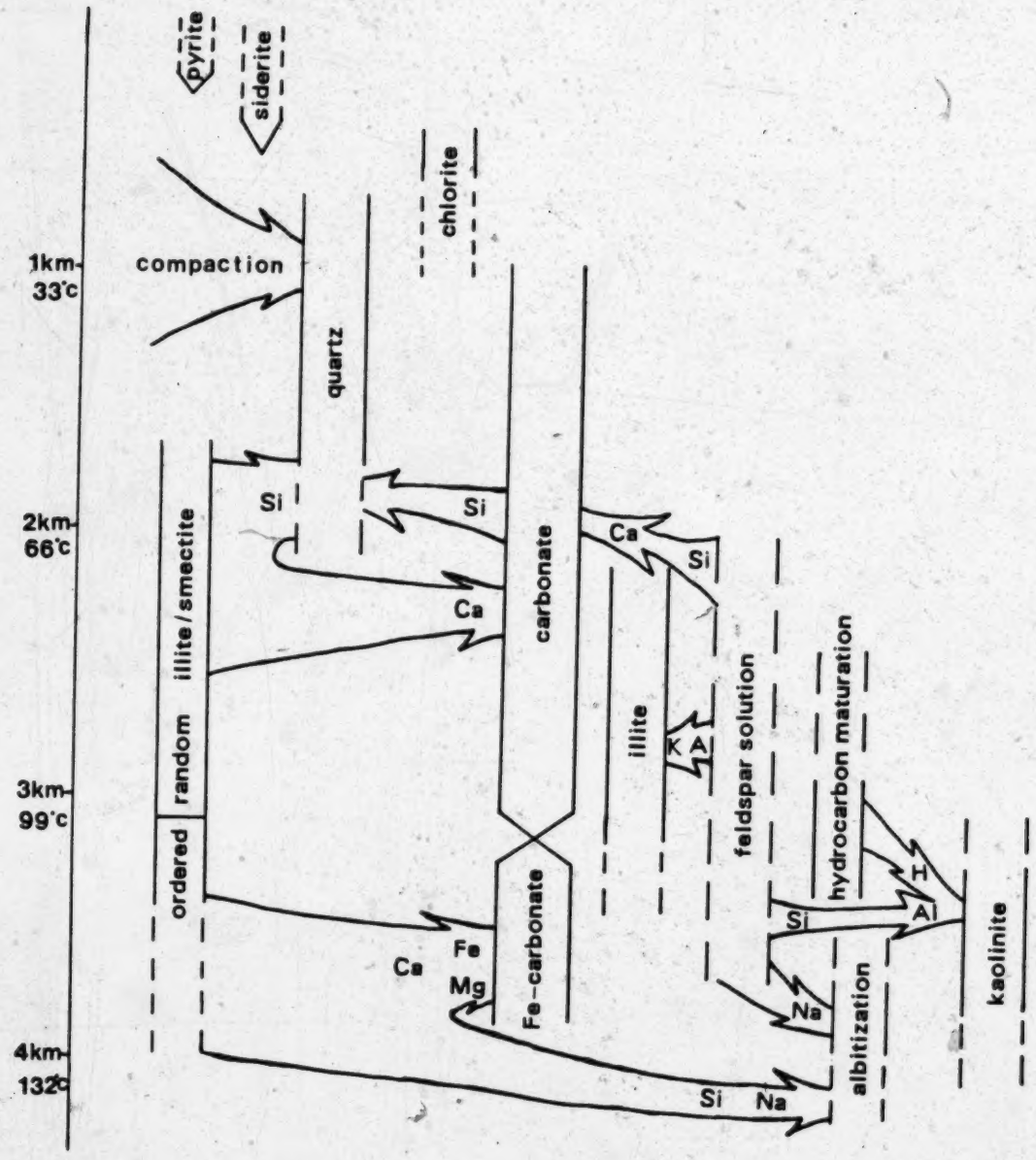

Figure 3.9 Diagenetic Model

(after Perry and Hower, 1970; Hower et al., 1976 ; Boles and Franks, 1979 and Boles, 1981)

Quartz overgrowths can form over a wide temperature range (50-100°C), with the upper limit occurring when SiO_2 is consumed in the formation of authigenic minerals such as albite (Boles, 1981). Carbonate may also occur over a wide temperature range (20-150°C), with the early carbonates precipitating from sea water or early pore fluids. The late carbonates (e.g., ankerite) may form as a result of complex mineral transformations which occur during late diagenesis. The illitization of smectite can provide the necessary Ca, Fe and Mg, with the Fe and Mg being released at $>$ 100°C (Boles and Franks, 1979) (Fig. 3.9).

The chlorite which occurs in trace amounts has probably formed early, prior to other authigenic clay minerals. This chlorite may occur as a simple transformation of biotite (noted in thin-section) and as an early authigenic clay mineral. Early authigenic chlorite, enveloped by prismatic quartz crystals, was identified within the Viking Formation in the Gilby field.

During late diagenesis a series of transformations occur within the clay minerals; these are discussed in an order which approximates the diagenetic sequence. The illite is believed to have formed from the recrystallization of detrital clays at the same time as the illite/smectite transformation was occurring. This transformation,

(1) $3.93K^{+} + 1.57$ smectite $\longrightarrow$ illite $+ 1.57Na^{+} + 3.14Ca^{2+} + 4.28Mg^{2+} + 4.78Fe^{3+} + 24.66Si^{4+} + 57O^{2-} + 15.7H_2O$ (Boles, 1981),

begins at approximately 60°C (Perry and Hower, 1970; Hower et al., 1976 and Boles, 1981) and shows an increase in illite layers with increased depth of burial. This transformation requires a source of K such as the leaching of K-feldspars. However, as little K-feldspar has been identified in the study area it is proposed that K has been leached elsewhere and transported into this system by pore fluids. As the illite/smectite transformation progresses the more aluminous smectite layers will be the first to react, followed by those which are Fe and Mg rich (Boles and Franks, 1979) (Fig. 3.9). The Fe and Mg rich smectite layers do not break down until the illite/smectite becomes ordered, about 100°C (Boles, 1981). This transformation releases Fe, Mg, Ca, Si and Na (Fig. 3.9). The Ca, Si and Na may be consumed by the formation of carbonates, quartz overgrowths and the albitization of feldspars. The Mg and Fe may be used in the ankeritization process (Fig. 3.9).

The large quantity of kaolinite may have formed from a variety of sources including precipitation from solution, transformation of feldspars and recrystallization of detrital clays. The precipitation of kaolinite from solution may be associated with the illite/smectite

transformation within the surrounding shales (eqn. 1). This transformation provides the necessary cations which are transported by the low pH fluid expelled from the shale. The extent to which this process will occur is questionable, as both the decarboxylation reactions and the illite/smectite transformation occur during late diagenesis, following migration of most compaction-expelled water. A second alternative is the complex transformation of feldspar to kaolinite, as follows:

(2) $2KAlSi_3O_8 + 2H^+ + 9H_2O \longrightarrow Al_2Si_2O_5(OH)_4 + 4H_4SiO_4 + 2K^+$ (Land and Milliken, 1981)

(3) $CaAl_2Si_2O_8 + 2H^+ + H_2O \longrightarrow Al_2Si_2O_5(OH)_4 + Ca^{2+}$ (Land and Milliken, 1981)

(4) $2NaAlSi_3O_8 + 2H^+ + H_2O \longrightarrow Al_2Si_2O_5(OH)_4 + 4SiO_2 + 2Na^+$ (Hutcheon, 1981)

These transformations of K-feldspar and plagioclase can release K, Ca, Na and Si (eqn. 2,3,4). The K may be used in the illite/smectite transformation (eqn. 1). Calcium may be used to form carbonate cement. The Si may be consumed to form quartz overgrowths or in conjunction with the Na in the albitization of plagioclase (eqn. 5), depending on the formation conditions.

The presence of minor amounts of albite suggests that albitization of feldspars may have occurred during late diagenesis. The main problem associated with this process is the large quantities of Na which are required, as shown by equation 5:

(5) $CaAl_2Si_2O_8 + 2Na^+ + 4H_4SiO_4 \longrightarrow 2NaAlSi_3O_8 + Ca^{2+} + 8H_2O$ (Land and Milliken, 1981).

However, most feldspar within the Viking Formation was identified as oligoclase (An_{10-30}), which would require smaller amounts of Na than indicated in eqn. 5. Three possible sources for the Na are the transformation of plagioclase to kaolinite (eqn. 4), illitization of smectite (eqn. 1) and/or the presence of Na-rich pore water (connate water) (Middleton, 1972).

The present formation conditions could not initiate the diagenetic sequence which was observed. This would suggest that the maximum burial depth of the Viking Formation was substantially greater than present day. Cretaceous formations such as the Viking may have had maximum burial depths of 3600 metres and formation temperatures of 149°C (Magara, 1976). Evidence which suggests these formation conditions are albitization, the illite/smectite transformation and the presence of hydrocarbons. Generally the albitization process is considered to occur at depths greater than 3400 metres, with temperatures in excess of 120°C (Middleton, 1972; Milliken et al., 1981; Land and Milliken, 1981 and Boles, 1981). The illite/smectite transformation has produced a regularly interstratified mixed-layer clay with >50% illite layers indicating a formation temperatures of >100°C. Finally, hydrocarbon

maturation and emplacement from the adjacent shales has occurred indicating a higher formation temperature than present day.

In summary, the Viking Formation has undergone both early and late stages of diagenesis. Early diagenesis is characterized by a variety of cements including pyrite and siderite. Evidence of this stage of diagenesis, predominately siderite cement, is well preserved within the lower portion of the fine-grained sandstone. The zones of siderite cement may represent fluctuations in the energy of the depositional environment, with low energy favouring the formation of siderite. Finally, the formation of quartz overgrowths within the lower sandstone unit further reduced permeability, thereby limiting subsequent diagenetic reactions.

The upper portion of the sandstone was not totally cemented at the end of the early diagenetic stage because of a higher depositional energy which inhibited the formation of pyrite and siderite cements. This sandstone has followed the same diagenetic sequence as the overlying coarse-grained sandstone and conglomerate. The formation of quartz overgrowths as a result of compaction did not severely reduce permeability, allowing the complex transformations of late diagenesis to occur. As the depth of burial increases the main driving force for the quartz overgrowths changed from compaction to the illitization of smectite. The Ca which is released in association with the Si may form carbonate cement, possibly dolomite. Also, fluid migration in conjunction with increased temperature and pressure results in the formation of authigenic clays. Pore-lining illite and illite/smectite was followed by pore-filling kaolinite, a result of the change from alkaline to acidic conditions. This change in pH is a result of the degradation of organic matter within the surrounding shales. Also, with increasing temperature the illite/smectite becomes ordered, releasing Fe and Mg for the ankeritization of the dolomite. The final stage of diagenesis may be the albitization of plagioclase feldspar. The diagenetic sequence is halted at this level within the reservoir rock containing hydrocarbons.

IV. RESERVOIR STUDY

A. HARMATTAN EAST RESERVOIR

This Viking reservoir is a stratigraphic trap in which the porous reservoir rocks are conglomerate and medium or coarse-grained sandstone. The trap is sealed by the overlying Lloydminster Shales, which act as a cap, and by the lateral thinning of the reservoir rock itself into fine-grained lithologies. The base of the reservoir is constrained by the low permeability of the fine-grained sandstone and the underlying Joli Fou Shales.

Hydrocarbons found within the Viking Formation are inferred to have originated from sediments within the Colorado Group (Deroo et al., 1977). The principal phase of hydrocarbon genesis occurred during the late Cretaceous, at maximum burial. The significance of this timing is that the oil formed when traps were available and that oil emplacement was a function of both the trapping mechanism(s) and communication between the reservoir and source rocks.

The configuration and lateral distribution of the producing horizons in the Harmattan East field are the result of depositional processes. The boundaries of the conglomerate extend from the north of Township 32, south to Township 30 (Fig. 4.1). The east/west boundaries, which are tentative, extend from Range 2 to Range 4, Township 32. The economically produceable portion of this Viking reservoir is approximated by the 2.0 metre isopach contour for the conglomerate (Fig. 4.6).

Hydrocarbon production in this reservoir is primarily from the conglomerate horizon. This horizon consists of three laterally continuous zones of conglomerate (Fig. 4.2, 4.3), each having high porosity (12%) and permeability (20-70 md) (Fig. 4.4). These zones are separated by pebbly sandstones of relatively low permeability (< 3 md). The conglomerate horizon attains its maximum thickness (4.5 metres) along the axis of the trough within the Harmattan East field. Moving laterally (north/south) from the trough each of the thick conglomerates grades into a series of fining-upward beds. A reduced thickness and vertical variations in porosity and permeability result from this change in depositional pattern.

Of secondary importance to hydrocarbon production is the medium or coarse-grained sandstone which lies below the conglomerate horizon. This sandstone has an average porosity of 10% but variable permeability (2-20 md), a result of authigenic cements. Low vertical

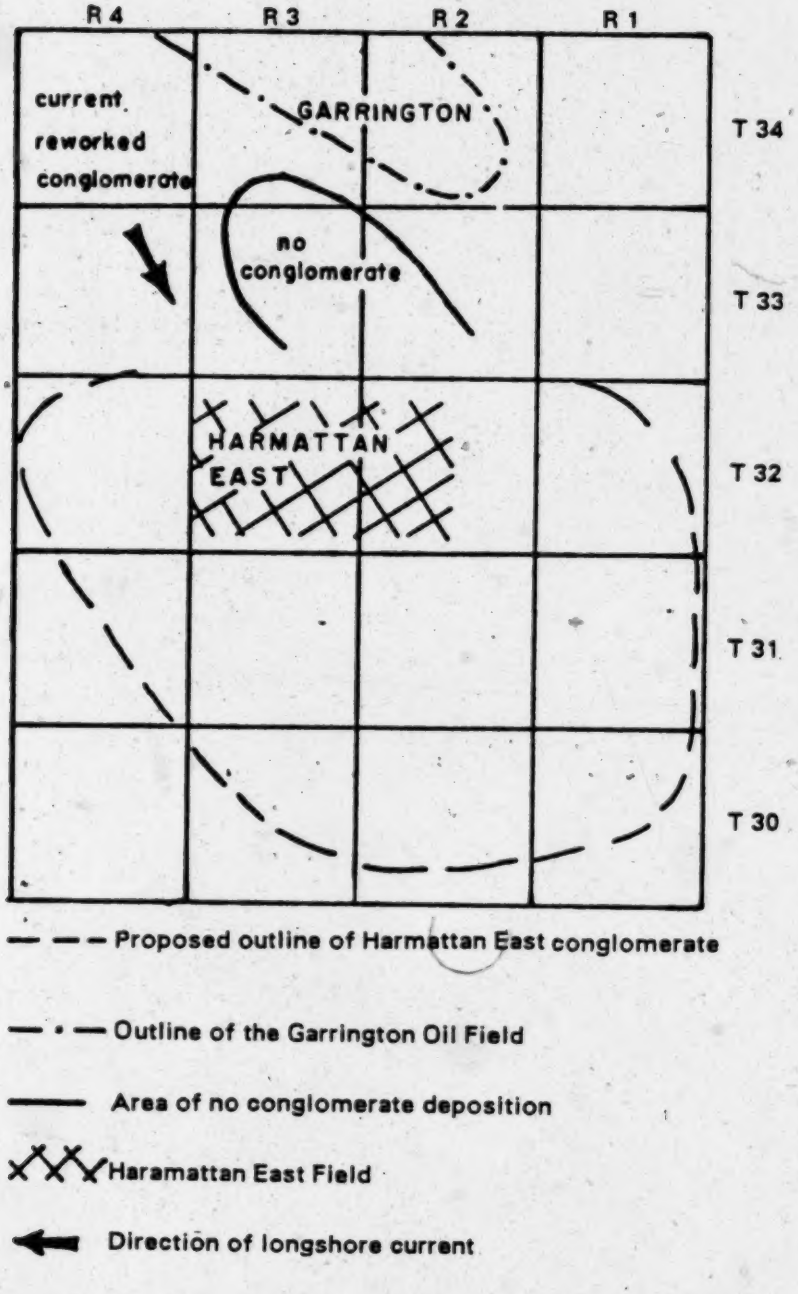

Figure 4.1 shows the skewed nature of the conglomerate which has originated from the Harmattan East field. Also, the northern margin of the Harmattan East field is located on the boundary between Township 32 and 33. At this location conglomerate, which is reworked by longshore currents, overlaps the Harmattan East conglomerate.

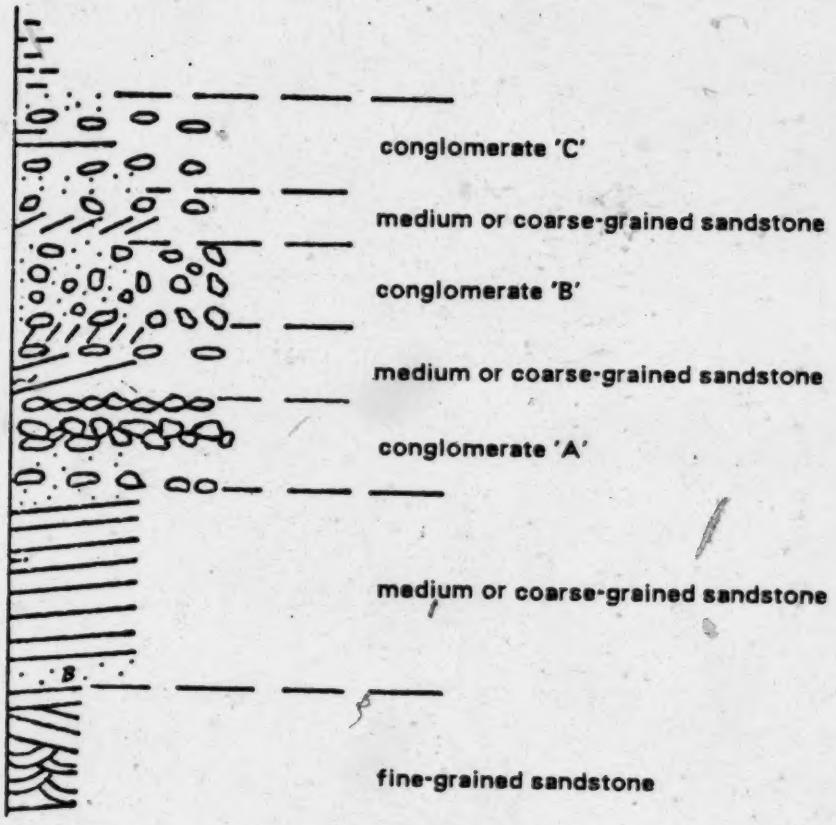

Figure 4.2 Harmattan East Lithology

Well Locations

2W5	3W5
1. 6-17-32	12. 16-10-32
2. 8-17-32	13. 16-11-32
3. 6-18-32	14. 8-12-32
4. 8-18-32	15. 14-12-32
5. 14-18-32	16. 6-13-32
6. 16-18-32	17. 16-13-32
7. 8-19-32	18. 16-14-32
8. 16-19-32	19. 16-15-32
9. 6-20-32	20. 6-16-32
10. 8-24-32	21. 8-19-32
11. 6-30-32	22. 6-22-32
	23. 16-22-32
	24. 6-23-32
	25. 16-23-32
	26. 14-24-32
	27. 6-25-32
	28. 6-27-32

LEGEND

Conglomerate

Medium or Coarse-grained Sandstone

Datum: 12 m below Base of Fish Scales

5 Metres

Figure 4.3

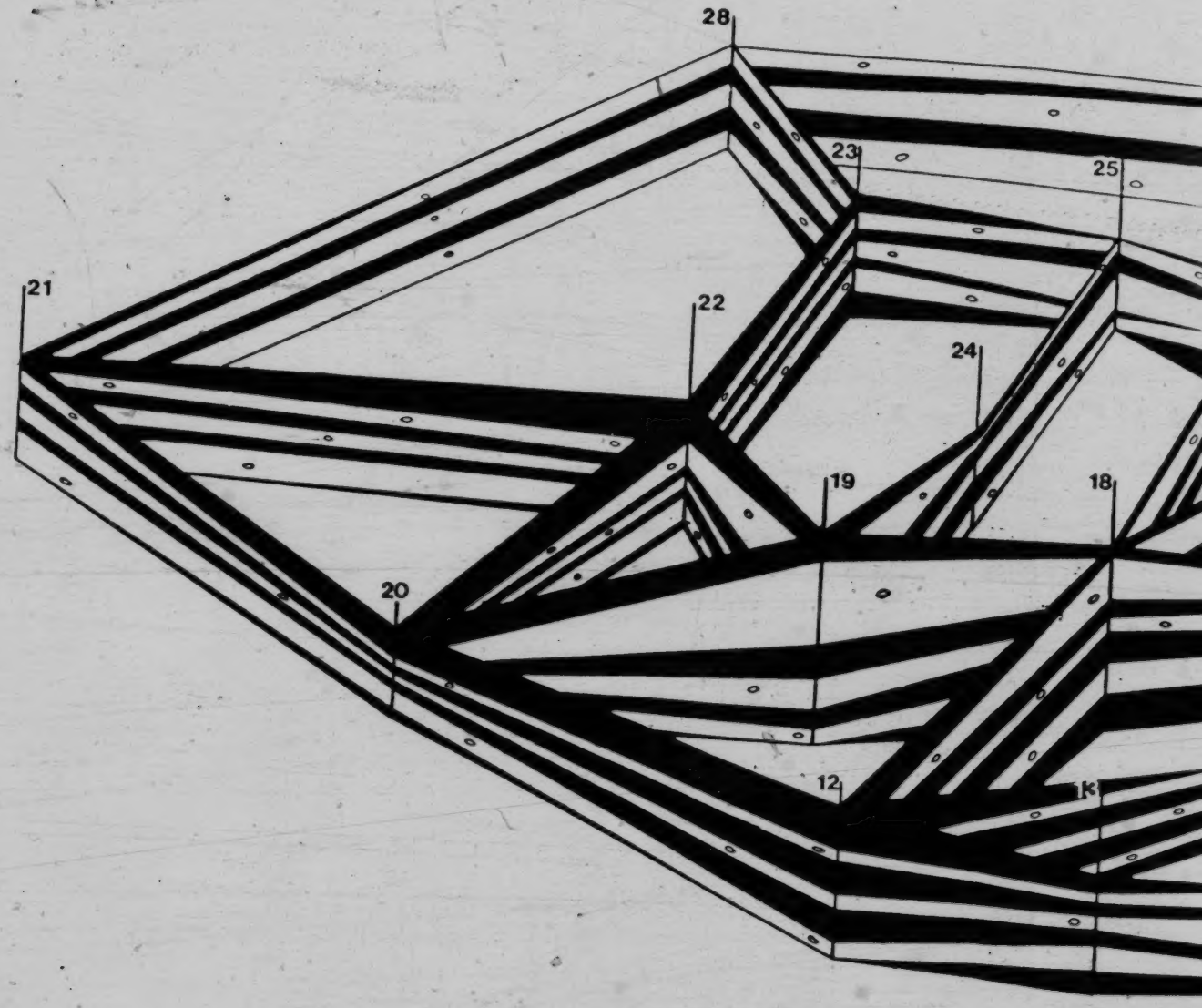
28
23
25
21
22
24
19
18
20
12

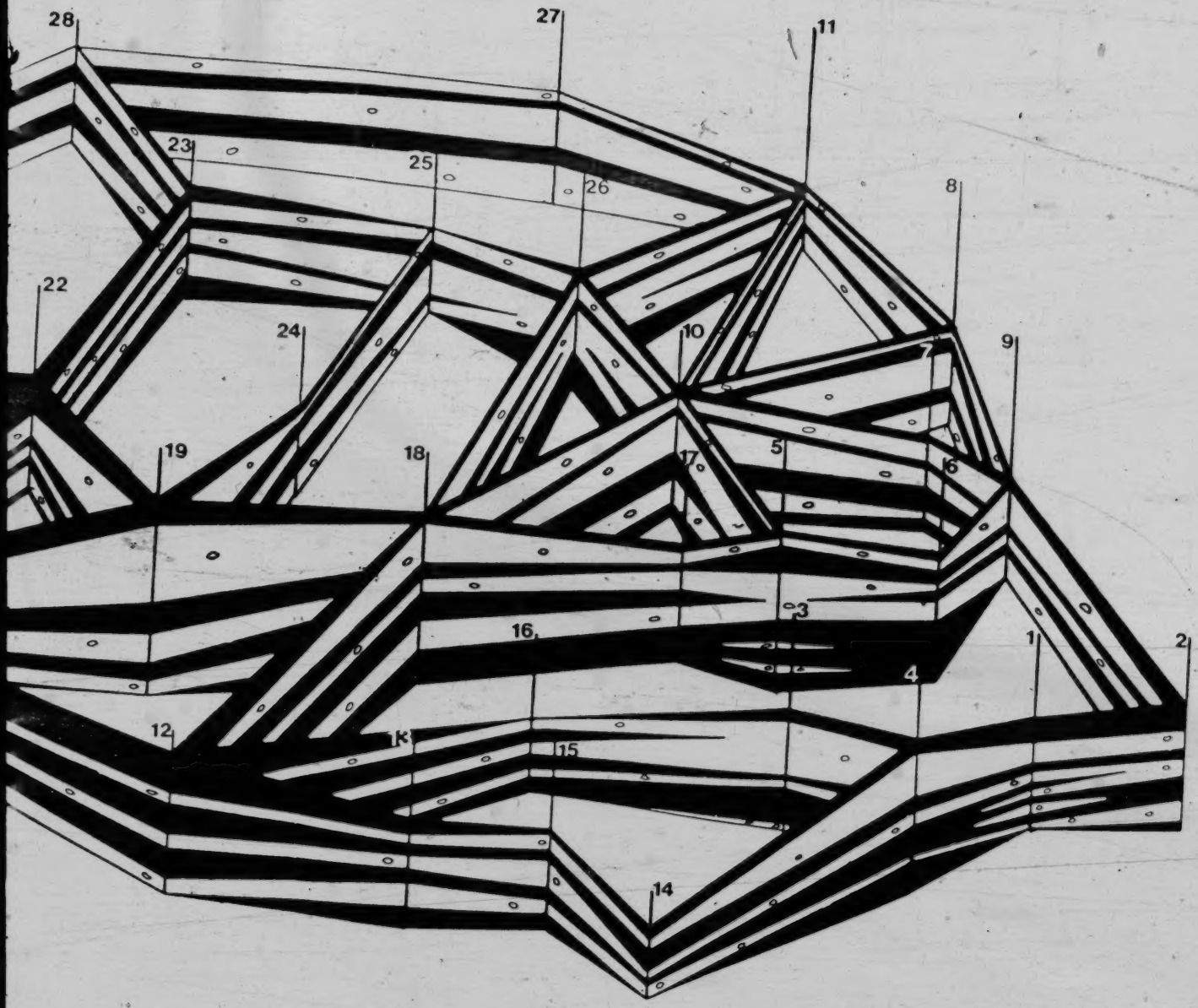
28
27
11
23
25
26
8
22
24
10
9
7
19
18
17
5
6
3
16
1
2
4
12
13
15
14

16-13-32 3W5

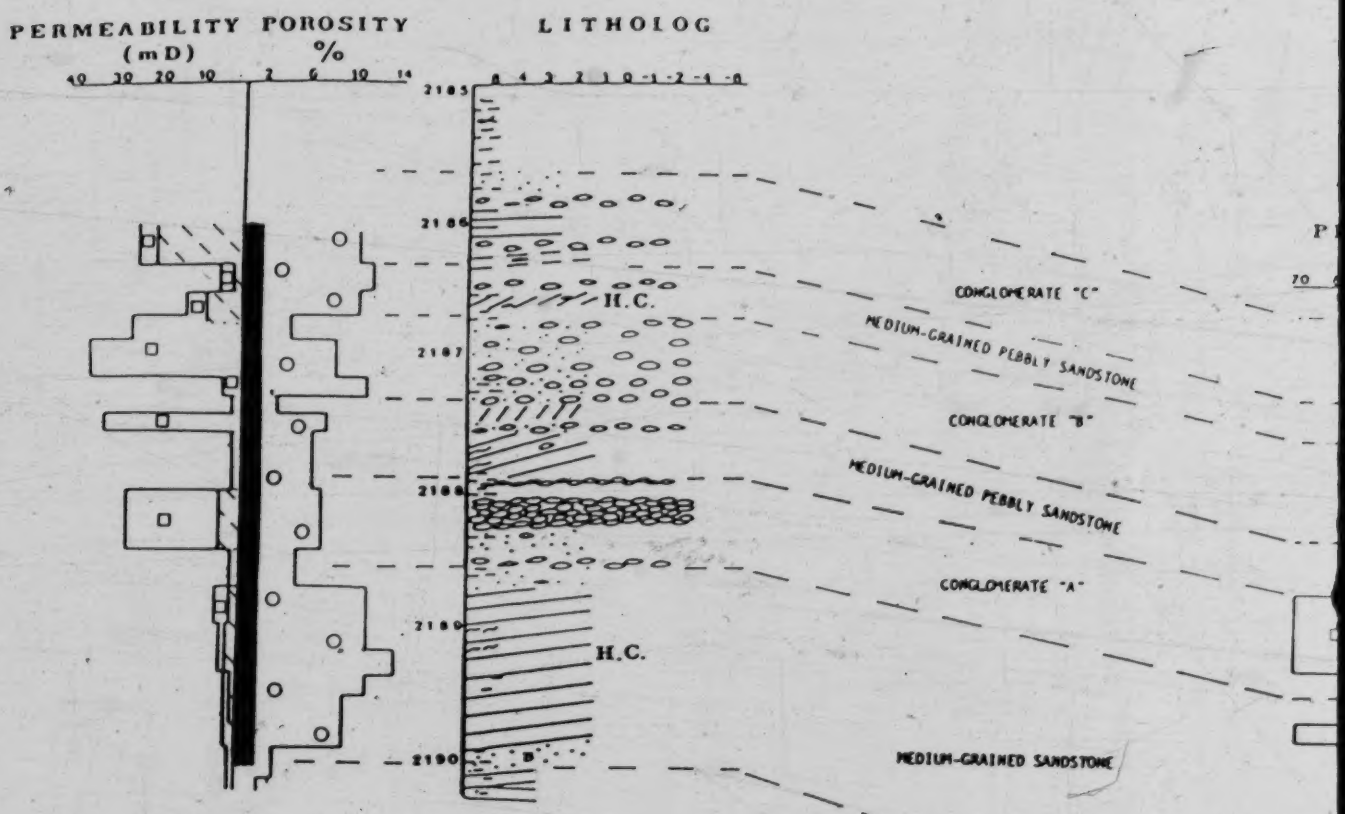

	OIL (m^3/24 HRS.)	GAS ($10^3 m^3$/24 HRS.)
Nov.	12.0	
Dec.		
Jan.	11.2	
Feb.	10.3	1.3

LEGEND

- POROSITY
- INTERVAL CORED
- STRATIGRAPHIC CORRELATION
- PERMEABILITY, VERTICAL (K_V)
- PERMEABILITY, HORIZONTAL (K_H)

Figure 4.4 CORRELATION OF POROSITY AND PERMEAB

STRATIGRAPHIC UNITS

6-18-32 2W5

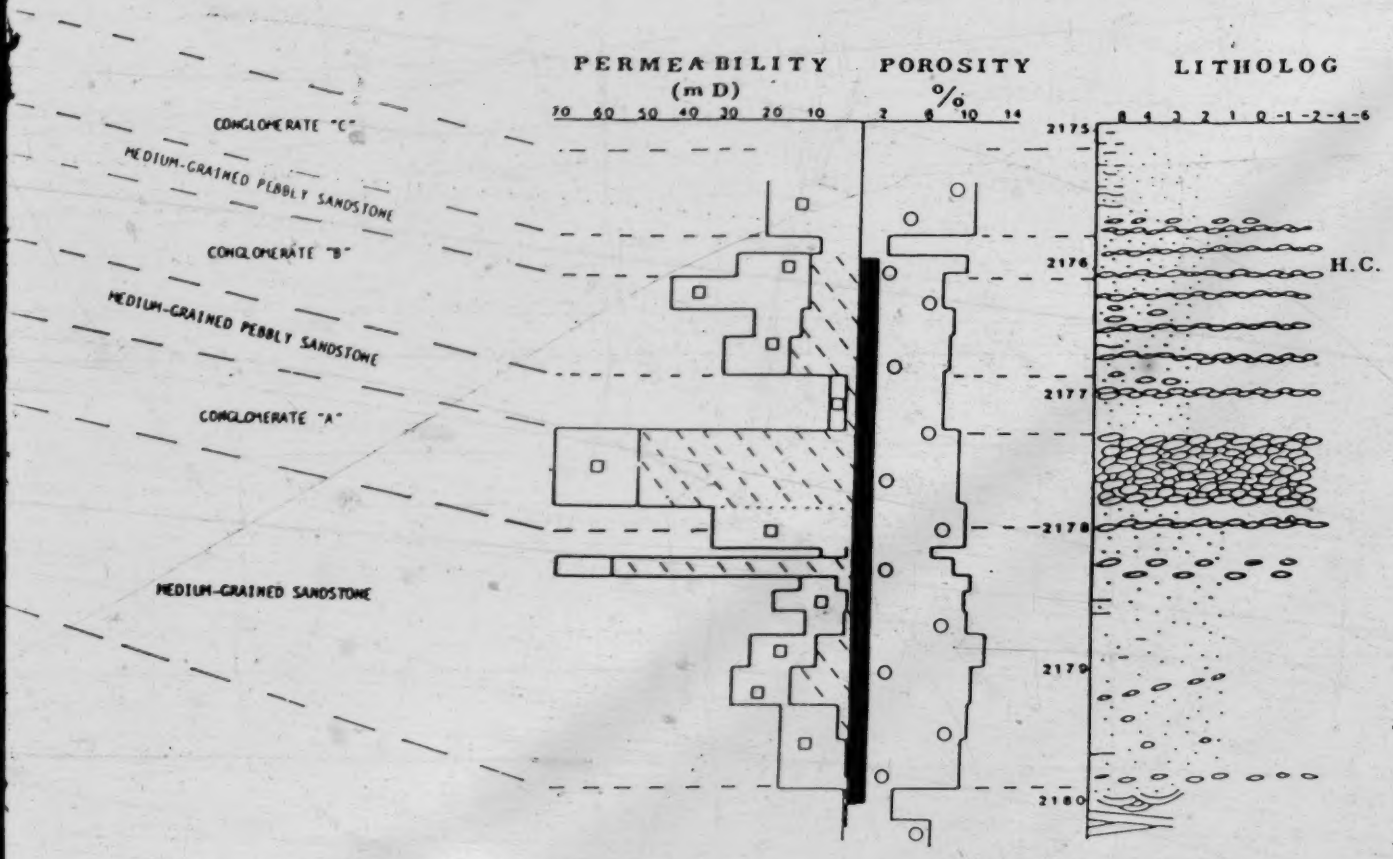

LEGEND

- POROSITY
- INTERVAL CORED
- STRATIGRAPHIC CORRELATION
- PERMEABILITY, VERTICAL (K_V)
- PERMEABILITY, HORIZONTAL (K_H)

	OIL (m^3/24 HRS.)	GAS ($10^3 m^3$/24 HRS.)
Dec.	6.0	
Jan.	15.3	
Feb.	15.0	1.6

OF POROSITY AND PERMEABILITY WITH

RATIGRAPHIC UNITS

2 of 2

permeability at the contact with the conglomerate causes poor communication between the two horizons.

B. FORMATION DAMAGE

Reservoir damage during development of this field could result from the migration of fines, sensitivity to fresh water and precipitation of ferric hydroxide gels, in decreasing order of importance (Almon and Davies, 1981). In the quartz-rich unit, most damage will arise from the cements which are in direct contact with pore fluids.

The most serious problem will be the migration-of-fines (mostly clay minerals with minor quartz). If fluid velocities are too high these fines may be dislodged and migrate within the pore system. Of particular concern is the diameter of the kaolinite crystals (10-15 μm), relative to the pore-throat diameter of the conglomerate (50-60 μm) and coarse-grained sandstone (20-30 μm) (Fig. 3.5). Migrating aggregates of kaolinite crystals may become trapped in the pore-throats, reducing permeability within this reservoir (Almon and Davies, 1981).

The illite and illite/smectite form fibrous networks on crystal facies and bridge pore-throats. The concern with these clay minerals is the large volume of microporosity which increases both the tortuosity and irreducible water saturation. Additional concerns include the possible breakage of clays during production and the separation of the illite/smectite and smectite due to swelling, adding to the migration of fines problem.

Chlorite was identified in all samples and must be considered if the reservoir is to be acidized. This chlorite may be partly dissolved by acids, liberating large quantities of iron. In the presence of oxygenated water, after the acid is spent, this iron will precipitate as a gelatinous ferric hydroxide $Fe(OH)_3$, plugging the pore-throats. However, chlorite is generally present in minor or trace amounts and will not have a major influence on reservoir damage. Iron-rich carbonates have also been identified. If acidized, these carbonates may cause the same problems as chlorite. Due to the patchy occurrence of the carbonates each well must be considered individually.

C. RESERVOIR EVALUATION

The quality of this Viking reservoir is controlled by sedimentology and mineralogy. The sedimentological control is a result of the depositional pattern of the conglomerate and directly influences the rate of primary production. Maximum production (maximum conglomerate thickness) is located along the axis of the trough within this field (Fig. 4.6a). Moving laterally (north/south) from the trough the rate of production decreases because of a decreased thickness of the conglomerate (Fig. 2.7). This thinner conglomerate also has lower porosity and permeability resulting from its fining-upward grain size.

The mineralogical control is a function of the abundance of both detrital and authigenic fine-grained material which exists within the pore system. The distribution of the detrital material, which is most abundant within and to the north of the trough, is controlled by longshore currents flowing to the southeast (Fig. 4.6b). The distribution of the authigenic material is in part related to the abundance of the detrital material, as a consistent level of diagenesis was attained throughout this reservoir. This detrital material may serve as a source for the authigenic minerals.

The abundance of fine-grained material is of secondary importance, provided that the rate of production is maintained at a low level. However, as a well stimulation program and secondary recovery techniques are used, the mineralogical controls will become more important. The effects of higher flushing rates, associated with well stimulation or secondary recovery techniques, was examined using 26 fractured wells from the Harmattan East field. Based on post-stimulation production rates the thickness of the conglomerate is no longer the primary controlling factor on reservoir quality (Fig. 4.6c). Of the 26 wells which were stimulated, seven were unsuccessful. Two of these seven wells (6-16-32 2W5 and 6-20-32 2W5) went to gas after stimulation, a result of their proximity to the gas/oil contact. The five remaining wells can be characterized as having >2 m of net pay, with a high percentage of fine-grained material throughout. Three of these wells (16-22-32 3W5, 16-23-32 3W5 and 16-25-32 3W5) are located to the north of the trough and have >2 m of conglomerate but poor production ($<2 m^3$/day). The two remaining wells (16-10-32 3W5 and 6-11-32 3W5) are located to the southwest of the trough and contain 2 m of coarse-grained sandstone and 1-2 m of conglomerate. As the low post-stimulation production rates of these five wells does not adequately reflect the thickness of the producing horizon it is proposed that the permeability may have been reduced by the

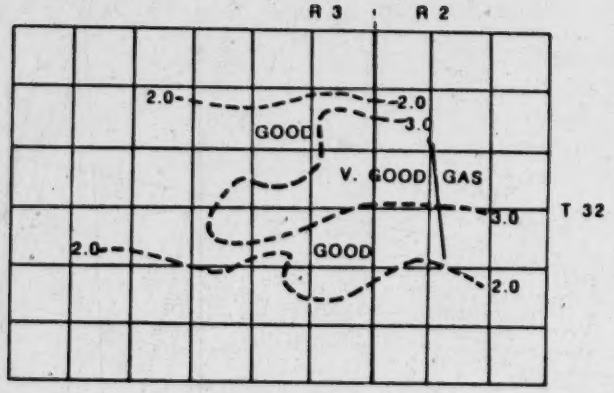

A reservoir, pre-stimulation

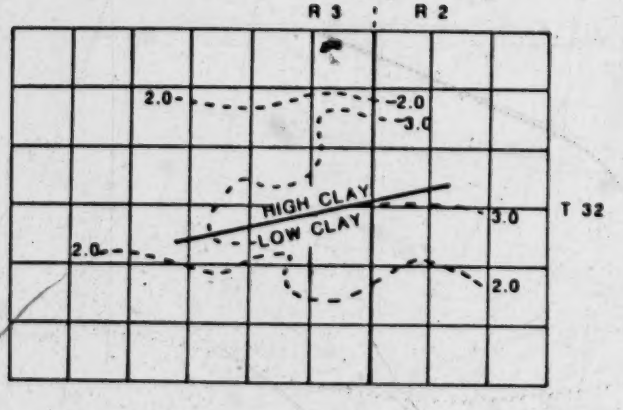

B distribution of fine-grained material

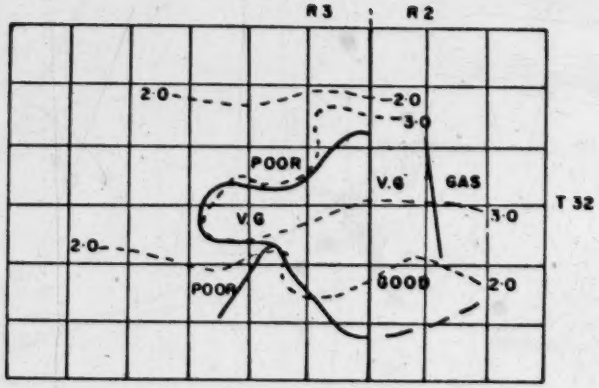

C reservoir, post-stimulation

LEGEND:

---2.0-- isopach of the conglomerate

GOOD rate of oil production

——— outline of reservoir

Figure 4.5 Harmattan East reservoir

migration of fines. This problem is restricted to areas which contain the greatest abundance of fine-grained material within the pore system. As a result of the high fluid velocities associated with the fracturing process this fine-grained material may have migrated, becoming trapped within pore-throats.

In summary, for primary production the reservoir quality is determined by the depositional pattern of the conglomerate. However, if stimulation or secondary recovery is attempted the mineralogical controls become important. Areas containing abundant fine-grained material may have production problems which will not occur throughout the field.

V. CONCLUSION

The Viking Formation within the Harmattan East field was deposited as a coarsening-upward clastic sequence. Deposition occurred approximately 5 km offshore of a northeasterly prograding, storm-dominated shoreline. This shoreline may have represented the seaward margin of a barrier-island complex.

This formation consists of three distinct facies associations: fine-grained sandstone, medium or coarse-grained sandstone and chert-pebble conglomerate. The two sandstones were transported into the lower shoreface environment by wave and/or storm-induced unidirectional currents. The conglomerate was transported into the lower shoreface or inner shelf environment by storm-induced, sediment gravity-flows. These gravity flows were focused along a trough created by the underlying sandstones. This results in the maximum thickness of the conglomerate (4.5 m) being located along the axis of the trough, decreasing laterally (north/south). The conglomerate shows only minor reworking because it was protected within the trough.

The Viking Formation consists of sublitharenites, which are primarily cemented by quartz and clay minerals, with lesser amounts of carbonate and pyrite. The clay minerals consist of predominately kaolinite and illite with smaller amounts of illite/smectite, chlorite and smectite. The conglomerate and coarse-grained sandstone contain mostly kaolinite, while illite is predominate in the fine-grained sandstone. This greater abundance of illite reflects a detrital contribution. The carbonates (siderite, dolomite and ankerite) generally represent 1-2% of the whole rock except in the lower portion of the fine-grained sandstone where siderite may reach a maximum of 20%.

The Viking Formation has undergone both early and late stages of diagenesis. Early diagenesis is characterized by the formation of pyrite, siderite, quartz overgrowths and chlorite. Late diagenesis is characterized by the illitization of smectite, formation of authigenic illite and later kaolinite, ankeritization of the dolomite and albitization of the feldspar. This diagenetic sequence was observed throughout the Viking Formation except in the lower portion of the fine-grained sandstone. This portion of the sandstone was well cemented during early diagenesis, reducing the permeability and limiting the effects of later diagenesis.

The producing horizon consists of three laterally continous zones of conglomerate overlying a medium or coarse-grained sandstone. For primary production the reservoir quality

will be determined by the depositional pattern of the conglomerate, if a low rate of production is maintained. However, if stimulation or secondary recovery (with high flushing rates) is attempted the mineralogy will have a significant influence on reservoir quality. Possible formation damage may result from the migration of fines, sensitivity to fresh water and precipitation of ferric hydroxide gels, in decreasing order of importance.

BIBLIOGRAPHY

Almon, W.R., 1981, Depositional Environment and Diagenesis of Permian Rotliegendes Sandstones in the Dutch Sector of the Southern North Sea, In Longstaffe, F.J. (ed.), Short course in Clays and the Resource Geologist: Mineralogical Association of Canada, p. 119-147.

___, and Davies, D.K., 1981, Formation damage and the crystal chemistry of clays, In Longstaffe, F.J. (ed.), Short course in clays and the resource geologists: Mineralogical Association of Canada, p. 81-103.

Amajor, L.C. 1978, Some Viking bentonites, south-central Alberta, Unpublished M.Sc. Thesis, University of Alberta, 104 pp.

___, 1980, Chronostratigraphy, depositional patterns and environmental analysis of sub-surface Lower Cretaceous (Albian) Viking reservoir sandstones in central Alberta and part of southwestern Saskatchewan, Ph.D. Thesis, University of Alberta, Edmonton, 596 pp.

___, 1984, Lower Cretaceous Viking barrier island, southwestern Alberta, Canada, Bulletin of the American Association of Petroleum Geologists, v.68, p. 448.

Amoco Canada Petroleum Company Limited, 1976. 1976-1977 thesis topics.

Bahan, W.G., 1951, Microfauna of the Joli Fou Formation in north-central Alberta, Unpublished M.Sc. thesis, University of Alberta, 43 pp.

Beach, F.K., 1955, Cardium, a turbidity current deposit, Bulletin of the Alberta Society of Petroleum Geologists, v. 3, p. 123-125.

___, 1956, Reply to DeWiel on turbidity current deposits, Journal of the Alberta Society of Petroleum Geologists, v. 4, p. 175-177.

___, 1962, Viking deposition (discussion), Journal of the Alberta Society of Petroleum Geologists, v. 10, p. 210-212.

Beaumont, E.A., 1980, Retrogradational shelf sedimentation: Viking Sandstone (Lower Cretaceous), central Alberta (abstract), Bulletin of the American Association of Petroleum Geologists, v. 64, p. 676.

___, 1984, Retrogradational shelf sedimentation: Lower Cretaceous Viking Formation, central Alberta, In Tillman, R.W. and Siemers, C.T. (eds.), Siliclastic Shelf Sediments: Tulsa, Oklahoma, Society of Economic Paleontologists and Mineralogists, Special Publication, No. 34, p. 163-177.

Berg, R.R., and Davies, D.K., 1968, Origin of Lower Cretaceous Muddy Sandstone at Bell Creek field, Montana, Bulletin of the American Association of Petroleum Geologists, v. 52, p. 1888-1898.

Berner, R.A., 1981, A new geochemical classification of sedimentary environments, Journal of Sedimentary Petrology, v. 51, p. 359-365.

Boersma, J.R., 1970, Distinguishing features of wave-ripple cross-stratification and morphology. Unpublished Ph.D. thesis, University of Utrecht, 65 pp.

Boles, J.R., 1978, Active ankerite cementation in the subsurface Eocene of Southwest Texas, Mineralogy and Petrology, v. 68, p. 13-22.

___, 1981, Clay diagenesis and effects on sandstone cementation (Case history from the Gulf Coast Tertiary). In F.J. Longstaffe (ed.), Short course in Clays and the Resource Geologist, Mineralogic Association of Canada, p. 81-103

___, and Franks, S.G., 1979, Clay diagenesis in Wilcox Sandstones of southwest Texas, Journal of Sedimentary Petrology, v. 49, p. 55-70.

Bouma, A.H., 1962, Sedimentology of some Flysch Deposits, Amsterdam, Elsevier, 168 pp.

Brenner, R.L. 1978, Sussex Sandstone of Wyoming - Example of Cretaceous offshore sedimentation, Bulletin of the American Association of Petroleum Geologists, v. 62, p. 181-200.

Bullock, D.B., 1950, A microfaunal study of the Basal Llyodminster Shale, Unpublished M.Sc. thesis, University of Alberta, 43 pp.

Cacchione, D.A., Drake, D.E., Grant, W.D. and Tate, G.B., 1984, Rippled scour depressions on the inner continental shelf off central California, Journal of Sedimentary Petrology, v. 54, p. 1280-1291.

Carpenter, A.B., 1978, Origin and chemical evolution of brines in sedimentary basins, Oklahoma Geological Survey Circular, no. 79, p. 60-77

Claypool, G.E., and Kaplan, I.R., 1974, The origin and distribution of methane in marine sediments, In natural gases in marine sediments, New York, Plenum Press, p. 99-139.

Clukey, W., Cacchione, D.A. and Nelson, C.H., 1980, Liquefaction potential of the Yukon prodelta, Bering Sea, Proceedings of the offshore Technology Conference, Houston, vol. 1, paper 3773, p. 315-325.

Curray, R.E., 1966, Observation of Alpine mudflows in the Tenmile Range, Central Colorado, Geological Society of America, v. 77, p. 771-776.

Davies, D.K., 1976, Models and concepts for exploration in Barrier Islands, In Saxena, R.S. (ed.), Sedimentary environments and hydrocarbons, American Association of Petroleum Geologists and NOGS short course, p. 77-115.

Dean, M.E., Longstaffe, F.J., Hein, F.J., Grant, S.K. and Robb, G.A., 1983, The Viking

Sandstone Project: Report #1, Mineralogical Studies of the Harmattan East Pool, April 1983, 89p. + 32 plates.

Delure, A.M., Hein, F.J., Dean, M.E., Longstaffe, F.J., Grant, S.K., Robb, G.A. and Jackson, H., 1984, The Viking Sandstone Project: Report #9, v. 3A, Regional Sedimentology, December 1984, 193 pp.

de Raaf, J.F.M., Boersma, J.F. and van Gelder, A., 1977, Wave generated structures and sequences from a shallow marine succession, Lower Carboniferous, County Cork, Ireland, Sedimentology, v. 24, p. 451-483.

Deroo, G., Powell, T.G., Tissot, B., McCrossan, R.G. and Hacquebard, P.A., 1977, The origin and migration of petroleum in the Western Canadian Sedimentary Basin, Alberta, A geochemical and thermal maturation study, Bulletin of the Geological Survey of Canada, no. 262, p. 1-114.

DeWiel, J.E.F. 1956, Viking and Cardium not turbidity current deposits, Bulletin of the Alberta Society of Petroleum Geologists, v. 4, p. 173-174.

Dickenson, W.R., 1971, Plate tectonic models of geosynclines, Earth and Planetary Science Letters, v. 10, p. 165-174

___, 1974, Plate tectonics and sedimentation, In Tectonics and sedimentation: Society of Economic Paleontologists and Mineralogists Special Publication 22, p 1-27.

___, 1976, Sedimentary basins developed during evolution of Mesozoic-Cenozoic arc trench system in western North American, Canadian Journal of Earth Sciences, v. 13, p. 1268-1287.

___, and Snyder, W.S., 1978, Plate tectonics of the Laramide orogeny in Mathews, V., III, (ed.), Laramide folding associated with basement block faulting in the western United

States, Geologic Society of America, Memoir 151, p. 355-366.

Douglas, R.J.W., Gabrielse, H., Wheller, J.O., Stott, D.F., Belyea, H.R., 1970, Geology of western Canada: Geological Survey of Canada, Economic Geology Report no. 1, p. 367-488.

Drake, D.D., 1976, Suspended sediment transport and mud deposition on continental shelves, In D.J. Stanley and D.J.P. Swift, (eds.), Marine sediment transport and environmental management, New York, John Wiley and Sons, p. 127-158.

Eisbacher, G.H., 1977, Mesozoic-Tertiary basin models for the Candian Cordilleran and their geological constraints, Canadian Journal of Earth Science, v. 14, p. 2414-2417.

Evans, W.E. 1970, Imbricate linear sandstone bodies of the Viking Formation in Dodsland-Hoosier area of southwestern Saskatchewan, Bulletin of the American Association of Petroleum Geologists, v. 54, p. 469-486.

Felix, D.W. and Gorsline, D.W. 1972, Newport submarine canyon, California:an example of the effects of shifting loci of sand supply upon canyon position, Marine Geology, v. 10, p.177-198.

Field, M.E. and Roy, P.S., 1984, Offshore transport and sand-body formation: evidence from a steep, high-energy shoreface, southeastern Australia, Journal of Sedimentary Petrology, vol. 54, p. 1292-1302.

Folk, R.L., 1968, Petrology of sedimentary rocks, Austin, Texas, Hemphill's book store.

Freeland, G.L., Stanley, D.J., Swift, D.J.P., and Lambert, D.N., 1981, The Hudson Shelf Valley: it's role in shelf sediment transport, Marine Geology, v. 42, p. 399-427.

Gammell, H.G., 1955, The Viking Member in central Alberta, Bulletin of the Alberta Society

of Petroleum Geologists, v. 3, p. 63-69.

Gautier, D.L., 1983, Diagenesis, In Rice, D.D. and Gautier, D.L. (authors), Patterns of Sedimentation, Diagenesis and Hydrocarbon Accumulation in Cretaceous Rocks of the Rocky Mountains, Society of Economic Paleontologists and Mineralogists, Special Publication 11, p. 4.1-4.4.

Glaister, R.P., 1958, Petrology of the Blairmore sandstone, Bulletin of the Alberta Society of Petroleum Geologists, v. 6, p. 43-49.

___, 1959, Lower Cretaceous of southern Alberta and adjoining areas, Bulletin of the American Association of Petroleum Geologists, v. 43, p. 590-640.

Hamblin, A.P. and Walker, R.G., 1979, Storm-dominated shallow marine deposits, The Fernie-Kootenay (Jurassic) transition, southern Rocky Mountains, Canadian Journal of Earth Science, v. 16, p. 1673-1690.

Harms, J.C., Southard, J.B., and Walker, R.G., 1982, Sturctures and sequences in clastic rocks, Society of Economic Paleontologists and Mineralogists, Short Course no. 9, 249 pp.

Hayes, M.O., 1967, Hurricanes as geologic agents, South Texas Coast, Bulletin of the American Association of Petroleum Geologists, v. 51, p. 937-956.

Hein, F.J., 1984, Deep-sea and fluvial braided channel conglomerates: A comparison of two case studies, In, Koster, E.H. and Steel, R.J. (eds.), Sedimentology of Gravels and Conglomerates, Canadian Society of Petroleum Geologists memoir 10, p. 33-49.

Howard, J.D. and Reineck, H.E., 1981, Depositional facies of high-energy beach-to-offshore sequence, comparison with low-energy sequence, Bulletin of the American Association of Petroleum Geologists, v. 65, p. 807-830.

Hower, J., Eslinger, E.V., Hower, M.E. and Perry, E.A., 1976, Mechanism of burial metamorphism of argillaceous sediments --1, Mineralogical and chemical evidence, Bulletin of the Geologic Society of America, v. 87, p. 725-737.

Hume, G.S., 1933, Oil and gas in western Canada, Geological Survey of Canada, Economic Geology Series No. 5, 359 pp.

Hunt, W.C., 1954, The Joseph Lake-Armena-Camrose producing trend, Alberta, In Clark, L.M. (ed.), Western Canada Sedimentary Basin, p. 452-463.

Hutcheon, I., 1981, Applications of thermodynamics to clay minerals and authigenic mineral equilibria, In Longstaffe, F.J. (ed.), Short course in Clays and the Resource Geologist, Mineralogical Association of Canada, p. 119-147.

Ignasiak, T.M., Kotlyar, L., Longstaffe, F.J., Strausz, O.P. and Montgomery, D.S., 1983, Separation and characterization of clay from Athabasca asphaltene, Fuel, v. 62, p. 353-362.

Jones, H.L. 1962, Viking deposition (discussion), Bulletin of the Alberta Society of Petroleum Geologists, v. 10, p. 212.

Jordon, T.E., 1981, Thrust loads and foreland basin evolution, Cretaceous, western United States, Bulletin of the American Association of Petroleum Geologists, v. 65, p. 2506-2520.

Karl, H.A., 1983, Factors that influence sediment transport at the shelf break, In Stanley D.J., Moore, G.T. (eds.) The Shelfbreak: Critical interface on continental margins, Society of Economic Paleontolgists and Mineralogists Special Publication 33, p. 219-233.

Kauffman, E.G., 1977, Geological and biological overview; Western Interior Cretaceous Basin, Mountain Geology, v. 14, p.75-99.

Kelts, K.R. and McKenzie, J.A., 1972, Diagenetic dolomite formation in Quaternary anoxic diatomaceous muds of Deep Sea Drilling Project Leg 64, Gulf of California: Initial Reports of the Deep Sea Drilling Project, v. 64, p. 553-569.

Koldijk, W.S. 1976, Gilby Viking 'B': A storm deposit, In Lernad, M.M. (ed.), The sedimentology of selected clastic oil and gas reservoirs in Alberta, Canadian Society of Petroleum Geologists, p. 62-77.

Komar, P.D., 1976, The transport of cohesionless sediments on continental shelves, , In D.J. Stanley and D.J.P. Swift, (eds.), Marine sediment transport and environmental management, New York, John Wiley and Sons, p. 23-28.

Kreisa, R.D. 1981, Storm-generated sedimentary structures in subtidal marine facies with examples from the Middle and Upper Ordovician of southwestern Virginia, Journal of Sedimentary Petrology, v. 51, p. 823-848.

Kumar, N. and J.E. Sanders, 1976, Characteristics of shoreface storm deposits: Modern and Ancient Examples, Journal of Sedimentary Petrology, v. 46, p. 145-162.

Land, L.S. and K.L. Milliken, 1981, Feldspar diagenesis in the Frio Formation, Brazoria County, Texas Gulf Coast. Geology, v. 9, p. 314-318.

Love, M., 1955, The Joffre Oil Field, geology and development, Oil in Canada, v. 7, p. 12884-12890.

Madsen, O.S., 1976, Wave climate of the continental margin: elements of its mathematical description, In Stanley, D.J., and Swift, D.J.P., (eds.) marine sediment transport and environmental Management, New York, John Wiley and Sons, p. 65-87.

Magdich, F.S., 1955, The Viking Formation in Saskatchewan: Unpublished M.Sc. Thesis, University of Saskatchewan, Saskatoon.

Margara, K., 1976, Thickness of removed sedimentary rocks, paleopore pressure, and paleotemperature, southwestern part of Western Canada Basin, Bulletin of the American Association of Petroleum Geologists, v. 60, p. 554-565.

McCubbin, D.G., 1982, Barrier Islands and Strand Plain Facies, In Scholle, P.A. and Spearing, D.R., (eds.), Sandstone Depositional Environments, American Association of Petroleum Geologists, memoir 31, p. 247-280.

McNeil, D.H., and Caldwell, W.G.E., 1981, Cretaceous rocks and their formainifera in the Manitoba escarpment, Geologic Association of Canada Special Paper 21, 439 pp.

Middleton, G.V. 1972, Albite of secondary origin in Charny Sandstone, Quebec, Journal of Sedimentary Petrology, v. 42, p.341-349.

Milliken, K.L., Land, L.S. and Loucks, R.G., 1981, History of burial diagenesis determined from isotopic geochemistry, Frio Formation, Brazoria County, Texas, American Association of Petroleum Geologists, v. 65, p. 1397-1413.

Mofjeld, H.O., 1976, Tidal currents, In D.J. Stanley and D.J.P. Swift, (eds.), Marine sediment transport and environmental management, New York, John Wiley and Sons, p. 53-64.

Morton, R.A., 1981, Formation of storm deposits by wind-forced currents in the Gulf of Mexico and the North Sea, Special Publication of the International Association of Sedimentologists, v. 5, p.385-396.

Murray, S.P., 1970, Bottom currents near the coast during Hurricane Camille, Journal of Geophysical Research, v. 75, p. 4579-4582.

Nauss, A.W., 1945, Cretaceous Stratigraphy of Vermilion area, Alberta, Canada, Bulletin of the American Association of Petroleum Geologists, v. 29, p. 1615-1618.

___, A.W., 1947, Cretaceous microfossils of the Vermillion area, Alberta, Journal of Paleontogy, v. 21, p. 329-343.

Nelson, C.H., 1982, Modern shallow-water graded sand layers from storm surges, Bering Shelf: A mimic of Bouma sequences and turbidite systems, Journal of Sedimentary Petrology, v. 52, p. 537-545.

North, B.R. and Caldwell, W.G.E., 1975, Foraminiferal faunas in the Cretaceous system of Saskatchewan, In Caldwell, W.G.E. (ed.), the Cretaceous system in the Western Interior of North America, Geological Association of Canada Special Paper, No. 13, p. 303-332.

Perry, E.A., Jr. and Hower, J., 1970, Burial diagenesis of Gulf Coast pelitic sediments, Clays and Clay Minerals, v. 18, p. 165-177.

Price, R.A., 1973, Large-scale gravitational flow of supracrustal rocks, southern Canadian Rockies, In DeJong, K.A., and Scholten, R., (eds.) Gravity and tectonics, New York, John Wiley and Sons, p. 491-502.

Reasoner, M.A. and Hunt, A.D., 1954, Smiley oil field, Saskatchewan, Bulletin of Canadian Mining and Metallurgy, v. 47, p. 612-617.

Reineck, H.E., and Singh, J.B., 1972, Genesis of laminated sand and graded rhythmites in storm-sand layers of shelf mud, Sedimentology, v. 18, p. 123-128.

Reinson, G.E., 1979, Barier Islands systems, In Walker, R.G. (ed.), Facies Models, Geoscience Canada Reprint Series 1, p. 57-74.

Rice, D.D., 1980, Coastal and deltaic sedimentation of Upper Cretaceous Eage Sandstone: relation to shallow gas accumulations, north-central Montana, Bulletin of the American Association of Petroleum Geologists, v. 64, p. 316-338.

___, 1983, Wide spread, shallow-marine, storm-generated sandstone units in the Upper Cretaceous Mosby Sandstone, central Montana, In Siemers, C.T., and Tillman, R.W. (eds.) Siliciclastic shelf sediments: Society of Economic Paleontologists and Mineralogists, Special Publication 35, p. 143-161.

___, and Gautier, D.L., 1983, Patterns of sedimentation, diagenesis, and hydrocarbon accumulation in Cretaceous rocks of the Rocky Mountains, Society of Economic Paleontologists and Mineralogists, short course no. 11, 253 pp.

Robb, G.A., Longstaffe, F.J., Hein, F.J., Dean, M.E., DeIure, A. and Grant, S.K., 1984, The Viking Sandstone Project: Report #9, v. 1, Geological Studies of the Garrington Oil Field, October 1984, 284p. + 7 maps + 12 plates.

Rodolfo, K.S., Buss, B.A., and Pilkey, O.H., 1971, Suspended sediment increase due to hurricane Gerda in continental shelf waters off Cape Lookout, North Carolina, Journal of Sedimentary Petrology, v. 41, p. 1121-1125.

Roessingh, H.K., 1959, Viking deposition in the southern Alberta Plains, Alberta Society of Petroleum Geologists, 9th Annual Field Conference, p. 130-137.

Rudkin, R.A., 1964, Chapter II: Lower Cretaceous, In McCrossan, R.G., and Glaister, R.P.(eds.), Geological history of western Canada, Canadian Society of Petroleum Geologists, Calgary, Alberta, p. 156-168.

Sallenger, A.H., Dingler, J.R. and Hunter, R., 1978, Coastal processes and morphology of the Bering Sea coast off Alaska, In Environment assessment of the Alaskan Continental Shelf: Annual Report of Principal Investigators for the year ending March 1978, United States Department of Commerce National Oceanic and Atmospheric Administration, Environmental Reserarch Labratory, Boulder Colorado, v. 12, p. 451-470.

Sampson, R.J., 1978, Surface II graphics system, Kansas Geological Survey, Lawrence, Kansas, 240 pp.

Shelton, J.W., 1973, Models of sand and sandstone deposits: a methodology for determining sand genesis and trend, Viking Sandstone, Cretaceous, Joffre Field, Alberta, Bulletin of the Oklahoma Geologic Survey, v. 118, p. 91-94.

Simpson, F., 1975, Marine lithofacies and biofacies of the Colorado Group (Middle Albian to Santonian), in Saskatchewan, In Caldwell, W.G.E. (ed.), The Cretaceous system in the Western Interior of North America, Geological Association of Canada, Special Paper no. 13, p. 553-587.

Smith, J.D. and Hopkins, T.S., 1972, Sediment transport on the continetal shelf off Washington and Oregon in light or recent current measurements, In D.J. Stanley and D.J.P. Swift, (eds.), Marine sediment transport and environmental management, New York, John Wiley and Sons, p. 143-180.

Slater, R.D., 1984, Prediction of tides in epeiric seas with a numerical model: The Cretaceous Seaway of North America, (abstract), In program with abstract, Canadian Society of Petroleum Geologists, Research Symposium, Sedimentology of shelf sands and sandstones, Calgary, Alberta, p. 62.

Slipper, S.E., 1918, Viking Gas Field, Structure of Area: Geological Survey Summary Department 1917, Part C, p. 8c.

Stansberry, G.F., 1957, The Viking Formation, Central Alberta, Unpublished M.Sc. Thesis, University of Alberta, 124 pp.

Stelck, C.R., 1975a, The Upper Albian *Miliammina manitobensis* zone in northeastern British Columbia: In Caldwell, W.G.E. (ed.), The Cretaceous system in the Western Interior of North America, Geological Association of Canada, Special Paper no. 13, p.

253-275.

__1975b, Basement control of Cretaceous sand sequences in Western Canada, In Caldwell, W.G.E. (ed.), The Cretaceous system in the Western Interior of North America, Geological Association of Canada, Special Paper no. 13, 666 pp.

__ 1958, Stratigraphic position of Viking sand, Bulletin of the Alberta Society of Petroleum Geologists, v. 6, p. 2-7.

Strides, A.H., 1982. Offshore tidal sands, New York, Chapman and Hall, 222 p.

Surdam, R.C., Boese, S. and Crossey, L.T., 1982, Role of organic and inorganic reactions in development of secondary porosity in sandstones (abstract), Bulletin of the American Association of Petroleum Geologists, v. 66, p. 635.

Swift, D.J.P., 1976a, Coastal sedimentation, In Stanley, D.J., and Swift, D.J.P., (eds.) Marine sediment transport and environmental management, New York, John Wiley and Sons, p 255-310.

Swift, D.J.P., 1976b, Continential shelf sedimentation, In D.J. Stanley and D.J.P. Swift, (eds.), Marine sediment transport and environmental management, New York, John Wiley and Sons, p. 311-350.

Thomas, M.B., 1977, Depth-porosity relationships in the Viking and Cardium Formations of central Alberta, unpublished M.Sc. Thesis, University of Calgary, 147 pp.

Tizzard, P.G., 1974, Viking deposition in the Suffield area, Alberta, unpublished M.Sc. Thesis, University of Alberta, 126 pp.

Tizzard, P.G., and Lerbekmo, J.F., 1975, Depositional history of the Viking formation, Suffield area, Alberta, Canada, Bulletin of the Canadian Society of Petroleum

Geologists, v. 23, p. 715-752.

Walker, R.G., 1975, Generalized facies models for resedimented conglomerates of turbidite association, Bulletin of the Geological Association of America, v. 88, p. 737-748.

___, 1979, Facies Model 7: Shallow marine sands. In Walker, R.G., (ed.), Facies Models: Geoscience Canada, Reprint Series 1, p. 75-89.

Weimer, R.J., 1983, Relation of unconformities, tectonics, and sea level changes, Cretaceous of the Denver Basin and adjacent areas, In Reynolds, M.W. and Dolly, E.D. (eds.), Mesozoic paleogeography of west-central United States: Denver, Rocky Mountain Section, Society of Economic Paleontologists and Mineralogists, p. 359-376.

Wheeler, J.O., Aitken, J.D., Berry, M.J., Gabrielse, H., Hutchison, W.W., Jacogy, W.R., Monger, J.W.H., Niblett, E.R., Norris, D.K., Price, R.A., and Stacey, R.A., 1972, The Cordilleran structural province, In Price, R.A., and Douglas, J.W. (eds.), Variations in tectonic styles in Canada, Geological Association of Canada, Special Paper no. 11, p. 1-82.

Williams, G.D., and Stelck, C.R., 1975, Speculations on the Cretaceous paleogeography of North America, In Caldwell, W.G.E. (ed.), The Cretaceous system in the Western Interior of North America, Geological Association of Canada, Special Paper no. 13, p. 1-7.

VI. APPENDIX I

Percentage of each subfacies within Conglomerate Association

Location	Subfacies																			
	2A	2B	2C	3A	3C	4A	4B	4C	5A	5B	6A	7A	7C	8A	8B	8C	9A	9B	9C	10B
6-7-32 2W5	-	-	-	26	-	4	-	-	-	-	-	-	-	14	4	-	30	12	10	t
16-7-32 2W5	-	-	-	-	-	-	-	-	89	-	-	-	-	-	-	-	11	-	-	
6-17-32 2W5	11	-	-	8	-	21	-	2	-	-	-	-	-	-	15	-	30	3	-	3
8-19-32 2W5	-	-	17	25	-	-	-	-	56	-	-	-	-	-	-	-	-	-	-	2
16-19-32 2W5	8	-	-	21	2	10	-	-	-	6	-	5	-	5	1	-	14	20	7	1
6-30-32 2W5	-	-	-	51	-	-	-	-	-	-	-	-	-	13	-	-	35	-	-	
16-10-32 3W5	-	-	-	6	-	-	-	-	10	-	-	-	1	-	29	2	18	21	3	11
16-11-32 3W5	-	-	48	11	-	2	-	-	3	-	-	-	-	5	-	-	19	-	12	t
14-12-32 3W5	-	-	-	46	-	-	-	-	-	-	-	5	-	5	-	-	40	5	-	
6-13-32 3W5	-	-	-	-	-	20	-	-	8	-	t	-	-	-	2	-	69	-	-	2
8-13-32 3W5	-	-	-	23	-	-	-	-	8	-	4	-	-	20	-	-	20	25	-	t
16-14-32 3W5	-	-	-	42	-	-	-	-	-	-	-	7	-	-	3	-	3	-	45	1
16-15-32 3W5	-	-	-	30	-	-	-	-	15	-	-	-	-	-	4	-	22	3	23	
6-16-32 3W5	-	-	-	10	-	-	-	-	-	-	-	-	-	-	15	17	32	22	-	5
6-22-32 3W5	-	-	-	13	-	t	-	-	43	-	2	-	-	38	-	-	-	-	-	5

Percentage of each subfacies within Conglomerate Association (continued)

Location	Subfacies																			
	2A	2B	2C	3A	3C	4A	4B	4C	5A	5B	6A	7A	7C	8A	8B	8C	9A	9B	9C	10B
16-22-32 3W5	-	-	-	37	-	7	-	-	14	-	23	-	-	-	-	-	26	-	-	t
6-23-32 3W5	-	-	12	-	-	7	-	-	48	-	-	-	-	-	-	1	30	-	-	t
16-23-32 3W5	-	-	-	-	-	4	-	-	16	-	51	6	-	-	-	-	18	4	-	
8-24-32 3W5	-	-	-	13	-	2	-	-	26	-	-	-	-	7	-	-	29	10	12	1
14-24-32 3W5	-	-	-	14	-	-	9	-	8	-	-	-	-	t	-	-	54	12	4	t
6-25-32 3W5	-	-	-	14	-	-	6	-	27	42	-	t	-	-	2	-	1	7	-	2
6-27-32 3W5	-	-	-	8	-	11	-	-	20	-	-	1	-	3	-	-	47	6	4	1
16-28-32 3W5	-	-	-	21	9	-	-	-	27	-	-	-	-	-	-	-	4	36	-	3
15-14V-32 4W5	-	-	-	46	-	3	-	-	-	-	-	-	-	-	4	-	47	-	-	

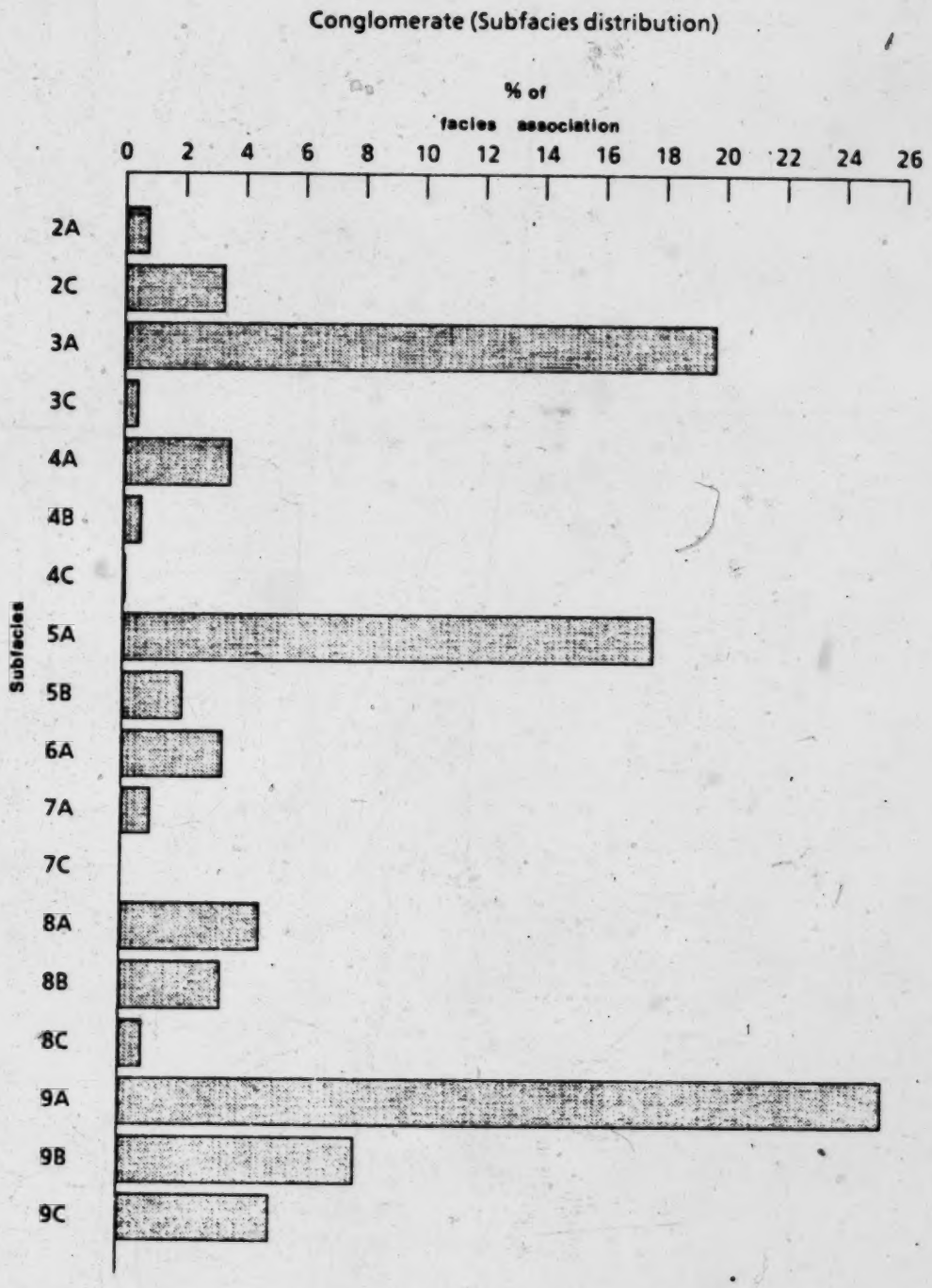
Conglomerate (Subfacies distribution)
% of
facies association
0 2 4 6 8 10 12 14 16 18 20 22 24 26
Subfacies
2A
2C
3A
3C
4A
4B
4C
5A
5B
6A
7A
7C
8A
8B
8C
9A
9B
9C

Percentage of each subfacies within Medium or Coarse Sand Association

Location	Subfacies									
	2A	3A	3B	7A	8A	8B	9A	9B	9C	10B
6-7-32 2W5	-	-	-	-	-	23	35	43	-	
16-7-32 2W5	-	-	-	-	-	-	3	55	42	t
6-17-32 2W5	-	-	-	-	-	-	-	-	-	
8-19-32 2W5	-	-	t	47	-	-	2	6	43	2
16-19-32 2W5	-	-	-	-	-	-	-	-	-	
6-30-32 2W5	-	-	-	-	-	-	-	-	-	
16-10-32 3W5	4	1	-	-	-	11	5	-	73	7
16-11-32 3W5	-	-	-	-	28	72	-	-	-	
14-12-32 3W5	-	-	-	-	-	-	-	100	-	
6-13-32 3W5	-	-	-	-	-	53	47	-	-	
8-13-32 3W5	-	-	-	-	11	10	27	43	-	9
16-14-32 3W5	-	-	-	-	-	8	-	-	91	1
16-15-32 3W5	-	-	-	-	-	-	-	-	-	
6-16-32 3W5	-	-	-	-	-	-	-	-	-	
6-22-32 3W5	-	-	-	-	13	-	30	11	30	17

Percentage of each subfacies within Medium or Coarse Sand Association (continued)

Location	Subfacies									
	2A	3A	3B	7A	8A	8B	9A	9B	9C	10B
16-22-32 3W5	-	-	-	-	9	-	90	-	-	1
6-23-32 3W5	-	-	-	-	-	-	-	-	-	
16-23-32 3W5	-	-	-	-	-	-	-	-	-	
8-24-32 3W5	-	-	-	-	25	-	-	75	-	
14-24-32 3W5	-	-	-	-	-	-	-	-	-	
6-25-32 3W5	-	-	-	-	-	-	-	-	-	
6-27-32 3W5	-	-	-	-	-	-	-	-	-	
16-28-32 3W5	-	-	-	-	60	-	24	-	-	6
15-14V-32 4W5	-	-	-	-	-	-	-	-	-	

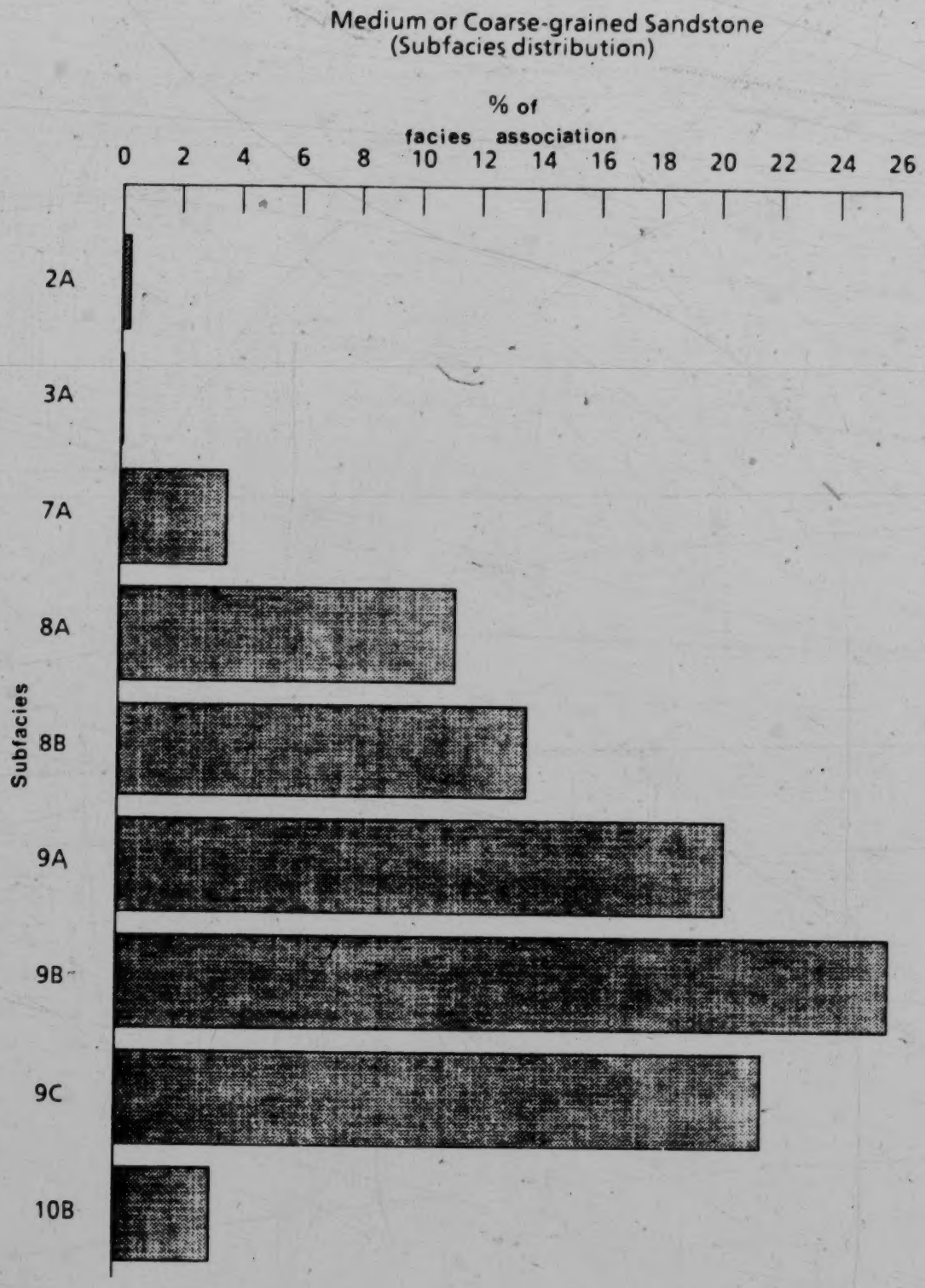
Medium or Coarse-grained Sandstone
(Subfacies distribution)
% of
facies association
0 2 4 6 8 10 12 14 16 18 20 22 24 26
Subfacies
2A
3A
7A
8A
8B
9A
9B
9C
10B

Percentage of each subfacies within Fine Sand Association

Location	Subfacies																		
	1A	1B	2A	2B	2C	2D	2E	2F	2G	3A	4A	5A	5B	7A	8A	8B	9A	9B	9C	10B
6-7-32 2W5	18	-	9	-	58	1	1	1	3	t	-	-	-	-	t	5	-	-	2	t
16-7-32 2W5	11	-	-	5	77	-	-	5	-	1	-	-	-	-	-	-	-	-	-	t
6-17-32 2W5	t	-	1	2	4	t	t	6	-	-	-	-	-	-	15	-	30	3	-	3
8-19-32 2W5	32	-	5	-	51	-	1	-	-	4	-	-	-	-	6	-	-	-	-	2
16-19-32 2W5	13	-	6	16	50	t	3	4	2	t	4	-	-	-	-	t	-	-	-	1
6-30-32 2W5	44	-	24	-	28	t	t	2	-	-	-	-	-	-	-	-	-	-	-	t
16-10-32 3W5	4	-	6	54	30	t	t	-	-	-	-	-	-	-	2	3	-	-	-	1
16-11-32 3W5	-	-	t	16	66	6	2	-	-	6	-	-	-	-	t	-	-	-	-	3
14-12-32 3W5	t	-	5	26	47	2	t	t	4	t	-	-	-	-	-	15	-	t	-	2
6-13-32 3W5	-	-	5	71	24	-	-	-	-	-	-	-	-	-	-	-	-	-	-	
8-13-32 3W5	-	-	6	-	77	t	-	-	-	1	-	-	-	-	-	13	-	-	-	2
16-14-32 3W5	5	-	t	9	58	1	-	-	-	4	-	-	-	-	-	15	-	1	7	t
16-15-32 3W5	-	-	-	-	96	-	-	-	-	-	-	-	-	-	-	-	-	-	-	4
6-16-32 3W5	2	-	2	10	81	-	-	-	-	4	-	-	-	-	-	-	-	-	-	1
6-22-32 3W5	-	-	91	-	8	-	-	-	-	-	-	-	-	-	-	-	-	-	-	1

Percentage of each subfacies within Fine Sand Association (continued)

Location	Subfacies																			
	1A	1B	2A	2B	2C	2D	2E	2F	2G	3A	4A	5A	5B	7A	8A	8B	9A	9B	9C	10B
16-22-32 3W5	t	-	11	27	28	2	-	14	15	1	-	-	-	t	-	-	-	-	-	3
6-23-32 3W5	8	4	-	12	71	-	1	-	-	t	-	-	-	-	-	t	-	-	-	3
16-23-32 3W5	17	-	20	30	13	t	t	6	5	3	-	-	t	-	2	-	-	-	-	2
8-24-32 3W5	31	-	22	-	28	1	2	-	5	5	1	-	-	t	1	-	2	t	-	2
14-24-32 3W5	-	-	-	-	100	-	-	-	-	-	-	-	-	-	-	-	-	-	-	
6-25-32 3W5	-	-	3	36	43	6	-	13	-	-	-	-	-	-	-	-	-	-	-	2
6-27-32 3W5	-	-	21	8	61	-	1	-	-	3	-	-	-	-	2	-	-	-	-	3
16-28-32 3W5	-	-	-	21	9	-	-	-	27	-	-	-	-	-	-	-	4	36	-	3
15-14V-32 4W5	14	-	8	16	36	1	2	-	-	4	t	2	-	-	-	16	-	-	-	1

Fine-grained Sandstone (Subfacies distribution)

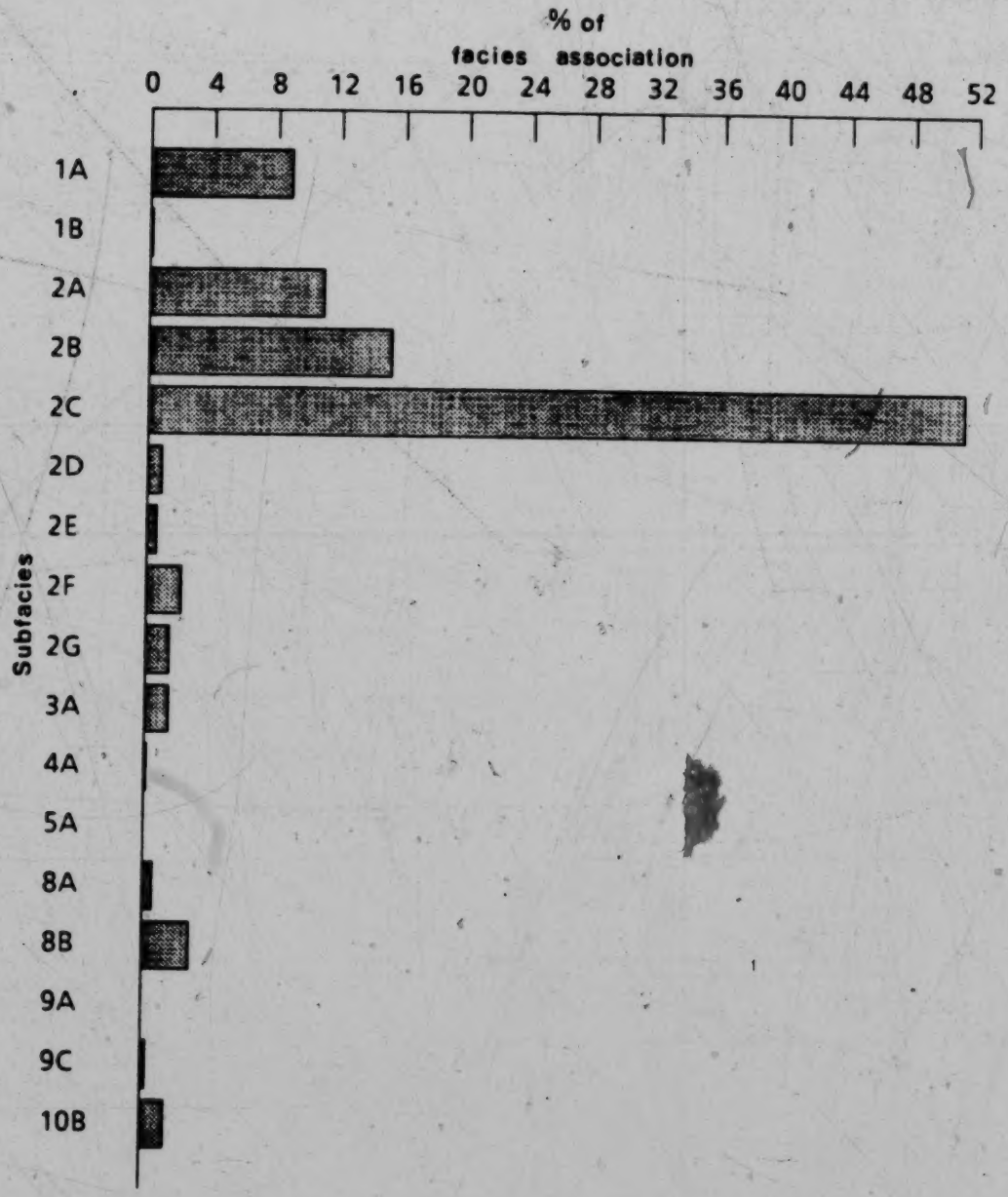

VII. APPENDIX II

LITHOLOGS

9-26-30 3W5
6-10-31 2W5
6-18-31 2W5
11-16-31 4W5
7-28-31 4W5
6-7-32 2W5
16-7-32 2W5
6-17-32 2W5
8-17-32 2W5
6-18-32 2W5
8-18-32 2W5
14-18-32 2W5
16-18-32 2W5
8-19-32 2W5
16-19-32 2W5
6-20-32 2W5
6-30-32 2W5
16-10-32 3W5
16-11-32 3W5
8-12-32 3W5
14-12-32 3W5
6-13-32 3W5
8-13-32 3W5
16-13-32 3W5
14-14-32 3W5
16-14-32 3W5
16-15-32 3W5
6-16-32 3W5
16-21-32 3W5
6-22-32 3W5
8-22-32 3W5
14-22-32 3W5
16-22-32 3W5
6-23-32 3W5
8-23-32 3W5
14-23-32 3W5
16-23-32 3W5
6-24-32 3W5
8-24-32 3W5
14-24-32 3W5
16-24-32 3W5
6-25-32 3W5
16-25-32 3W5
6-27-32 3W5
16-28-32 3W5
15-14V-32 4W5
11-18-32 4W5
7-24V-32 4W5
5-27-32 4W5
10-23-33 2W5
3-19-33 4W5
5-19-33 4W5
7-19-33 4W5
11-31-33 4W5

9-26-30 3W5

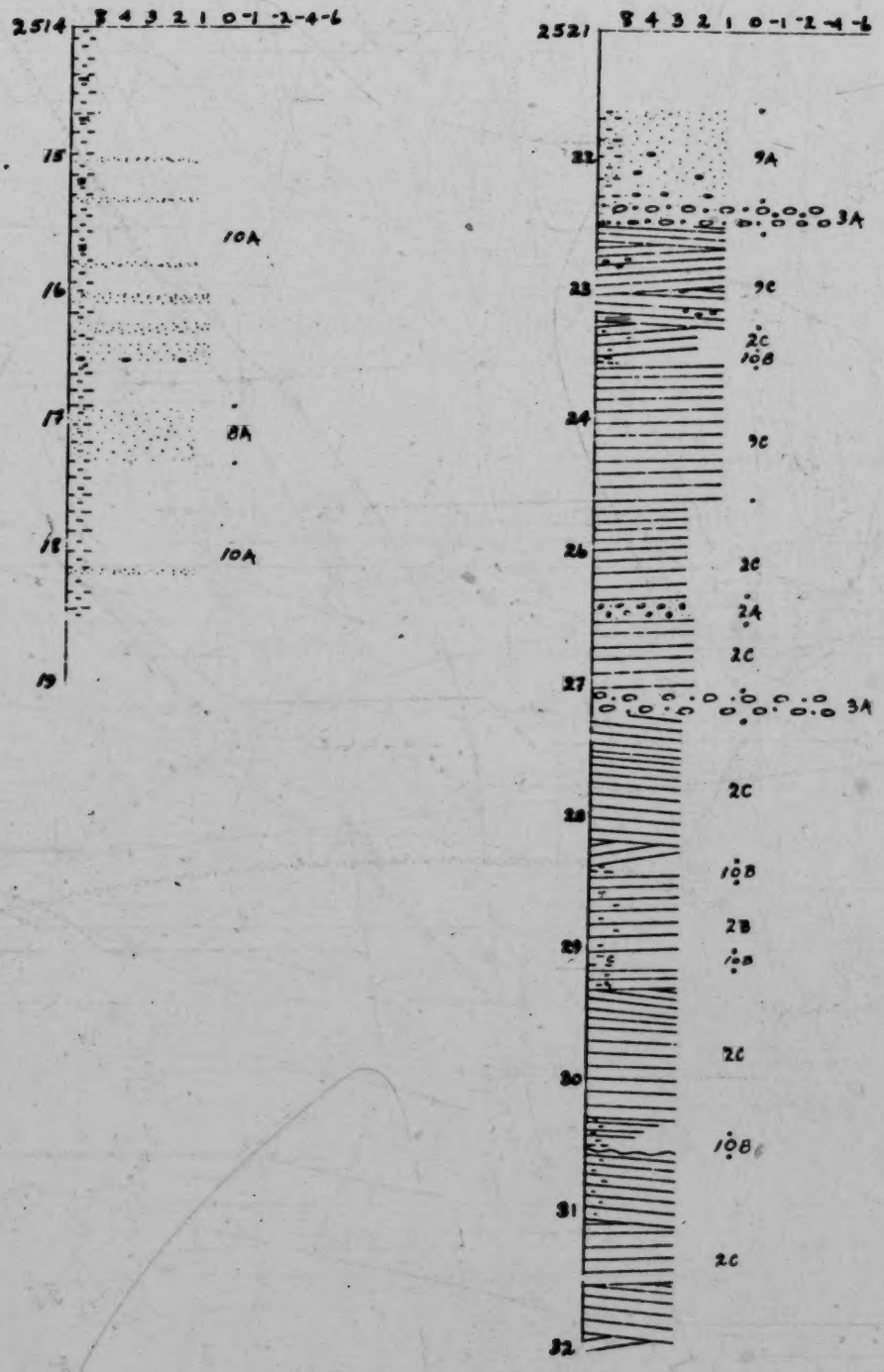
2514
8 4 3 2 1 0 -1 -2 -4 -6
15
16
17
18
19
10A
8A
10A
2521
8 4 3 2 1 0 -1 -2 -4 -6
22
23
24
25
26
27
28
29
30
31
32
9A
3A
9C
2C
10B
9C
2C
2A
2C
3A
2C
10B
2B
10B
2C
10B
2C

9-26-30 3W5 cont'd

6-10-31 2W5

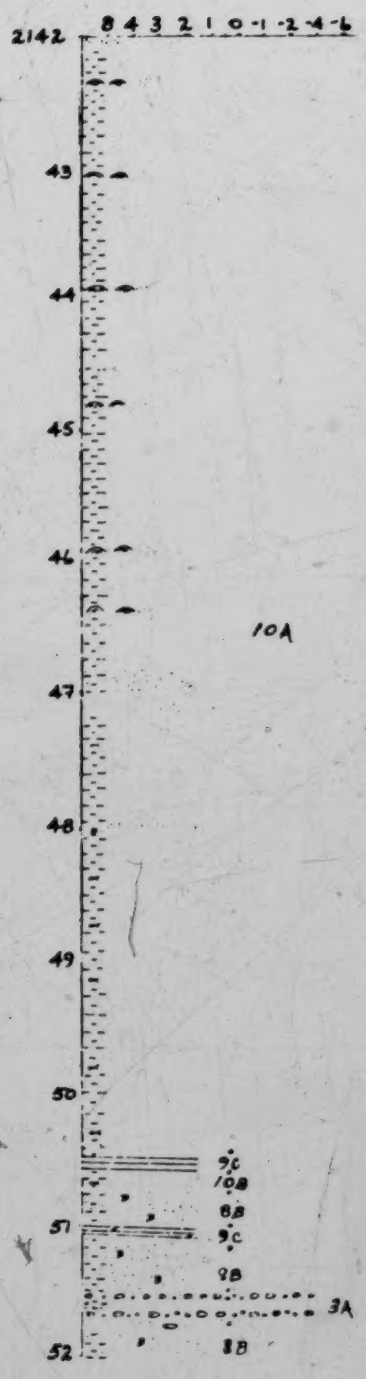
2142
8 4 3 2 1 0 -1 -2 -4 -6
43
44
45
46
47
48
49
50
51
52
10A
9C
10B
8B
9C
8B
3A
8B

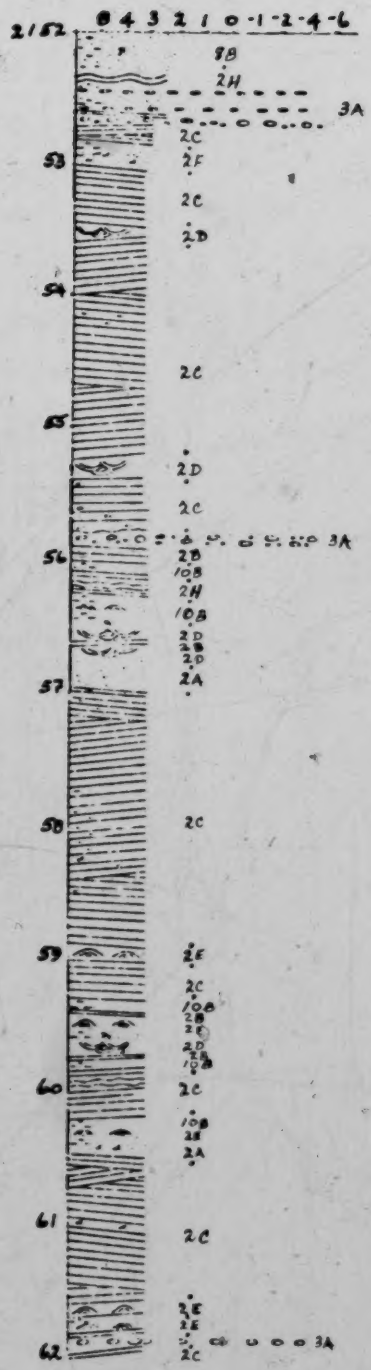
2152
8 4 3 2 1 0 -1 -2 -4 -6
8B
2H
3A
2C
53
2F
2C
2D
54
2C
55
2D
2C
56
3A
2B
10B
2H
10B
2D
2B
2D
2A
57
2C
58
59
2E
2C
10B
2B
2C
2D
2B
10B
60
2C
10B
2B
2A
61
2C
2E
2E
62
2C
3A

6-10-31 2W5 cont'd

6-18-31 2W5

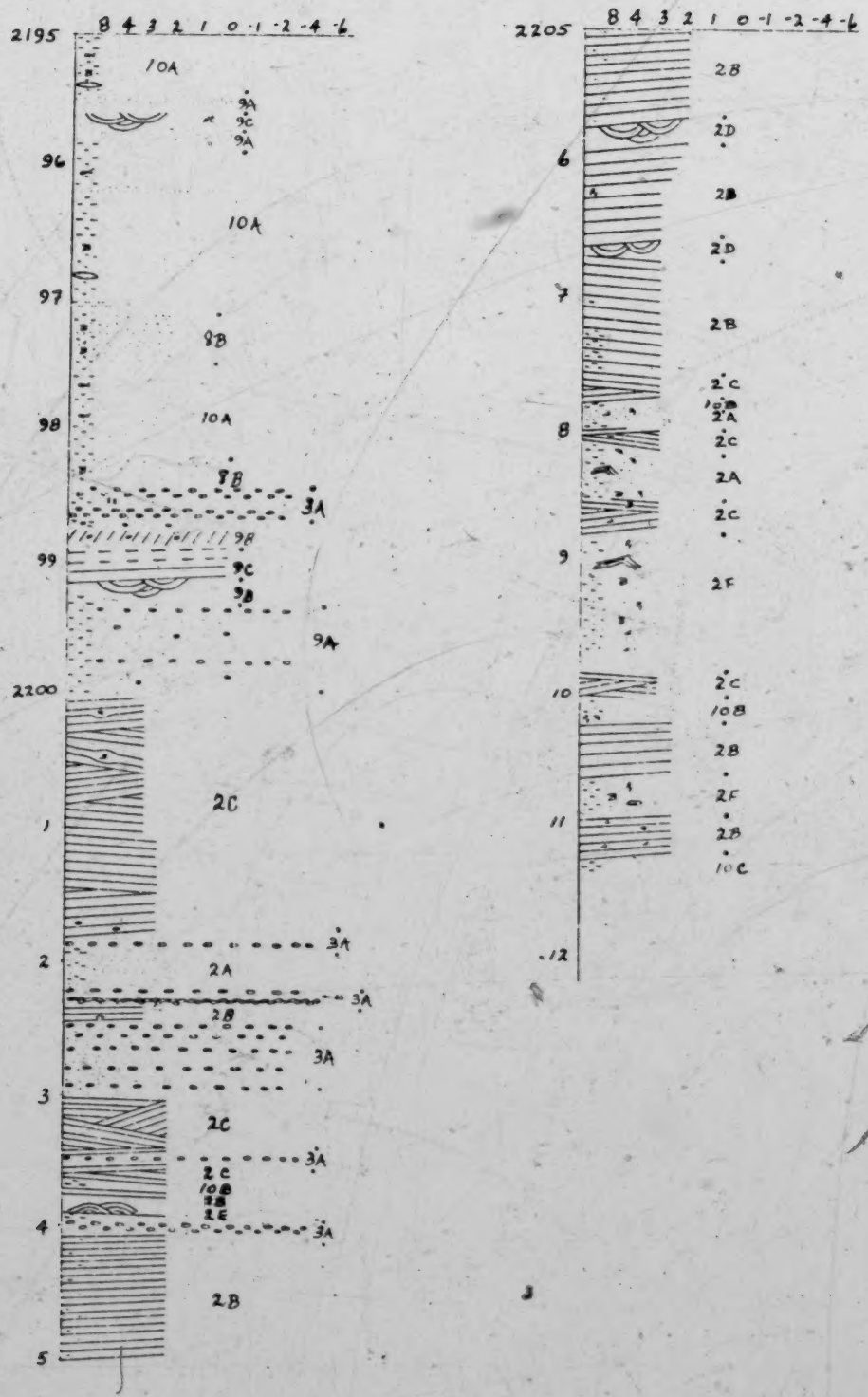
8 4 3 2 1 0 -1 -2 -4 -6
2195
96
97
98
99
2200
1
2
3
4
5
10A
9A
9C
9A
10A
9B
10A
9B
3A
9B
9C
9B
9A
2C
3A
2A
3A
2B
3A
2C
3A
2C
10B
2B
2E
3A
2B
2205
6
7
8
9
10
11
12
2B
2D
2B
2D
2B
2C
10B
2A
2C
2A
2C
2F
2C
10B
2B
2F
2B
10C

11-16-31 4W5

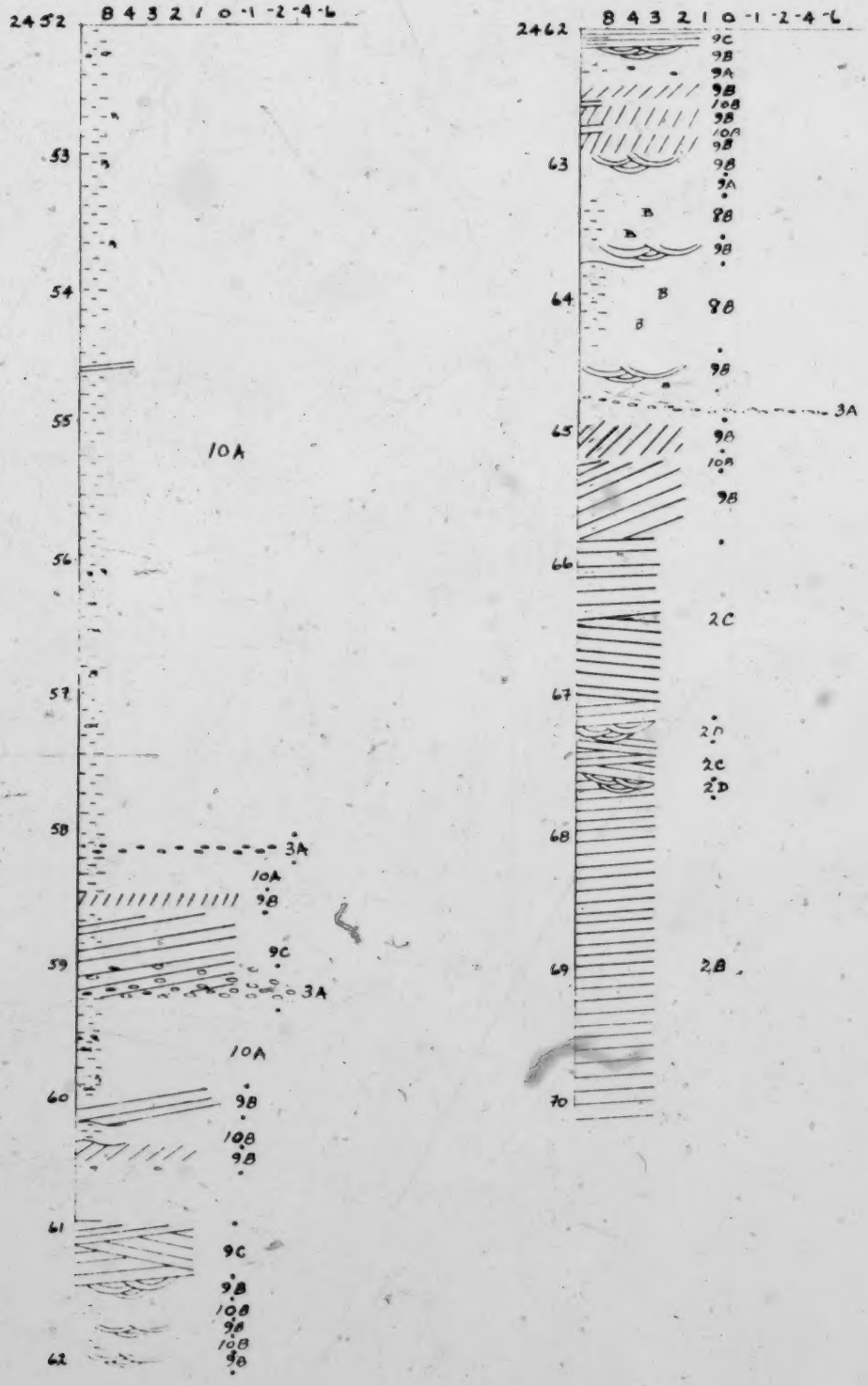
2452
8 4 3 2 1 0 -1 -2 -4 -6
53
54
55
56
57
58
59
60
61
62
10A
3A
10A
9B
9C
3A
10A
9B
10B
9B
9C
9B
10B
9B
10B
9B
2462
8 4 3 2 1 0 -1 -2 -4 -6
63
64
65
66
67
68
69
70
9C
9B
9A
9B
10B
9B
10B
9B
9B
9A
B
8B
B
9B
B
8B
B
9B
3A
9B
10B
9B
2C
2D
2C
2D
2B

7-28-31 4W5

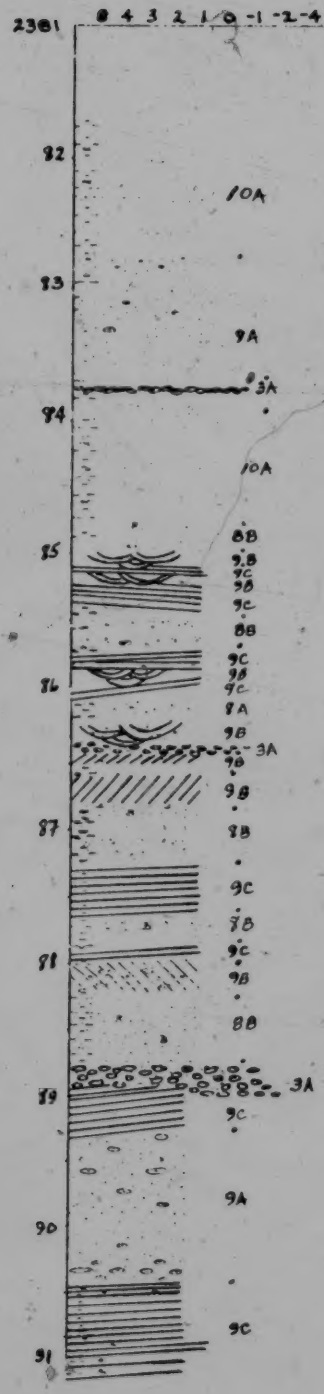
8 4 3 2 1 0 -1 -2 -4 -6
2381
82
83
84
85
86
87
88
89
90
91
10A
9A
3A
10A
8B
9B
9C
9B
9C
8B
9C
9B
9C
8A
9B
3A
9B
9B
8B
9C
9B
9C
9B
8B
3A
9C
9A
9C

6-7-32 2W5

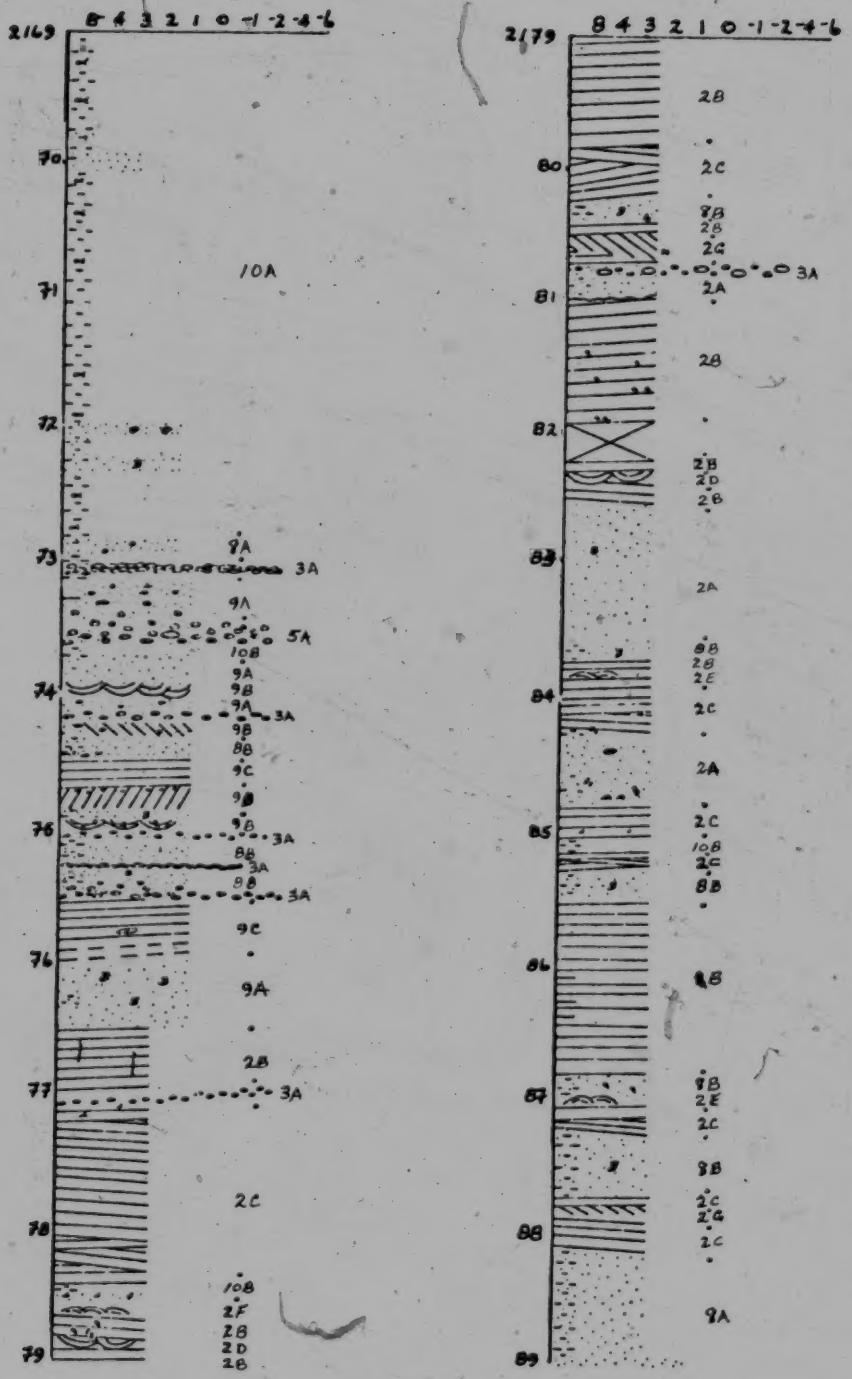
8 4 3 2 1 0 -1 -2 -4 -6
2169
70
71
72
73
74
75
76
77
78
79
10A
9A
3A
5A
10B
9B
9C
2B
2C
2F
2D
2179
80
81
82
83
84
85
86
87
88
89
2E
2G
2A

6-7-32 2W5 cont'd

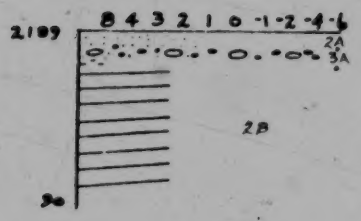

16-7-32 2W5

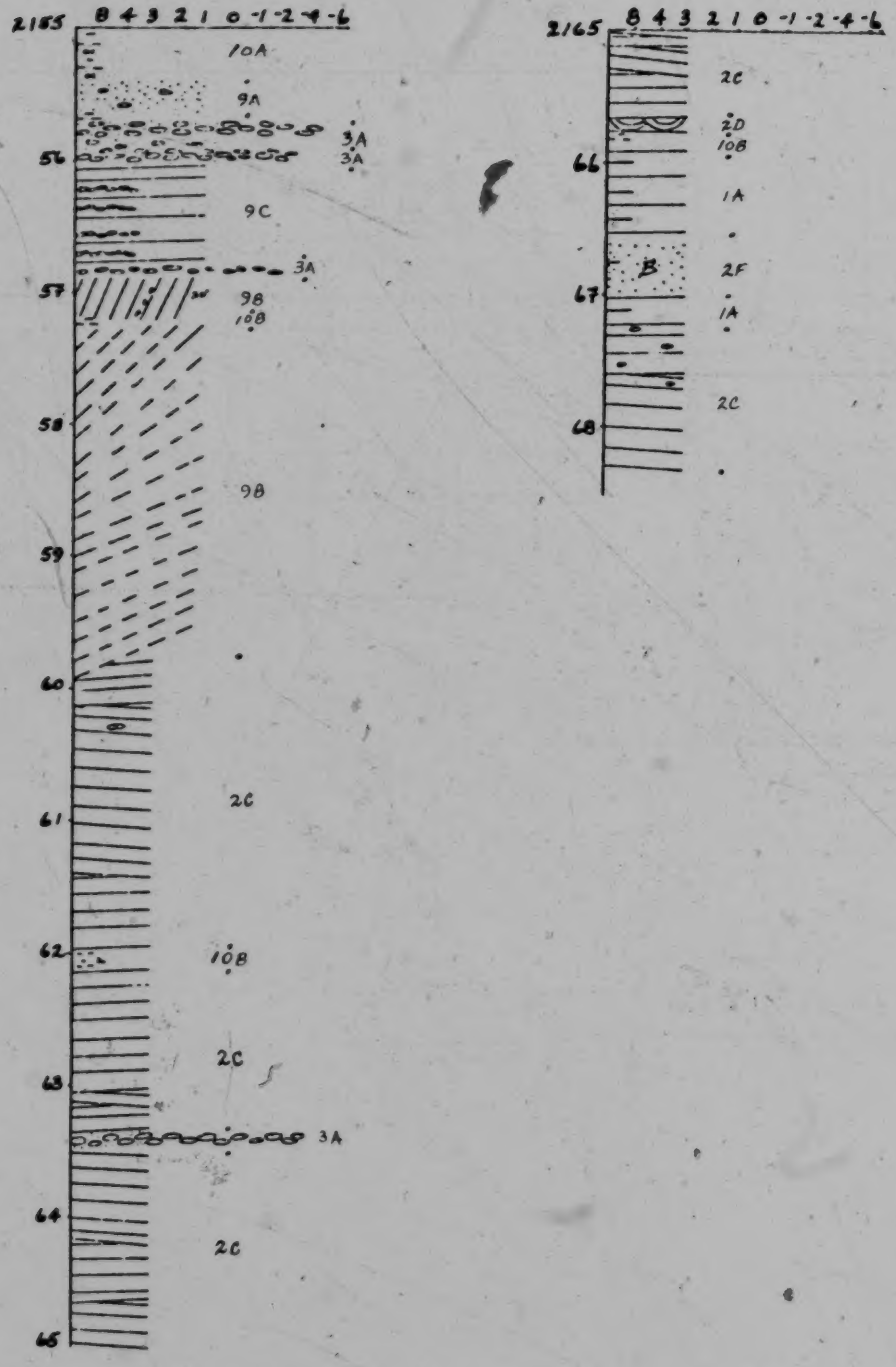
2165
8 4 3 2 1 0 -1 -2 -4 -6
10A
9A
3A
3A
9C
3A
9B
10B
9B
2C
10B
2C
3A
2C
56
57
58
59
60
61
62
63
64
65
2165
8 4 3 2 1 0 -1 -2 -4 -6
2C
2D
10B
1A
2F
1A
2C
66
67
68

6-17-32 2W5

8 4 3 2 1 0 -1 -2 -4 -6
2133
34
35
36
37
38
39
40
41
42
43
4A
5A
9A
3A
9B
3A
10B
3A
8B
2C
8A
2C
8B
2D
2B
10B
2A
1A
2C
2D
2C
10B
1A
2E
2B
1A
2B
1A
10B
2E
2A
1A
2E
8B
2C
2D
2B
10B
2C
2E
2A
1E
2C
2A
2C
2A
1A
2B
10B

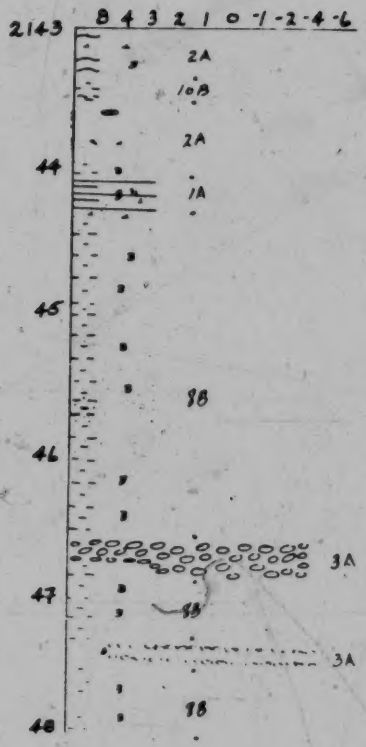
8 4 3 2 1 0 -1 -2 -4 -6
2143
44
45
46
47
48
2A
10B
2A
1A
8B
3A
8B
3A
8B

8-17-32 2W5

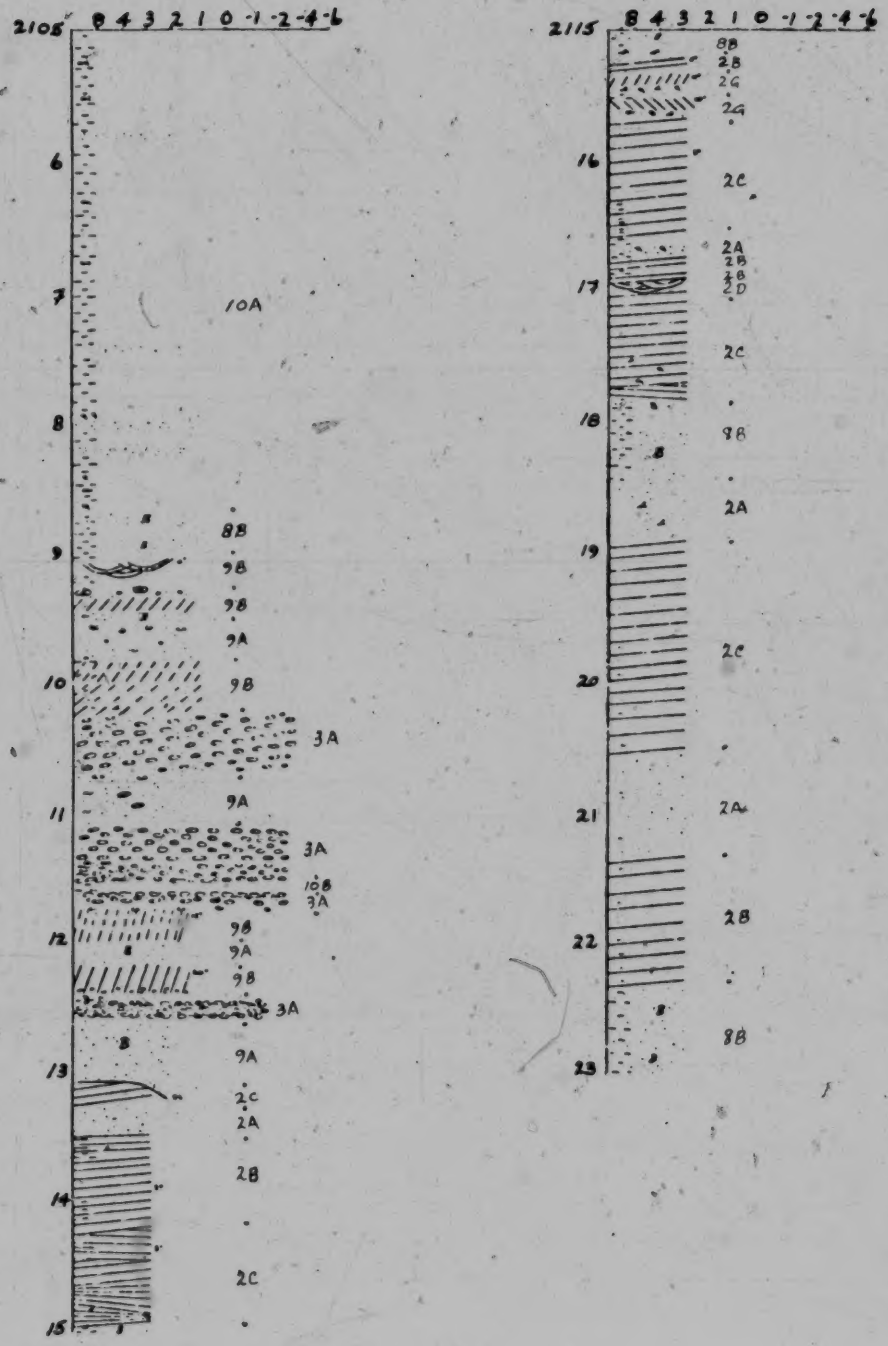
2105
8 4 3 2 1 0 -1 -2 -4 -6
6
7
8
9
10
11
12
13
14
15
10A
8B
9B
9B
9A
9B
3A
9A
3A
10B
3A
9B
9A
9B
3A
9A
2C
2A
2B
2C
2115
8 4 3 2 1 0 -1 -2 -4 -6
8B
2B
2C
2A
16
17
18
19
20
21
22
23
2C
2A
2B
2D
2C
9B
2A
2C
2A
2B
8B

6-18-32 2W5

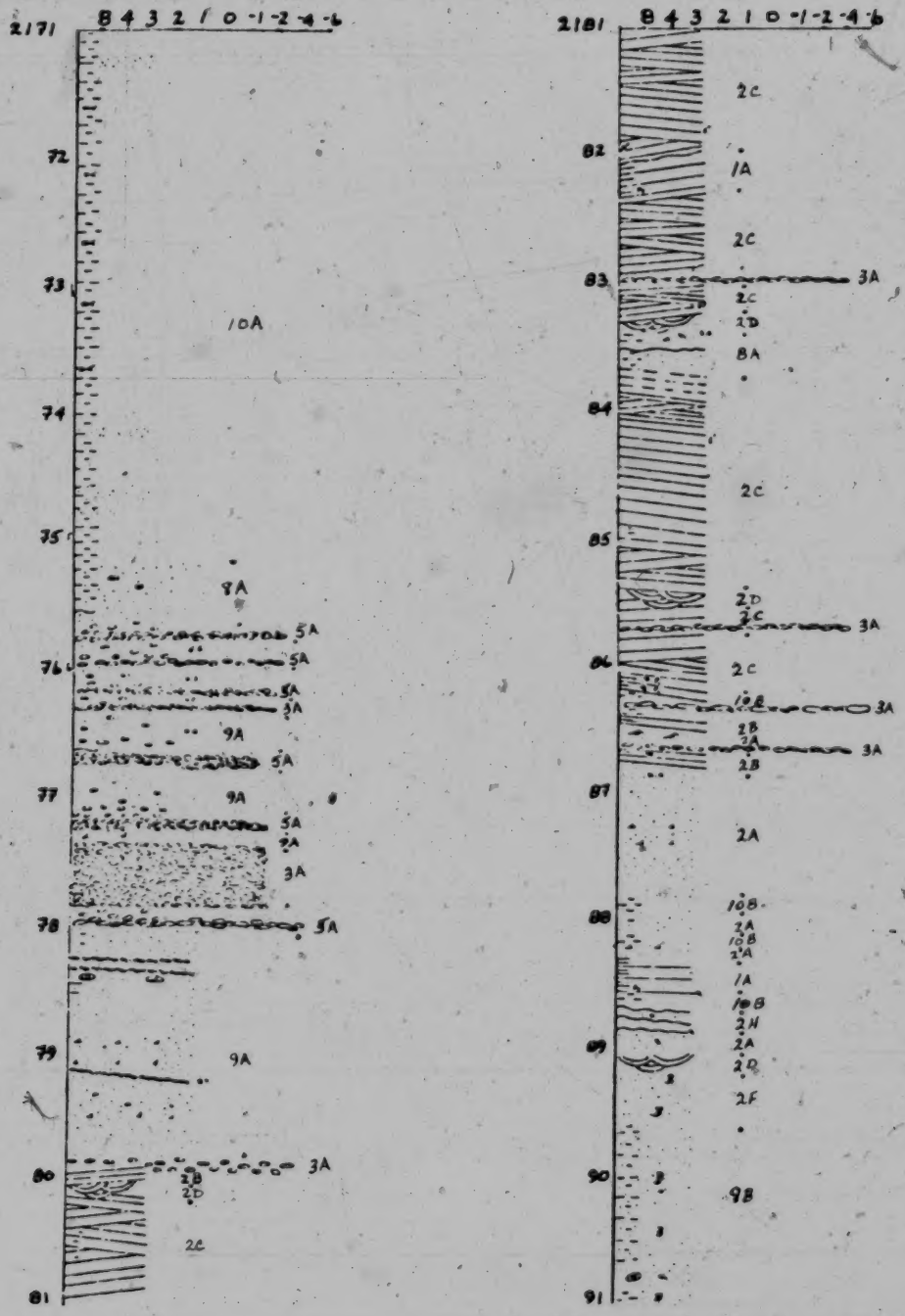
2171
8 4 3 2 1 0 -1 -2 -4 -6
72
73
74
75
76
77
78
79
80
81
10A
9A
5A
9A
5A
9A
5A
2A
3A
5A
9A
3A
2B
2D
2C
2181
8 4 3 2 1 0 -1 -2 -4 -6
82
83
84
85
86
87
88
89
90
91
2C
1A
2C
3A
2C
2D
8A
2C
2D
2C
3A
2C
10B
3A
2B
3A
3A
2B
2A
10B
2A
10B
2A
1A
10B
2H
2A
2D
2F
9B

6-18-32 2W5 cont'd

8-18-32 2W5

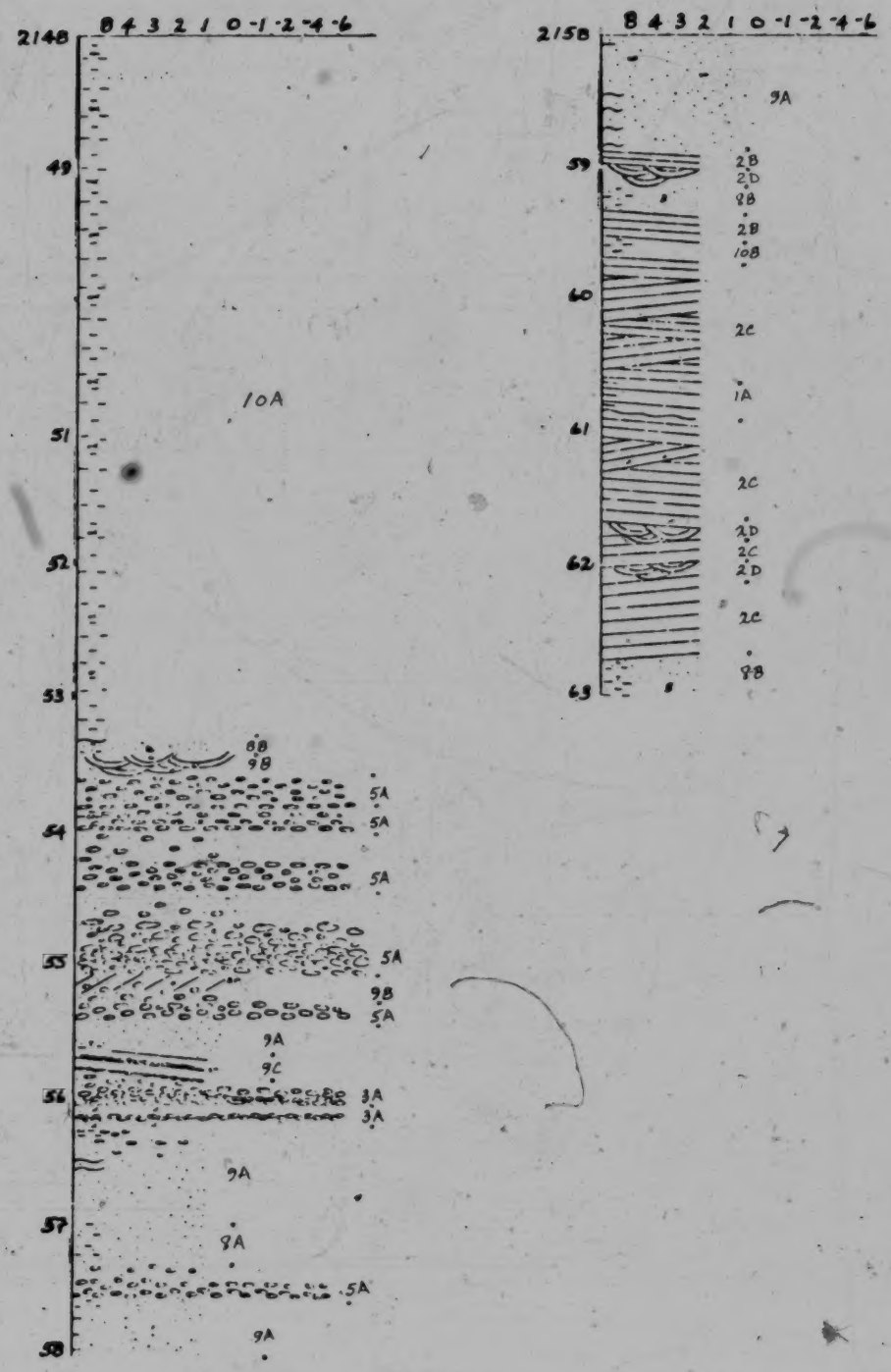
2148
8 4 3 2 1 0 -1 -2 -4 -6
49
10A
51
52
53
8B
9B
5A
54
5A
5A
55
5A
9B
5A
9A
9C
56
3A
3A
9A
57
9A
5A
9A
58
2158
8 4 3 2 1 0 -1 -2 -4 -6
9A
59
2B
2D
8B
2B
10B
60
2C
1A
61
2C
2D
2C
62
2D
2C
8B
63

14-18-32 2W5

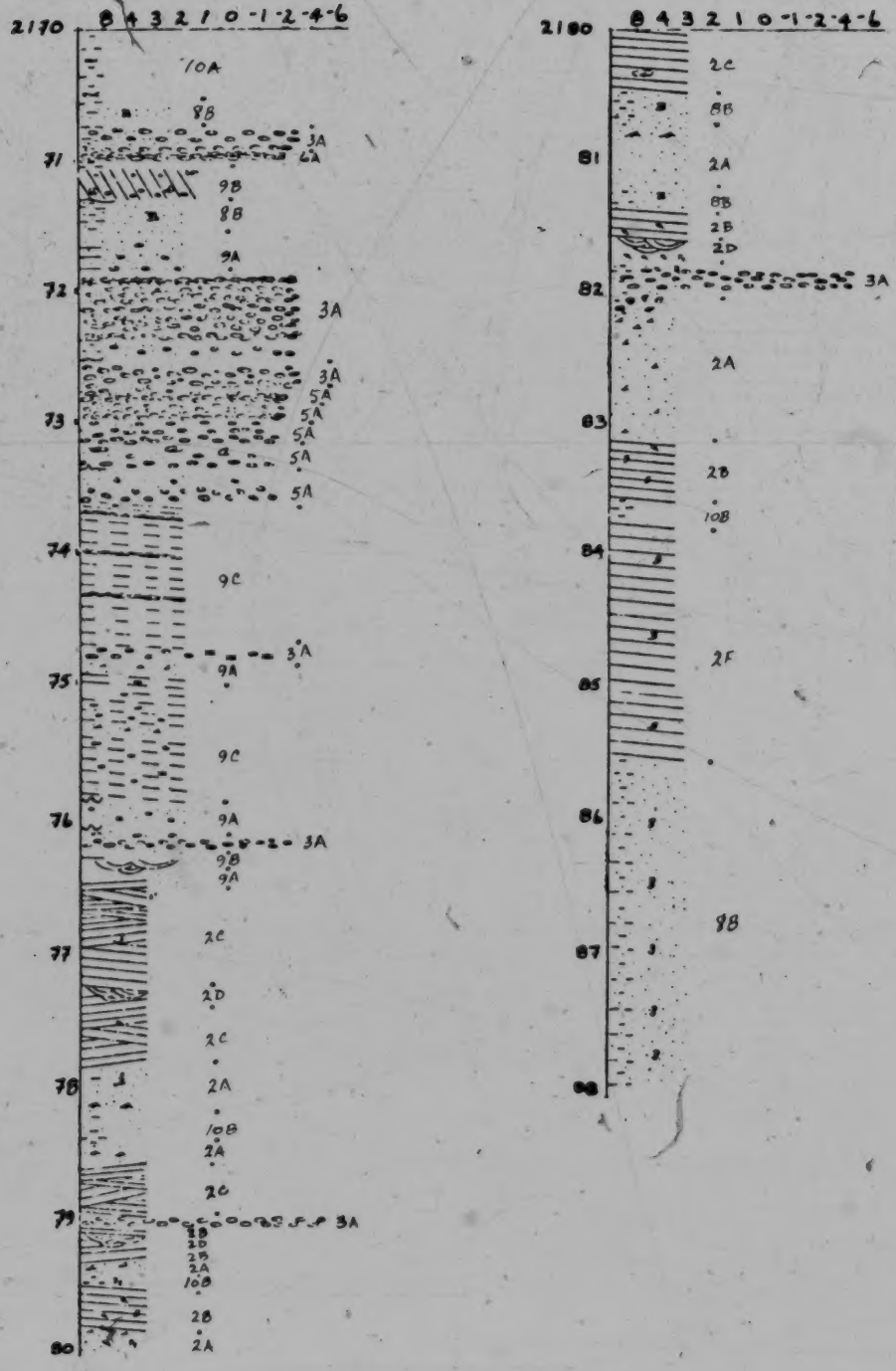
2170
8 4 3 2 1 0 -1 -2 -4 -6
10A
8B
3A
4A
9B
8B
9A
3A
3A
5A
5A
5A
5A
5A
9C
3A
9A
9C
9A
3A
9B
9A
2C
2D
2C
2A
10B
2A
2C
3A
2B
2D
2B
2A
10B
2B
2A
71
72
73
74
75
76
77
78
79
80
2180
8 4 3 2 1 0 -1 -2 -4 -6
2C
8B
2A
8B
2B
2D
3A
2A
2B
10B
2F
9B
81
82
83
84
85
86
87
88

16-18-32 2W5

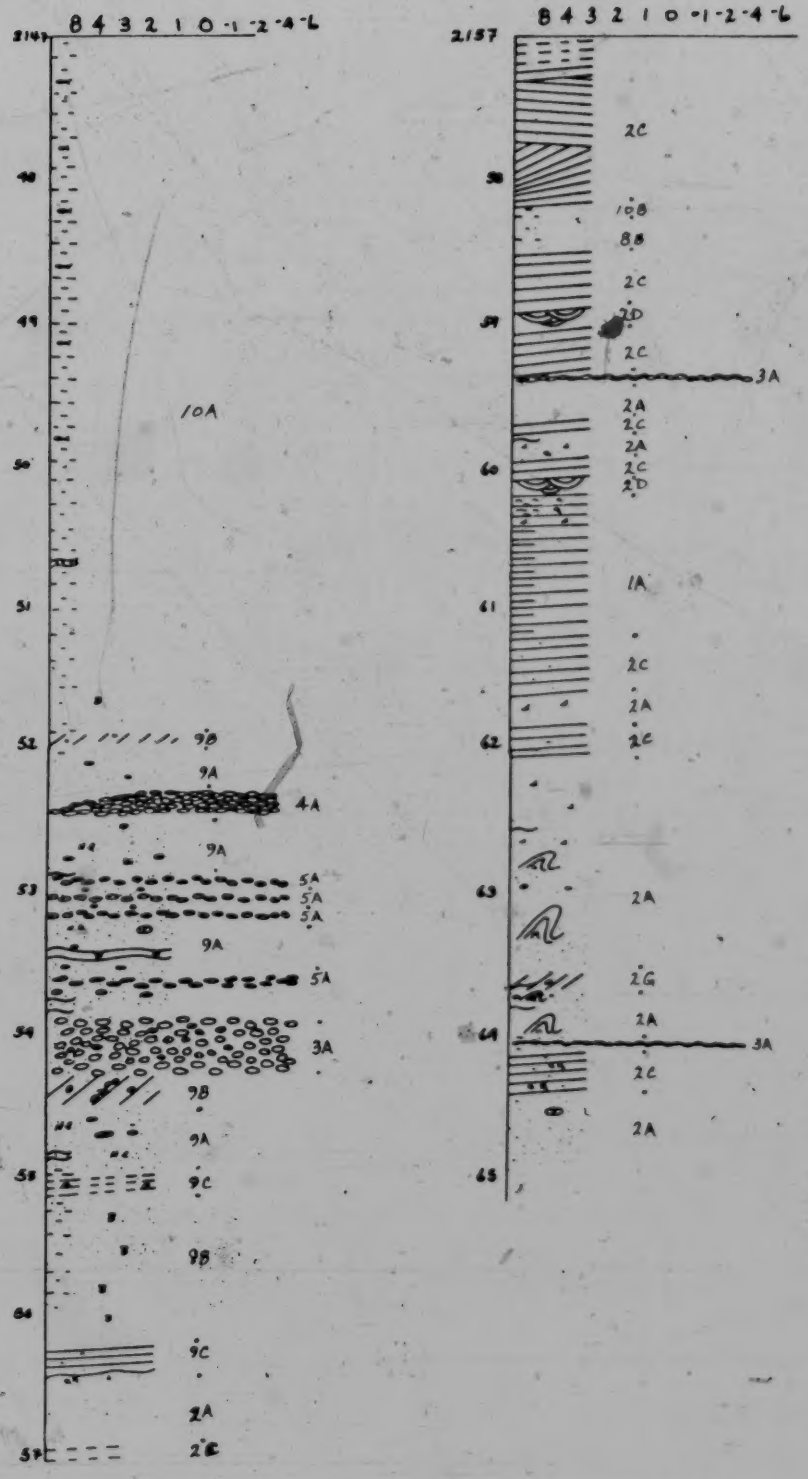
8 4 3 2 1 0 -1 -2 -4 -6
2147
48
49
50
51
52
53
54
55
56
57
10A
9D
9A
4A
9A
5A
5A
5A
9A
5A
3A
9B
9A
9C
9B
9C
2A
2C
8 4 3 2 1 0 -1 -2 -4 -6
2157
58
59
60
61
62
63
64
65
2C
10B
8B
2C
2D
2C
3A
2A
2C
2A
2C
2D
1A
2C
2A
2C
2A
2G
2A
3A
2C
2A

8-19-32 2W5

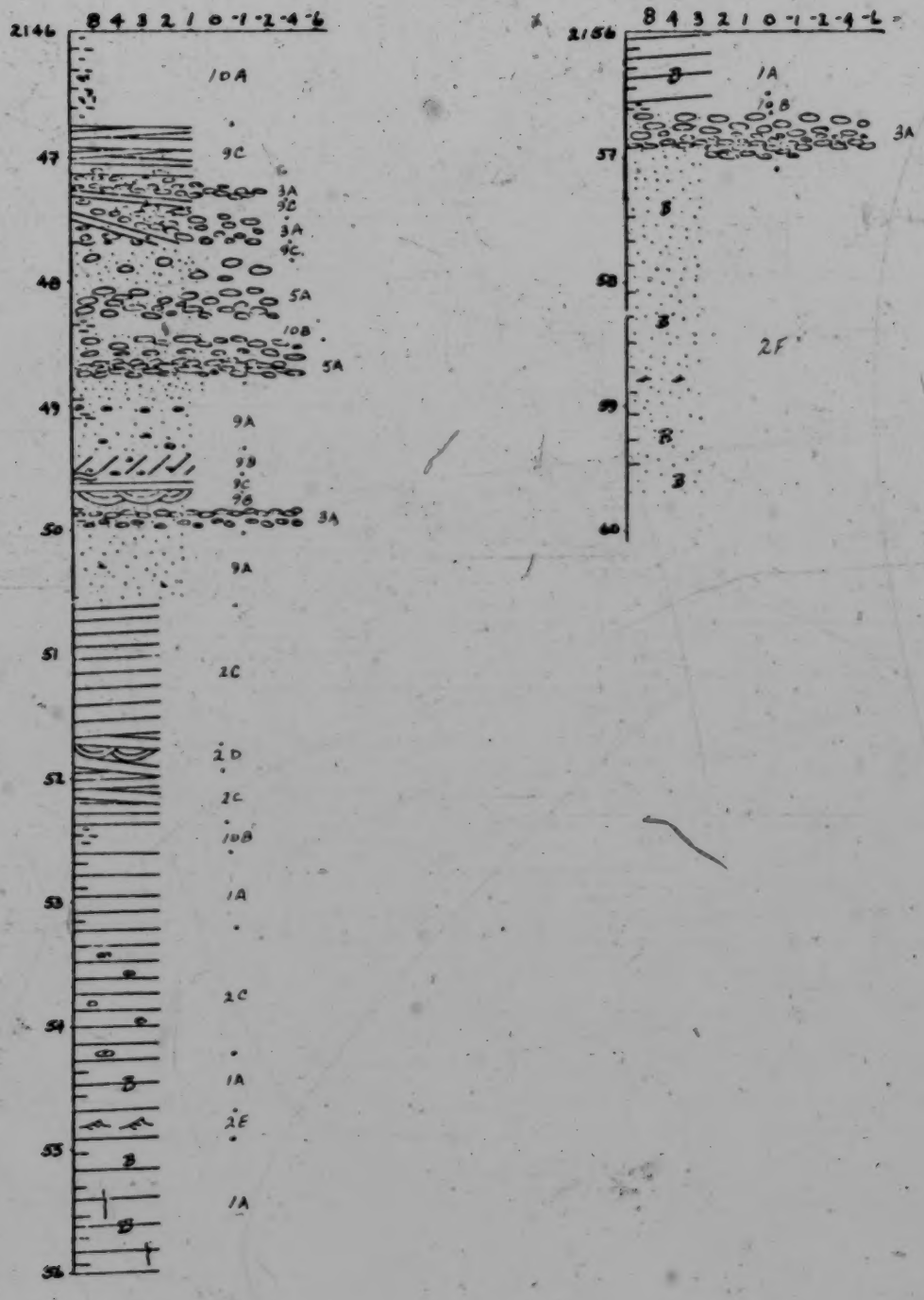
8 4 3 2 1 0 -1 -2 -4 -6
2146
47
48
49
50
51
52
53
54
55
56
10A
9C
3A
9C
3A
9C
5A
10B
5A
9A
9B
9C
9B
3A
9A
2C
2D
2C
10B
1A
2C
1A
2E
1A
8 4 3 2 1 0 -1 -2 -4 -6
2156
57
58
59
60
1A
10B
3A
2F

16-19-32 2W5

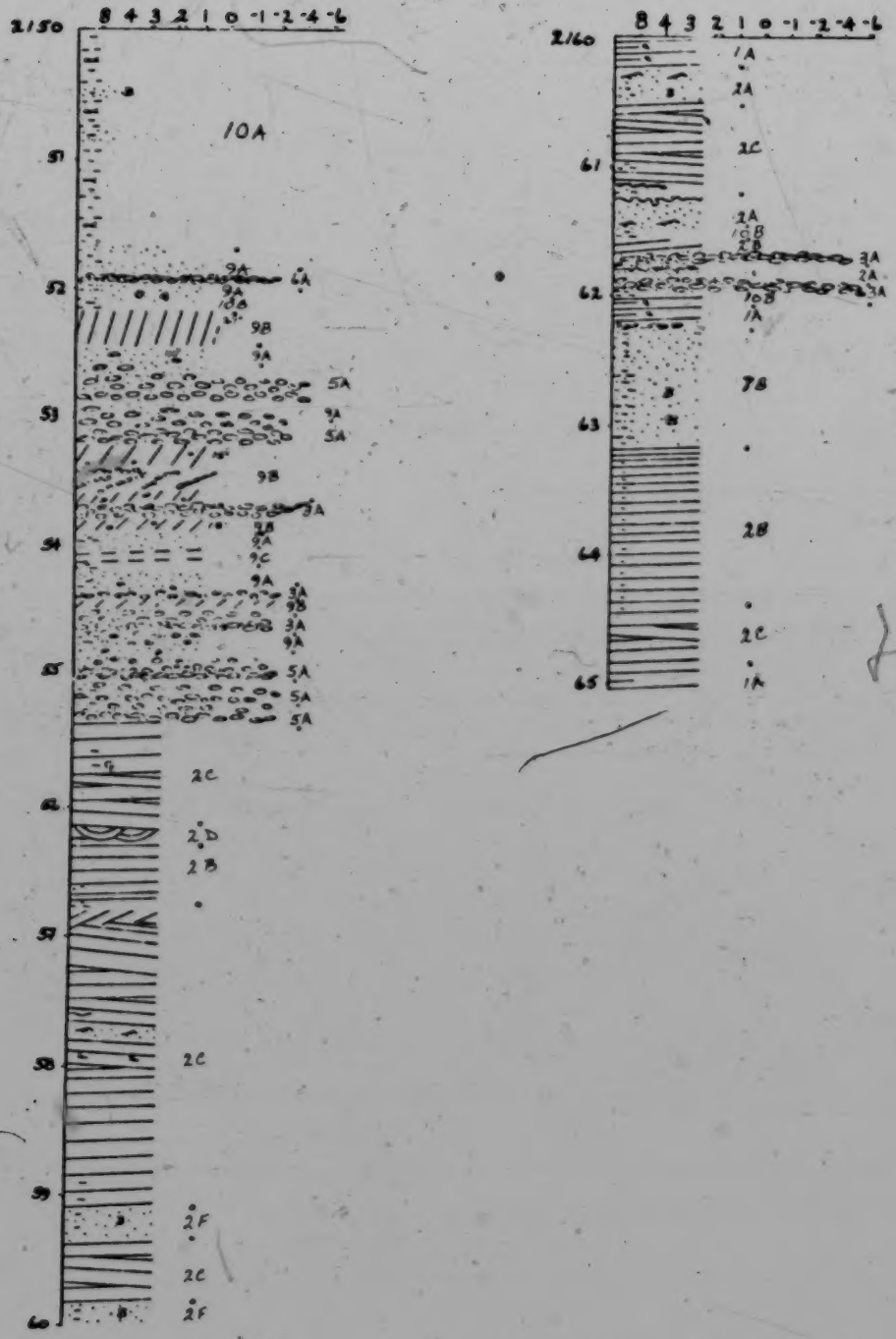
2150
8 4 3 2 1 0 -1 -2 -4 -6
51
52
53
54
55
56
57
58
59
60
10A
9A
4A
10A
9B
9A
5A
9A
5A
9B
9A
3A
9A
9C
9A
3A
9B
3A
9A
5A
5A
5A
2C
2D
2B
2C
2F
2C
2F
2160
8 4 3 2 1 0 -1 -2 -4 -6
61
62
63
64
65
1A
2A
2C
2A
1C
1B
2B
3A
2A
3A
10B
1A
7B
2B
2C
1A

6-20-32 2W5

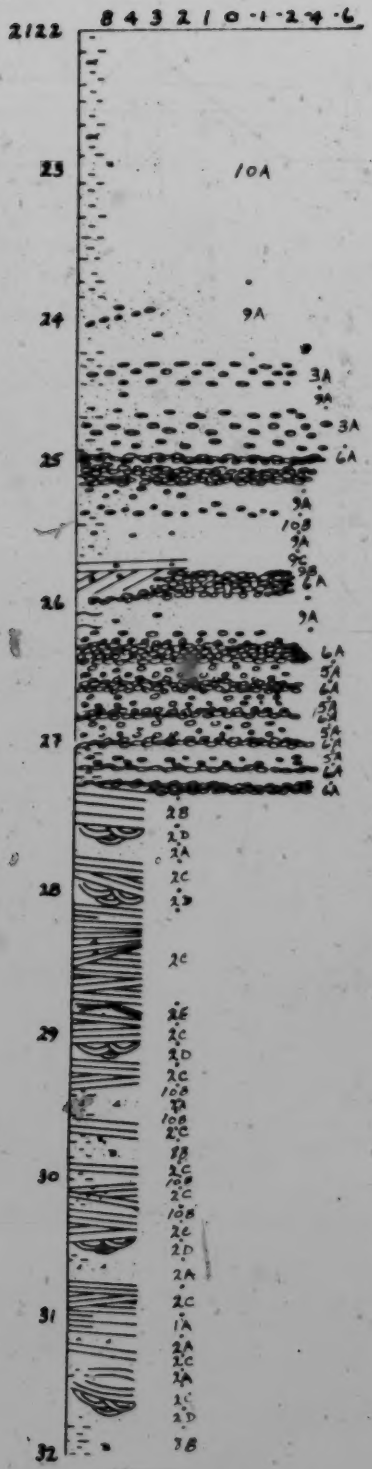
8 4 3 2 1 0 -1 -2 -4 -6
2122
23
24
25
26
27
28
29
30
31
32
10A
9A
3A
6A
5A
2B
2D
2A
2C
2E
1A
10B
9C
8B

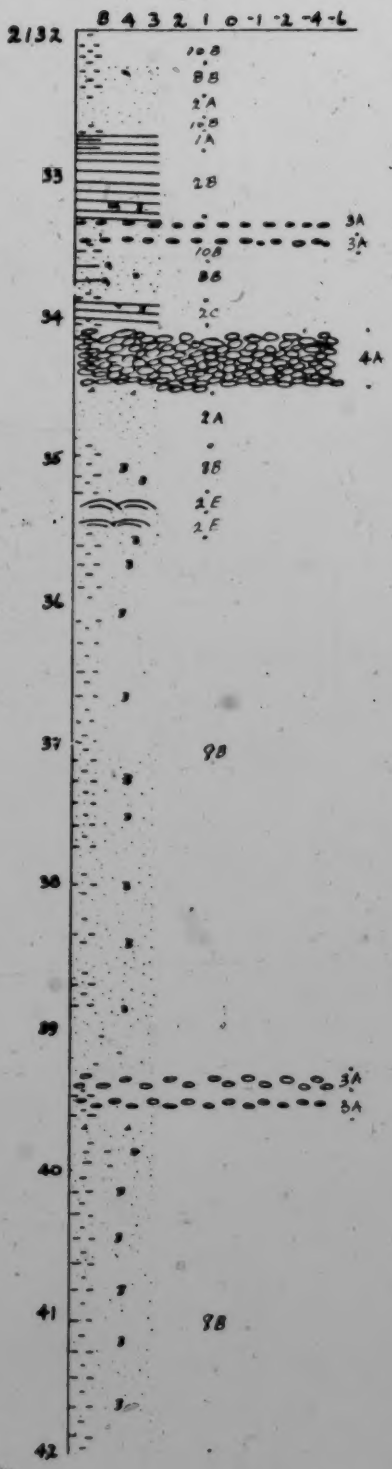
8 4 3 2 1 0 -1 -2 -4 -6
2132
33
34
35
36
37
38
39
40
41
42
10B
8B
2A
1A
2B
3A
2C
4A
2E
9B
8A

6-20-32 2W5 cont'd

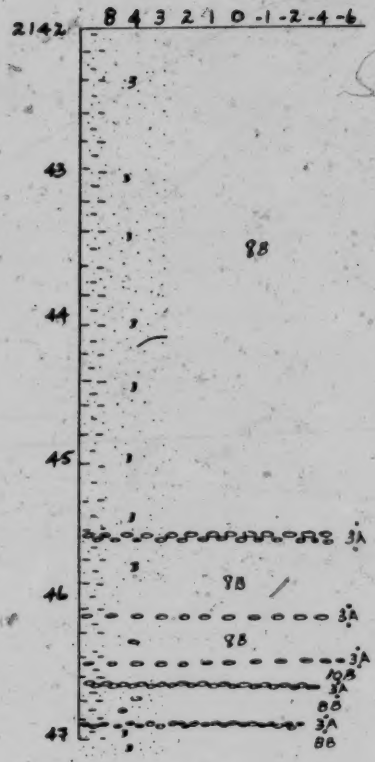

BIOTURBATED TO 2158

6-30-32 2W5

2/69
8 4 3 2 1 0 -1 -2 -4 -6
70
71
72
73
74
75
76
77
78
79
10A
9A
5A
3A
2C
2B
10B
2A
1A

2/79
8 4 3 2 1 0 -1 -2 -4 -6
80
81
82
83
84
1A
1D
2A
2C
2B
3

16-10-32 3W5

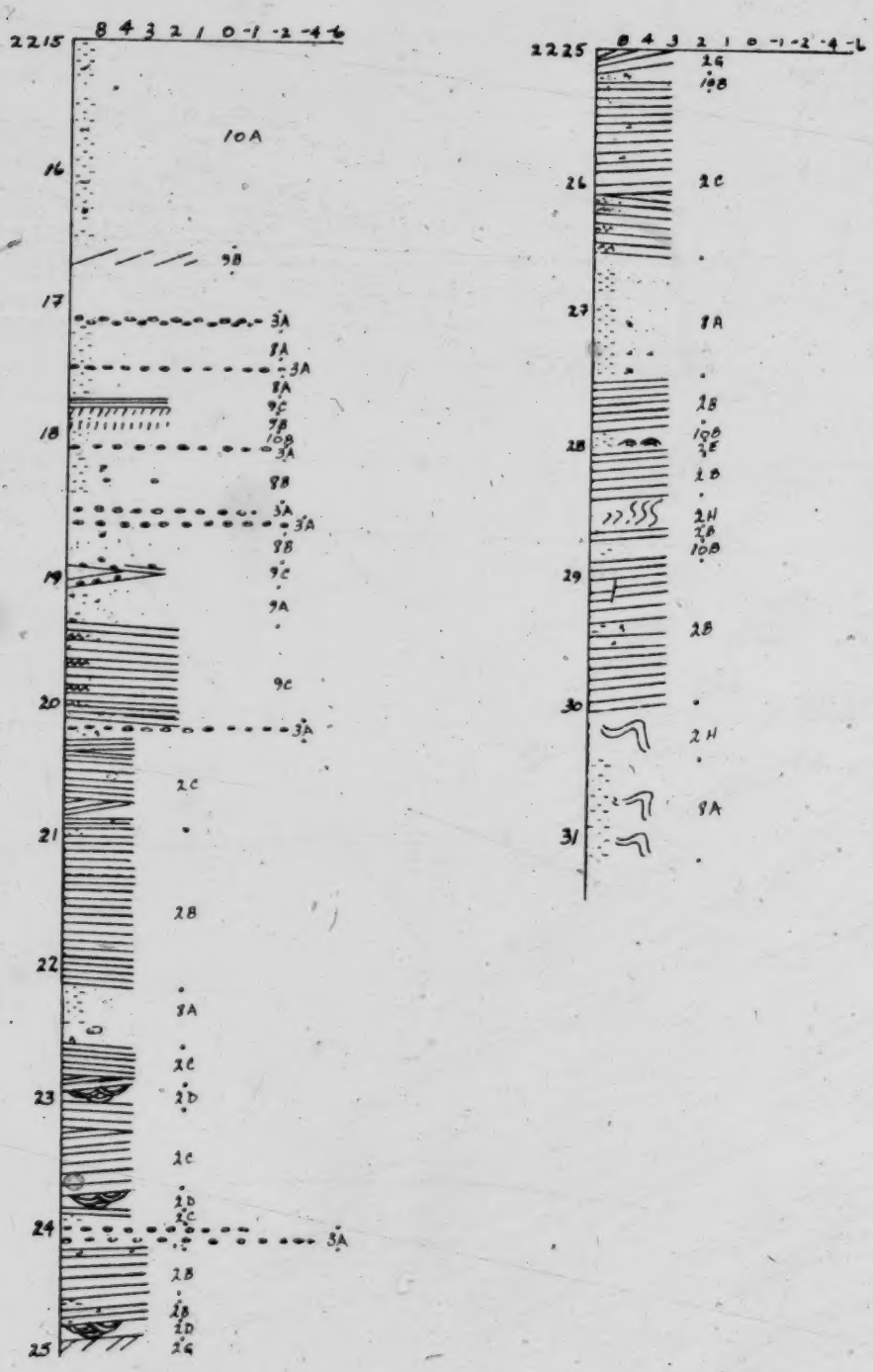
2215
8 4 3 2 1 0 -1 -2 -4 -6
16
17
18
19
20
21
22
23
24
25
10A
9B
3A
1A
9C
9B
10B
9A
2C
2B
2D
2E
2225
26
27
28
29
30
31
2G
10B
2C
1A
2B
10B
2F
2D
2H
2A
10B
2B
2H
1A

16-11-32 3W5

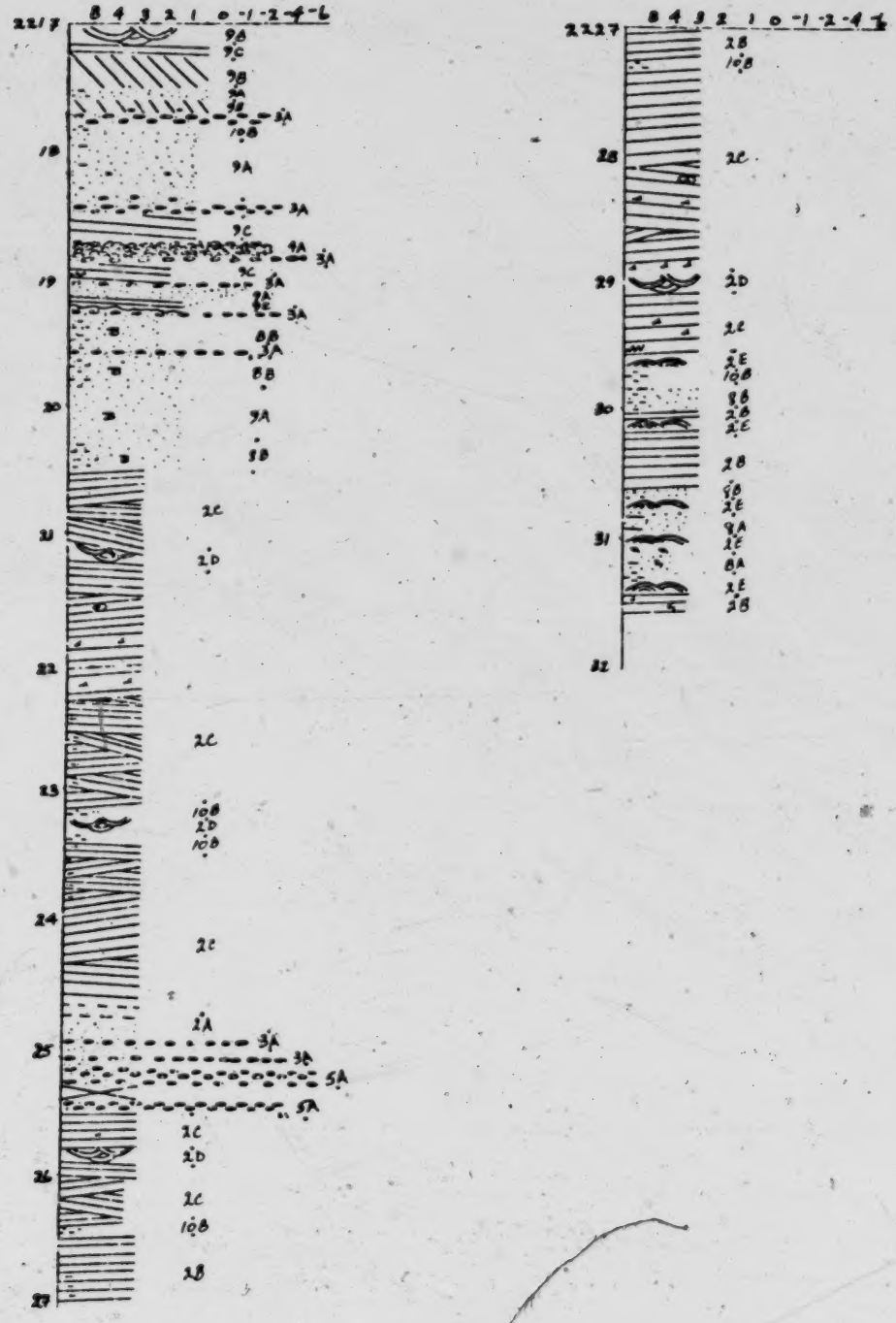

8-12-32 3W5

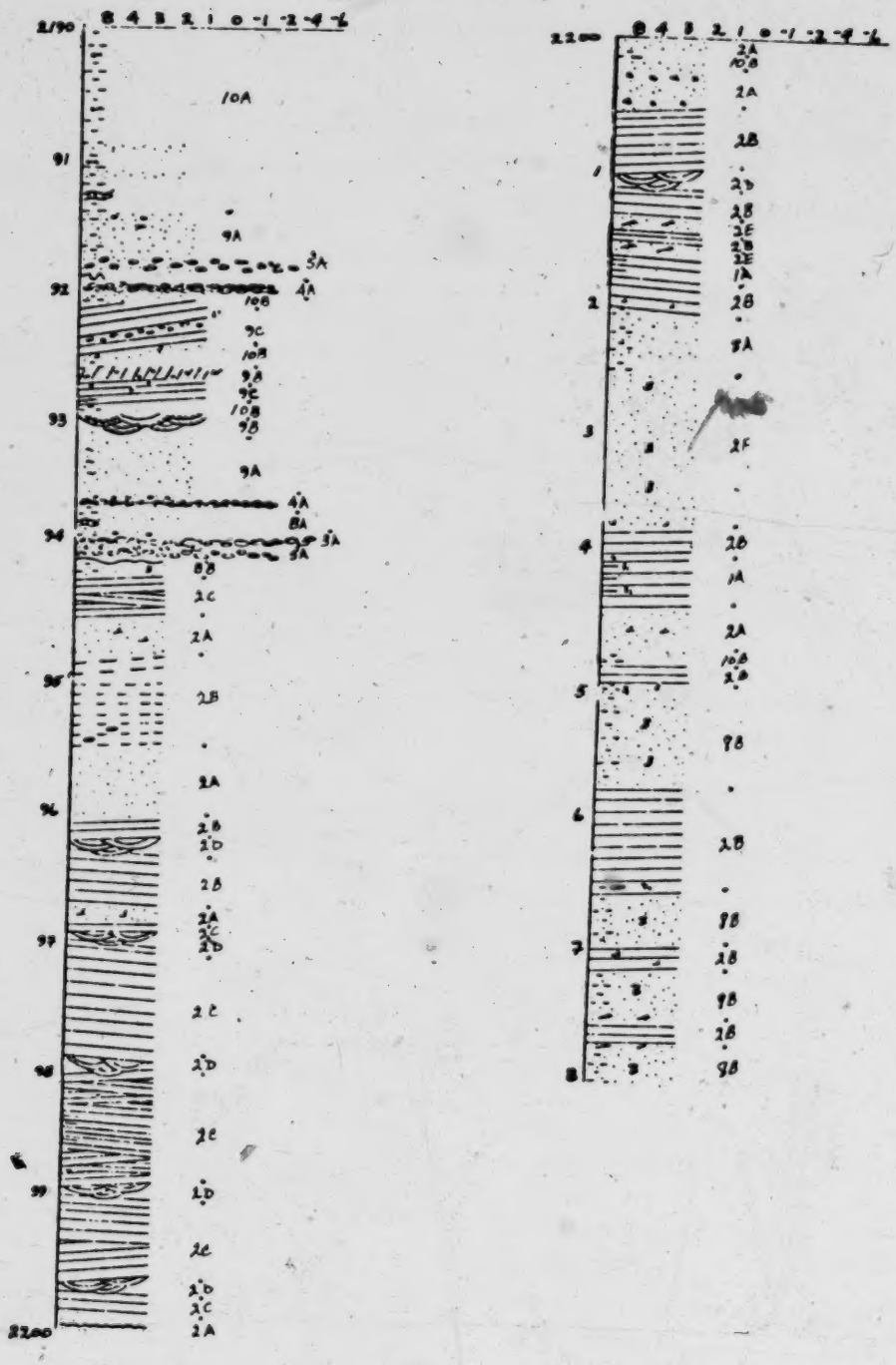
2190
91
92
93
94
95
96
97
98
99
2200
10A
9A
3A
4A
10B
9C
9B
8A
8B
2C
2A
2B
2D
2E
1A
2200
1
2
3
4
5
6
7
8
2F
9B

14-12-32 3W5

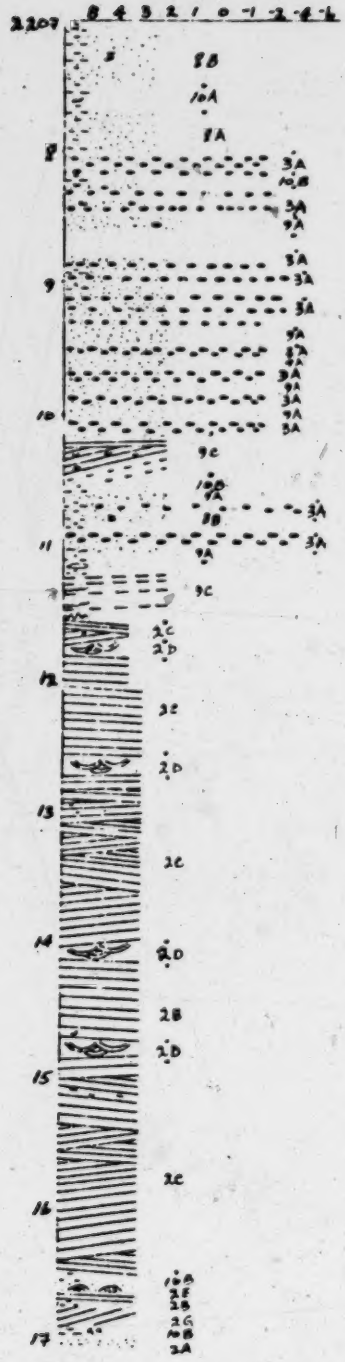
3207
8 4 3 2 1 0 -1 -2 -4 -6
8
9
10
11
12
13
14
15
16
17
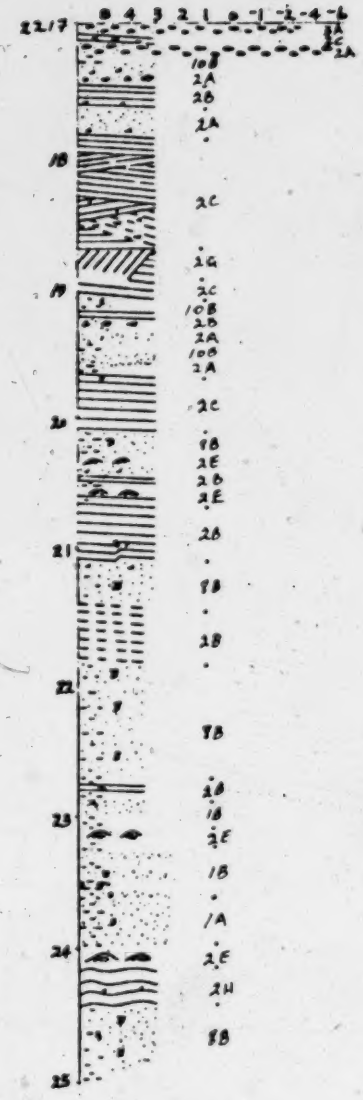
2217
8 4 3 2 1 0 -1 -2 -4 -6
18
19
20
21
22
23
24
25

6-13-32 3W5

8-13-32 3W5

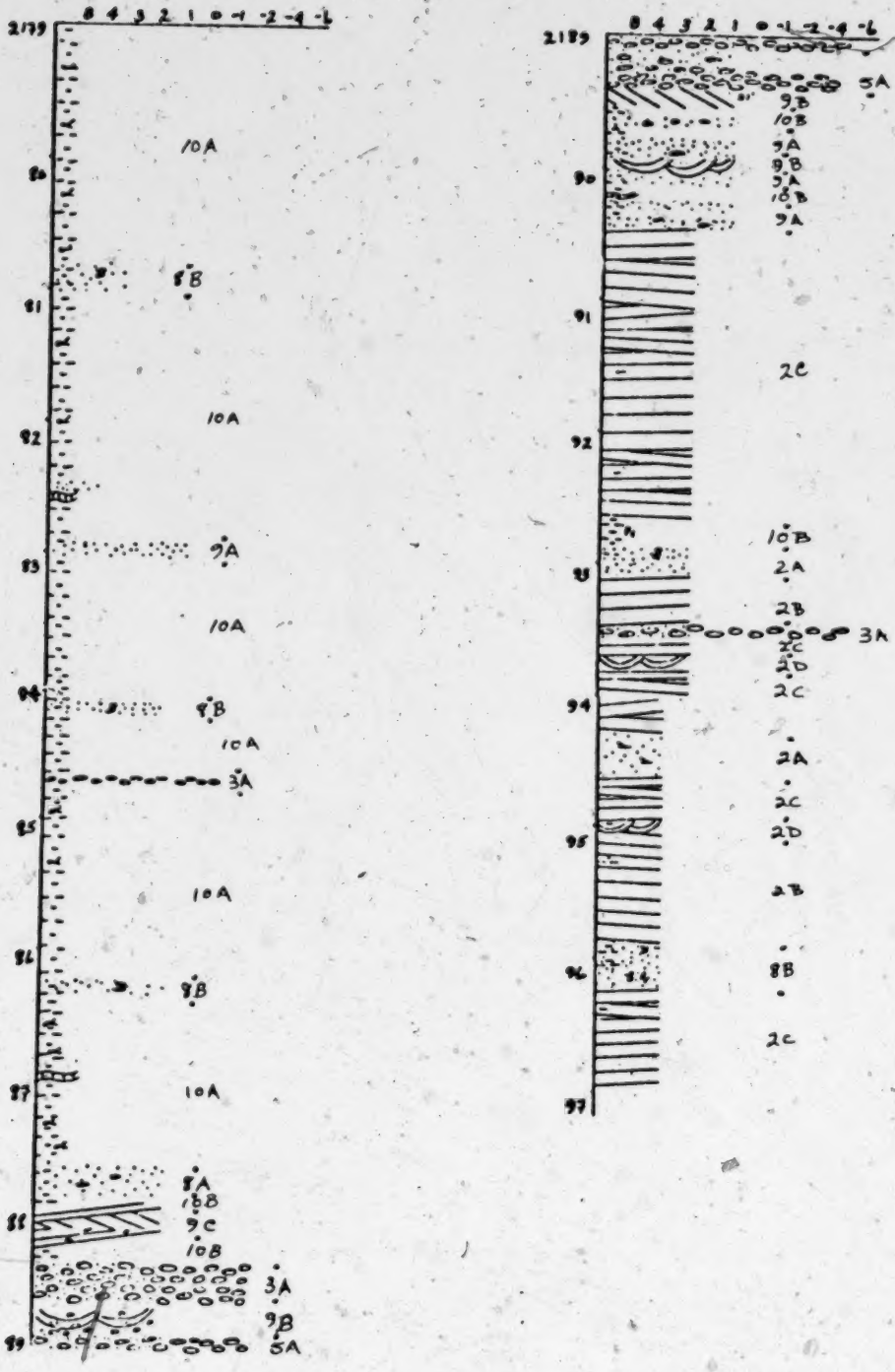
8 4 3 2 1 0 -1 -2 -4 -6
2179
10A
8B
10A
9A
10A
9B
10A
3A
10A
9B
10A
9A
1BB
9C
10B
3A
9B
5A
8 4 3 2 1 0 -1 -2 -4 -6
2189
5A
9B
10B
9A
9B
9A
10B
9A
2C
10B
2A
2B
3A
2C
2D
2C
2A
2C
2D
2B
8B
2C

16-13-32 3W5

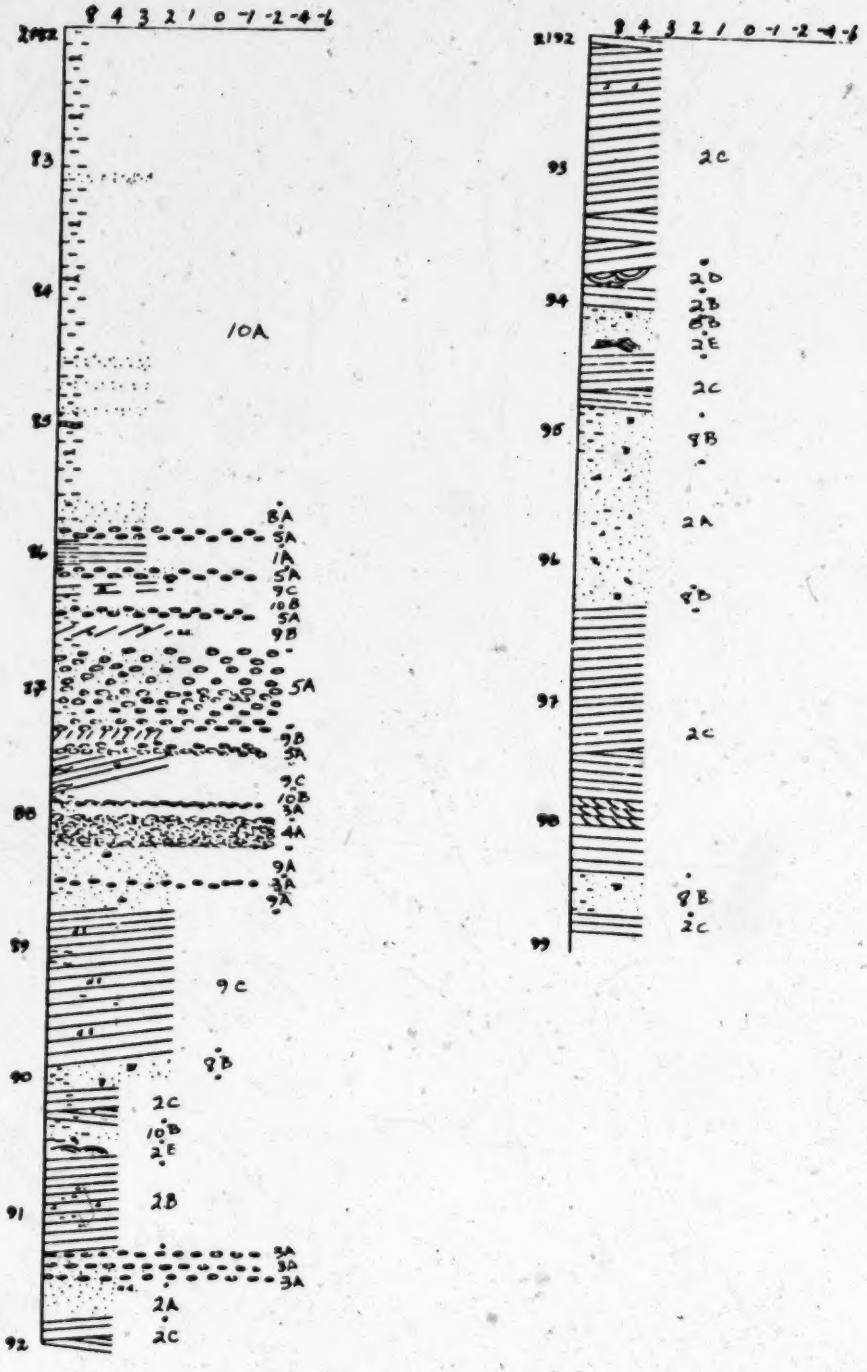
8 4 3 2 1 0 -1 -2 -4 -6
2192
93
94
95
96
97
98
99
10A
8A
5A
1A
5A
9C
10B
5A
9B
5A
9B
5A
9C
10B
5A
4A
9A
3A
9A
9C
8B
2C
10B
2E
2B
3A
3A
3A
2A
2C
2C
2D
2B
8B
2E
2C
8B
2A
8D
2C
8B
2C

14-14-32 3W5

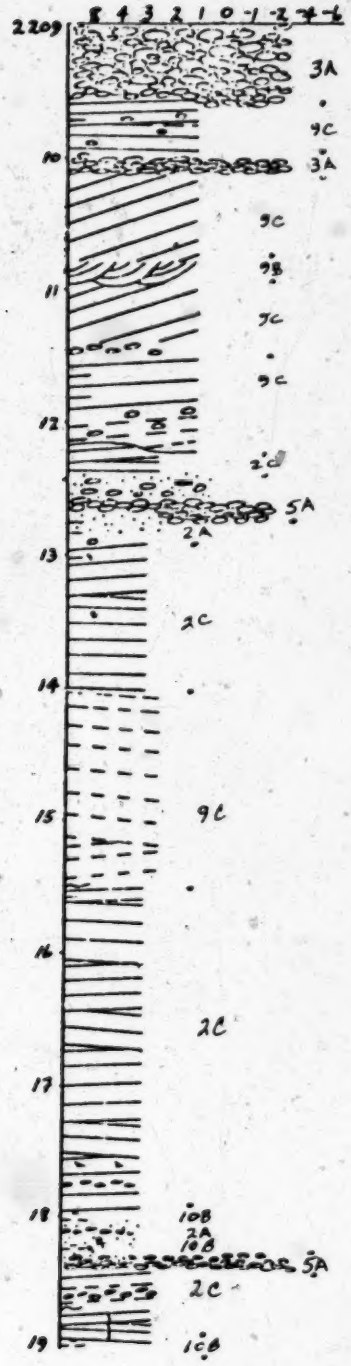
8 4 3 2 1 0 -1 -2 -4 -6
2209
3A
9C
10
3A
9C
9B
11
7C
9C
12
2C
5A
2A
13
2C
14
9C
15
16
2C
17
18
10B
2A
10B
5A
2C
19
10B

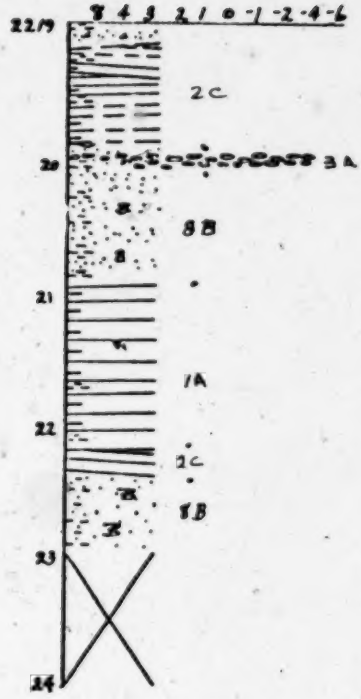
8 4 3 2 1 0 -1 -2 -4 -6
2219
2C
20
3A
8B
8
21
1A
22
2C
8B
23
24

16-14-32 3W5

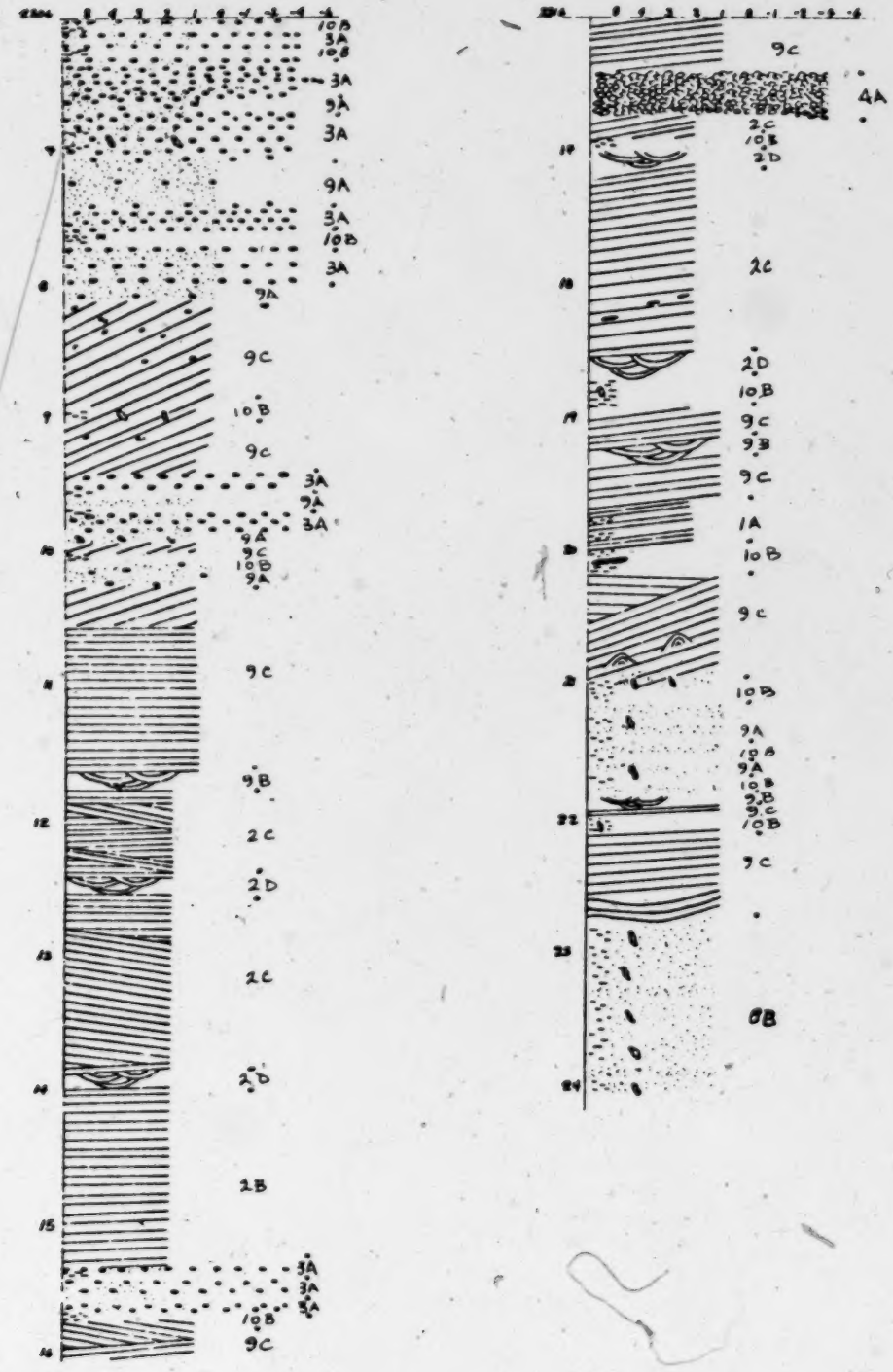
10B
3A
10B
3A
9A
3A
9A
3A
10B
3A
9A
9C
10B
9C
3A
9A
3A
9A
9C
10B
9A
9C
9B
2C
2D
2C
2D
2B
3A
3A
3A
10B
9C
9C
4A
2C
10B
2D
2C
2D
10B
9C
9B
9C
1A
10B
9C
10B
9A
10B
9A
10B
2B
9C
10B
9C
OB

16-15-32 3W5

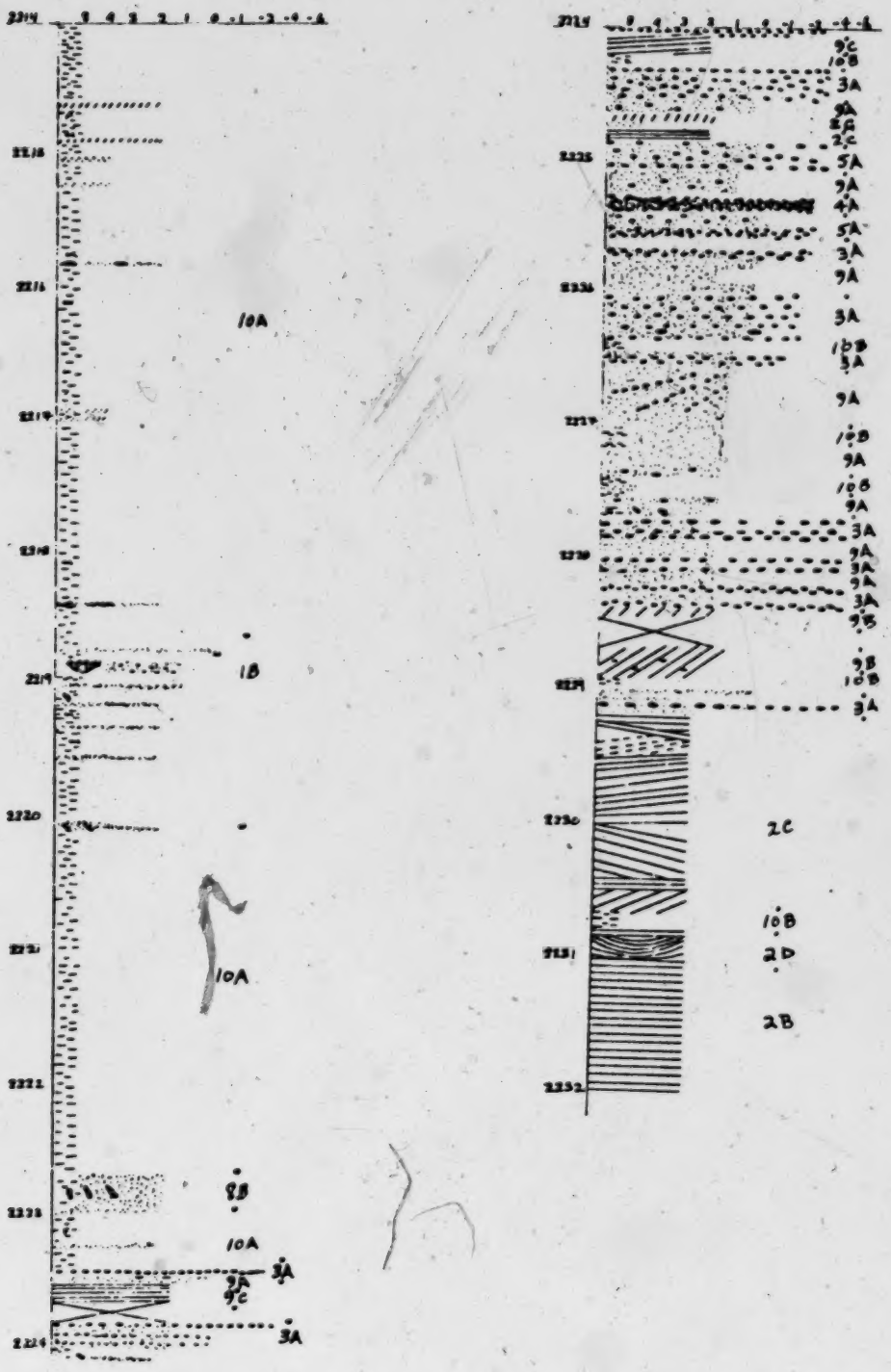
10A
1B
10A
9B
10A
3A
9A
9C
3A
9C
10B
3A
9A
2C
5A
9A
4A
5A
3A
9A
3A
10B
3A
9A
10B
9A
10B
9A
3A
9A
3A
9A
3A
9B
9B
10B
3A
2C
10B
2D
2B

6-16-32 3W5

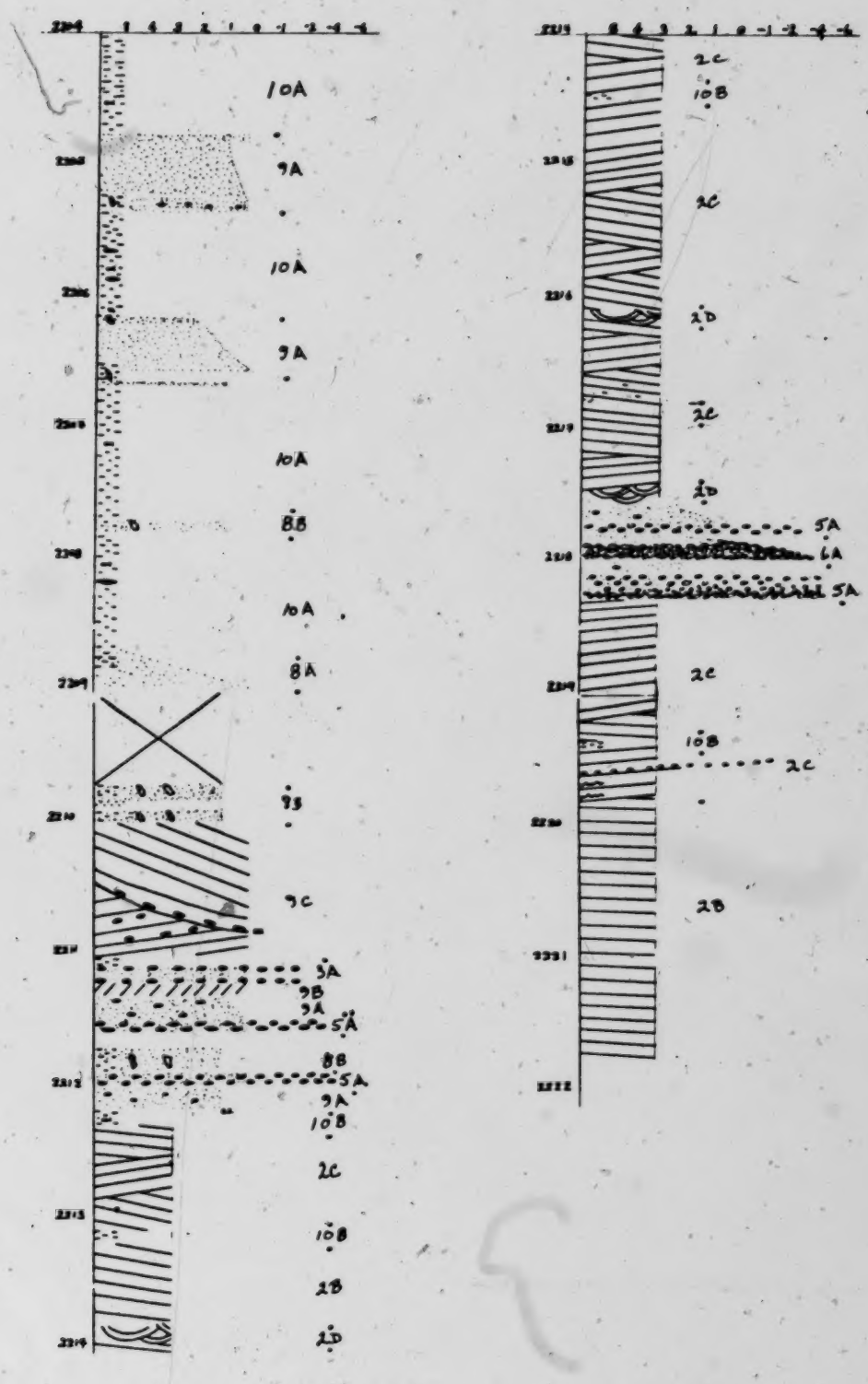
10A
9A
10A
9A
10A
8B
10A
8A
9B
9C
5A
9B
5A
5A
8B
5A
9A
10B
2C
10B
2B
2D
2C
2D
2C
1D
5A
6A
5A
2C
10B
2C
2B

16-21-32 3W5

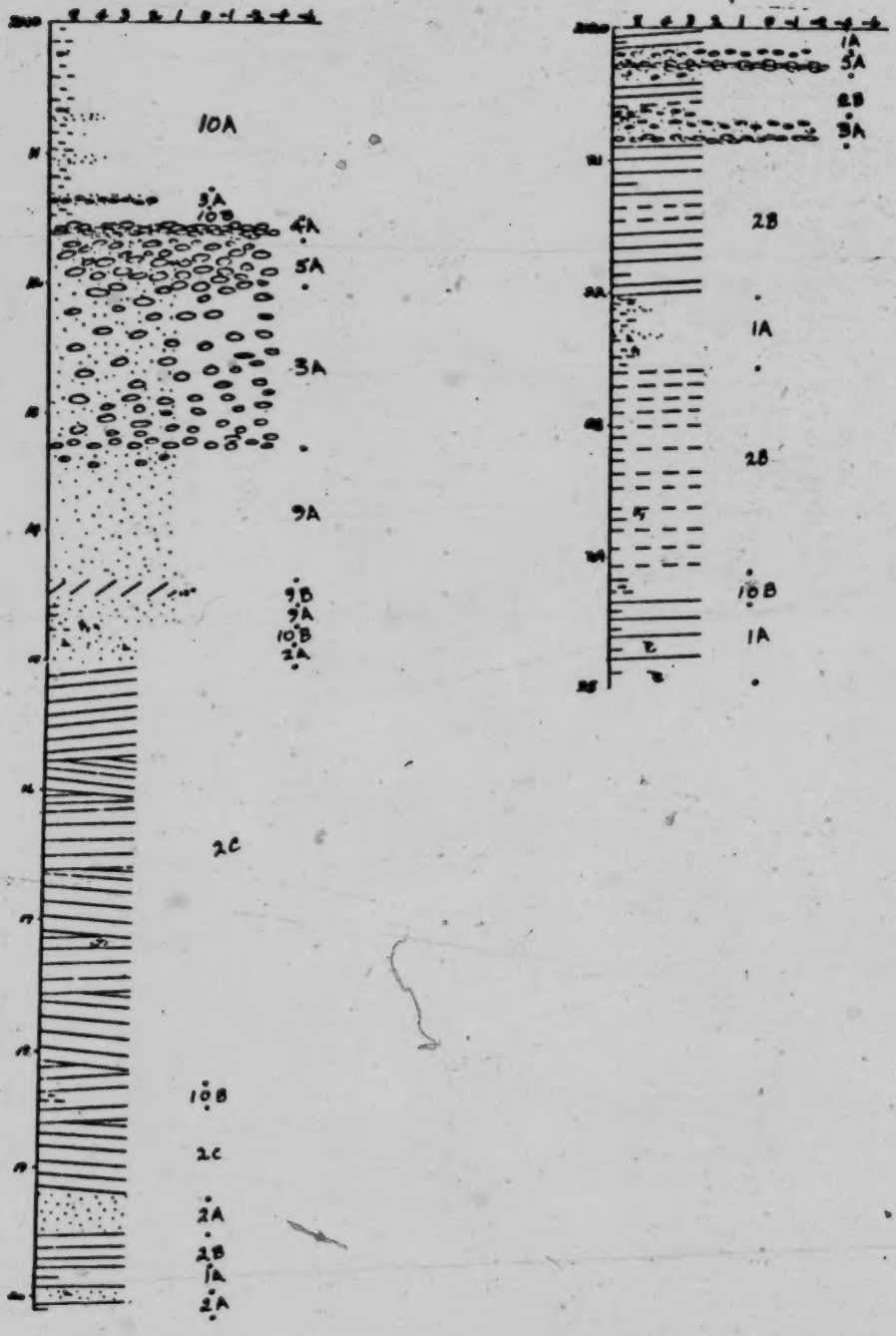
10A
3A
10B
4A
5A
3A
9A
9B
9A
10B
2A
2C
10B
2C
2A
2B
1A
2A
1A
5A
2B
3A
2B
1A
2B
10B
1A

6-22-32 3W5

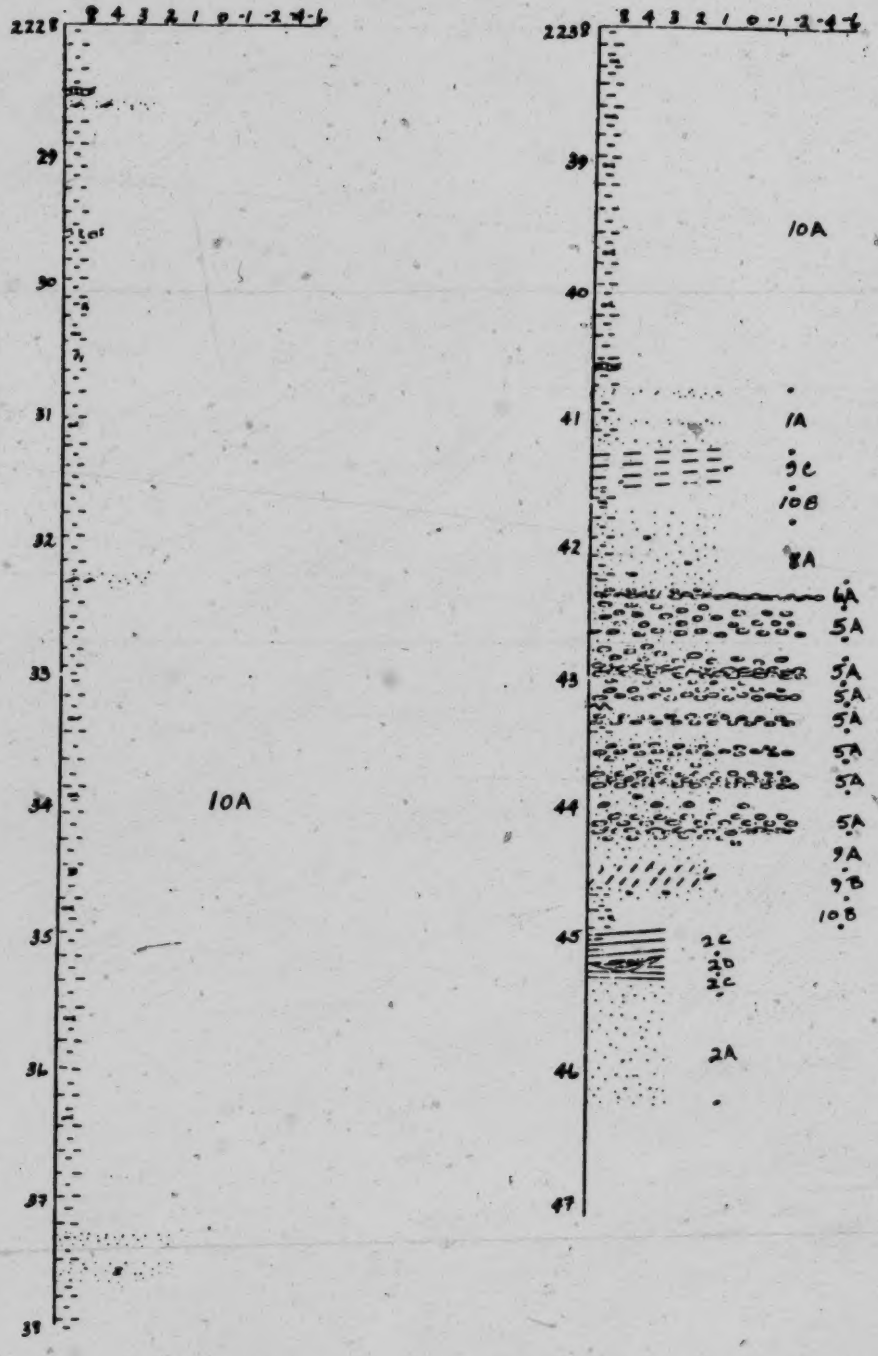
2228
29
30
31
32
33
34
35
36
37
38
10A
2239
39
40
41
42
43
44
45
46
47
10A
1A
9C
10B
8A
4A
5A
5A
5A
5A
5A
5A
5A
9A
9B
10B
2C
2D
2C
2A

16-22-32 3W5

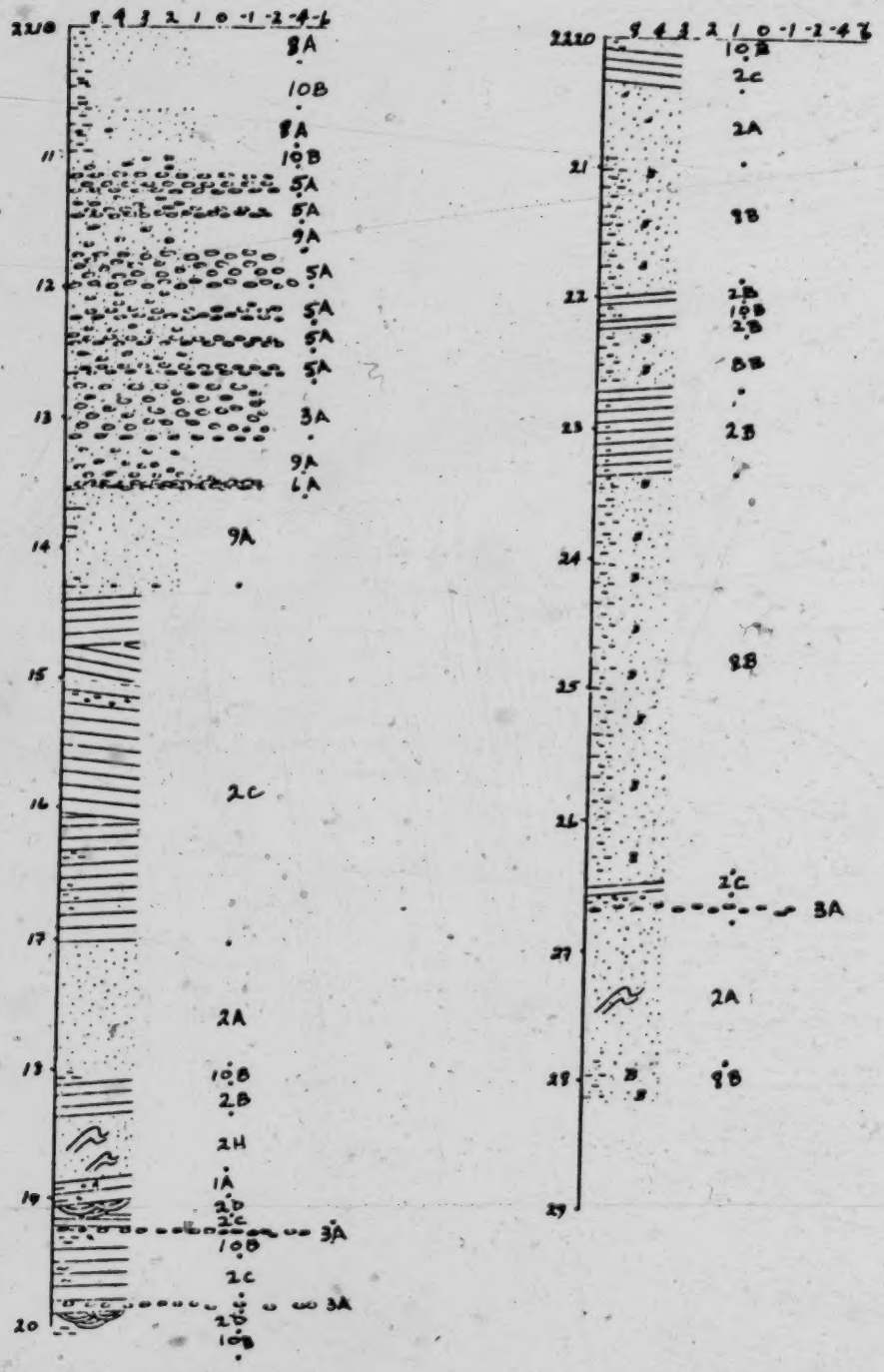
2210
9 4 3 2 1 0 -1 -2 -4 -6
8A
10B
8A
10B
5A
5A
9A
5A
5A
5A
5A
3A
9A
6A
9A
2C
2A
10B
2B
2H
1A
2D
2C
3A
10B
2C
3A
2D
10B
11
12
13
14
15
16
17
18
19
20
21
22
23
24
25
26
27
28
29
10B
2C
2A
2B
10B
2B
2B
2B
2C
3A
2A
2B

8-22-32 3W5

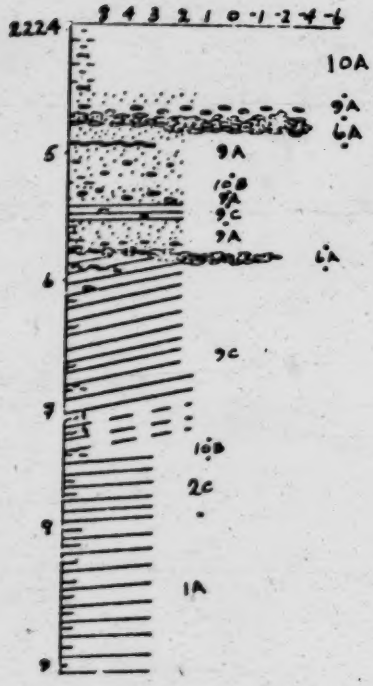

14-22-32 3W5

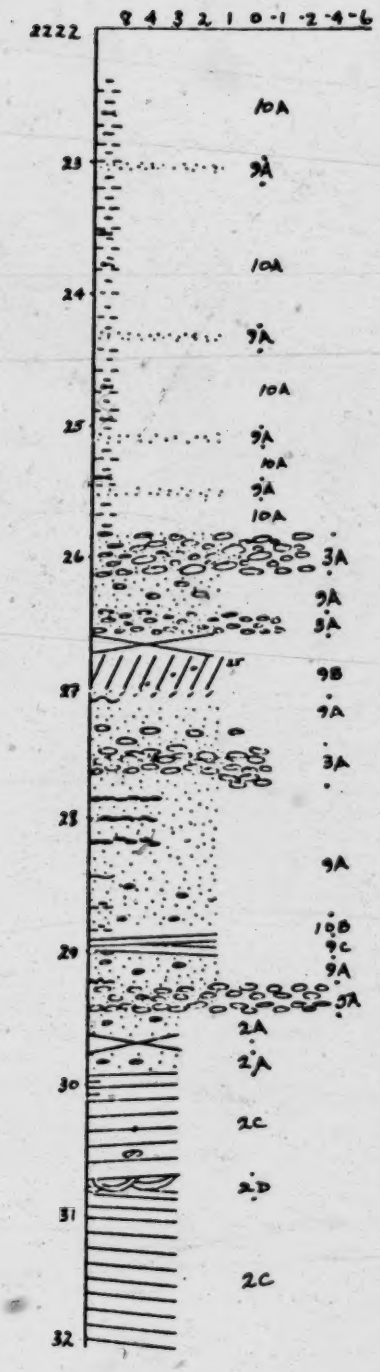
8 4 3 2 1 0 -1 -2 -4 -6
2222
23
24
25
26
27
28
29
30
31
32
10A
9A
10A
9A
10A
9A
10A
9A
10A
3A
9A
3A
9B
9A
3A
9A
10B
9C
9A
9A
2A
2A
2C
2D
2C

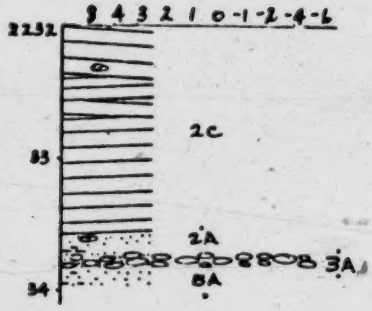
8 4 3 2 1 0 -1 -2 -4 -6
2232
33
34
2C
2A
3A
8A

6-23-32 3W5

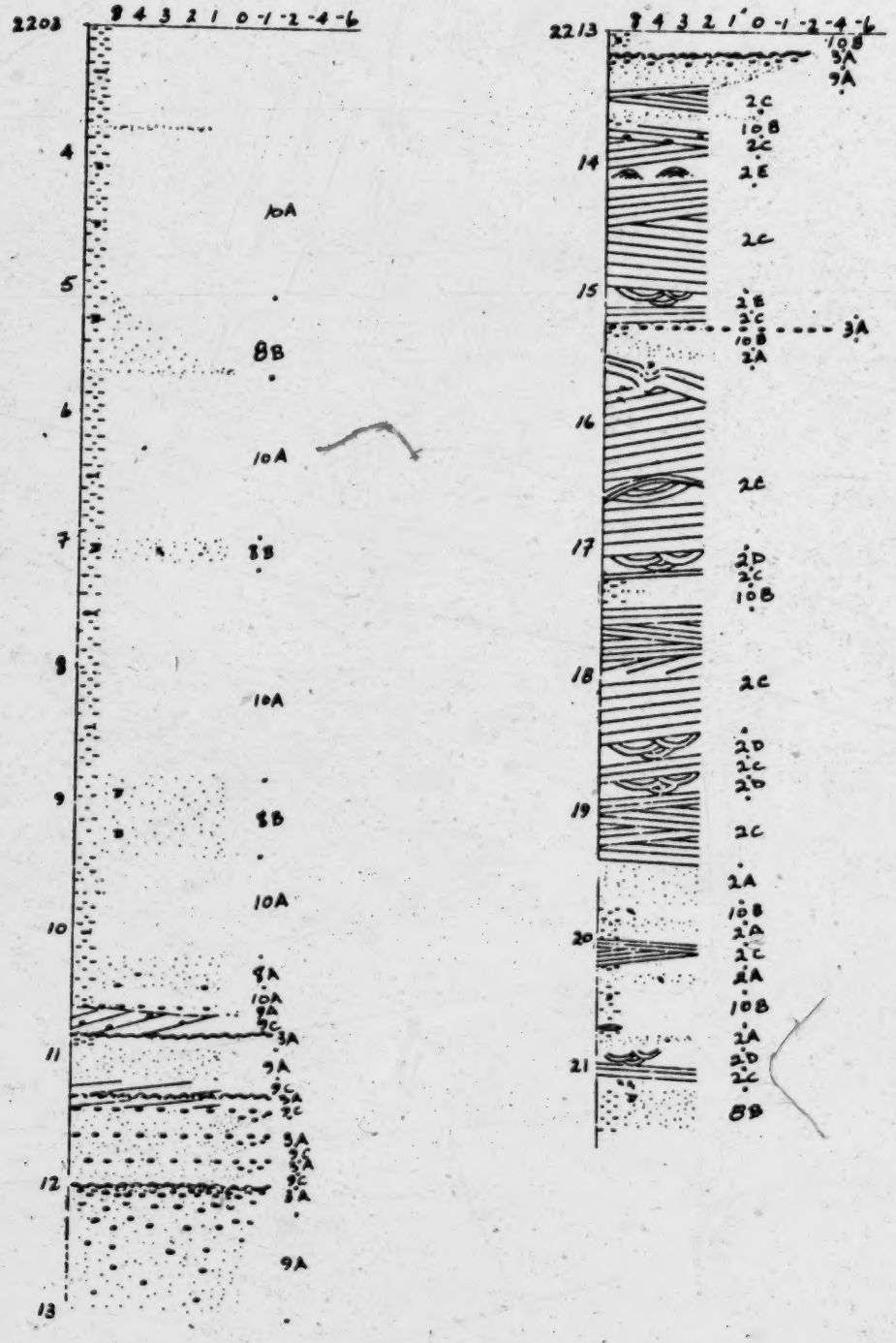
2203
8 4 3 2 1 0 -1 -2 -4 -6
4
5
6
7
8
9
10
11
12
13
10A
8B
10A
8B
10A
8B
10A
9A
10A
9A
2C
3A
9A
9C
2C
9A
2C
3A
2C
3A
9C
3A
9A
2213
8 4 3 2 1 0 -1 -2 -4 -6
10B
3A
9A
2C
10B
2C
14
2E
2C
15
2E
2C
10B
3A
2A
16
2C
17
2D
2C
10B
18
2C
2D
2C
2D
19
2C
2A
10B
20
2A
2C
2A
10B
2A
21
2D
2C
8B

8-23-32 3W5

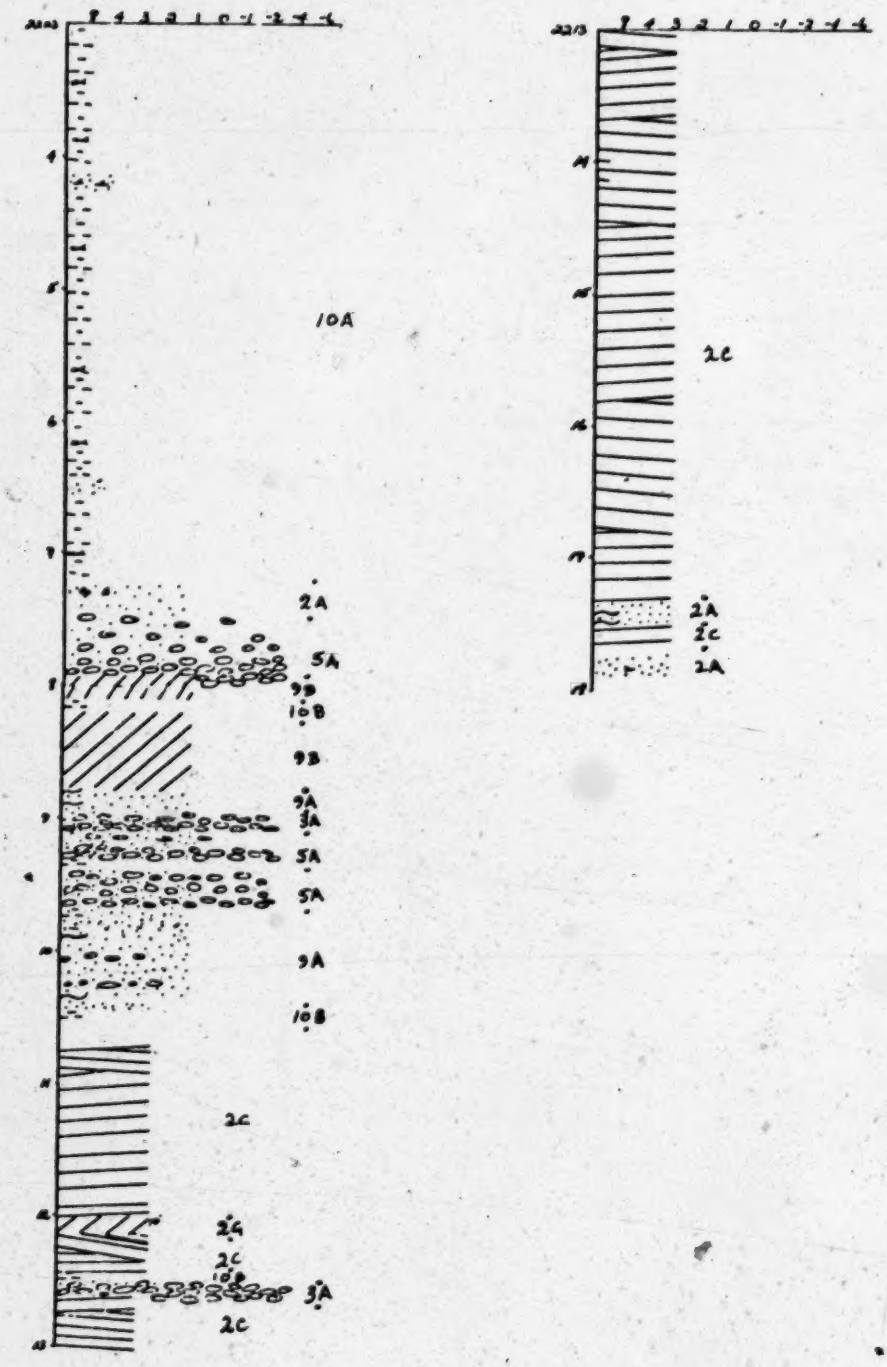

14-23-32 3W5

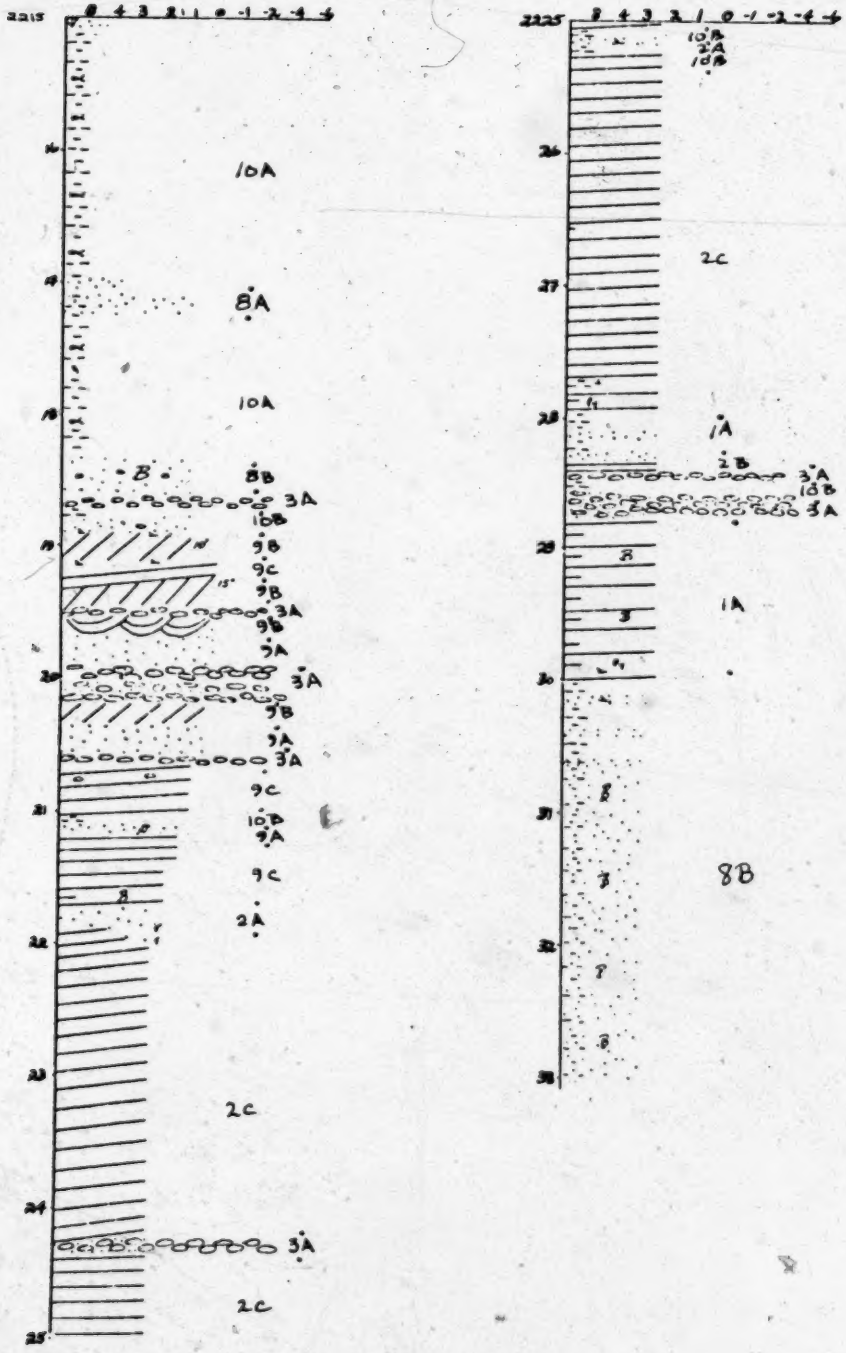
2215
8 4 3 2 1 0 -1 -2 -4 -6
10A
8A
10A
8B
3A
10B
9B
9C
9B
3A
9B
9A
3A
9B
9A
3A
9C
10B
9A
9C
2A
2C
3A
2C
2225
8 4 3 2 1 0 -1 -2 -4 -6
10B
2A
10B
2C
1A
2B
3A
10B
3A
1A
8B

16-23-32 3W5

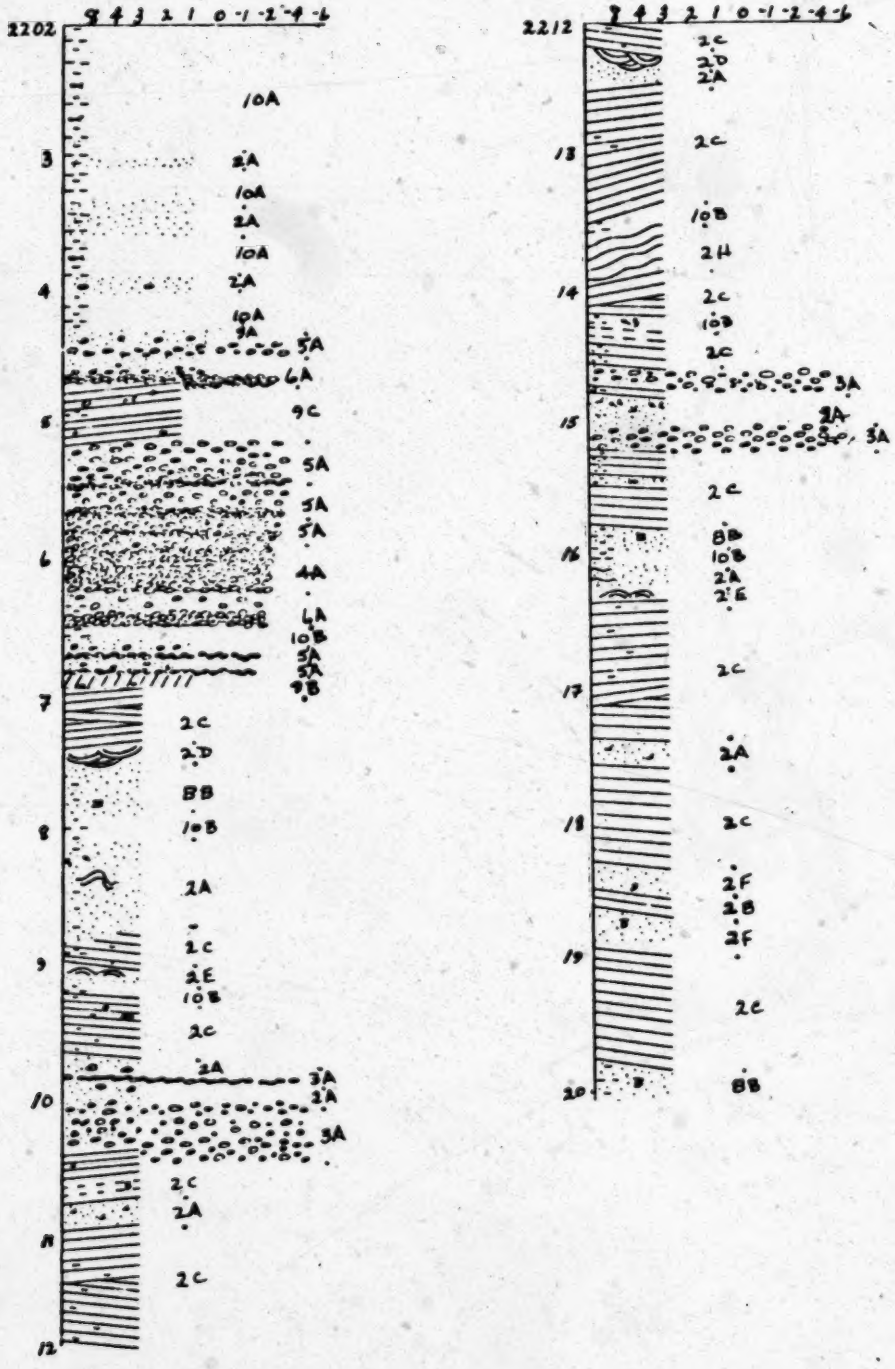
2202
3 4 3 2 1 0 -1 -2 -4 -6
10A
3
2A
10A
2A
10A
4
2A
10A
3A
5A
6A
5
9C
5A
5A
5A
6
4A
4A
10B
5A
5A
9B
7
2C
2D
BB
8
10B
2A
2C
9
2E
10B
2C
2A
3A
10
2A
3A
2C
2A
11
2C
12
2212
3 4 3 2 1 0 -1 -2 -4 -6
2C
2D
2A
2C
13
10B
2H
14
2C
10B
2C
3A
2A
15
3A
3A
2C
BB
16
10B
2A
2E
2C
17
2A
2C
18
2F
2B
2F
19
2C
BB
20

6-24-32 3W5

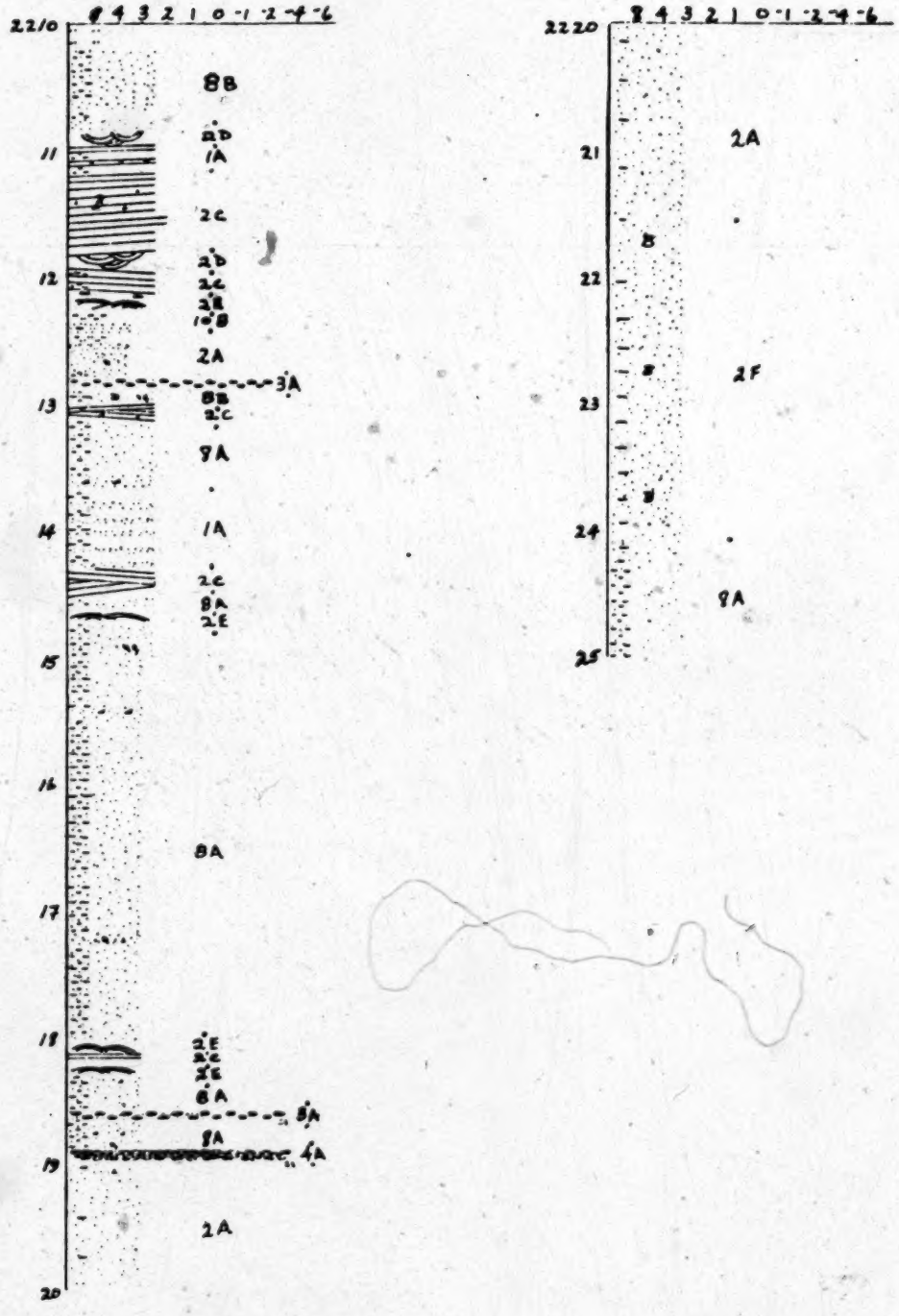
8 4 3 2 1 0 -1 -2 -4 -6
2210
11
12
13
14
15
16
17
18
19
20
8B
2D
1A
2C
2D
2C
2E
1B
2A
3A
8B
2C
8A
1A
2C
8A
2E
8A
2E
2C
2E
8A
8A
4A
2A
2220
21
22
23
24
25
2A
B
2F
8A

8-24-32 3W5

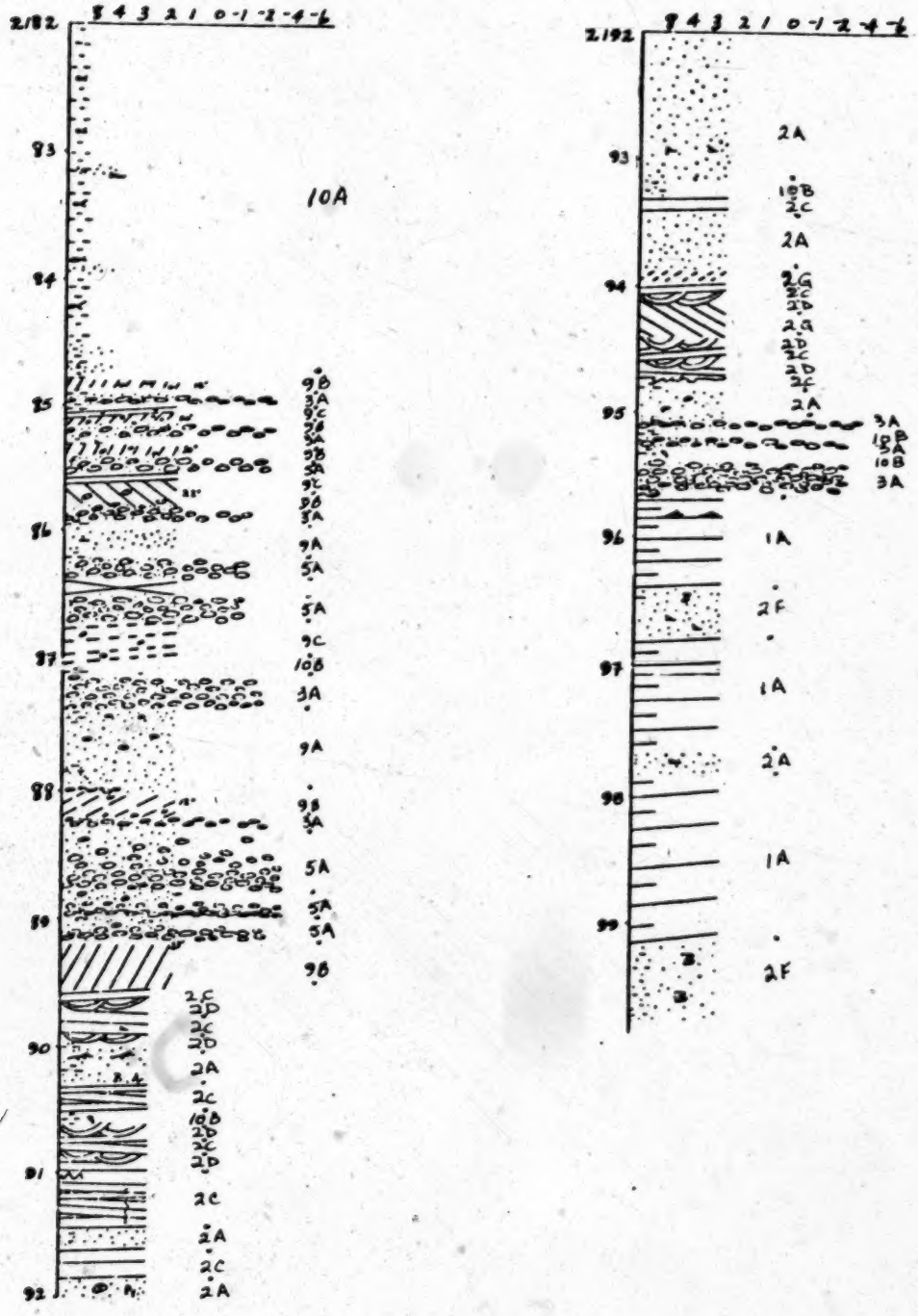

14-24-32 3W5

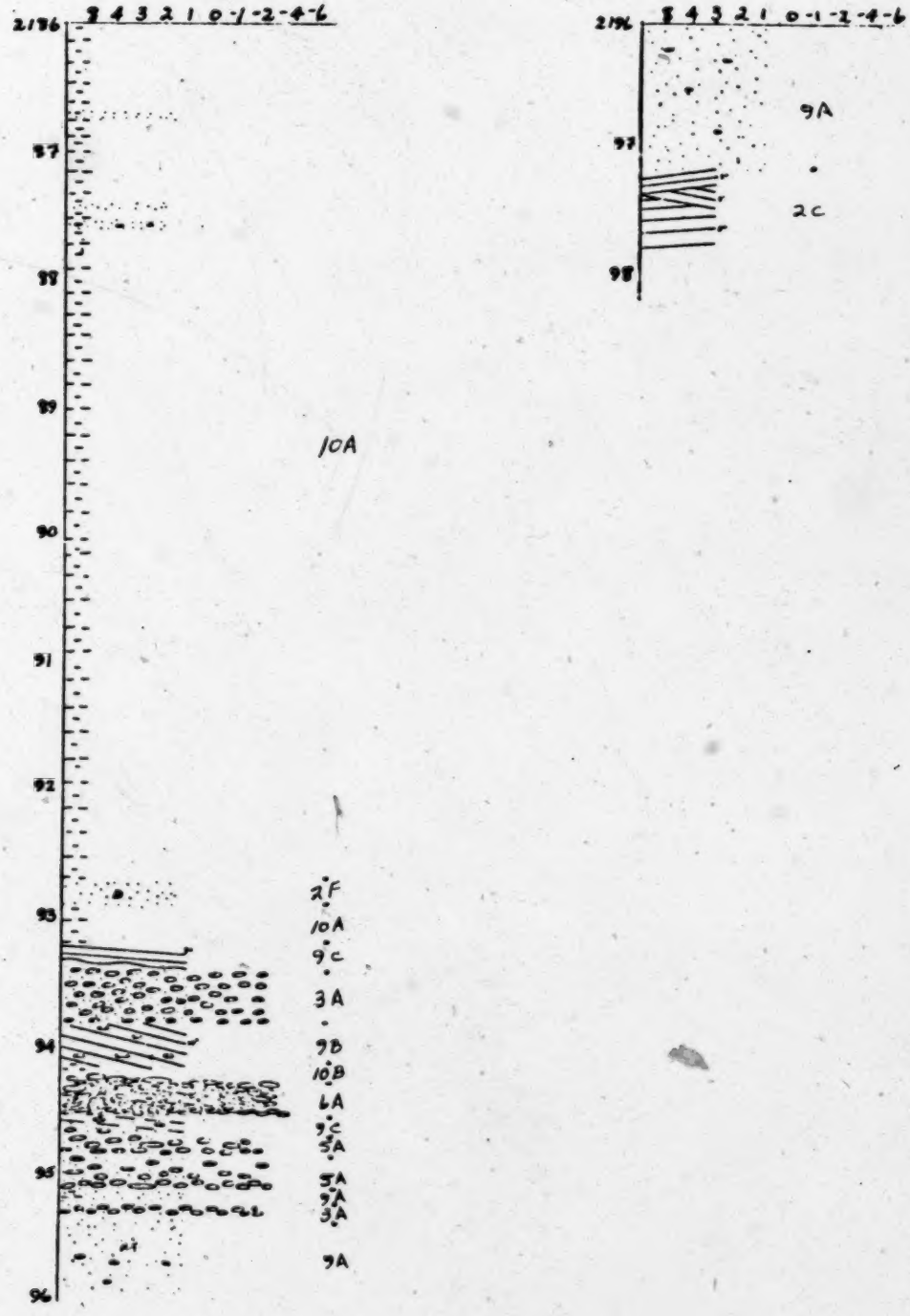
2196
8 4 3 2 1 0 -1 -2 -4 -6
97
98
99
90
91
92
93
94
95
96
10A
2F
10A
9C
3A
9B
10B
4A
9C
5A
5A
9A
3A
9A
2196
8 4 3 2 1 0 -1 -2 -4 -6
97
98
9A
2C

16-24-32 3W5

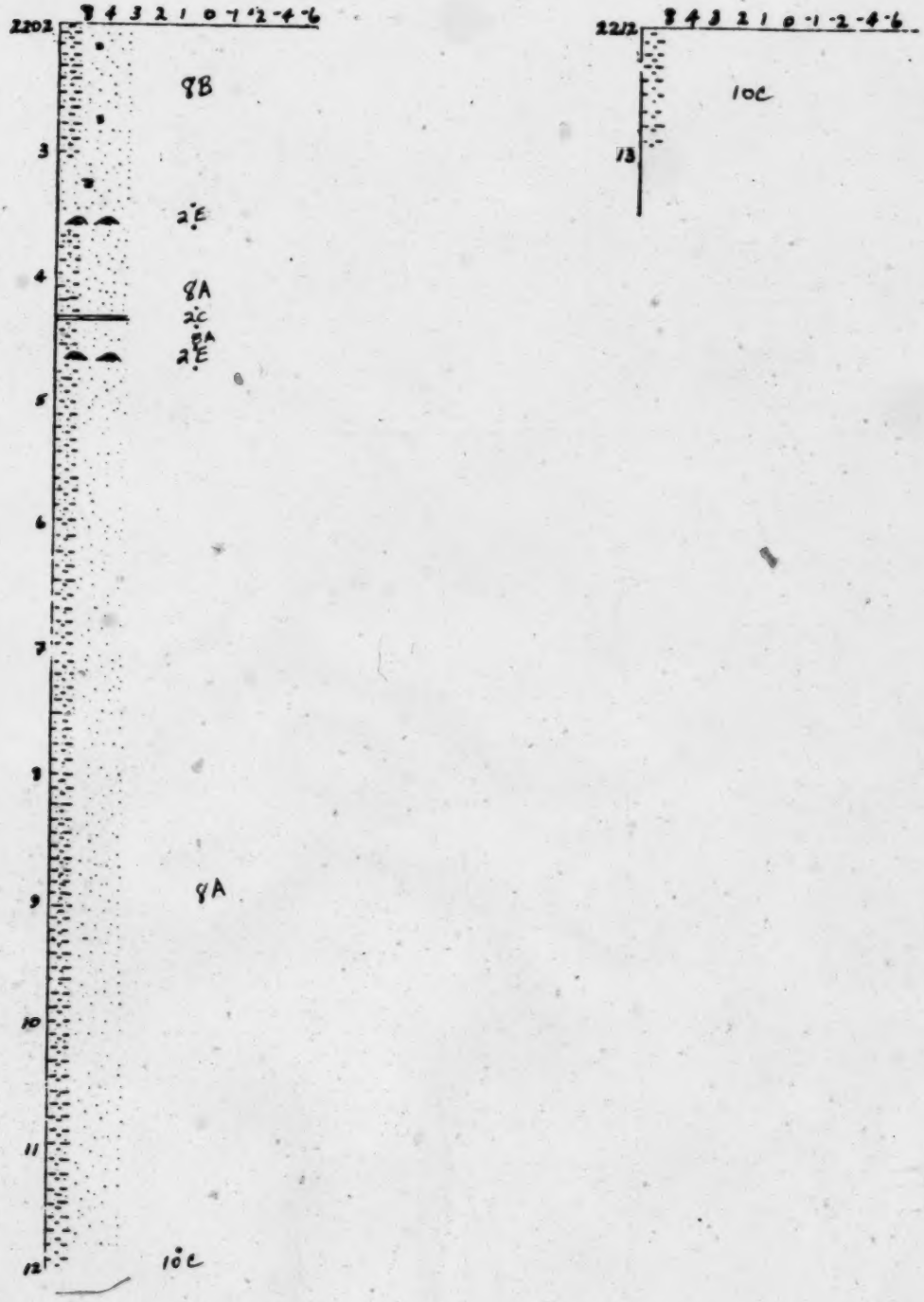
8 4 3 2 1 0 -1 -2 -4 -6
2202
3
4
5
6
7
8
9
10
11
12
8B
2E
8A
2C
8A
2E
8A
10C
8 4 3 2 1 0 -1 -2 -4 -6
2212
13
10C

6-25-32 3W5

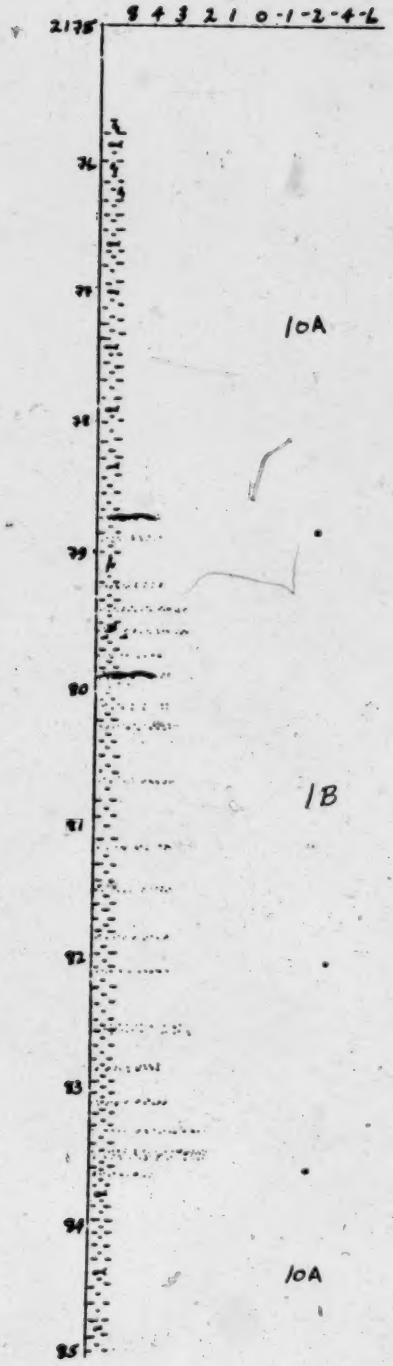
8 4 3 2 1 0 -1 -2 -4 -6
2178
10A
1B
10A

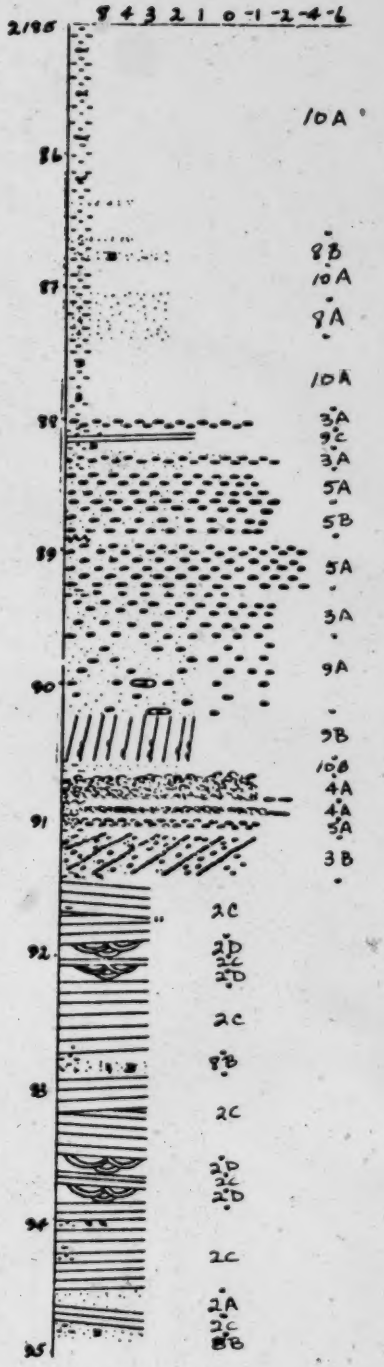
8 4 3 2 1 0 -1 -2 -4 -6
2195
10A
8B
10A
8A
10A
3A
9C
3A
5A
5B
5A
3A
9A
9B
10B
4A
4A
5A
3B
2C
2D
2C
2D
2C
8B
2C
2D
2C
2D
2C
2A
2C
8B

16-25-32 3W5

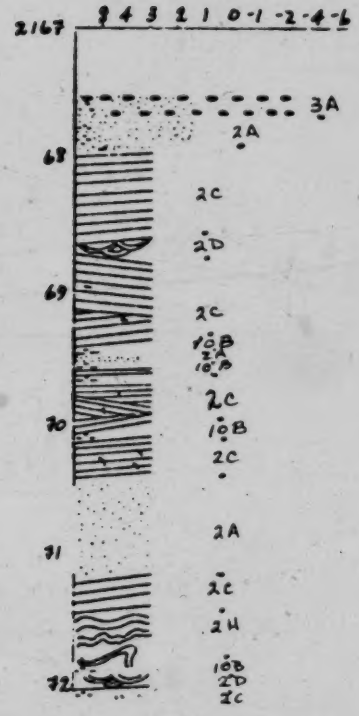
2167
3 4 3 2 1 0 -1 -2 -4 -6
3A
2A
68
2C
2D
69
2C
10B
2A
10B
2C
70
10B
2C
2A
71
2C
2H
10B
72
2D
2C

6-27-32 3W5

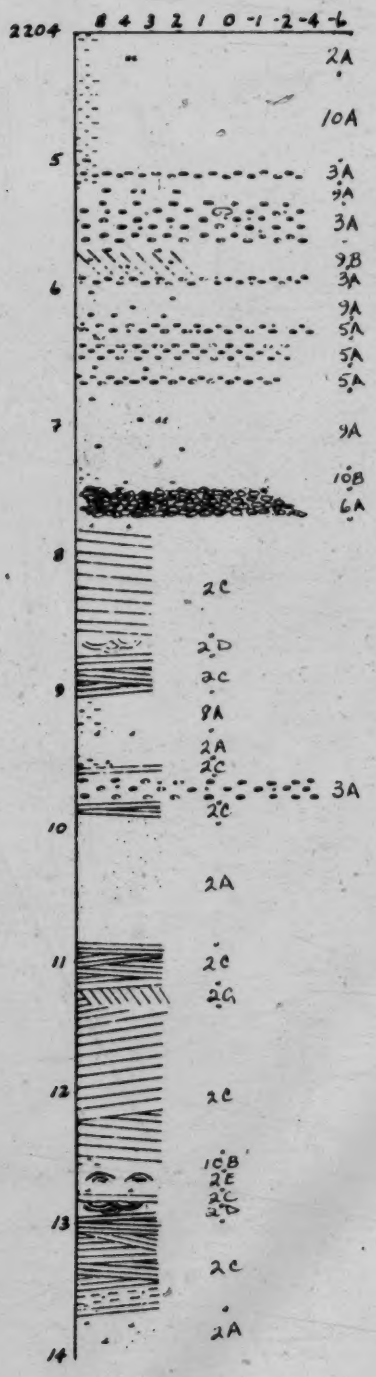
2204
8 4 3 2 1 0 -1 -2 -4 -6
2A
10A
5
3A
9A
3A
9B
6
3A
9A
5A
5A
5A
7
9A
10B
6A
8
2C
2D
2C
9
8A
2A
2C
3A
2C
10
2A
11
2C
2G
12
2C
10B
2E
2C
2D
13
2C
2A
14

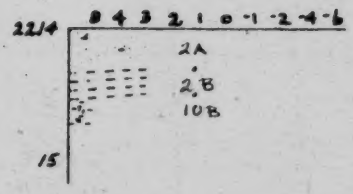
2214
8 4 3 2 1 0 -1 -2 -4 -6
2A
2B
10B
15

16-28-32 3W5

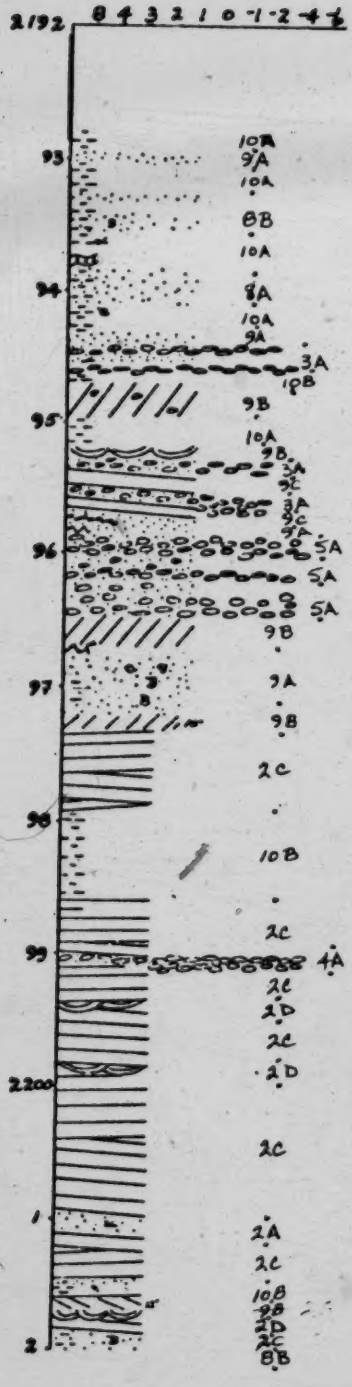
2192
8 4 3 2 1 0 -1 -2 -4 -6
93
94
95
96
97
98
99
2200
1
2
10B
9A
10A
8B
10A
8A
10A
9A
3A
10B
9B
10A
2B
3A
2C
3A
5C
7A
5A
5A
5A
9B
9A
9B
2C
10B
2C
1A
2C
2D
2C
2D
2C
2A
2C
10B
9B
2D
2C
8B

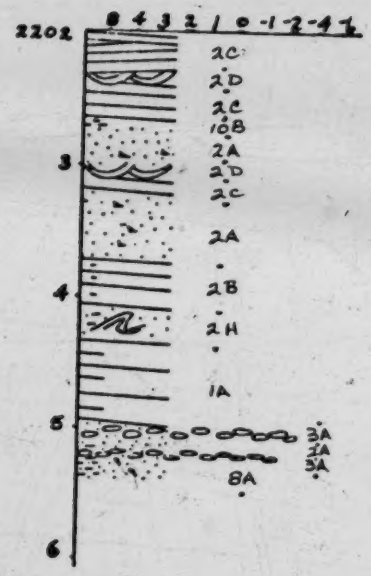
2202
8 4 3 2 1 0 -1 -2 -4 -6
3
4
5
6
2C
2D
2C
10B
2A
2D
2C
2A
2B
2H
1A
3A
2A
3A
8A

15-14V-32 4W5

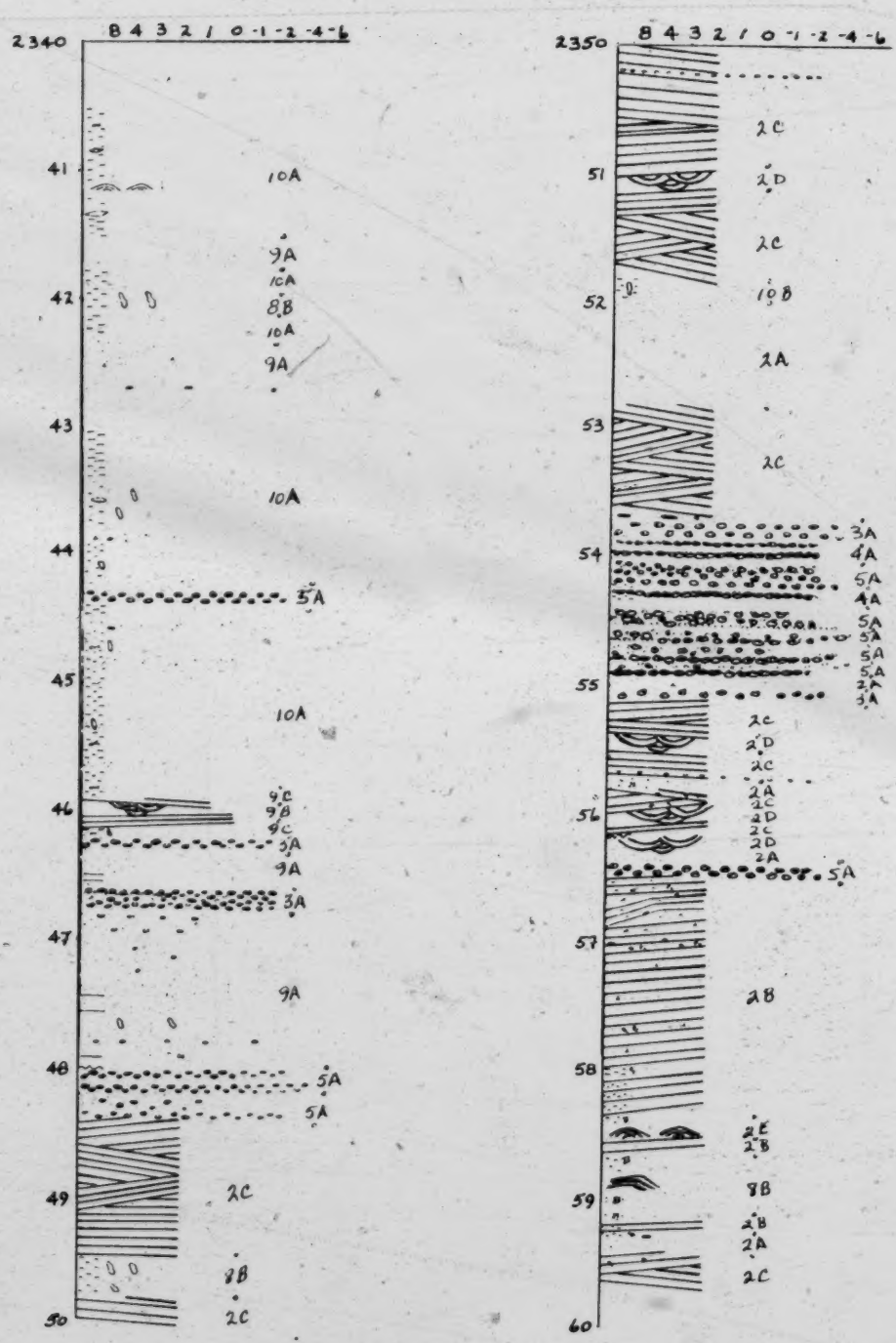
2340
8 4 3 2 1 0 -1 -2 -4 -6
41
42
43
44
45
46
47
48
49
50
10A
9A
10A
8B
10A
9A
10A
5A
10A
9C
9B
9C
5A
9A
3A
9A
5A
5A
2C
8B
2C
2350
8 4 3 2 1 0 -1 -2 -4 -6
51
52
53
54
55
56
57
58
59
60
2C
2D
2C
10B
2A
2C
3A
4A
5A
4A
5A
5A
5A
5A
2A
3A
2C
2D
2C
2A
2C
2D
2C
2D
2A
5A
2B
2E
2B
8B
2B
2A
2C

15-14V-32 4W5 cont'd

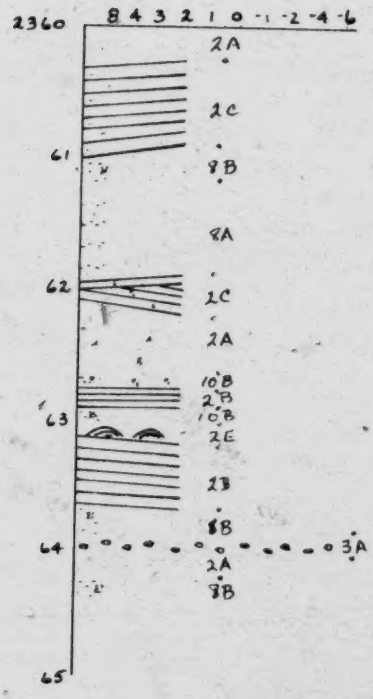

11-18-32 4W5

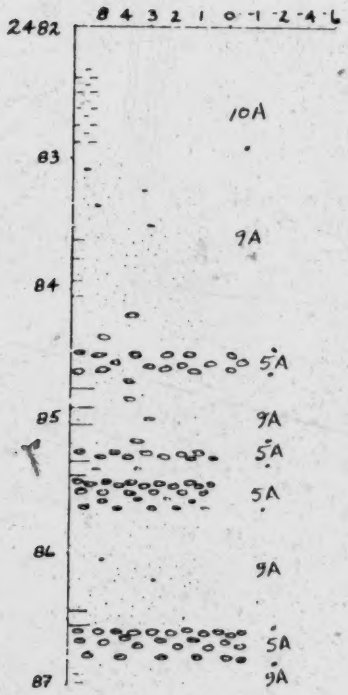

7-24V-32 4W5

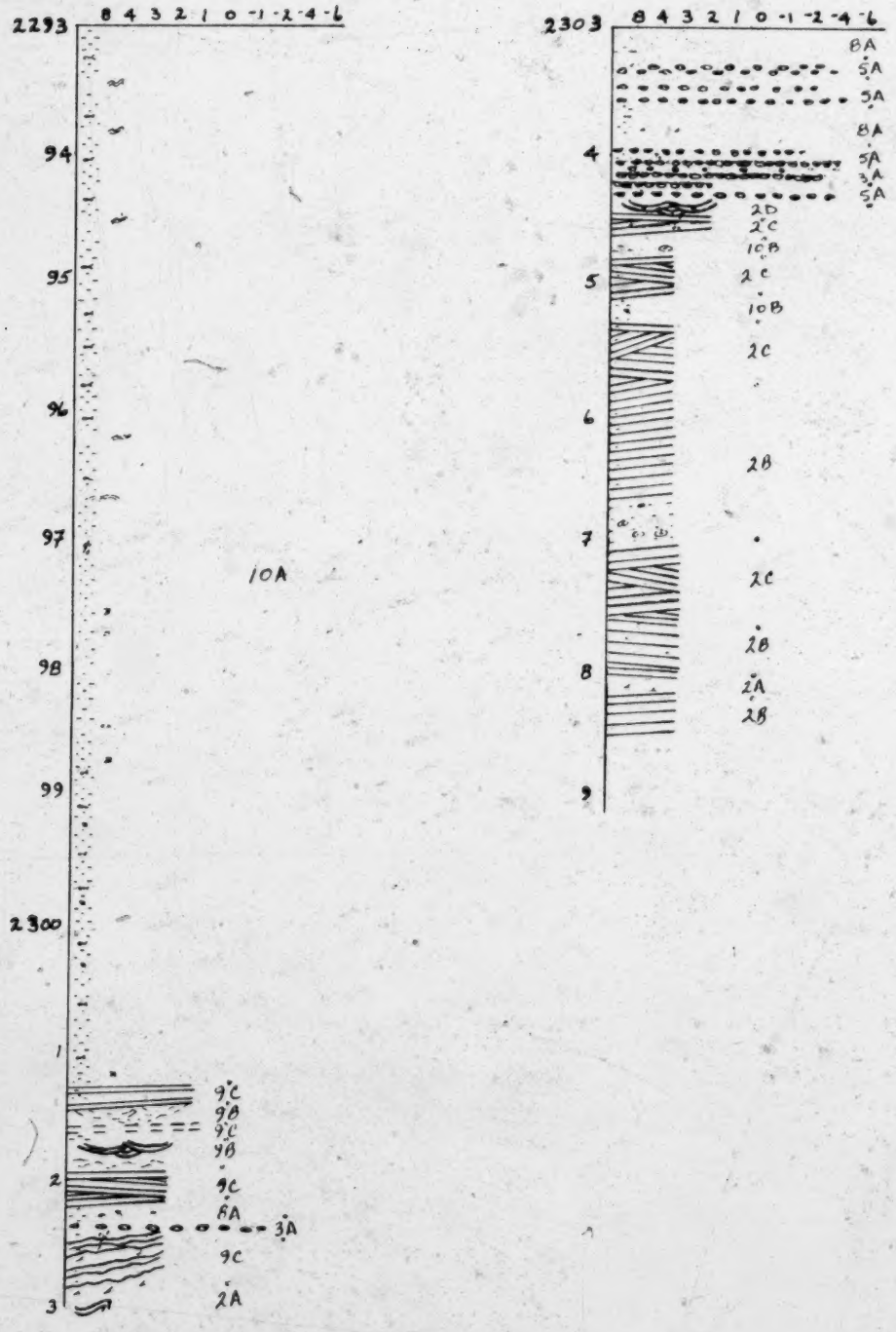
8 4 3 2 1 0 -1 -2 -4 -6
2293
94
95
96
97
98
99
2300
1
2
3
10A
9C
9B
9C
9B
9C
8A
3A
9C
2A
2303
4
5
6
7
8
9
8A
5A
3A
5A
8A
5A
3A
5A
2D
2C
10B
2C
10B
2C
2B
2C
2B
2A
2B

5-27-32 4W5

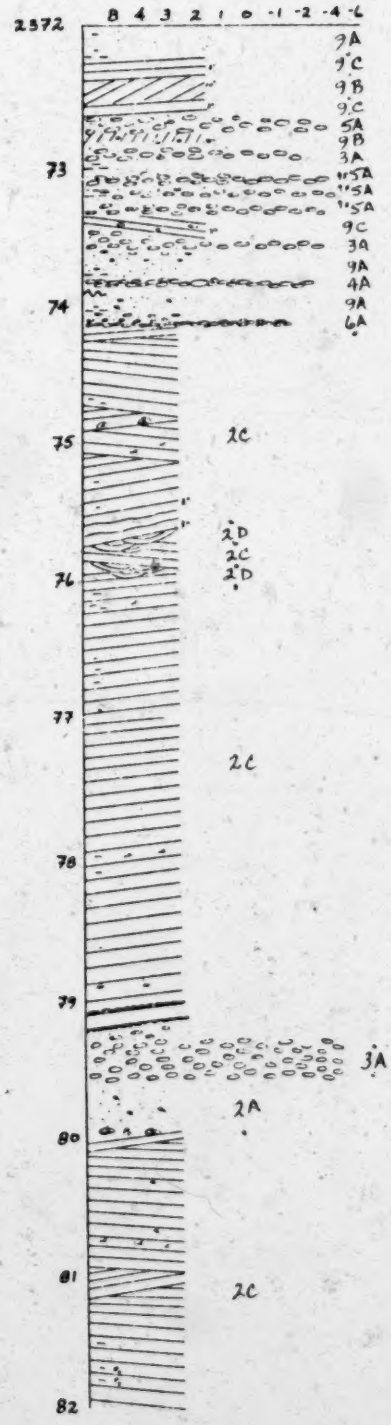
2372
B 4 3 2 1 0 -1 -2 -4 -6
9A
9C
9B
9C
5A
9B
3A
73
11 5A
11 5A
11 5A
9C
3A
9A
4A
74
9A
6A
75
2C
2D
2C
76
2D
77
2C
78
79
3A
2A
80
81
2C
82

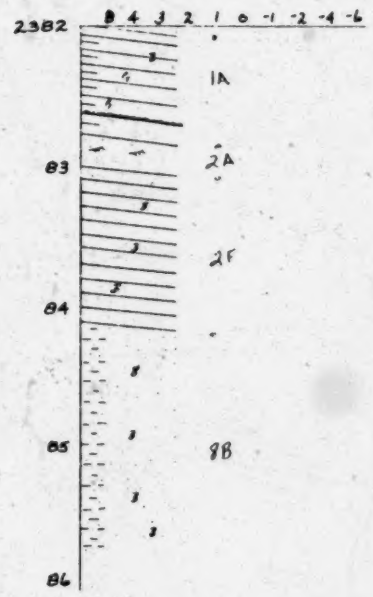
2382
B 4 3 2 1 0 -1 -2 -4 -6
1A
83
2A
2F
84
85
8B
86

10-23-33 2W5

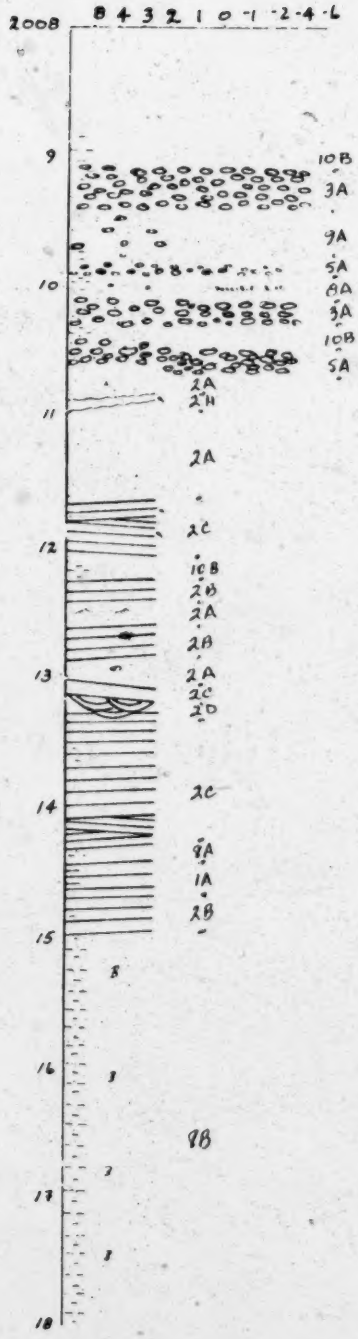
2008
8 4 3 2 1 0 -1 -2 -4 -6
9
10
11
12
13
14
15
16
17
18
10B
3A
9A
5A
8A
3A
10B
5A
2A
2H
2A
2C
10B
2B
2A
2B
2A
2C
2D
2C
9A
1A
2B
8B

3-19-33 4W5

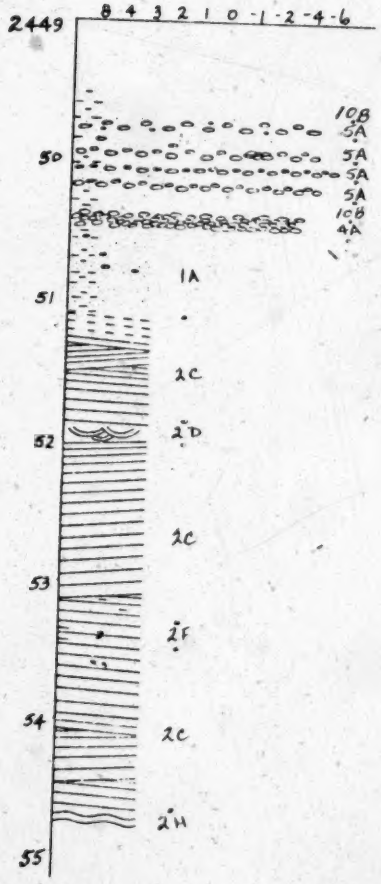
8 4 3 2 1 0 -1 -2 -4 -6
2449
50
51
52
53
54
55
10B
5A
5A
5A
5A
10B
4A
1A
2C
2D
2C
2F
2C
2H

5-19-33 4W5

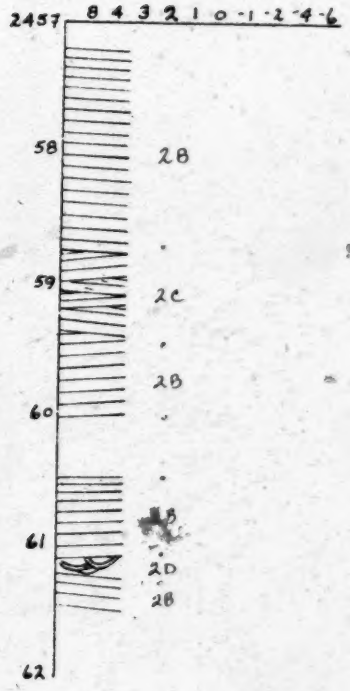

7-19-33 4W5

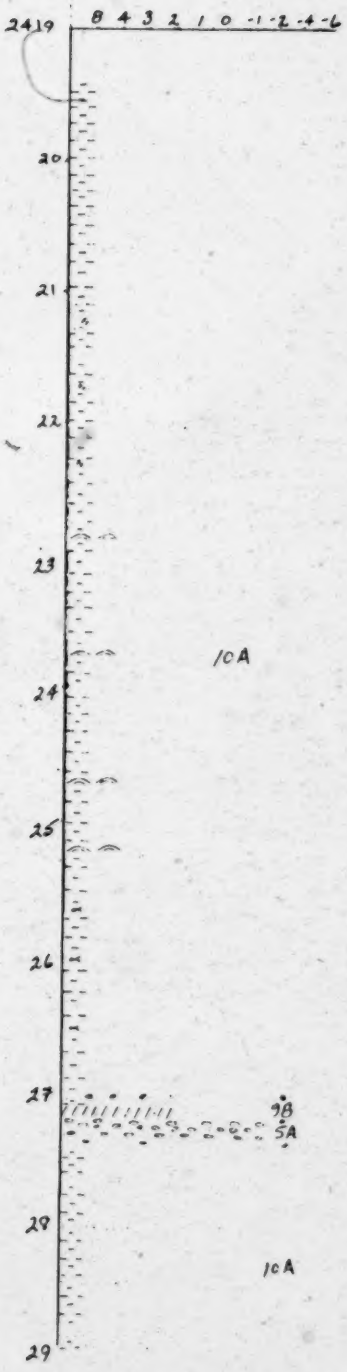
2419
8 4 3 2 1 0 -1 -2 -4 -6
20
21
22
23
24
25
26
27
29
29
10A
9B
5A
10A

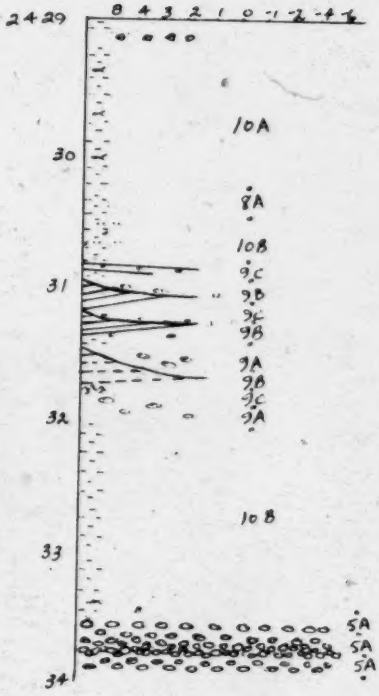
2429
8 4 3 2 1 0 -1 -2 -4 -6
30
31
32
33
34
10A
8A
10B
9C
9B
9C
9B
9A
9B
9C
9A
10B
5A
5A
5A

11-31-33 4W5

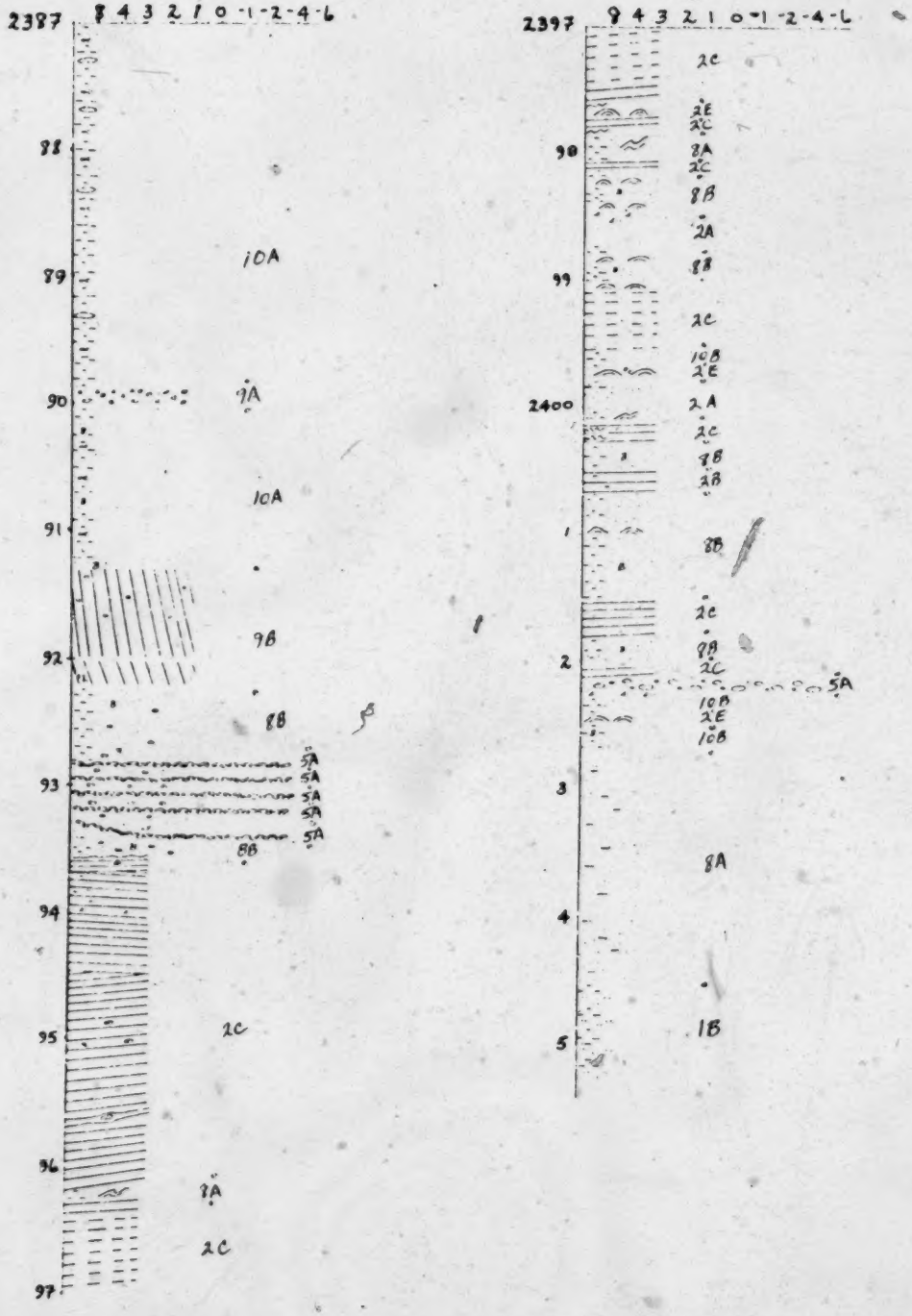
2387
8 4 3 2 1 0 -1 -2 -4 -6
88
89
90
91
92
93
94
95
96
97
10A
9A
10A
9B
8B
5A
5A
5A
5A
5A
8B
2C
2A
2C
2397
8 4 3 2 1 0 -1 -2 -4 -6
2C
2E
2C
98
8A
2C
8B
2A
99
8B
2C
10B
2E
2400
2A
2C
8B
2B
1
8B
2C
8B
2
2C
5A
10B
2E
10B
3
8A
4
5
1B